AD NUMBER

ADB063220

LIMITATION CHANGES

TO:

Approved for public release; distribution is unlimited.

FROM:

Distribution authorized to U.S. Gov't. agencies only; Test and Evaluation; 26 JAN 1982. Other requests shall be referred to Naval Underwater Systems Center, New London, CT.

AUTHORITY

NUWC ltr 9 Mar 1994

AD NUMBER

ADB063220

LIMITATION CHANGES

TO:

Approved for public release; distribution is unlimited.

FROM:

Distribution authorized to U.S. Gov't. agencies only; Test and Evaluation; 26 JAN 1982. Other requests shall be referred to Naval Underwater Systems Center, New London, CT.

AUTHORITY

NUWC ltr 9 Mar 1954

NUSC Technical Document 6059
26 January 1982

Principles of Sonar Installation

Harrison T. Loeser
Engineering and Technical Support Department

Naval Underwater Systems Center
Newport, Rhode Island / New London, Connecticut

Preface

This document was prepared under NUSC Project No. A60425, Principal Investigator, H. T. Loeser (Code 4101), Sponsoring Activity, Naval Sea Systems Command, H. Demattia (SEA 61R4).

The information assembled here was derived from many sources and it proved impractical, if not impossible, to give acknowledgment when due. However, all sources are included in the bibliographies that accompany each chapter.

Preparation of this document was supported, in part, by work under the following contracts:

N00140-76-O-6962	Tractor, Inc.	Chapters 1, 5
N66604-78-M-3886	Rockwell International	Chapters 1, 2, 3
N66604-78-M-6282	Bolt Beranek & Newman	Chapters 2, 3
N66604-79-M-1956	Woodmont Systems	Chapter 4

Reviewed and Approved: 26 January 1982

J. F. Kelly, Jr.
Head, Engineering and Technical Support Department

The author of this document is located at the
New London Laboratory, Naval Underwater Systems Center,
New London, Connecticut 06320.

REPORT DOCUMENTATION PAGE		READ INSTRUCTIONS BEFORE COMPLETING FORM
1. REPORT NUMBER TD 6059	2. GOVT ACCESSION NO. AD-B063 220L	3. RECIPIENT'S CATALOG NUMBER
4. TITLE (and Subtitle) PRINCIPLES OF SONAR INSTALLATION		5. TYPE OF REPORT & PERIOD COVERED 6. PERFORMING ORG. REPORT NUMBER
7. AUTHOR(s) Harrison T. Loeser		8. CONTRACT OR GRANT NUMBER(s)
9. PERFORMING ORGANIZATION NAME AND ADDRESS Naval Underwater Systems Center New London Laboratory New London, CT 06320		10. PROGRAM ELEMENT, PROJECT, TASK AREA & WORK UNIT NUMBERS A60425
11. CONTROLLING OFFICE NAME AND ADDRESS Naval Sea Systems Command (SEA 61R4) Washington, D. C. 20360		12. REPORT DATE 26 January 1982 13. NUMBER OF PAGES 247
14. MONITORING AGENCY NAME & ADDRESS(if different from Controlling Office)		15. SECURITY CLASS. (of this report) UNCLASSIFIED 15a. DECLASSIFICATION/ DOWNGRADING SCHEDULE

16. DISTRIBUTION STATEMENT (of this Report)

Distribution limited to U.S. Government agencies only: Test and Evaluation, 26 JAN 82 (date). Other requests for this document must be referred to the Naval Underwater Systems Center.

17. DISTRIBUTION STATEMENT (of the abstract entered in Block 20, if different from Report)

18. SUPPLEMENTARY NOTES

19. KEY WORDS (Continue on reverse side if necessary and identify by block number)

1. Acoustic Control
2. Acoustic Phenomena
3. Array Installation
4. Elastomers
5. EMI
6. Noise Generation
7. Ship Installation
8. Sonar
9. Sonar Fundamentals
10. Vibration

20. ABSTRACT (Continue on reverse side if necessary and identify by block number)

This document provides information useful to designers and constructors of anti-submarine warfare ships. The fundamentals of sonar, noise generation and transmission, vibration control, acoustic phenomena, elastomers, acoustic shipboard sonar uses, and sonar installation, and electromagnetic interference are discussed.

DD FORM 1 JAN 73 1473 EDITION OF 1 NOV 65 IS OBSOLETE
S/N 0102-014-6601

TABLE OF CONTENTS

TABLE OF CONTENTS (CONT'D)

TABLE OF CONTENTS (CONT'D)

TABLE OF CONTENTS (CONT'D)

Page

CHAPTER IV
ELASTOMERS

TABLE OF CONTENTS (CONT'D)

TABLE OF CONTENTS (CONT'D)

LIST OF ILLUSTRATIONS

LIST OF ILLUSTRATIONS (CONT'D)

LIST OF ILLUSTRATIONS (CONT'D)

LIST OF ILLUSTRATIONS (CONT'D)

LIST OF ILLUSTRATIONS (CONT'D)

LIST OF ILLUSTRATIONS (CONT'D)

LIST OF ILLUSTRATIONS (CONT'D)

LIST OF TABLES

LIST OF TABLES (CONT'D)

Principles of Sonar Installation

CHAPTER I
SONAR FUNDAMENTALS

GLOSSARY

a	Radius (L)
A	Absorption (dB)
A-D	Analog to Digital
AG	Array Gain (dB)
AM	Amplitude Modulation
AMLC	Amplitude Modulation Locked Carrier
B	Bulk Modulus
B_f	Root Mean Square Phase Deviation
BT	Bathythermograph
BW	Beamwidth (3 dB Down Points)
c	Speed of Sound (L/T)
CDM	Companded Delta Modulation
CDMX	Code Division Multiplexing
CPCM	Companded Pulse Code Modulation
CZ	Convergence Zone
d	Ratio of Signal Plus Noise-to-Noise
d_h	Hydrophone Separation (L)
D	Depth (L)
D_R	Directivity
D_D	Degradation in Signal Gain (dB)
dB	Decibel
D/E	Depression/Elevation (from Horizontal Plane)
DI	Directivity Index (dB)
DM	Delta Modulation
DPCM	Delta Pulse Code Modulation
DSB	Double Side Band
DSL	Deep Scattering Layer
DT	Detection Threshold (dB)
E	Root Mean Square Relative Amplitude Fluctuations
f	Frequency (1/T)
FDM	Frequency Division Multiplexing
FM	Frequency Modulation
FSK	Frequency Shift Keying
GS	Array Signal Gain (dB)
GN	Array Noise Gain (dB)
Hz	Hertz (1/T)
I	Intensity (F/LT)
k	Wave Number ($2\pi/\lambda$) (1/L)
kHz	Kilohertz (1/T)
kyd	Kiloyard (L)
L	Length of Array (L)
MRA	Main Response Axis
MUX	Multiplexing
n	Index of Refraction
N	Number
NL	Noise Level
p	Pressure (F/L^2)
Pa	Pascal
PCM	Pulse Code Modulation
P(D)	Probability of Detection
P(FA)	Probability of False Alarm

PM	Phase Modulation
PPM	Pulse Position Modulation
PQM	Phase Quadrature Modulation
PSK	Phase Shift Keying
r	Range (L)
r_e	Ratio of Successive Array Element Spacing
r_L	Radial Distance from Center (L)
R	Array Element Spacing Ratio
RAP	Reliable Acoustic Path
RL	Reverberation Level (dB)
ROC	Receiver Operating Characteristic
SL	Source Level (dB)
SOFAR	Sound Fixing and Ranging
SSB	Single Side Band
T	Temperature
t	Time (T)
TDM	Time Division Multiplexing
TL	Transmission Loss (dB)
TS	Target Strength (dB)
W	Bandwidth
XBT	Expendable Bathythermograph
α_R	Angle
α	Absorption Coefficient (dB/kyd)
α_S	Percent Sound Speed Error
β	Angle
ε	Error or Difference
λ	Wavelength (L)
λ_o	Wavelength of Array Design Frequency (L)
θ	Angle
μPa	Micro Pascal
π	3.1415927
ϱ	Mass Density (FT^2/L^4)
σ	Coherence of Noise
τ	Time Interval (T)

CHAPTER I
SONAR FUNDAMENTALS

1.0. INTRODUCTION

According to Webster's New Collegiate Dictionary, sound is "mechanical radiant energy transmitted by longitudinal waves in air or other material media"; sonar is the acronym for "sound navigation and ranging." Sound waves cause pressure changes and particle motion in the medium. Although either pressure or particle velocity can be used to excite sonar sensors, pressure is most commonly employed.

Sound is the only form of energy capable of penetrating the sea to appreciable distances; other forms, such as radio waves and light, are subject to attenuation that is several orders of magnitude greater than that of sound in sea water. Therefore, anv underwater system designed to perform a function over great distances in the ocean uses sound as its basic energy source.

1.1. APPLICATIONS

Military applications of sound by the Navy include systems that operate in frequency ranges from less than one to many thousands of Hertz. At the low end of this spectrum is the pressure mine, which responds to the reduction of pressure on the sea floor when a vessel is overhead. The signature of the vessel, which is well below 1 Hz, is not truly an acoustic disturbance. It is considered to be a hydrodynamic effect readily detected by the pressure sensor. Acoustic mines operate in the range of a few-to-tens of Hertz, where ships make a considerable amount of noise at frequencies so low that they are difficult to detect.

Passive surveillance sonars operate at low frequencies, where surface ships produce the maximum acoustic output and long ranges are possible. Active echo ranging sonars for submarine detection operate at higher frequencies because of the required array and transducer size, target reflection, and reverberation.

Because of their small size, acoustic homing torpedos use still higher frequency bands to obtain directional information from the relatively small front end of the array. Sonars for detecting small objects or defining the shapes of submerged bodies require even higher frequencies. These systems operate at such extremely high frequencies in order to obtain the narrow beams and short pulse lengths required to reduce the reverberation accompanying echoes from a mine on the ocean floor.

Non-military uses for sound and sonar include (1) depth sounders (the oldest and still the most important device), (2) beacons, (3) transponders, (4) sonar release mechanisms, (5) fish finders, (6) counters and trackers, and (7) telemetry systems that use acoustic beams instead of wire links. Because these and other such devices must be physically small and need not operate over the great distances required for military purposes, they employ frequencies in the kilohertz ranges. Figure 1.1 is a graphic presentation of the acoustic spectrum and shows the uses of the various frequency bands.

1.2. ACOUSTIC UNITS

Although sonar sensors are usually pressure sensitive, sonar calculations are made in terms of *intensity*, which is defined as sound power per unit area. It is proportional to the square of

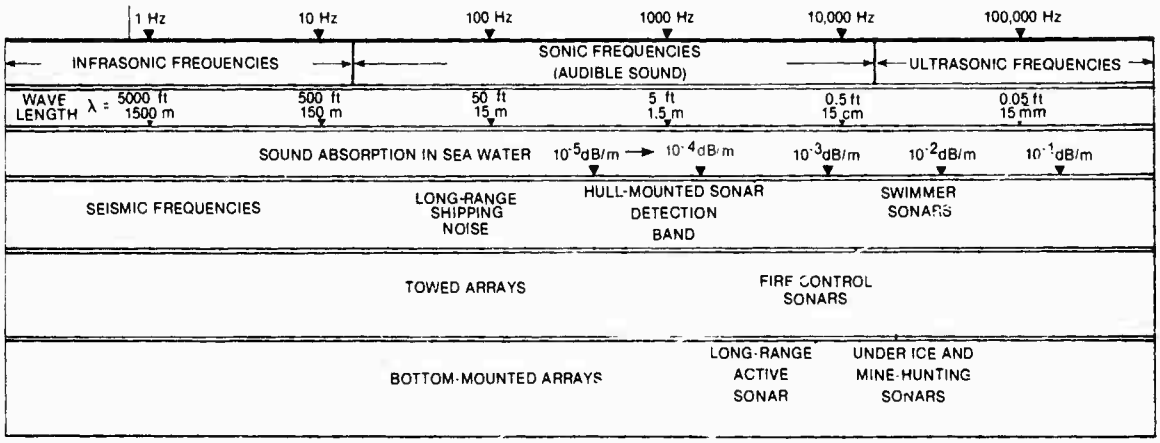

Figure 1.1. Acoustic Spectrum

the pressure in accordance with the expression

$$I = p^2/\varrho c,$$

where the proportionality factor ϱc is the product of the density and sound speed of the sea water medium.

Logarithms of the ratios of intensities, expressed in decibels, are used for sonar calculations instead of linear numbers. Thus,

$$\text{Decibels} = 10 \log (I/I_{ref}),$$

where I is the intensity of a sound wave and I_{ref} is the intensity of a reference wave. The reference wave is assumed to be a plane wave of root-mean-square pressure equal to 1 μPa. The level of a sound wave is the number of decibels that define it. For example, a sound wave having an intensity 100 times greater than that of the reference wave (and therefore a pressure 10 times greater) would have a level of 20 dB//1 μPa. All sonar calculation results are expressed in decibels because it permits the multiplication of quantities by adding the decibel equivalents; this was a great advantage before the pocket calculator became available, and still is.

(FOR MORE INFORMATION CONCERNING *Acoustic Units refer to Albers, 1960; Beranek, 1954; Horton, 1959; Kinsler and Frey, 1962; Officer, 1958; Urick, 1975.*)

1.3. PROPAGATION OF SOUND IN THE SEA

The level of sound radiated from a source in the ocean is attenuated by spreading and other processes such as absorption, scattering, and diffraction. Spreading causes the weakening of intensity as the radiated energy is dispersed over an area that increases with distance. Scattering, diffraction, and absorption weaken the signal by removing energy from the acoustic beam. Scattering and diffraction result in the redistribution of sound in the sea; absorption is the loss of sound to heat. Transmission loss (TL) is used to express the sum of these attenuation losses, i.e.,

$$TL = 10 \log (I_1/I_r),$$

where I_1 is the intensity 0.9 m (1 yd) from the source and I_r is the intensity at r yd. Although TL is a positive number of decibels (since I_1 is always greater than I_r), it appears with a negative sign in sonar equations because it is a loss.

1.3.1. SPREADING

Two types of spreading that occur are spherical and cylindrical (see figure 1.2). Spherical spreading occurs when the sound spreads uniformly over a sphere (or hemisphere)

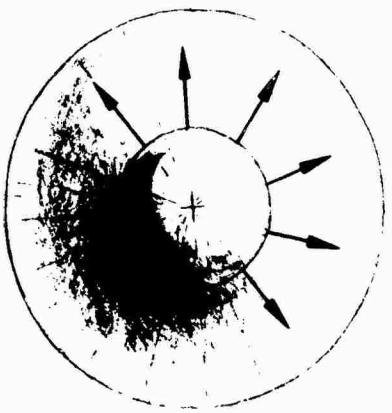

Figure 1.2a. Free Field: Spherical Spreading

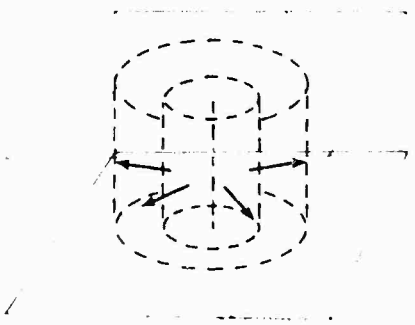

Figure 1.2b. Ducts: Cylindrical Spreading

Figure 1.2. Spherical and Cylindrical Spreading

that expands with distance. Since the area of such a sphere increases as the square of r, the intensity (energy/area) varies as $1/r^2$ and, therefore,

$$TL = 20 \log r + c.$$

Cylindrical spreading occurs when the sound spreads uniformly over a cylinder (or half cylinder) that expands with distance. Because the area of such a cylinder increases as the first power of r, the intensity (energy/area) varies as $1/r$ and, therefore,

$$TL = 10 \log r + c.$$

Cylindrical spreading occurs in a sound channel duct beyond the range at which the duct is said to be *full* of sound.

1.3.2. ABSORPTION OF SOUND IN THE SEA

A major attenuation component affecting TL is absorption; it represents a conversion of sound to heat that causes a loss. Since the amount of intensity lost to heat for a given distance is proportional to the original intensity, the TL (measured in decibels) increases linearly with range. Therefore, absorption is subject to a different range law than is spreading. Combining the two losses yields

$$TL = 20 \log r + \alpha r \times 10^{-3},$$

where α is the absorption coefficient in dB/kyd and r is expressed in yards.

The absorption coefficient, α, generally increases as the square of the frequency, except for some flatter portions of the spectrum where changes in basic physical processes occur. Figure 1.3 shows values of α versus frequency at

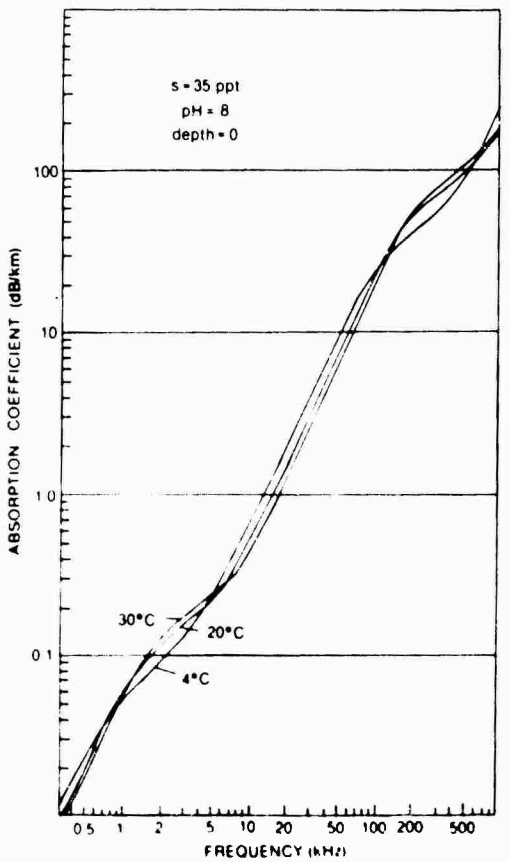

Figure 1.3. Absorption Coefficient versus Frequency

zero depth (i.e., at the surface) for various temperatures. As can be seen, α is generally less (by a factor of approximately 2 in the 5 to 50 kHz range) in warm water than in cold water. Therefore, sonar systems operating at frequencies where α is appreciable are likely to achieve greater ranges in warm waters.

The processes responsible for the absorption of sound in sea water are ionic-relaxation mechanisms involving two of the many salts in the ocean. They are boric acid (H_3BO_3), which influences the range below 1 kHz and magnesium sulphate ($MgSO_4$), which influences the 1 to 100 kHz range.

The absorption coefficient decreases with increasing depth. Figure 1.4 shows the fraction of the surface value as a function of frequency at two temperatures for depths of 3 and 6 km (3.3 and 6.6 kyd). As can be seen, the effect is significant; deep paths in the sea suffer only a fraction of the absorption loss encounted by paths near the surface.

The plot in figure 1.3 should not be extrapolated below the frequencies shown because there is evidence that α flattens out with frequency at the low end. This occurs in the region of 0.003 dB/kyd for reasons that are not yet understood.

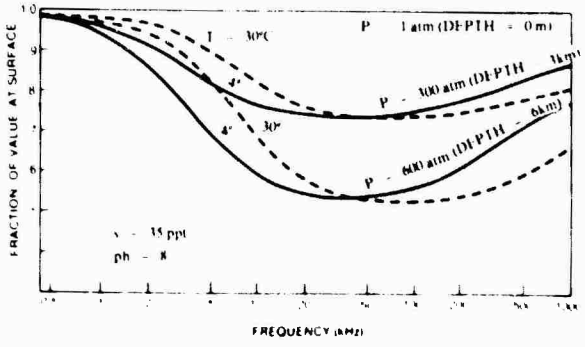

Figure 1.4. Decrease of Absorption Coefficient with Depth

1.3.3. SPREADING, ABSORPTION, AND ACHIEVABLE RANGES

The losses mentioned so far account for the total loss under many conditions and serve as a guide for predicting average loss when there is no interest in special circumstances and the range is not too great. Spherical spreading predictions apply up to ranges where multipath propagation effects begin to be important, at high angles to the horizontal (for bottom bounce sonars), and in (rare) isovelocity water. Such spreading even exists in ducts when the trapping of sound is compensated for by leakage of sound. Thus,

$$TL = 20 \log r + \alpha r \times 10^{-3}$$

is a useful approximation under the above conditions.

Therefore, if α is assumed to be 10 dB/kyd, the spreading loss out to 1 kyd (0.9 km) is approximately 60 dB and the absorption loss is only about 10 dB. However, between 9 and 18 km (10 and 20 kyd) the loss becomes, respectively, 6 and 100 dB showing that attenuation, not spreading, is the major limitation on long-range sonars at high frequencies. Attenuation effects at normal ranges are negligible on passive detection and surveillance sonars because they operate in the frequency range of a few hundred Hertz.

The importance of absorption in limiting range is demonstrated by the following: Since,

$$TL = 20 \log r + \alpha r \times 10^{-3}$$

then (note that 20 log e = 8.67), by taking differentials,

$$d(TL)/dr = 8.67/r + \alpha \times 10^{-3}.$$

The rates of absorption loss and spreading loss are, therefore, equal at a range where

$$8.67/r = \alpha \times 10^{-3}.$$

or

$$r_c = 8.67/(\alpha \times 10^{-3}).$$

Beyond this range, absorption dominates. Transmission loss caused by absorption is

$$A = \alpha r \times 10^{-3} \text{ dB}$$

and, hence,

$$r = A/(\alpha \times 10^{-3});$$

therefore, if we let r_{10} be the range at which $A \approx 10$ dB, then

$$r_{10} = 10/(\alpha \times 10^{-3}),$$

Figure 1.5 shows this range as a function of frequency. It illustrates that high frequency sonar systems experience high attenuation at much shorter ranges than low frequency systems.

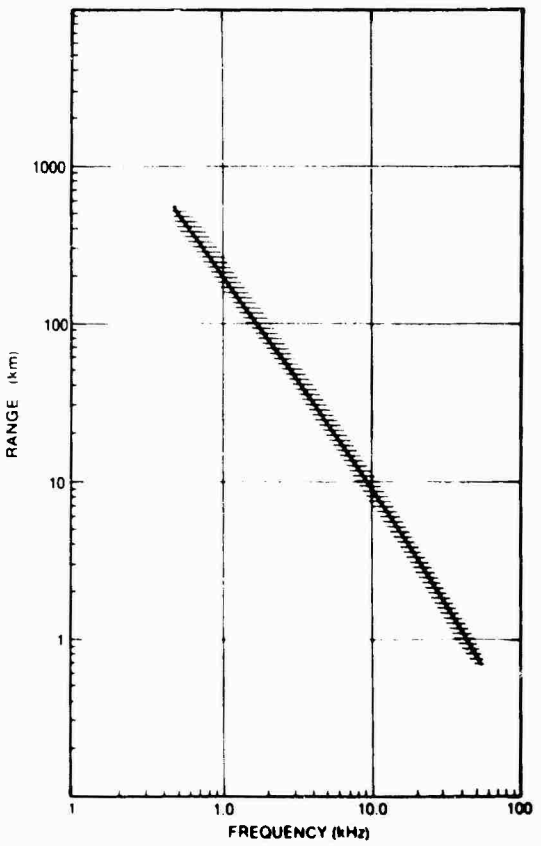

Figure 1.5. Range at which Absorption Approximates 10 dB

1.3.4. IRREGULAR SPREADING

The sea is inhomogeneous and the speed of sound varies with location. Therefore, the sound emitted by a source is distributed irregularly into areas of high acoustic intensity such as convergence zones, caustics, and focusing regions and areas of low intensity such as shadow zones.

1.3.5. REFRACTION AND RAY BENDING

The variation of the sound speed with depth in the sea is termed the *sound speed profile*. This speed-depth function is extremely important in modifying the simple spreading laws described above and in determining the sound field at a distance.

The speed of sound in sea water is determined by temperature, salinity, and depth; it increases when any one of these factors increases. Although only three variables influence speed, the relationship is very complicated. A simple formula for calculating speed is

$$c = 1449 + 4.59T - 0.053T^2 + 0.0163D,$$

where

c = speed of sound (m/sec),
T = temperature in degrees centigrade, and
D = depth in meters.

This expression gives the speed of sound in meters per second to one part in a thousand. Salinity is not considered here because, compared with temperature, it is a negligible factor; expressions that include salinity are available.

Speed is generally determined by using a bathythermograph (BT) to measure T as a function of D. Figure 1.6 shows a cutaway view of the expendable bathythermograph (XBT) that is deployed by surface ships. The XBT employs a thermistor bead that senses temperature changes through changes in the electrical resistance. The signal is communicated to the ship via a fine wire as the instrument descends at a known rate of speed. A similar instrument, the BT-AN/SSQ-36, is deployed by aircraft in the same manner as that used to drop sonobuoys.

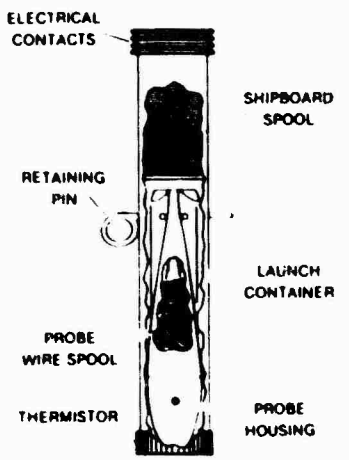

Figure 1.6. Cut-Away View of XBT

Sound speed profiles have been determined for many locations in the oceans using various equipment, including velocimeters for direct measurements. It can be seen in figure 1.7, which shows typical speed profiles for two latitudes, that speed decreases with depth at shallow depths (*negative gradient*) and increases with depth at deep depths (*positive gradient*). This is because the temperature decreases at shallow depths and the speed increases with depth in the deep isothermal layer. This reversal of gradient results in a *depth of minimum speed*, to which sound is continuously returned as it propagates outward from its source because of downward refraction in the negative gradient above, and upward refraction in the positive gradient below. Figure 1.7 also shows that the depth of minimum speed is shallower at the higher latitudes until, eventually, it is just beneath the ice in the Arctic Ocean.

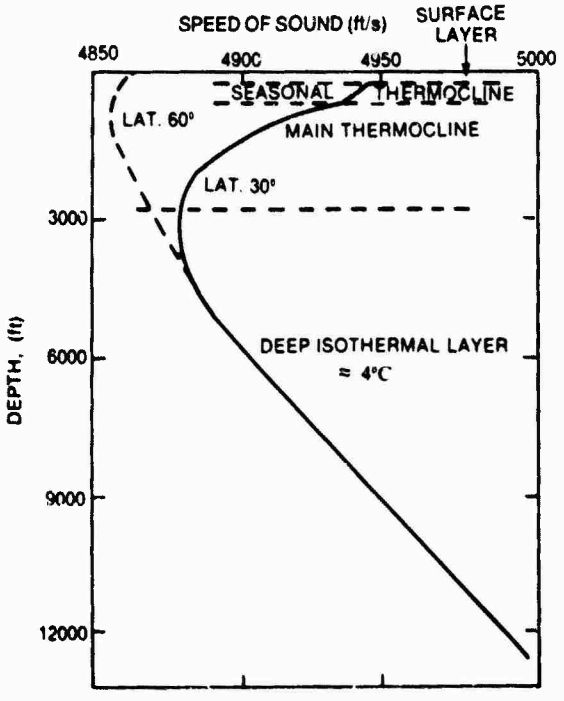

Figure 1.7. Sound Speed Profiles at Two Latitudes

The shallower portion of a speed profile shows daily, seasonal, and ephemeral changes and is, of course, highly variable. Therefore, sonar systems that employ near-surface propagation paths are subject to such vagaries while those that use deep source paths are not.

1.3.6. SNELL'S LAW AND RAY TRACING

If a sound speed profile is divided into layers and the speed is assumed to be constant in each one, the sound is refracted according to Snell's Law when traveling between layers. A simple derivation of this law for two layers of constant speed separated by a plane is presented in figure 1.8.

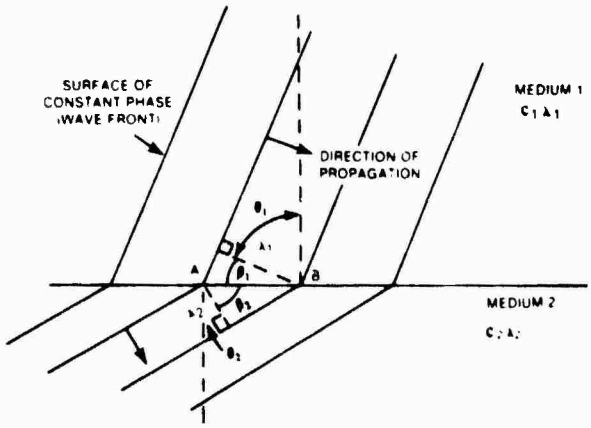

Figure 1.8. Derivation of Snell's Law

This relationship provides the basis for ray-trace computer programs where successive rays begin at the source at pre-set vertical angles and are traced from layer-to-layer to the range desired. Horizontal changes in water depth and speed profile are readily accommodated by such programs. A ray-trace diagram provides a visualization of the sound and, by measuring the vertical distance between rays at a particular point, the spreading loss.There are normal mode and wave-theory programs that are more sophisticated and general than is the ray-trace program, but none is as visually effective.

1.3.7. SURFACE DUCT

A surface duct develops when the near surface waters become mixed by wind-caused turbulence and an isothermal layer is produced. The layer is characterized by a positive gradient because of the depth effect on speed. The sound travels outward from the source in a succession of upward arcs that repeatedly encounter the surface of the sea (see figure 1.9a). There is a shadow zone below the layer into which only weak diffracted and surface-scattered sound can penetrate. When the mixed layer is absent (see figure 1.9b) the shadow region extends all the way to the surface. This shadow, cast by the surface, is not *acoustically black* (i.e., devoid of sound from the source), but the sound within it is weak and incoherent.

When the duct is thick and the surface calm, the surface duct provides an excellent low-loss channel for long sonar ranges. But when the duct is thin or not well developed, or the sea surface rough, the surface duct is subject to excessive losses. When the surface duct is *lossy* (i.e., characterized by high losses caused by poor reflection from a rough sea surface), or absent, long ranges can be reached only by bouncing the sound signal off the bottom. The layer depth and wind speed determine the quality of surface duct transmission.

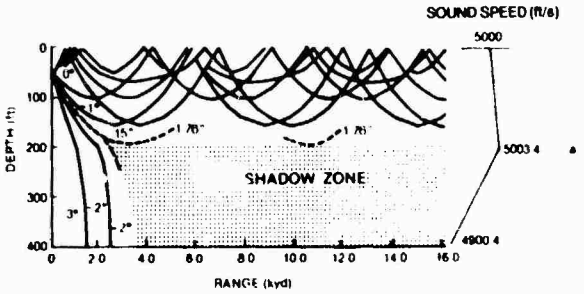

Figure 1.9a. Surface Duct Present

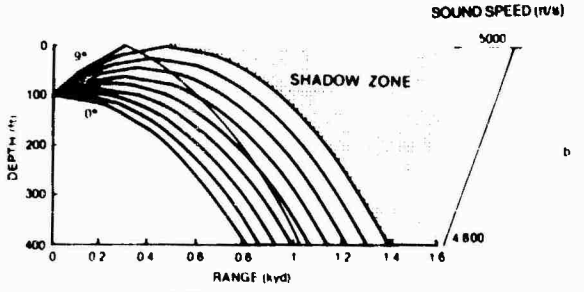

Figure 1.9b. Surface Duct Absent

Figure 1.9. Ray Diagrams

1.3.8. DEEP OCEAN DUCTS AND CONVERGENCE ZONES

Because of the characteristic sound speed profile of the deep ocean, sound rays from a deep source form a series of downward and upward arcs. These refracted paths carry sound out to great distances with little loss beyond that caused by spreading and absorption. Figure 1.10 shows ray diagrams for three source

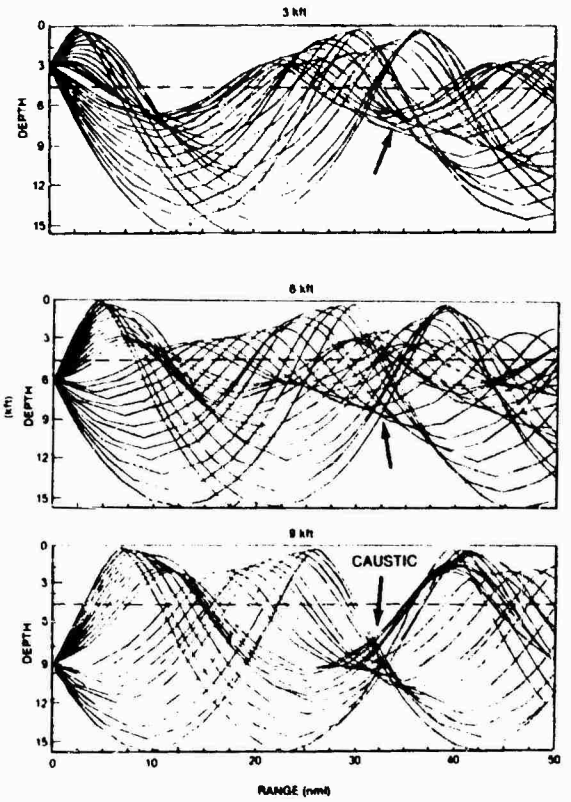

Figure 1.10. Ray Diagrams at Three Depths in the Deep Ocean Duct

depths. When the source is at the depth of minimum speed, indicated by the dashed line, transmission is good. A long-range shot is received as a crescendo of sound that reaches maximum and abruptly stops. Such a signal is known as a sound fixing and ranging (SOFAR) transmission, which refers to an acoustic technique for aviation-rescue that triangulates on a short, received signal. In addition to the refracted rays shown in figure 1.10, bottom and surface refracted rays exist that complicate the diagrams; however, they do not carry ap-

preciable amounts of sound to long ranges because of surface and bottom losses. The arrows in figure 1.10 denote caustics, i.e., areas where the sound is concentrated.

The deep ocean duct acts as a lens. It creates convergence zones (CZs) and shadow zones in which, respectively, the received intensity is greater or less than elsewhere. When both source and receiver are at a shallow depth, rays that have undergone one refraction at a deep depth converge. This region is known as the CZ or first CZ, since they repeat themselves at regular range intervals. Figure 1.11 shows two adjacent CZs between 60 and 70 km (68 and 78 kyd) at the surface; they merge into one zone when the source is at the surface. In order for a CZ to exist, the speed profile must extend to a depth (the critical depth) where the speed is the same as that at the depth of the source; that is, the water must be deeper than the critical depth.

Figure 1.12a shows the surface temperature and water depth required for the existence of a CZ. Figure 1.12b shows that the range to the CZ is also determined by surface temperature. For mid-latitudes, the CZ is a circular-band approximately 5 to 8 km (5.5 to 9 kyd) wide surrounding a source at a distance of 35 to 60 km (38 to 63 kyd) (figure 1.12b), where transmission loss tends to be 5 to 15 dB less than when there is no zone. Thus, targets transiting a zone are readily detectable for short periods. The short detection times are the result of the narrow range width of the zone.

1.3.9. SHALLOW WATER

Shallow water in the ocean is considered to be waters of depth of less than 200 m (100 fm). There are many such areas including those off the coast of the U.S.S.R., the United Kingdom, Argentina, and Southeast Asia.

Sound propagation is variable and unpredictable in shallow water. It is often good out to a few nautical miles because the sound is trapped and cylindrical spreading or bottom focusing applies, but it becomes poor at longer ranges because of boundary losses. In shallow water, sound travels outward from a source by repeated encounters with one or both of the lossy boundaries. The method for predicting transmission loss at high frequencies and short ranges is the same as for deep water areas. At lower frequencies, out to ranges reached by surveillance sonars, the transmission loss is generally unpredictable because it is influenced by sea state, speed profiles, fish population, and bottom characteristics.

1.3.10. TRANSMISSION LOSS IN DUCTS

Transmission loss in a duct can be expressed as

$$TL = 10 \log r + 10 \log r_o + (\alpha + \alpha_L) r \times 10^{-3},$$

where

r = range,
r_o = range where duct is full of sound and cylindrical spreading begins,
α = ordinary absorption coefficient (dB/km), and
α_L = duct leakage coefficient (dB/km).

For a particular duct, r_o can be crudely estimated from a ray diagram but α_L must be derived from field data. There is a cutoff frequency below which any duct ceases acting as a duct and α_L becomes extremely high.

1.3.11. SEA SURFACE EFFECTS

The boundary of the sea exerts many, often profound, effects on the performance of sonar systems that operate at shallow depths near the surface (where many U.S. Navy systems operate). Among these effects are that the sea surface:

1. Causes a reflection loss for sound that is incident upon it. The loss is 2 to 3 dB at frequencies near 24 kHz and essentially 0 dB below 1 kHz. It is a function of sea state, increasing at higher states.
2. Scatters sound, causing the principal loss in surface ducts.
3. Reflects scattered sound back toward the source, causing surface reverberation.
4. Causes interference with the direct sound, which creates the Lloyd Mirror Effect when the sea is not too rough and the frequency not too

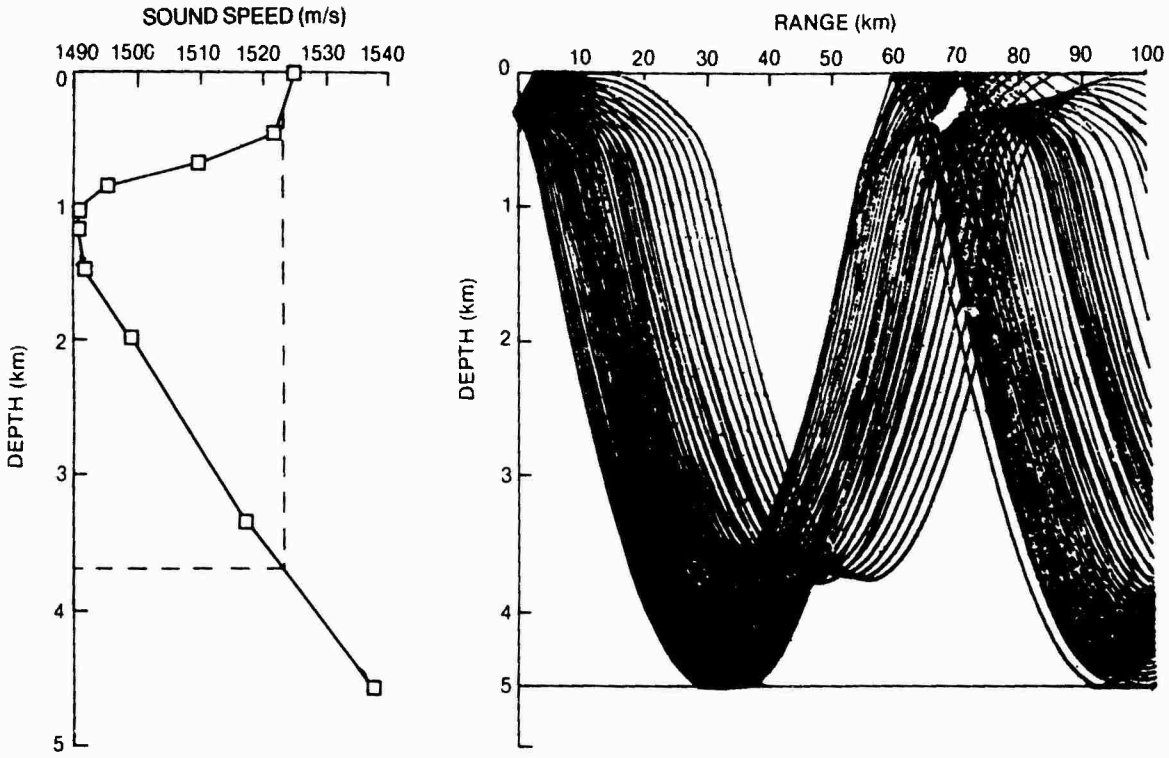

Figure 1.11. Sound Speed Profile and Ray Diagram Showing CZs

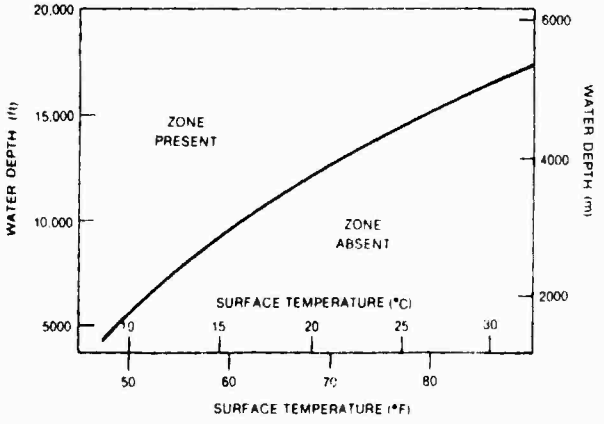

Figure 1.12a. Conditions for Existence of a CZ

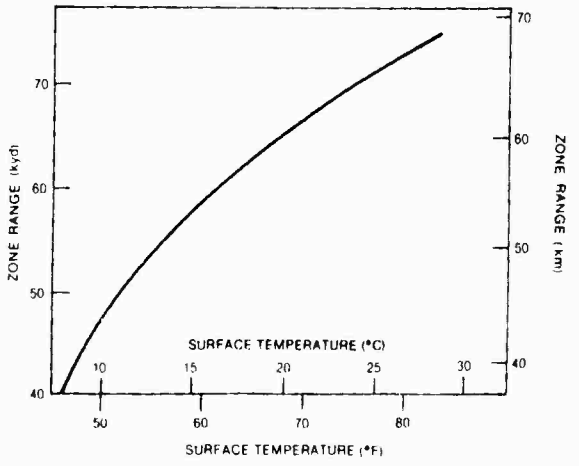

Figure 1.12b. Range to CZ versus Surface Temperature

Figure 1.12. Conditions for the Existence of a CZ, and Range to CZ versus Surface Temperature

high.

5. Creates a shadow zone when a negative gradient exists near the surface.

6. Imposes its own motion, exhibited as modulation side bands, on continuous wave sinusoidal incident sound waves.

7. Affects reverberation and transmission via the bubbly layer beneath it.

8. Makes noise; it is the principal source of ambient noise in the absence of shipping.

9. Reduces the output of a shallow source when it is less than ¼-wavelength below the surface.

10. Causes platform motion that influences operator performance and requires that surface ship beamformers be stabilized.

1.3.12. BOTTOM EFFECTS

The sea bottom also has a great influence on sonar performance and has the following characteristics:

1. It is lossy, i.e., is subject to a loss of as much as 30 dB, which greatly affects bottom bounce sonar propagation. Figure 1.13 presents typical bottom loss versus grazing angle curves. Ocean charts normally accompany the curves (the charts are classified) to show the area in which they are applicable.

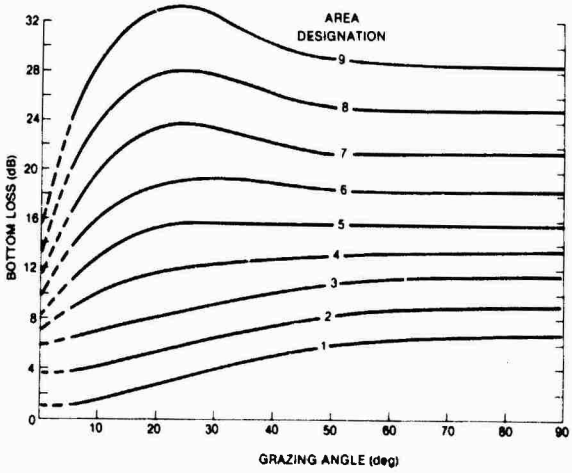

Figure 1.13. Typical Bottom Loss Curves (1 to 4 khz)

2. Although its characteristics vary, it provides less acoustic discontinuity than the sea surface so that sound can easily enter; this results in the losses described.

3. It is penetrable to great depths and distances by low frequency sound, which may enter it and then be refracted back into the water.

4. It is stationary, exhibiting none of the motional effects of the surface.

5. It is more variable in its properties than the surface, often changing suddenly over short distances.

6. It is difficult to access and therefore a less well known boundary than the sea surface.

(For more information concerning *Propagation of Sound in the Sea* refer to *Albers, 1960; Brekhovskikh, 1960; Fisher and Simmons, 1977; Greenspan and Tschiegg, 1959; Hale, 1961; Horton, 1959; Leroy, 1969; Marsh and Schulkin, 1962; NDRC, 1969; Officer, 1958; Schulkin, 1962; Tolstoy and Clay, 1966; TRACOR, 1965; Urick and Hoover, 1956; Urick, 1975; Urick, 1965; Urick, 1963; Webb and Tucker, 1970; Weinberg, 1979.)*

1.4. AMBIENT NOISE IN THE SEA

The term *ambient noise* refers to the prevailing noise background in the sea that is not associated with the hydrophone or its platform. Table 1.1 lists the major causes and spectral characteristics of ambient noise over the 1 Hz to 50 kHz frequency range.

Table 1.1 Sources of Ambient Noise in the Deep Sea

Frequency Range (Hz)	Source	Spectral Slope dB/Oct	Remarks
<1	Tides, Seismic Unrest, Waves	Variable	Little known tides cause Tones in Spectrum
1 to 20	Surface Waves	-8 to -10	Recent Investigations
20 to 500	Shipping	3 to -6	Strong in Ship Lanes
500 to 50,000	Sea Surface	-5 to -6	Well Defined Levels Process of Generation Uncertain
> 50,000	Thermal Agitation	6	

1.4.1. WIND AND SHIPPING NOISE

Wind and shipping noise are the two most important ambient noise sources. Wind noise originates locally at the surface and pours down, like rain, on hydrophones in the sea, whereas shipping noise originates at a distance, often at ranges of hundreds of miles.

Figure 1.14 shows the idealized average spectra of ambient noise in deep water. Note that shipping noise dominates the spectrum out to a few hundred Hertz and then wind noise predominates. Table 1.2 summarizes wind and shipping noise characteristics.

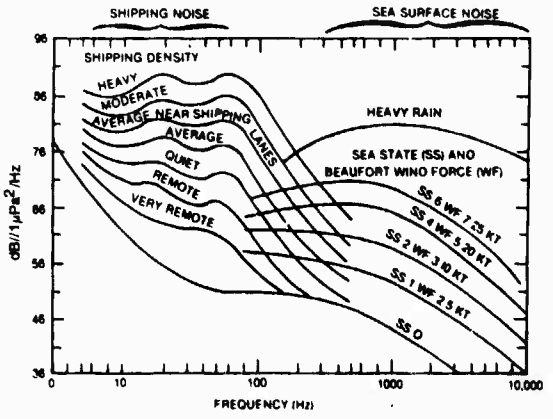

Figure 1.14. Typical Deep Water Ambient Noise Spectra

Table 1.2. Summary of the Characteristics of the Two Principal Types of Ambient Noise

Shipping Noise	Wind Noise
Originates in distant shipping.	Originates locally on the sea surface.
Dominant at low frequencies (100 Hz and below in deep water).	Dominant at high frequencies (1000 Hz and above).
Travels over deep refracted and reflected paths.	Travels over direct paths.
Is not dependent on wind speed.	Is wind-speed dependent at the rate of 6 dB/wind speed doubled.
Arrives primarily from low angles. Time delay correlograms show a peak near zero time delays.	Arrives primarily from high angles. Time delay correlograms show a peak at time delays corresponding to upward angles between 45° and 80°.
Is relatively unimportant in shallow water except for nearby ship sources.	Tends to dominate the spectrum in shallow water when identifiable ship traffic and biological noise sources are absent.

1.4.2. AMBIENT NOISE CHARACTERISTICS

Ambient noise decreases with depth. The quietest place in the water column is at or near the deep sea bed where refraction and bathymetric shielding provide a natural screen for long-range shipping noise. Conversely, the noisiest place is in the surface duct, which acts as a trap for noise and signals.

Another important characteristic of ambient noise is its azimuthal and vertical directionality. In azimuth, directionality depends upon the distribution in bearing of distant shipping noise about the receiving array. In the vertical, shipping noise is received horizontally and wind noise vertically. It is only when shipping and wind noise are equal that the ambient noise background is approximately isotropic.

1.4.3. BIOLOGICAL NOISE

Various biological sounds emanating from soniferous fish, whales, and snapping shrimp contribute to the ambient noise background at many locations. Such noise is an intermittent and, often, severe source in shallow water. All sorts of squeaks, moans, groans, chirps, and roars occur in biologically active waters. Also, in warmer waters over hard rough bottoms, snapping shrimp make a persistent high frequency sound by rubbing their claws together; this noise degrades the performance of sonar systems that operate in the kilohertz band.

(For more information concerning *Ambient Noise in the Sea* refer to *Albers, 1960; Axelrod, 1965; Horton, 1959; NDRC, 1969; Officer, 1958; Tolstoy and Clay, 1966; TRACOR, 1965; Urick, 1975; Urick, 1966; Weinberg, 1979.*)

1.5. REVERBERATION

Reverberation is the backscattering of sound caused by various inhomogeneities in the sea. It is exhibited as a decaying, quivering blast of sound following the emission of a sonar generated noise signal. As in a room, reverberation in the sea is the result of the scattering back of sound toward the source.

1.5.1. CAUSES OF REVERBERATION

Figure 1.15 shows reverberation contributors measured using a nondirectional hydrophone to record the noise of a nondirectional shot source. The first major component is surface reverberation (point A) that originates at the surface and rapidly decays because of distance of travel, angle at the surface, and downward refraction. The decay is interrupted, or reversed, by a return from the deep scattering layer (point B) and then by bottom reflection (point C). The bottom return is usually multiple and has several peaks. The bottom reflected return is followed by bottom reverberations from the ocean floor (point D) and subsequent bottom reflections (not shown in the figure). Many of the influences can be reduced or eliminated by employing directional sonar systems. Such systems are subject only to reverberation from scatterers in the path of the sound beam.

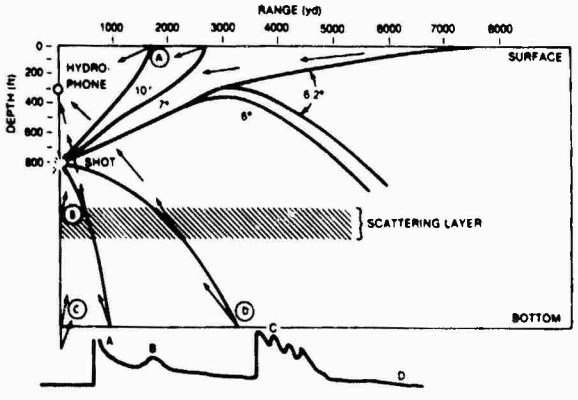

Figure 1.15. Reverberation Contributors

1.5.2. SCATTERING STRENGTH

The important oceanographic parameter in relation to reverberation is the scattering strength of a unit volume of sea water 0.765 m^3 (1 yd^3) or of a unit area of sea surface or bottom 0.836 m^2 (1 yd^2). This quantity is 10 times the log of the ratio of the backscattered intensity (referred to 0.9 m, or 1 yd) to the incident intensity. Its magnitude is determined by at-sea measurements.

The scattering strength of the deep scattering layer averages -70 to -80 dB; that of the sea surface increases with wind speed and grazing angle, averaging about -40 dB at low angles and a 10 knot wind speed. The scattering strength of the bottom, which varies with the type of bottom and increases with grazing angle, is approximately -30 dB for a sand bottom at a 10° grazing angle.

Scattering strength values are necessary for reverberation calculations. Their sum (in decibels) and the size of the reverberating volume or area (in dB//1 yd^3, or 1 yd^2) is a quantity similar to the strength of a sonar target. That is, it is the effective strength of the reverberation exhibited as unwanted noise in the signal reflected from the target.

1.5.3. DEEP SCATTERING LAYER

The deep scattering layer (DSL), where biological scatterers exist, creates much of the volume reverberation that degrades deep-water sonar system performance. The predominant scatterers are swim bladder fish below 20 kHz and plankton (e.g., siphonophores and shrimp) at higher frequencies.The DSL is characterized by a peculiar diurnal migration in depth; it rises to the surface at sunset and descends to a few hundred feet or yards at sunrise in all of the oceans of the world. The DSL is often the source of the reverberation accompanying echoes from targets in the first CZ when employing active sonar systems.

The influence of reverberation on active sonar performance depends on the power output of the system and prevailing oceanographic conditions. High power sonars are usually reverberation-limited; i.e., their echoes occur in a background of reverberation. Also, this is usually the case for all active sonars operating in shallow water because the surface and bottom are repeatedly encountered in propagation to a distant target and back.

(For more information concerning *Reverberation* refer to *Albers, 1960; Horton, 1959; Merklinger, 1968; NDRC, 1969; Officer, 1958; TRACOR, 1965; Urick, 1975; Weinberg, 1979.*)

1.6. DETECTION OF SIGNALS

The detection of a signal in a background of noise or reverberation is the most important, and the most difficult, function of sonar systems. Until the target is detected, other functions, such as classification and attack, cannot be accomplished.

1.6.1. SIMPLE DETECTION THEORY

In order to detect a signal in a background of noise, a *threshold* must be set, such that when it is exceeded a detection is made. The detection will be correct when a signal does indeed exist; it will be incorrect, i.e., a *false alarm*, when the threshold is exceeded by a noise spike instead of a true signal. There are two independent probabilities that the threshold will be exceeded for a given setting; they are the probability of detection (P(D)), in which it is exceeded by signal- plus-noise, and the probability of a false alarm (P(FA)), in which it is exceeded by noise alone.

The relationship between P(D), P(FA), and SNR is represented by the receiver operating characteristic (ROC) curves shown in figure 1.16. The parameter, d, of the family of curves is the required (signal + noise-to-noise) ratio for the output of the signal processor to detect

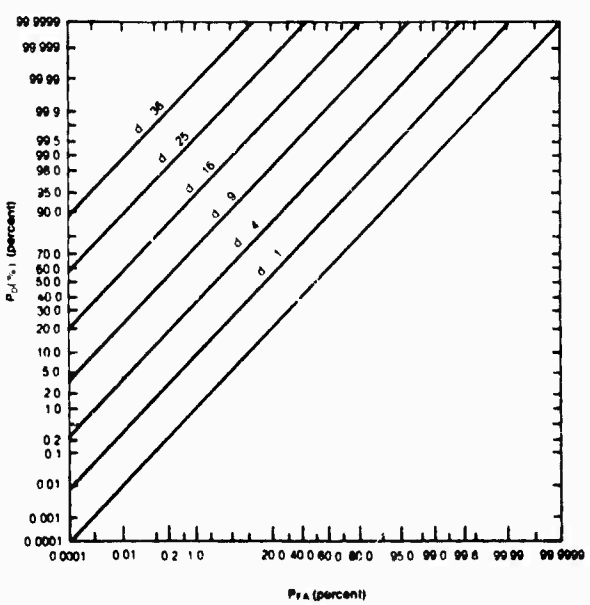

Figure 1.16. ROC Curves

selected probabilities. The required signal-to-noise ratio (SNR) at the input to the processor for a simple energy detector (i.e. one that squares and integrates the voltage at its input (see figure 1.17)) is given by

$$DT = 5 \log(dw/\tau),$$

where

w = bandwidth
τ = integration time

and DT is the detection threshold defined as 10 times the log of the signal power in the receiver bandwidth to the noise power in a 1 Hz band.

The DT is the SNR required at the array terminals to accomplish detection at the probability levels defined by the appropriate P(D) and P(FA) values using the selected bandwidth and integration time. Thus, SNR is the key factor in detection.

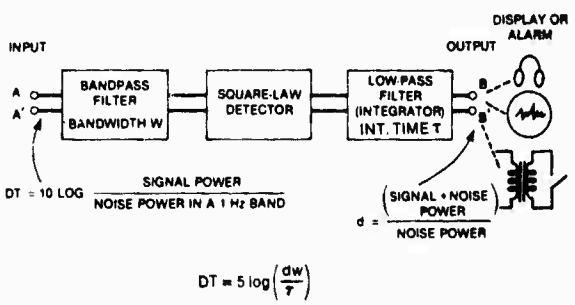

Figure 1.17. Elemental Energy Detector

1.6.2. ESTIMATED DETECTION THRESHOLD

The first step in estimating the DT is to select a desired P(D) and a tolerable P(FA) (which is usually very small, on the order of 10^{-4} to 10^{-6}). Then a value of d is taken from the ROC curves (figure 1.16) and DT is calculated using the above equation; the pre-detector bandwidth, w, and the post-detector integration time, τ. Corrections are usually required to this calculation to compensate for signal fluctuations, small correlation-length bandwidth products, and multiple signals.

(For more information concerning *Detection of Signals* refer to *Allen and Westerfield, 1964; Jeffress, 1967; Lawson, 1950; NDRC, 1969; Swets, 1954; Urick, 1975; Woodward, 1953.*)

1.7. SONAR EQUATIONS

Sonar equations are the relationships between certain quantities termed *sonar parameters*, which depend upon the ocean medium (i.e., propagation, ambient noise, and reverberation), the target, and the system and platform employed. Sonar parameters provide convenient categories for the inclusion and quantification of the numerous and diverse effects of underwater sound. The sonar parameters are the

1. source level (SL) of the target for passive sonars and the projector for active sonars,
2. transmission loss (TL),
3. target strength (TS), which is the ratio (in decibels) of the echo intensity (at 0.9 m (1 yd) from the target) to the incident intensity,
4. noise level (NL), which is measured by a nondirectional hydrophone and expressed in a 1 Hz bandwidth (this includes the sum of ambient and own ship noise),
5. array gain (AG), which is the improvment in SNR produced by a sonar array,
6. reverberation level (RL), which is the level of a plane wave that produces the same output as the reverberation noise, and
7. detection threshold (DT), which is the SNR at the array terminals required for detection.

Applying these parameters to the sonar equations we have, for passive sonar,

$$SL - TL = NL - AG + DT;$$

for active sonar (noise background),

$$SL - 2(TL) + TS = NL - AG + DT;$$

and for active sonar (reverberation background),

$$SL - 2(TL) + TS = RL + DT.$$

The desired parameters are solved for in terms of known parameters. For example, parameters such as SI (active), NL, and AG are selected in terms of the desired capability (i.e., DT, range (TL), ambient conditions (RL), target chacteristics (SL (passive) or TS (active)). The *best* compromise solution for a system design is obtained by applying the equations using a trial-and-error method. The medium parameters (TL (the only one for which range is a factor), NL (ambient), and RL) are solved for when predictions are desired for a particular system. The equations may also be used to solve for target parameters such as SL (passive) and TS when the other parameters are known.

(For more information concerning *Sonar Equations* refer to *Albers, 1960; Horton, 1959; NDRC, 1969; Officer, 1958; TRACOR, 1965; Urick, 1975; Urick, 1962.*)

1.8. BEAMFORMING

Beamforming is the process of listening to or transmitting sound from an array at selected angles. It reduces the unwanted noise at the processor by amplifying the signals arriving from the selected angle and provides bearing and depression/elevation (D/E) angle information concerning the target.Beamforming is used in the transmit mode to reduce the power required by concentrating it in the direction of the target and narrowing the illuminated sector to decrease unwanted reverberations and echoes from targets that are not of interest.

The basic beamforming process is as follows:

1. If the hydrophone elements of an array such as that shown in figure 1.18 are spaced at a distance, d_h, and a pure tone signal arrives at an angle θ from point, A, it will arrive at each element in turn as shown in figure 1.19. The time delay between arrivals is

$$\Delta T = (d_h \sin \theta)/c.$$

2. If the signals are delayed by the proper time delay, i.e.,

H - 1 by $3\Delta T$,
H - 2 by $2\Delta T$,
H - 3 by $1\Delta T$,

and

H - 4 by 0,

and then added, the sound arriving from angle θ is multiplied by a factor of four. Signals arriving from other angles will not be amplified as much. A plot of the amplification factor versus angle, i.e., a beam pattern, is shown in figure 1.20. It is characterized by a main lobe and side lobes separated by nulls or areas where the signal is very low. The angle subtended on the main lobe between the half-power, or -3 dB, down points is described as the beamwidth. If

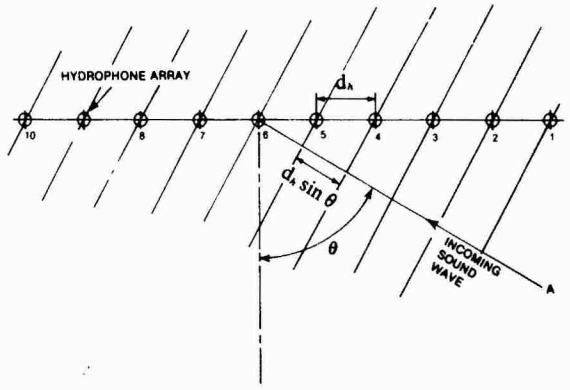

Figure 1.18. Sound Wave Striking Hydrophone Array

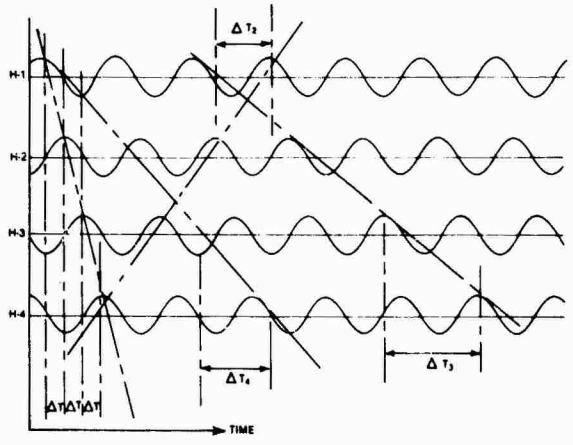

Figure 1.19. Signal Arrivals at Four Hydrophones

beams are formed at many angles, the arrival angle may be determined by finding the beam having the maximum signal.

In a similar manner, a beam of acoustic energy may be transmitted from an active array by timing the signal from each transducer. The phrase *principle of reciprocity* refers to the fact that beamforming calculations are the same for active and passive sonar arrays. The principle, enunciated by Helmholtz, is sometimes referred to as the *Helmholtz Reciprocity Principle*. It states that the location of a source (active transducer) and of a field point (hydrophone) can be interchanged without altering the pressure measured at the field point. More simply, sound acts the same when traveling in either direction.

It is apparent that for time delays other than the appropriate one for angle θ (i.e., ΔT_2, ΔT_3, or ΔT_4), the arrival angle will also be characterized by amplified signals. If the side lobes equal the main lobe, they are known as grating lobes. Grating lobes may be eliminated by spacing the hydrophones closer than $\lambda/2$ (in which case the configuration approximates a continuous line array) or by spacially shading the array (this will be discussed later).

The simple array of single hydrophones described above is axially symmetrical so that the beam pattern formed is actually a rotation of the plot in figure 1.20 about the axis A-A. Therefore, a beam is shaped like a cone when viewed in three dimensions and the target may be anywhere on the surface of the cone.

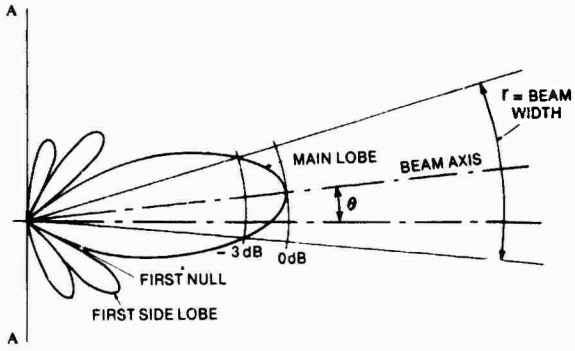

Figure 1.20. Example of Beam Pattern

(For more information concerning *Beamforming* refer to *Applied Hydro-Acoustics, Inc., 1976; Horton, 1959; King, et al., 1960; TRACOR, 1965; Von Winkle, 1963.*)

1.9. ARRAY CHARACTERISTICS

1.9.1. DEPRESSION/ELEVATION ANGLE (AREA ARRAYS)

The term *depression elevation* (D/E) refers to an angle that is depressed below or elevated above the horizontal plane. An area array, either flat plane, spherical, cylindrical, or conformal can provide (D/E) and azimuth angle and improve the SNR. It also eliminates ambiguities inherent in the line array beam patterns. The beams from area arrays, being formed in two directions, provide pencil beams for greater directional information and spacial discrimination against noise.

1.9.2. DIRECTIVITY INDEX AND ARRAY GAIN

The directivity index (DI) measures the directivity (D_R) of the array. Array directivity is the ratio of the power per unit solid angle radiated (or received) in the direction of the maximum amplitude pattern to the average radiated power per unit solid angle. It is usually defined as the number of decibels above the decibel value of an isotropic radiator (receiver) whose directivity is unity. Therefore,

$$DI = 10 \log D_R.$$

When L (for a uniform line source) $>> \lambda$

$$D_R = 2L/\lambda \quad (\text{i.e., } DI = 10 \log 2L/\lambda).$$

The actual DI varies with L/λ for the continuous line array as shown in figure 1.21, but, for practical purposes, the approximation is sufficient to describe it. There is little change in directivity for small steering angles and it increases (figure 1.22) as the steering angle increases.

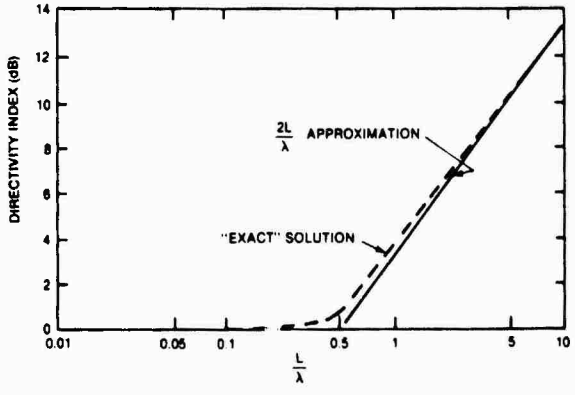

Figure 1.21. Directivity Index versus Frequency for Continuous Linear Array

Array gain is the improvement in the SNR of the array, i.e.,

$$AG = \text{signal gain (dB)} - \text{noise gain (dB)} = G_S - G_N$$

For a unidirectional signal in isotropic noise, AG = DI.

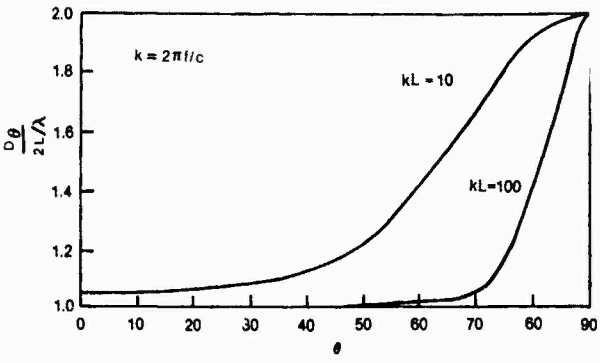

Figure 1.22. Increased Directivity with Increased Steering Angle

1.9.3. ARRAY SHADING AND SPACING

Shading the element responses and varying element spacing may be used to improve the main lobe and reduce the side lobes. Shading refers to increasing or decreasing the gain on any element signal before it goes to the processor. The total half-power, -3 dB beamwidth, for a simple, equally spaced line array is

$$BW_3 = 0.886 \lambda/L \text{ (in radians)}$$

or

$$50.8 \lambda/L \text{ (in degrees).}$$

A plot of the beamwidth versus array length for broadside and various steering angles is presented in figure 1.23.

Side lobes occur at angle θ when

$$(\pi L/\lambda) \sin \theta = \tan [(\pi L/\lambda) \sin \theta].$$

The roots of this equation are

$$(\pi L/\lambda) \sin \theta = 4.49, 7.73, \text{ and } 10.9,$$

$$\theta = \arcsin 4.49\lambda/\pi L, 7.73\lambda/\pi L,$$

or

$$10.9\lambda/\pi L.$$

One characteristic of the simple array, where the elements all have the same amplitude and phase, is the relatively great height of the first side lobe. Array element distributions can be formulated such that the side lobes are as low as desired.

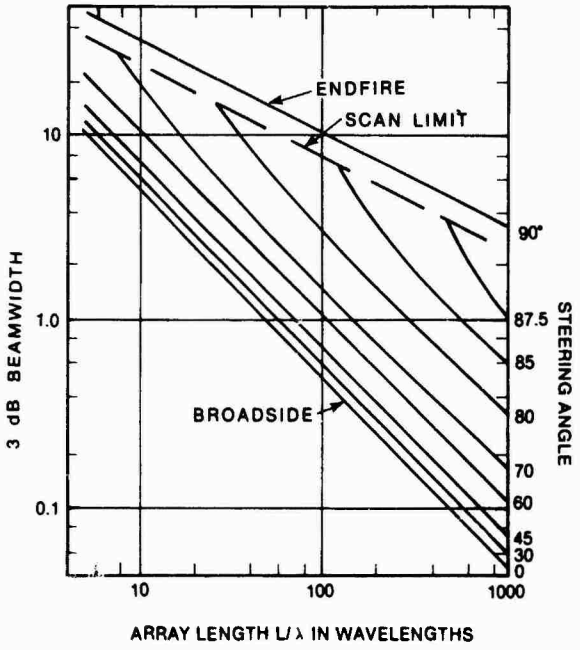

Figure 1.23. Beamwidth versus Array Length and Steering Angle

A gabled array is one in which the amplitude decreases uniformly from the central element to the ends. The first side lobe will have a height that is only 0.25 percent of the main beam height instead of the 5 percent height for the uniform array. A binomial array has a non-uniform distribution because the elements are weighted according to the coefficients of binomial expansions. The important characteristic of a binomial array is that it has no side lobes.

Among the various types of shading is Dolph-Chebyshev, which is non-uniform and provides the narrowest possible main lobe beamwidth for a specified side lobe reduction or the lowest side lobe reduction for a specified main lobe beamwidth. Taylor shading is a variation of Dolph-Chebyshev that produces lower side lobes outside of the center region. Cosine-on-pedestal shading also provides side lobe reduction. The disadvantage of side lobe reduction is that it broadens the main beam.

The side lobe level and beamwidth can also be controlled by varying the spacing of the elements. Element spacing may be geometrically tapered as in figure 1.24a. The ratio of the maximum spacing to the minimum spacing is defined as R and the common ratio of successive spacings is

$$r_e = R^{[1/(N-2)]},$$

where N = number of elements. An eleven element array designed for maximum resolution is shown in figure 1.24b, where the numbers indicate relative inter-element spacing. For some arrays, a statistical approach is used. The elements are randomly placed over an aperture according to a given distribution function.

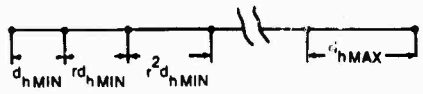

Figure 1.24a. Geometrically Spaced Tapered Array

Figure 1.24b. Minimum Redundancy Array

Figure 1.24. Varied Hydrophone Spacing

In general, the beam pattern function of a non-uniform array is characterized by a sharp main beam followed by a region of low side lobes, the *clean sweep region*, which is then followed by a region of moderately high side lobes, the *plateau region* (see figure 1.25).

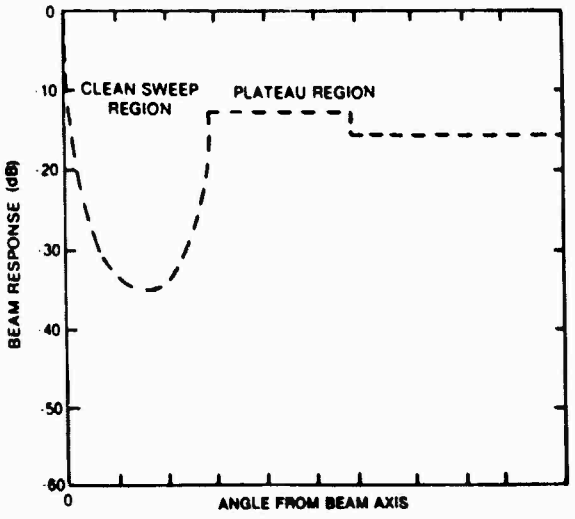

Figure 1.25. Non-Uniform Array Beam Pattern

The array gain of non-uniformly spaced arrays depends on the properties of the beam pattern and noise field. At low frequencies and isotropic noise,

$$AG \approx 10 \log 2L/\lambda.$$

At high frequencies, $L>>\lambda$, the gain achieves a value of

$$AG \approx 10 \log N,$$

where N = the number of elements.

Spacial tapering permits higher resolution or a significant reduction in the number of elements. It also permits a wider bandwidth, without grating lobes, and a very good first side lobe reduction.

(For more information concerning *Array Characteristics* refer to *Applied Hydro-Acoustics Research, Inc., 1976; Anderson, 1962; King, et al., 1960; Ishimaru, 1962; Tracor, 1965.*)

1.10. BEAMFORMER

The beamformer provides the proper time delays and shading of signals from the various hydrophones and sums them to form the input from the selected angle. The signal is then transmitted to the detection and tracking system. This complicated data processing system will not be presented here in detail. However, because array installation design may adversely influence beamformer performance, the effects of installation parameters on the beamforming process will be discussed below.

1.11. CAUSES OF PERFORMANCE DEGRADATION

1.11.1. GENERAL

Degradation of array performance may be the result of poor quality control when manufacturing hydrophones and electronic preamplifiers. It may also be caused by cross-talk in the signal lines or mechanical problems such as the location of the elements, reflection from ships structure, refraction in lens-shaped domes, and self-noise. The effects of various causes of array degradation will be discussed in this section. In general, types of arrays other than line arrays will produce somewhat different effects.

1.11.2. PHASE AND AMPLITUDE ERRORS

The effect of random errors in amplitude and phase on side lobe suppression for a 25 element Dolph-Chebyshev linear array is shown in figure 1.26.

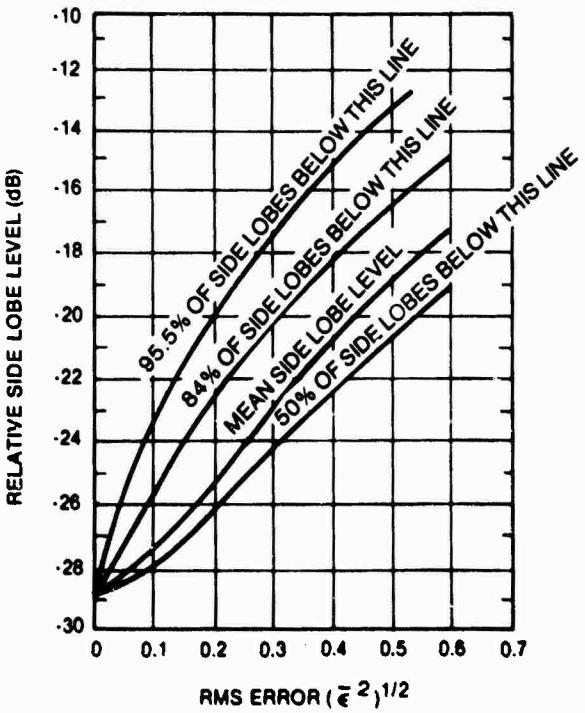

Figure 1.26. Amplitude and Phase Errors (Line Array)

$\bar{\epsilon}^2$ = TOTAL MEAN SQUARE ERROR = $\bar{\Delta}^2 + \bar{\zeta}^2$

$\bar{\Delta}^2$ = MEAN SQUARE AMPLITUDE ERROR
$\bar{\zeta}^2$ = MEAN SQUARE PHASE ERROR (RADIANS)

1.11.3. HYDROPHONE LOCATION

The effects on side lobe levels of errors in element location for 5 Dolph-Chebyshev arrays are illustrated in figure 1.27. The side lobe level increase is influenced by the number of elements and the initial side lobe level.

CURVE	NUMBER ELEMENTS	SIDE LOBE LEVEL (dB)
A	24	-40
B	24	-30
C	24	-20
D	48	-40
E	144	-40

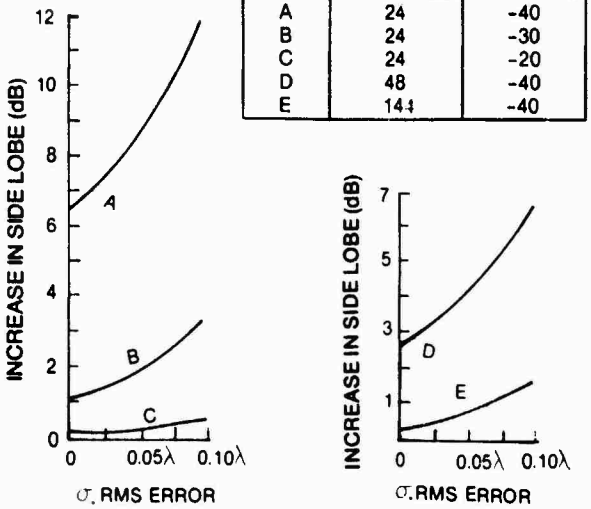

Figure 1.27. Effect of Hydrophone Location Errors on Five Line Arrays

1.11.4. SOUND SPEED VARIATIONS

Beam pointing errors result from variations in the local sound speed in the vicinity of the array. If the percent of sound speed error is

$$\varepsilon = 100\,|(C_e - C)/C\,|,$$

where

C_e = assumed speed and
C = actual speed,

the beampointing error is

$$\delta\theta = \theta - \sin^{-1}\,[100 \sin\theta/(100 + \varepsilon)].$$

Figure 1.28 shows the error caused by this effect.

1.11.5. REFLECTIONS

If the sonar array is located such that arrivals from some angles reflect into it from own ship structure, the beamformer will show spurious targets. Similarly, if some array elements receive reflections that cause spurious time delays, there may be a canceling effect and

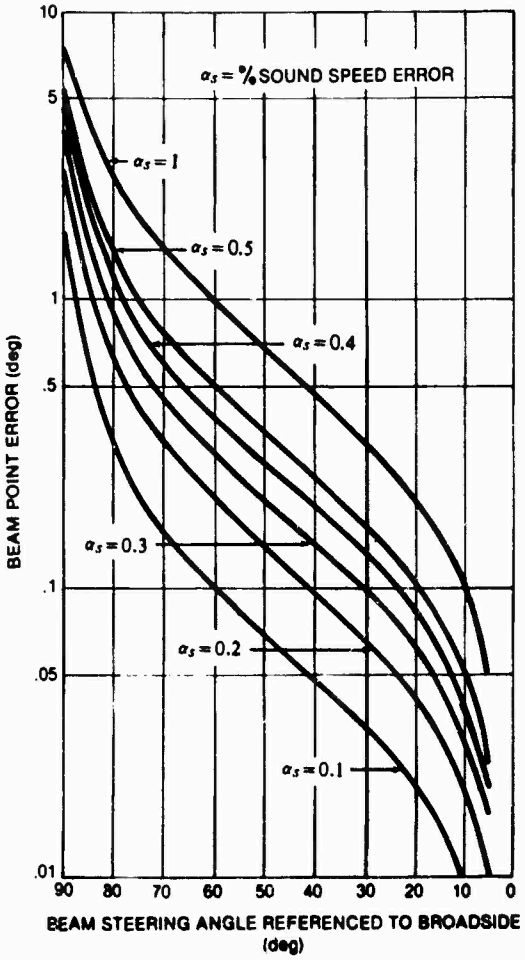

Figure 1.28. Beampointing Errors

performance will be degraded. Also, locating compliant material near array hydrophones effectively reflects the signal 180° out-of-phase and greatly reduces the received signal. For this reason air flasks, reflector tiles, air bubbles, foamed plastic and other acoustically compliant materials should be located as far from an array as possible or shadowed by baffles.

1.11.6. SELF-NOISE

The self-noise variation over the length of the array for large passive systems may negate the advantage of array size by reducing hydrophone effectiveness in noisy areas. When there are varying noise levels at the hydrophones, the optimum array signal is obtained by shading using the ratio

$$K_i/K_1 = (N_1/N_i)^2,$$

where

K_i = amplification of noisy phone,
K_1 = amplification of normal phone,
N_i = noise of noisy phone, and
N_1 = noise of normal phone.

Increasing the amplification of the *ith* hydrophone above this ratio reduces array SNR. Therefore, the amount of shading required for any hydrophone is a measure of its value to the array. It is apparent from the ratio plotted in figure 1.29 that a noise level increase of over 5 dB would make a hydrophone practically useless. Thus, there is no point in increasing the length of an array by adding a hydrophone if it is in a noisy area and cannot be baffled.

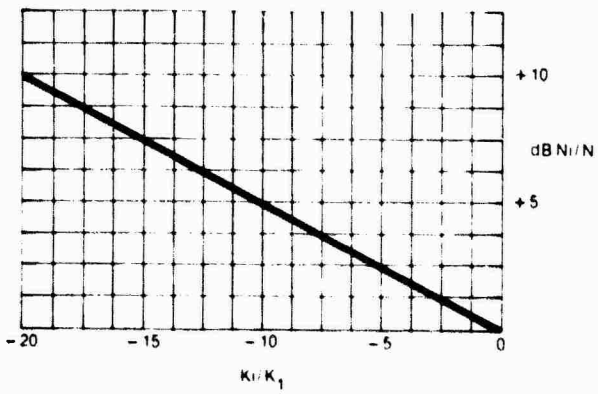

Figure 1.29. Required Shading of Noisy Hydrophone for Optimum SNR

1.11.7. SIGNAL AND NOISE FLUCTUATIONS

Random amplitude and phase fluctuations in the signals and noise arriving at each element of an array caused by the effects mentioned above will degrade array SNR gain from the ideal. The effect of such fluctuations on signal and noise is determined from the change in the value of the squared, time-averaged output signal voltage.

The array signal gain at a given frequency is defined as

$$G_S = \frac{\text{average output signal power of array}}{\text{average output signal power of reference receiver}}.$$

The degradation in signal gain resulting from the fluctuations in amplitude and phase may be defined as D_D, where

$$D_D = G_F - G_I.$$

Here D_D is defined such that it will always be negative in the direction of peak response with G_F being the signal gain including fluctuations and G_I, which is given as 10 log N^2, is the ideal signal gain. Amplitude and phase variations reduce the signal gain in the direction of peak response.

Two cases of signal gain degradation caused by phase and amplitude fluctuations are of interest. If there are no amplitude fluctuations, the expression for D_D is

$$D_D = 10 \log [(1 - e^{-B_f^2}/N) + (e^{-B_f^2})],$$

where B_f is the rms phase deviation. If there are no phase fluctuations, D_D is

$$D_D = 10 \log [(E^2/N + 1)/(E^2 + 1)],$$

where E is the rms relative amplitude fluctuation.

Figure 1.30 shows a plot of the first of these expressions for a 40-element (N = 40) array and shows the reduction in array signal gain due to phase fluctuations only; the abscissa represents the root mean square deviation of the fluctuation in phase angle. Figure 1.31 illustrates the second of these expressions, also for N = 40, and shows the reduction in array signal gain from amplitude fluctuations only. It is apparent from the figures that large phase fluctuations degrade array signal gain to a greater extent than do large amplitude fluctuations.

Array noise gain can be treated much the same, except that the effects of array response in directions other than the steered direction must be considered. The definition of array noise gain is similar to that for the signal gain, i.e.,

$$G_N = \frac{\text{average output noise power of array}}{\text{average output noise power of reference receiver}}.$$

However, compared with the signal gain case, the average output noise power will contain

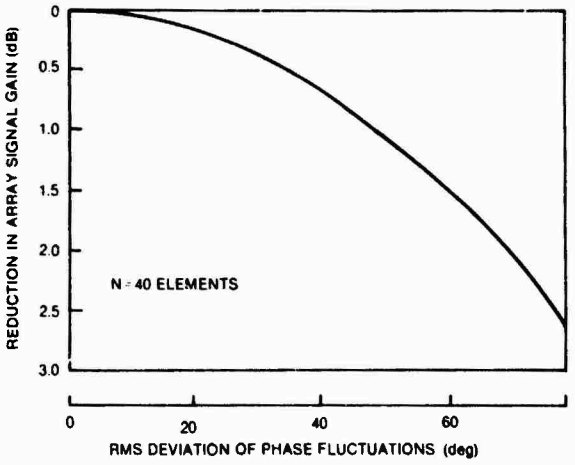

Figure 1.30. Gain Degradation Caused by Phase Fluctuations (Line Array)

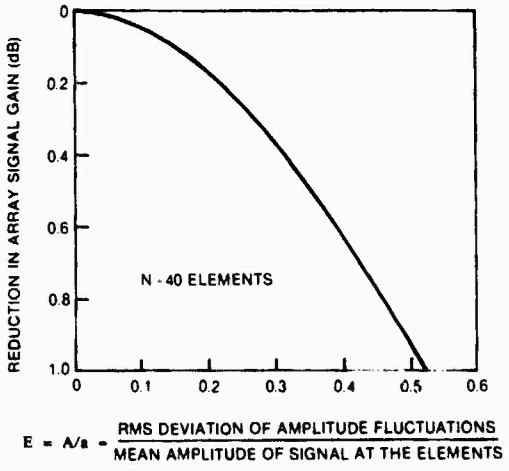

Figure 1.31. Gain Degradation Caused by Amplitude Fluctuations (Line Array)

components from all possible directions. It is generally assumed that the noise background is three-dimensional and isotropic but this is not always true. It can be shown that, for a line array having a constant phase correlation coefficient in a three-dimensional isotropic noise field, the amplitude and phase fluctuations at a given frequency modify the *ideal*, or errorless noise gain, so that it is closer to the value of 10 log N. This is demonstrated in figure 1.32 for an 8-element, equally spaced array. The ideal noise gain is represented by the solid line and the actual is denoted by the dashed line; both are plotted versus d_h/λ. This graph has a similar form for other values of N.

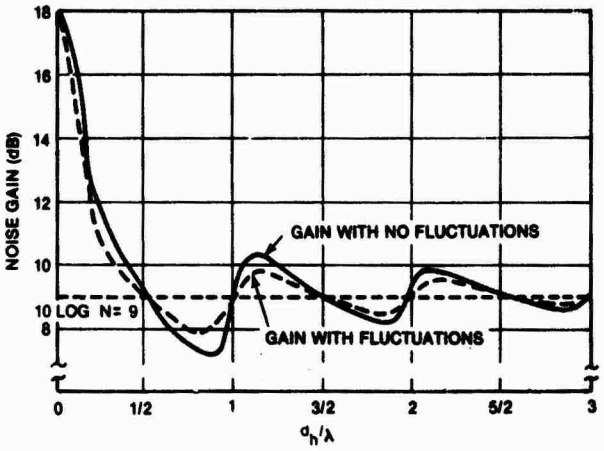

Figure 1.32. Amplitude and Phase Fluctuation Effects (Line Array)

It is apparent from figure 1.32 that the noise gain will be 10 log N (where N is the number of array elements) for the typical line array employing half-wavelength ($d_h/\lambda = ½$) element spacing. For spacing of less than half-wavelength, the noise gain can increase substantially; for spacing greater than half-wavelength it will remain close to the value of 10 log N. The above results are valid for fluctuation errors between the source and the point at which the output is measured. They include fluctuations in the (1) environment, (2) hydrophone performance, (3) dome effects, and (4) telemetry system.

It is important to note when calculating AG that G_S and G_N may have been derived for wavelengths that are not the same. For example, G_S for an array at the signal frequency corresponding to the typical half-wavelength element spacing can be calculated. The value of G_N at this frequency will, in accordance with figure 1.32, be 10 log N. However, for lower noise frequencies, the quantity d_h/λ, where λ is the noise wavelength, will become small and G_N will become large reducing array gain correspondingly.

1.11.8. COHERENCE EFFECTS

Signal and noise coherence will also effect array gain. Signals at two hydrophones are said to be coherent when their time variations display similar patterns; the level can be measured by cross correlating the signals. It can

be shown that when both signal and noise are either completely coherent or completely incoherent array gain will be 0 dB.

When the signal is perfectly coherent and the noise is completely incoherent the gain for an array having N elements will be

$$AG = 10 \log N.$$

When a perfectly coherent signal is in a background of only partially coherent noise, the expression for array gain becomes

$$AG = 10 \log N / [1 + (N-1)\, o\,],$$

where o = noise coherence,

which is less than 10 log N. Thus, array gain is reduced as the signal coherence decreases or the noise coherence increases.

1.11.9. FREQUENCY EFFECTS

For an unshaded line array of N elements of uniform spacing d_h, the DI or ideal AG in a three-dimensional isotropic ambient noise field is given by

$$AG = 10 \log \{[2(N-1)d_h]/\lambda\}.$$

If the design frequency f_o is such that $d = \lambda_o/2$, then the expression can be rewritten as

$$AG = 10 \log [(N-1)f/f_o],$$

where f = received signal frequency.

It is apparent that, for a fixed number of elements, N, the array gain will increase with frequency at a rate of 3 dB/oct.

It was shown earlier (1.9.3.) that the -3 dB beamwidth (measured in degrees) of a line array at broadside is approximately

$$BW_3 = 50.8^\circ \lambda/[(N-1)\lambda_o/2]$$

or

$$BW_3 = [101.6^\circ/(N-1)][f_o/f],$$

where the array length is $(N-1)\lambda_o/2$. Thus, the broadside beamwidth varies inversely with frequency and the corresponding array gain can be written as

$$AG = 10 \log (101.6^\circ/BW_3).$$

1.11.10. STEERING ANGLE

The beamwidth of a scanned line array varies as $|\cos \theta|^{-1}$, where θ is measured from broadside. The beamwidth is minimal at broadside and increases toward endfire. Because of the slope of the cosine function, the rate of increase is slow near broadside and the beamwidth actually remains within 20 percent of its minimum value over a sector of nearly 70 deg centered at broadside. In a three-dimensional isotropic ambient noise field the gain of a line array is independent of steering angle θ since the $|\cos \theta|^{-1}$ beam broadening factor is cancelled by a geometrical cos θ dependence of the solid or three- dimensional beam. As a result, array performance measured, e.g., by an estimated detection range, is essentially independent of array heading and steering direction.

1.11.11. LOST HYDROPHONES (LINE ARRAY)

Array performance will, of course be effected by the loss of one or more hydrophones or hydrophone groups. Consider the computed normalized DI plotted as a function of the fractional number of lost hydrophones as shown in figure 1.33 for a very long array. The upper and lower solid lines represent the maximum and minimum DI values for a given percentage of lost hydrophones and the dashed line represents the average DI. The DI for an array having a given number of lost hydrophones will depend on their exact location along the array. Thus, different configurations having the same number of lost hydrophones will exhibit different DIs. It is apparent from figure 1.33 that, on the average, the DI for a long array will decrease by about 1 dB for a 20 percent loss of hydrophones. Note that the side lobe level is also effected. Consider the broadside beampattern of a very long shaded array that is shown in figure 1.34.

Figures 1.35 through 1.38 illustrate the changes that occur as greater numbers of hydrophones are lost. For long arrays the indicated average generally increases in side lobe

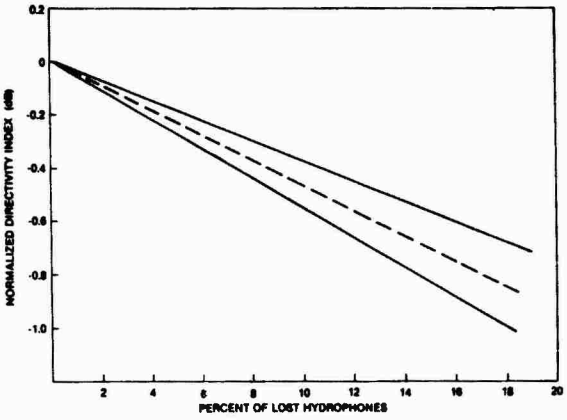

Figure 1.33. Directivity Index versus Percent of Lost Hydrophones

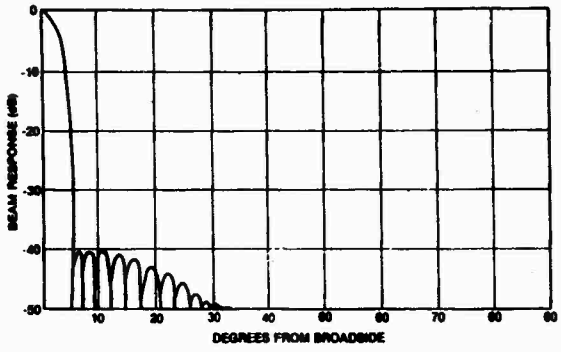

Figure 1.34. Broadside Beampattern with No Lost Hydrophones

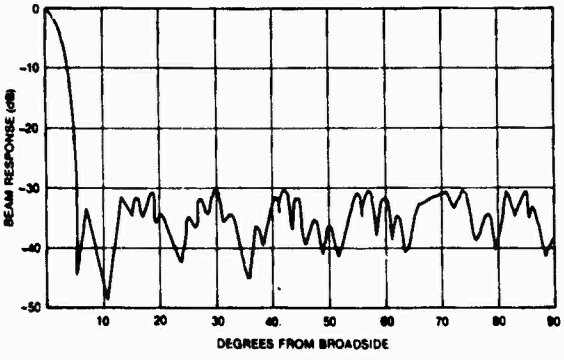

Figure 1.35. Broadside Beampattern with 4 Percent Hydrophone Loss

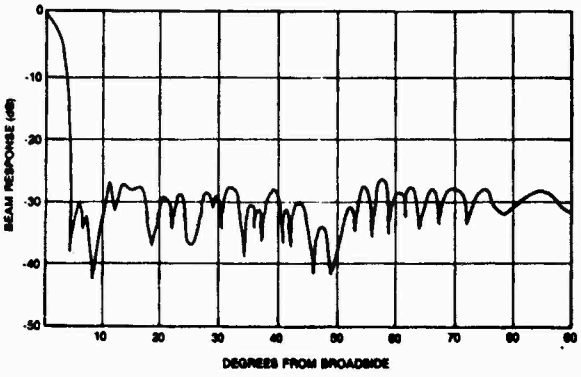

Figure 1.36. Broadside Beampattern with 9 Percent Hydrophone Loss

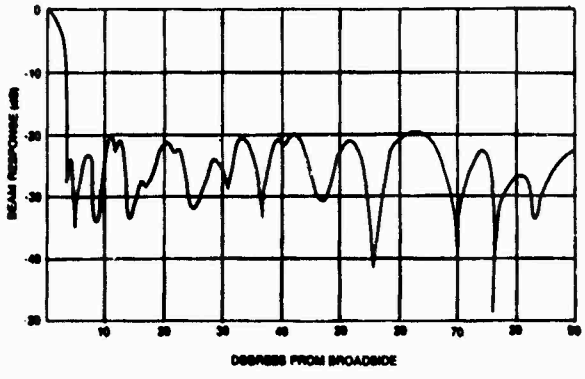

Figure 1.37. Broadside Beampattern with 12 Percent Hydrophone Loss

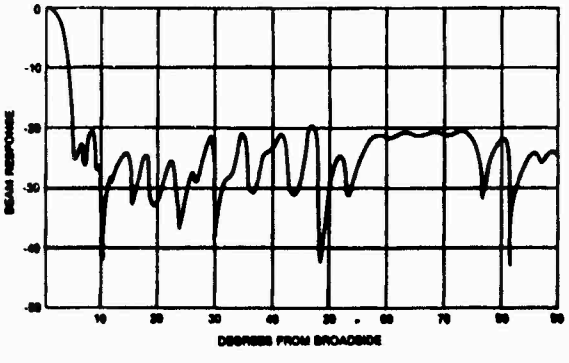

Figure 1.38. Broadside Beampattern with 18 Percent Hydrophone Loss

level with an increasing percentage of lost hydrophones. The average remains approximately the same for any configuration of lost hydrophones as long as the configuration is relatively uniform across the array.

It can generally be concluded that the effect of lost hydrophones on the DI of a very long array is minimal. The increase in the side lobe level, however, will be quite severe even if only 4 percent are lost.

1.11.12. BEAM SCALLOPING

Beam scalloping can cause a reduction in DI. It occurs when a point source target is located between adjacent beams where the response is less than the maximum or design value of either beam. That is, beam loss occurs when the target is not located on the main response axis (MRA) of some beam in the pattern. The actual reduction in DI below the MRA value depends primarily on the response level at the beam crossover points. It thus depends on the beamwidth and on the total number of beams formed.

Figure 1.39 shows a typical graph of scalloping loss versus d_h/λ, where d_h is the hydrophone element (or group) spacing in the array. The curve illustrates conventional time-delay beamforming, in which the scalloping loss decreases with decreasing frequency (or increasing wave length). As the frequency decreases from its design value, the beamwidth increases and adjacent beams cross at response levels above the design level, the scalloping loss then decreases.

As frequency increases, beamwidth decreases, adjacent beams cross at response levels below the design level, and scalloping loss becomes greater. When full azimuthal coverage is desired, beam crossovers should be set well above -3 dB at the design frequency so that the scalloping loss is kept to a minimum (about 1 dB) over most bands of interest. Although equipments such as frequency independent beamformers are employed, enough beams should be formed at the design frequency to ensure a crossover level well above -3 dB for a less than 1 dB scalloping loss at all frequencies.

1.11.13. SAMPLING LOSS

In conventional beamforming, the main beam is steered by time-delaying the signals from each element before summing to form the beam. In more current systems, however, the hydrophone signals are quantized in both amplitude and time. That is, the signals reaching the beamformer are digitized samples of the hydrophone analog output taken at discrete time intervals. When employing time sampled data for steering beams, the general approach is to use the sample having the time delay closest to that required (i.e., the *closest sample* method). It becomes apparent, then, that conventional beamformer performance will be effected by the sampling rate.

If the phase error resulting from the sampling is uniformly distributed, array signal gain degradation will be of the form shown in figure 1.40 for a uniformly weighted array and randomly steered beam. The figure plots the *over*

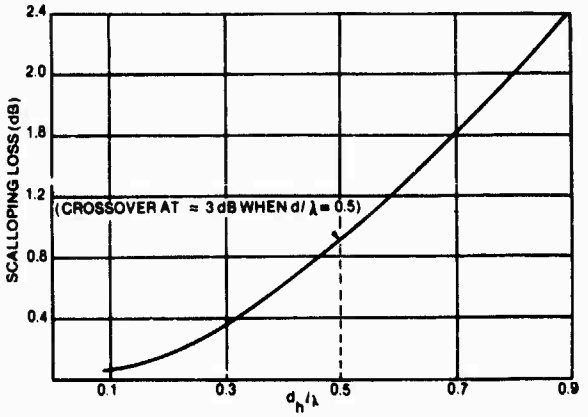

Figure 1.39. Typical Scalloping Loss for Conventional Beamformer

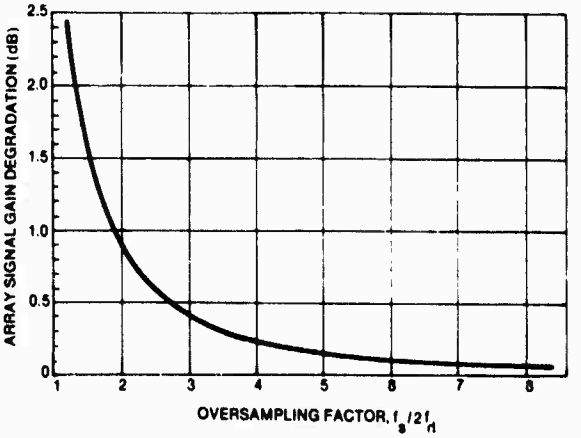

Figure 1.40. Time Delay Beamformer Loss Caused by Time Quantization

sampling factor, or ratio of the sampling rate, f_s, to twice the design frequency against array signal gain degradation. It shows that array signal gain degradation decreases as the sampling rate is increased and that the over sampling factor should be at least 3. Although the results are for a uniformly weighted array, they are approximately valid for shaded arrays.

The phase errors caused by sampling or time-delay quantization can lead to severe problems in respect to controlling the side lobe level of the beam pattern. If the closest sample method is used for beam steering, the maximum phase error introduced by sampling is given by

$$\varepsilon_{max}\,(\text{degrees}) = \pm\,(f/f_s)\,180°,$$

where f_s is the sampling rate (or frequency) and f is the frequency of interest. For example, the maximum phase error, ε_{max}, for a periodic signal that is sampled twice during each period is ± 90°.

It can be shown that for certain amplitude shaded arrays having design frequency f_D,

$$\varepsilon_{max} = \pm\,(f_D/f_s)\,180°$$

greater than 9° may lead to severe side lobe degradation. That is, if the sampling rate, f_s, is not at least 20 times the design frequency f_D, the sidelobe level will increase above its shaded level and a significant number of grating lobes will be introduced into the beampattern. Because sampling at this rate (20 × f_D) is generally unfeasible for a long array, other approaches, such as interpolating between fewer samples, must be employed using time domain beamforming to reduce the phase error.

1.11.14. WIDEBAND SIGNALS

The application of the proper phase steering to only one frequency in a band causes a beam pointing error at other frequencies and a loss in response to wideband signals; the wider the input bandwidth of the beamformer, the greater the degradation in performance. The response of a beamformer to a wideband signal can be evaluated by computing its output power density from the product of the source power density and the beampattern. The beamformer loss has been evaluated for a zonal source power density spectrum and the results are plotted in figure 1.41 as a function of $BN(d_h/c)\sin\beta$, where B is the bandwidth and β is the steering angle. It is apparent from the figure that maximum degradation occurs at endfire ($\beta = \pi/2$) and that there is no loss at broadside ($\beta = 0$). It should also be noted that the Nd_h/c term along the abscissa in figure 1.41 is approximately equal to the transit time, τ, of a sound wave along the entire line array.

1.11.15. FREQUENCY BIN SCALLOPING

It is apparent from figure 1.41 that narrowband pre-filtering will decrease wideband beamformer loss. The narrowband filters are not perfect, however, and will result in *picket fence* or *frequency scalloping* loss (see figure 1.42). Generally, frequency bin

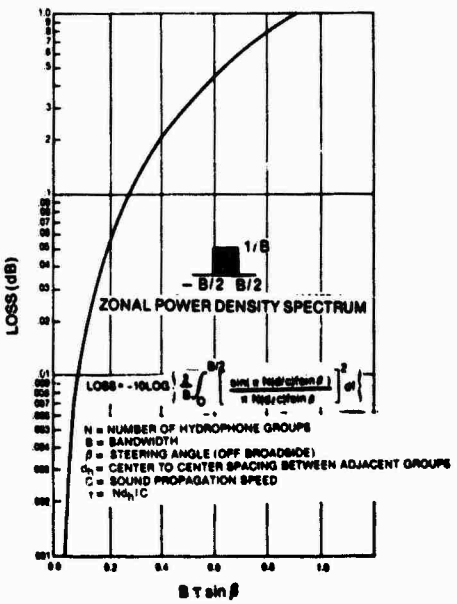

Figure 1.41. Beamformer Loss for a Uniformly Weighted Array and Randomly Steered Beam

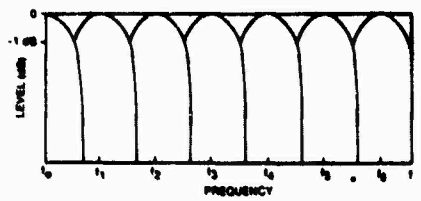

Figure 1.42. Narrowband Filtering

scalloping causes a smaller degradation. It is actually similar to the beam scalloping loss discussed earlier and occurs because the transfer characteristics of the individual filters are not perfectly flat across the respective bands.

1.11.16. OPERATOR PERFORMANCE

Any operator's capacity for searching a display and recognizing the presence of a target is, naturally, limited. It is generally conceded that operator's contribute an approximately 7 dB loss in recognition differential unalerted and about 6 dB alerted.

(For more information concerning *Causes of Performance Degradation* refer to *Applied Hydro-Acoustics Research, 1976; Blackman and Tukey, 1959; Lawson and Uhlenbeck, 1950; Peterson, et al., 1954; Swets, 1964; TRACOR, 1965; Urick, 1973; Von Winkle, 1963.*)

1.12. TELEMETRY SYSTEM CONSTRAINTS

The telemetry system conveys power from inboard electronics to the hydrophones in the array and returns the hydrophone data. Its function is to provide

1. transmission of electrical power and command signals from the inboard sonar system,
2. transmission of hydrophone and other data from the array to the inboard sonar system,
3. minimal degradation of SNR power density ratio (usually less than 1 dB) at the telemetry output,
4. minimal spurious cross-products or cross-talk at the output,
5. controlled channel-to-channel gain and phase variation,
6. adequate dynamic range and frequency bandpass, and
7. availability and reliability for a broad range of environmental conditions (e.g., static pressure, shock, and fatigue).

Because the telemetry functions listed above require a separate system, they impose various constraints on overall performance. The large number of sensors in contemporary arrays require that the telemetry system transmit encoded, mutiplexed, and/or modulated data along a common carrier. Tables 1.3, 1.4, and 1.5 list some of the more frequently used techniques and systems. Table 1.6 compares telemetry methods and table 1.7 lists their characteristics.

Encoding is the process of sampling an analog signal and arranging, or coding, the resultant digital samples to retain as much information as

Table 1.3. Typical Telemetry Techniques

Encoding Techniques
(Linear) Pulse Code Modulation (PCM)
Differential Pulse Code Modulation (DPCM)
Delta Modulation (DM)
Companding Pulse Code Modulation (CPCM)
Companding Delta Modulation (CDM)
Multiplexing Techniques
Time Division Multiplexing (TDM)
Frequency-Division Multiplexing (FDM)
Code-Division Multiplexing (CDM)
Modulation Techniques
Amplitude Modulation (AM)
Frequency Modulation (FM)
Phase Modulation (PM)

Table 1.4. Telemetry Multiplex Candidates

Multiple Twisted Pair Cable
Frequency Division Multiplex (FDM)
Type:
Single Sideband-Amplitude Modulation (SSB-AM)
Double Sideband-Amplitude Modulation (DSB-AM)
Double Sideband-Amplitude Modulation with Locked Carrier (DSB-AMLC)
Phase Quadrature Multiplexing-Amplitude Modulation (PQM-AM)
Frequency Modulation (FM)
Tiered Frequency Modulation (FM-FM)
Time Division Multiplex (TDM)
Type:
Pulse Position Modulation (PPM)
(Linear) Pulse Code Modulation (PCM)
Companded Pulse Code Modulation (CPCM)
Simple Delta Modulation (DM)
Companded Delta Modulation (CDM)

Table 1.5. Telemetry System Comparisons

DSB-AM	High Power, High Cost, Low commonality, Restricted to One Octave
DSB-AMLC	High Power, Low Commonality, High Cost, Moderate Improvement Risk
PQM-AM	Susceptible to Crosstalk (Error), Complex Receiver High Cost, High Development Risk
FM	Limited Expansion Capability, Low Commonality, Noise Susceptibility, High Cost, Moderate to High Development Risk
FM-FM	Low Commonality, Complex Electronics, High Cost, Moderate to High Development Risk
PCM	Moderately Complex Electronics, Large Bandwidth, Medium Cost, Moderate Development Risk
CPCM	Moderately Complex Electronics, Large Bandwidth, Medium Cost, Moderate Development Risk
DM	High Bandwidth (Clockrate), Poor Expansion Capability Limited System Accuracy, Restricted Dynamic Range

Table 1.7. Telemetry System Characteristics

Physical Characteristics

- Length of Cables
- Size of Array
- Number of Telemetry Channels
- Maximum Pressure
- Hull Penetration

Electronic Characteristics

- Hydrophone Preamp Bypass
- Hydrophone Preamp Gain Control Variability (from Inboard)
- Type of Analog to Digital Conversion (Encloding)
- Sampling Rate for All Sensors
- Number of Bits of Quantization per Sample
- Data Rate Through Cables
- Maximum Permissible Bit Error Rate
- Maximum Channel-to-Channel Gain Variation
- Maximum Channel-to-Channel Phase Variation
- Mean Time Between Failures (MTBF)
- Prime Power for Entire Cable Telemetry Subsystem

Table 1.6. Frequency and Time Division Multiplex Comparison

	Frequency DM					Time DM				
Characteristics	DSB-AM	DSB-AMLC	PQM-AM	FM	FM-FM	PCM	CPCM	DM	CDM	Hardware
System Accuracy	Med 2*	Med 2	Med 2	Med 2	Med 2	High 2	High 3	Low 1.5	Med 2	High 3
Dynamic Range	High 3	High 3	High 3	Med 2	Med 2	Med 2	High 2	Med 1	Med 2	High 3
Reliability	High 3	High 3	Med 2	Med 2	Med 2	Med 2	Med 2	Med 2.5	Med 2.5	High 3
Cost	High 1	High 1	High 1	High 1	High 1	Med 2	Med 2	Low 3	Low 3	Low 3
Standardization (Commonality)	Low 1	Low 1	Low 1	Low 1	Low 13	High 3	High 3	High 3	High 3	High 3
Bandwidth-Clockrate	Med 2	Med 2	Low 3	Med 2	Med 2.5	Med 2	Med 2	High 1	Med 2	Low 3
Power (Current)	High 1	High 1	High 1	Med 2	Med 2	Med 2	Med 2	Low 3	Med 3	Low 3
Receivers/Transmitters (Number-Complexity)	High 1	High 1	High 1	High 1	High 1	Med 2.5	Med 2.5	Low 3	Med 2.5	Low 3
Expansion Capability	Low 1	Med 2	Med 2.5	Low 1	Med 2	High 3	High 3	Low 1	Med 2.5	Low 1
Size (Weight)	Lge	Lge	Med	Med	Med	Med	Med	Sml	Sml	Lge
Noise Susceptibility (RFI) (Distortion)	High 1	Med 2	High 1.5	High 1.5	High 1.5	Low 3	Low 3	Low 2	Low 3	Med 2
Flexibility	Low 1	Low 1	Low 1	Med 2	Med 2.5	High 3	High 3	Med 2	Med 2.5	Low 1
Relative Score:	18	20	21	19	21	30	30	26	31	28

*Relative Merit:
Poor - 0
Good - 1-2
Better - 3

possible. For example, delta modulation is a process for encoding analog signals where the output of the modulator is a series of digital *ones* and *zeros* (one-bit quantization). The rate at which the ones appear at the output is directly proportional to the rate of increase of the amplitude of the input analog signal. Integrating the train of ones and zeros over the proper time interval reproduces the original analog signal.

Other encoding methods are given in table 1.3. When no encoding is used, the analog sensor signals are transmitted directly through the cable telemetry system. Uniform, or linear pulse code modulation (PCM), is the time sampling of the analog signal and yields a stream of digital sample groups where the coding of the ones and zeros within each group represents the amplitude of the analog signal at discrete time intervals. Differential PCM (DPCM) is the quantization of the change from the preceding sample amplitude value to the current one into two or more discrete quanta or levels. Companded PCM (CPCM) and companded delta modulation (CDM) employ nonuniform mapping of analog amplitude samples into bits of quantized data.

The particular encoding technique used depends on the processing method employed (i.e., spectral analysis, averaging, and so on). Digital transmission provides a minimum of cross-talk and signal degradation when compared with analog transmission. Delta modulation requires simpler circuitry than does PCM, but PCM is characterized by a wider dynamic range for a given binary bit rate. The DPCM produces a better slope-overload performance (i.e., a steep increase in analog input voltage) than delta modulation but the circuitry is more complex. On the other hand, companding encoding techniques provide better signal-to-distortion ratios than do uniform encoding schemes.

Multiplexing refers to the means of combining many hydrophone signals, without mutual interference, on a common carrier such as coaxial cable. Time-division multiplexing (TDM) separates the encoded signals, in time, from each sensor on the carrier. Other multiplexing techniques are frequency-division multiplexing (FDM) and code-division multiplexing (CDM). When multiplexing is not employed, a pair of twisted wires is used for each hydrophone but the method creates a very bulky cable when large numbers of hydrophones are involved. Hybrid systems, such as twisted pairs from the hydrophones to a group connection by an A/D conversion and TDM for transmission to the FDM could be used, but oscillator and filter costs are high. The CDM is usually considered only when the number of hydrophones is small (i.e., approximately 10).

(U) Amplitude modulation (AM) is the method of impressing an analog signal on a sinusoidal carrier. Double sideband AM (DSAM) distributes the signal symmetrically about the carrier frequency. Signal sideband AM (SSBAM) retains only that part of the spectrum above the carrier. Frequency modulation (FM) and phase modulation (PM) may also be used. No modultion is required if TDM, CDMX, or twisted wire pairs are employed. The FDM requires some modulation; in this case, AM is simpler, less expensive, and requires less frequency spectrum than FM. However, FM (or PM) suppress cross-talk more effectively.

When digital encoding is employed FM becomes frequency shift keying (FSK), which means that the FM is applied to a square wave (digital pulse). The resultant translation is FSK. Similarly, digital coding of PM becomes phase shift keying (PSK). A spectral representation of some of the waveforms discussed above are shown in figure 1.43.

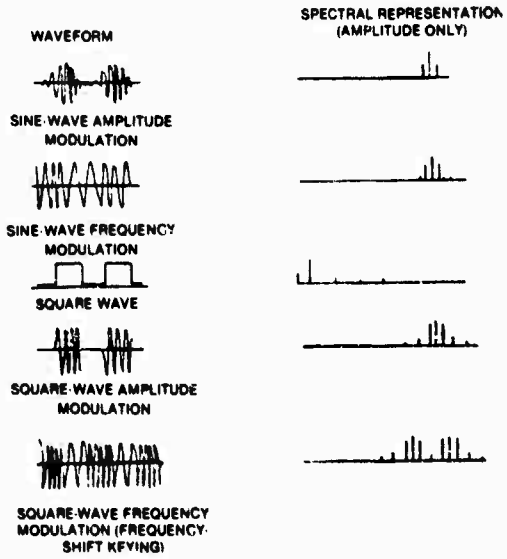

Figure 1.43. Fourier Spectra for Typical Periodic Waveforms

Table 1.4 lists a series of potential telemetry multiplexing schemes, many of which are in use. It also lists some potential modulation techniques that can be used with the FDM of analog signals. Hardwired, or twisted pair systems are bulky and require many leads. Single sideband amplitude modulation is characterized by complex receiving systems.

Table 1.6 compares various telemetry methods. The rating presented is arbitrary and the values would change to suit the application. The characteristics that must be specified for a system are listed in table 1.7.

(For more information concerning *Telemetry System Constraints* refer to *Applied Hydro-Acoustics Research, Inc., 1976; TRACOR, 1965.*)

1.13. RANGING

Active ranging is achieved by transmitting a pulse of acoustic energy toward the target and timing the return echo. The time is then multiplied by the speed of sound and divided by two. Passive ranging is more complicated and less accurate. It can be performed using the four basic methods shown in figure 1.44, in addition to ship maneuvering techniques (e.g., the Ekelund method).

The first method depends on simple triangulation and its accuracy depends on the precision with which the baseline and angles to the target are known. The range error is the greatest at maximum ranges. Geometrical considerations (see figure 1.45) show that for average towed array cable lengths, an error of 3° in can cause a 10 percent error at a range of 13.5 km (15 kyd). Variations in the towed array

DOMAIN / MODE	GEOMETRIC ANGULAR DOMAIN	TIME DIFFERENCE DOMAIN
HORIZONTAL MODE	TOWED AND HULL ARRAY TRIANGULATION (1)	WAVE FRONT CURVATURES (3)
VERTICAL MODE	D/E ANGLE (2)	MULTIPATH ARRIVAL Δ t (4)

Figure 1.44. Range Finding Methods

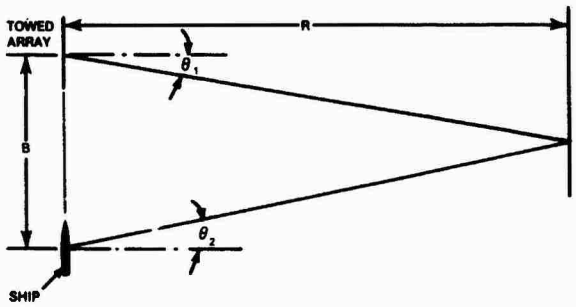

Figure 1.45. Range Finding using Triangulation

position or angle relative to the ship will result in range errors.

The second method uses the vertical arrival angle to estimate the range (see figure 1.46). The ray path may be calculated if the (1) approximate target and own ship depth; (2) sound speed profile depth curve for the water column; and (3) α, the angle at which the signal arrives are known. If there is more than one ray present, the estimate may be improved by calculating for more than one. Inaccurate measurements of α_R, the bottom reflected angle, or errors in calculating the ray path, will contribute to range errors. The geometry in figure 1.46 is exaggerated in the vertical dimension for clarity; a scaled version would show that small errors in angle cause substantial errors in range.

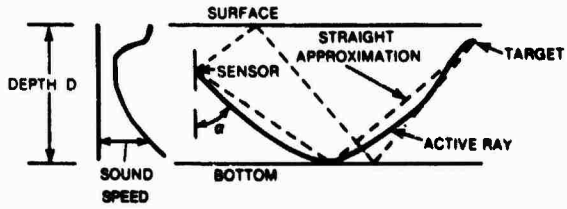

Figure 1.46. Range Finding using Arrival Angles or Time Delays

The third method uses the arrival times at three arrays to determine the wavefront curvature, i.e., the reciprocal of the range. Each array forms beams to improve the SNR in order to determine the arrivals as precisely as possible. The accuracy of the geometry of the three arrays and the precision with which the time differences are measured determine the accuracy of

the calculation. The angular alignment is also sensitive and there is the naval architecture problem of finding suitable locations for the arrays when constrained by alignment requirements. There is also the difficulty of separating multi-path arrivals. All of the above mentioned problems limit the effective range capability of this method.

The fourth method employs the difference in arrival time of various acoustic paths; two such paths are shown in figure 1.46. If the surface reflection and bottom-surface-target path are added, four paths may be considered. Since the paths move through the same water column, knowledge of the precise nature of the sound speed variation is not as critical as for method number two. However, extremely accurate correlation, to determine the time delay between multipaths, and identification of the time delays are important.

The four methods all have their advantages and disadvantages. In some instances, more than one is used to improve accuracy. The principal appplication of the techniques is to obtain a relatively quick, passive, rough estimate of range for use with bearing information and other data to obtain a target motion analysis (TMA) solution for target position, speed, and course.

1.14. OTHER SONAR TECHNOLOGY

1.14.1. ACOUSTIC LENSES

Acoustic lenses simplify the beam forming process. The liquid lens is a spherical shell, filled with a refractive medium, that focuses sound energy in the same manner an optical lens focuses light energy. Sound waves incident on the lens are refracted to form a high intensity focal region as shown in figure 1.47. The refraction is caused by a difference in acoustic wave speed in the lens media and surrounding water. The focusing ability is set by its diameter as measured in wavelengths for the frequency of interest.

A single hydrophone located in the focal region of the lens forms a highly directive beam pattern without the necessity of auxiliary beamforming electronics. A typical beam pattern is shown in figure 1.48; it was obtained

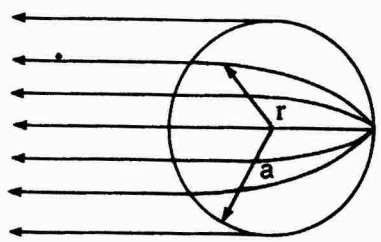

Figure 1.47. Focusing using a Luneburg Lens

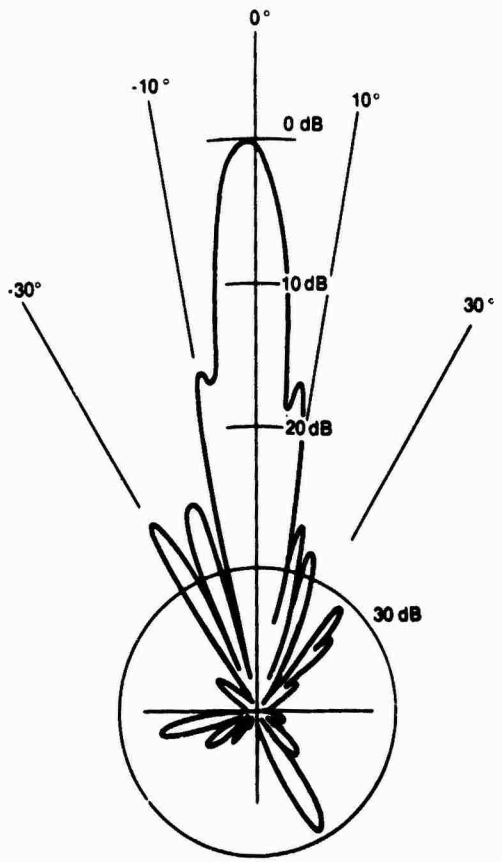

Figure 1.48. Beampattern of a 49 cm (18 in.) Diameter Liquid Lens at 30 kHz

using a 45 cm (18 in.) diameter liquid lens at a frequency of 30 kHz. Other liquid lenses having 15 cm (6 in.) diameters and 100 kHz operating frequencies have been developed. Liquid lenses may be used for active and passive search and acquisition and tracking. A large number of highly directive beams may be formed when one hydrophone is used per beam.

Various types of lenses may be built. For example, the Luneburg lens is a spherically symmetric, refracting structure composed of a nonhomogeneous fluid and has an index of refraction, n_L, given by

$$n_L = (2 - r_L^2/a^2),$$

where (refer to figure 1.47) a is the radius of the lens and r_L is the radial distance measured from the center of the lens. The index of refraction, n, of the medium is referenced to the speed of sound in water, c_w; thus, $n = c_w/c$, where c is the speed of sound in the medium. Figure 1.47 shows how a *bundle* of rays, representing an incident plane wave, is focused to a point on the surface of a Luneburg lens (focusing to a single point is termed *perfect focusing*). The speed of sound in a fluid is a function of the density of the fluid, ϱ, and the bulk modulus, B ,i.e.,

$$c = (B/\varrho)^{1/2}.$$

In order to vary the speed of sound in the water, B or ϱ must be made to vary. Toulis first described a practical method by using compliant metallic tubes and water. The effect is to vary B, while ϱ remains relatively constant. A compliant tube is a hollow, flattened tube having a cross section that is small compared with a wavelength and a compressibility much greater than that of water. A mixture of compliant tubes and water with the compliant tube occupying only a few percent of the total volume will have a refractive index sufficiently large to permit focusing in a spherical lens. The effective index can be made to vary throughout the lens by changing the spacing between the tubes. If the maximum tube spacing is small compared with the operating wavelength, a continuously varying index of refraction is approximated. The lens is comparatively light and nearly neutrally buoyant in water.

Other materials, such as rubber or steel, can be used to form the lens for particular purposes. Lenses constructed of such materials have not yet been employed for linear or spacial acoustic hydrophone arrays. However, their special characteristics may make them candidates for high frequency applications.

1.14.2. PARABOLIC REFLECTORS

Beamforming may also be accomplished by using parabolic reflectors. There are two types; one reflects from a hard, stiff surface such as a metal mirror and the other uses compliant tubes that form a pressure release surface. In order to obtain good reflection from an interface, there must be a discontinuity in the value of ϱc, or the acoustic impedence at the interface. This may be done by using either a significantly higher or significantly lower value of ϱc. When a higher value is used to provide a reflecting surface, the surface must be stiff and the equivalent of several wavelengths deep. This is not difficult for very high frequency, short wavelength tones but, as the frequency becomes lower and the wavelength longer, the mass involved becomes greater.

Therefore, for low frequencies it is necessary to use significantly lower values of ϱc by forming a compliant tube parabolic mirror that approximates a low impedance surface. Such a surface reflects at a 180° phase shift, whereas the hard surface reflects at a 0° phase shift.

1.14.3. PARAMETRIC SONAR

Parametric sonar operates on the principle of combining two tones projected simultaneously from the same source to form the sum and difference frequencies; the method is similar to heterodyning. The advantage of such a system is that the parametric difference frequency source affords a unique means of transmitting a narrow beam, virtually without side lobes, from a physically small tranducer. For applications such as deep water bathymetry, for which high resolution is required, a narrow beam must be produced at relatively low frequencies (where absorption is tolerable). For this and similar applications, the parametric source has advantages over conventional radiators.

The parametric acoustic radiator uses the nonlinearity of sound propagation to generate energy in the water at two or more difference frequencies. The difference frequency is generated in a relatively long, endfired, virtual array in the water column in front of the

projector where interaction between primary frequencies occurs. The virtual array, with its approximately exponential shading, produces difference frequencies having very low side lobes. Because the beamwidth depends on the length of the array and not on projector size, the narrow beam can be produced by a physically small transducer. The efficiency of the parametric radiator is relatively low (from 00.1 to 3 percent). However, it is feasible to generate source levels useful for one-way applications, such as communications, and for echo ranging.

Figure 1.49, which compares conventional and parametric systems using the same projector, illustrates the potential advantages of the parametric echo ranging source for a small scale situation. The narrow parametric beam without sidelobes eliminates surface reverberation and the target is unobscured. Such a system is valuable because it requires a small array and the narrow beamwidth it produces is an advantage in confined areas where reverberation is a problem.

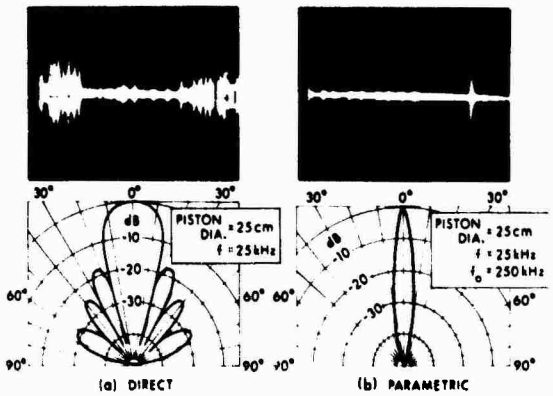

Figure 1.49. Echo Ranging Performance

(For more information concerning *Other Sonar Technology* refer to *Burdic, et al., 1972; Clay and Medwin, 1977; Corbett, et al., 1976; Gannon, 1974; Kock and Harvey, 1949; Kock, 1965; Konrad, 1979; Raytheon, 1973; Robertson, 1967; Sternberg, et al., 1978; Westervelt, 1963.)*

1.15. COMPUTER MODELING

The expanding capability of computers has made the modeling of most of the phenomena discussed in this chapter possible. The generic sonar model provides a comprehensive capability for evaluating sonar systems and investigating their operation in the ocean environment.

(For more information concerning *Computer Modeling* refer to *Weinberg, 1979.*)

ANNOTATED BIBLIOGRAPHY

Albers, V.M., *Underwater Acoustics Handbook*, Pennsylvania State University Press, PA, 1960.

Allen, W.B. and E.C. Westerfield, "Digital Compressed-time Correlators for Active Sonar," *Journal of the Acoustical Society of America*, vol. 36, p. 121, 1964.

Anderson, M.G., "Linear Arrays with Variable Inter-Element Spacing," *IRE Transactions on Antennas and Propagation*, AP-10, 137, March 1962.

Applied Hydro-Acoustics Institute, Inc.. *Handbook of Array Design Technology*, Prepared for NAVELEX (Code 320), 30 June 1976.

Axelrod, E.H., et al., "Vertical Directionality of Ambient Noise in the Deep Ocean," *Journal of the Acoustical Society of America*, vol. 37, p.77, 1965.

Beranek L.L., *Acoustics Measurements*, John Wiley and Sons, Inc., NY, 1949.

Blackman, R.B. and J.W. Tukey, *The Measurement of Power Spectra*, Dover Publications, Inc., NY, 1959.

Brekhovskikh, L.N., *Waves in Layered Media*, Academic Press, NY, 1960.

This is the best available theoretical treatment of propagation. It is applicable to radio and radar in the atmosphere as well as to underwater sound. Understanding the theory as presented is often difficult for the engineer, but the results are usually well summarized.

Burdic, W.S., E.V. Byron, and A. Boyles, "An Acoustic Compliant Tube Luneburg Lens," *Proceedings of the 29th Navy Symposium on Underwater Acoustics*, vol. 1, 2 November 1972.

Corbett, K.T., F.N. Middleton and R.L. Sternberg, "Non-Spherical Acoustic Lens Study," *Journal of the Acoustical Society of America*, vol. 59, no.5, May 1976.

Clay, C. S. and H. Medwin, *Acoustical Oceanography*, John Wiley and Sons, NY, 1977.

This textbook covers a variety of topics from an academic viewpoint. The appendices provide a useful reference.

Fisher, F.H. and V.P. Simmons, "Sound Absorption in Sea Water," *Journal of the Acoustical Society of America*, vol. 62, p. 558, 1977.

Greenspan, M. and C.E. Tschiegg, "Transistorized Velocimeter for Measuring the Speed of Sound in the Sea," *Journal of the Acoustical Society of America*, vol. 31, p. 1038, 1959.

Gannon, E., "Available Computer Programs for Parametric Sonar Research, Analysis, and Design," NUSC Technical Memorandum TD1X-10-74, 14 March 1974.

Hale, F.E., "Long Range Sound Propagation in the Deep Ocean," *Journal of the Acoustical Society of America*, vol. 33, p. 456, 1961.

Horton, J.W., *Fundamentals of Sonar*, 2nd edition, U.S. Naval Institute, MD, 1959.

Ishimaru, A., "Theory of Unequally Spaced Arrays," *IRE Transactions on Antennas and Propagation*, AP-10, 691, November 1962.

Jeffress, L.A., "Mathematical and Electrical Models for Auditory Detection," *Journal of the Acoustical Society of America*, vol. 44, p. 187, 1967.

King, D.D., R.F. Packard and R.C. Thomas, "Unequally Spaced, Broadband Antenna Arrays," *IRE Transactions on Antennas and Propagation*, AP-10, 380, July 1960.

Kinsler, L.E. and A.R. Frey, *Fundamentals of Acoustics*, 2nd edition, John Wiley and Sons, NY, 1962.

This is good reference for basic acoustics. It treats the subject in an elementary fashion with only a passing mention of underwater sound.

Kock, W.E. and F.K. Harvey, "Refracting

Sound Waves," *Journal of the Acoustical Society of America*, September 1949.

Kock, W.E., *Sound Waves and Light Waves*, Doubleday and Company, Inc., NY, 1965.

Konrad, W.L., "Application of the Parametric Source to Bottom and Subbottom Profiling," *Proceedings of the 1973 Symposium, Finite-Amplitude Wave Effects in Fluids*, Copenhagen, 1973.

Lawson, J.J. and G.E. Uhlenbeck, *Threshold Signals*, McGraw-Hill Book Company, Inc., NY, 1950.

Leroy, C.C., "Development of Simple Equations for Accurate and More Realistic Calculations of the Speed of Sound in Water," *Journal of the Acoustical Society of America*, vol. 46, p. 216, 1969.

Marsh, H.W. and M. Schulkin, "Shallow Water Transmission," *Journal of the Acoustical Society of America*, vol. 34, p. 863, 1962.

Merklinger, H.M., "Bottom Reverberation Measured with Explosive Charges Fired Deep in the Ocean," *Journal of the Acoustical Society of America*, vol. 44, p. 508, 1968.

National Defense Research Committee, *Physics of Sound in the Sea*, Division 6 Summary Technical Report 8, 1946. Reprinted by NAVMAT, 1969.

National Defense Research Committee, *Principles and Applications of Underwater Sound*, Division 6 Summary Technical Report 7, 1946. Reprinted by NAVMAT, 1969.

These two NRDC publications provide the basic theory and application of underwater sound as of the end of WW II. The material is still basically valid and includes chapters by some of the eminent physicists engaged in ASW during the war.

Officer, C.B., *Introduction to the Theory of Sound Transmission*, McGraw-Hill Book Company, Inc., NY, 1958.

Peterson, W.W., T.G. Birdsall and W.C. Fox, "The Theory of Signal Detectability," *IRE Transactions on Information Theory*, pp. 171-212, 1954.

Raytheon, *Acoustic Parameters and Installation Approaches for a Directional Submarine Communication Array*, Raytheon Final Report R-1360, 19 October 1973.

Robertson, G.H., "Operating Characteristics for a Linear Detector of CW Signals in Narrowband Gaussian Noise," *Bell System Technical Journal*, April 1967.

Schulkin, M., "Surface Coupled Losses in Surface Sound Channels," *Journal of the Acoustical Society of America*, vol. 44, p. 1152, 1962.

Schulkin, M. and H.W. Marsh, "Low Frequency Sound Absorption in the Ocean," *Journal of the Acoustical Society of America*, vol. 63, p. 43, 1978.

Sternberg, R.L., W.A. Anderson and G.T. Stevens, "Log-Periodic Acoustic Lens: Acoustic Filter Plate Study," *Journal of the Acoustical Society of America*, vol. 63, no. 5, May 1978.

Swets, J.A., ed., *Signal Detection and Recognition by Human Observers*, John Wiley and Sons, Inc., NY, 1964.

Tolstoy, I. and C.S. Clay, *Ocean Acoustics*, McGraw-Hill Book Company, Inc., NY, 1966.

This is of interest to the engineer with a good background in theory. It provides some practical examples concerning propagation.

TRACOR, *Introduction to Sonar Technology*, NAVSHIPS 0967-129-3010, Prepared for BUSHIPS, December 1965.

Urick, R.J. and R.M. Hoover, "Backscattering of Sound from the Sea Surface: Its Measurement, Causes, and Application to the Prediction of Reverberation Levels," *Journal of the Acoustical Society of America*, vol. 28, p. 1038, 1956.

Urick, R.J., *Principles of Underwater Sound*,

2nd edition, McGraw-Hill Book Company, Inc., NY, 1975.

This book is intended for the working engineer and concentrates on sonar equations. It summarizes each sonar parameter and solves some practical problems in design and prediction. However, the numerical data provided are limited because of the security classification of the more current information.

Urick, R.J., "Generalized Form of the Sonar Equations," *Journal of the Acoustical Society of America*, vol. 34, p. 547, 1962.

Urick, R.J., "Caustics and Convergence Zones in Deep Water Sound Transmission," *Journal of the Acoustical Society of America*, vol. 38, p. 348, 1965.

Urick, R.J., "Correlative Properties of Ambient Noise at Bermuda," *Journal of the Acoustical Society of America*, vol. 40, p. 1108, 1966.

Urick, R.J., "Low Frequency Sound Attenuation in the Deep Ocean," Paper Presented at Acoustical Society of America Meeting, May 1963.

Urick, R.J., *Fluctuations in Sonar: A Short Survey*, NOL Technical Report 73-217, 1973.

Westervelt, P.J., "Parametric Acoustic Array," *Journal of the Acoustical Society of America*, vol. 35, pp 535-537, 1963.

Von Winkle, W.A., *Increased Signal-to-Noise Ratio of a Summed Array Through Dynamic Shading*, USL Technical Report 579, 15 July 1963.

Webb, D.C. and M.J. Tucker, "Transmission Characteristics of the SOFAR Channel," *Journal of the Acoustical Society of America*, vol. 48, p. 767, 1970.

Weinberg, H., *Generic Sonar Model*, NUSC Technical Document 5971, 1 January 1979.

Woodward, P.M., *Probability and Information Theory*, Pergamon Press, 1953

Principles of Sonar Installation

CHAPTER II
NOISE GENERATION

GLOSSARY

A	Coefficient
A_c	Pipe Area at Choke Point (L^2)
A_o	Pipe Area at Point "o" (L^2)
a	Length of Plate (Direction of Flow) (L)
a_p	Radius (L)
a_D	Half-Distance Between Dipole Sources (L)
a_o	Mean Radius (L)
a_Q	Half-Distance Between Quadrupole Sources (L)
a_t	Time Varying Radius (L)
B	Number of Propeller Blades
b	Plate Width (L)
C_f	Oscillating Hydrodynamic Lift Coefficient
C_p	Pressure Coefficient
c	Sound Speed (L/T)
D	Water Depth (L)
D_P	Propeller Diameter (L)
D_R	Flexural Rigidity [$Eh^3/12(1-\nu^2)$] (FL)
E	Young's Modulus (F/L^2)
E_A	Acoustic Energy (FL)
F	Force (F)
f	Frequency (1/T)
f_c	Line Frequency Component (1/T)
f_n	Frequency of n^{th} Mode (1/T)
f_o	Frequency of Spectrum Peak (1/T)
h_v	Vortex Separation Distance (L)
h	Plate Thickness (L)
hp	Horsepower (550 ft-lb/sec) (LF/T)
J_o	Propeller Advance Ratio
K	Spring Constant (F/L)
K_c	Critical Cavitation Index
K_f	Flow Cavitation Index
K_i	Inception Cavitation Index
K_o	Operating Cavitation Index
K_{oc}	Operating Critical Cavitation Index
K_{tip}	Propeller Tip Cavitation Index
k	Wave Number ($2\pi/\lambda$) (1/L)
k_a	Acoustic Wave Number (1/L)
k_h	Hydrodynamic Wave Number (1/L)
k_r	Resonant Wave Number (1/L)
L	Length
L	Sound Level (dB)
L_e	Effective Length (L)
L_N	Noise Level (dB)
L_s	Diesel Engine Sound Constant (dB)
ℓ	Correlation Length of Vortex Shedding (L)
M	Mach Number
m	Mass (FT^2/L)
m	Order of Mode Vibration
N	Revolutions per Minute (1/T)
N	Number of Bubbles per Second
N	Noise Level (dB)

n	Rotational Speed (1/T)
n	Mode Number
P	Sound Pressure (F/L^2)
P_{crit}	Critical Cavitation Pressure (F/L^2)
P_i	Internal Pressure (F/L^2)
P_m	Impact Pressure (F/L^2)
P_{min}	Minimum Pressure in Pipe (F/L^2)
P_o	Pressure at Point "o" (F/L^2)
P_{out}	External Pressure (F/L^2)
P_v	Vapor Pressure (F/L^2)
Q_o	Pulsating Fluid Flux (L^3/T)
R	Resistance (Function of Application)
R_{rad}	Radiation Resistance (FT/L)
r	Radial Distance to a Point (Radius) (L)
r	Plate Damping Coefficient per Unit Area (FT/L^3)
$r_{c_{m,n}}$	Plate Critical Damping Coefficient per Unit Area for m,nth Mode (FT/L^3)
S	Strouhal Number (fl/V) (Dimensionless)
T	Time (T)
t	Time (T)
U	Velocity (L/T)
U_o	Flow Velocity (L/T)
U_o	Oscillating Velocity (L/T)
U_s	Source Velocity (L/T)
U_c	Mean Velocity of Eddies Along Plate (L/T)
V	Velocity (L/T)
V_{max}	Maximum Velocity (L/T)
V_o	Velocity at Point "o" (L/T)
V_o	Velocity of Ship (L/T)
V_o	Initial Bubble Volume (L^3)
V_{tip}	Propeller Tip Velocity (L/T)
W	Power (LF/T)
W_{AC}	Acoustic Power (LF/T)
W_{MECH}	Mechanical Power (LF/T)
X	Reactance (FT/L)
Z	Impedance (Function of Application)
Z_{RAD}	Radiation Impedance (FT/L)
z	Specific Acoustic Impedance (FT/L^3)
δ^*	Turbulent Boundary Layer Displacement Distance (L)
η	Efficiency
η_{AC}	Acoustic Efficiency
ξ	Change in Dimension (L)
ξ	Ratio of Initial and Final Radii
θ	Angle
λ	Wave Length (L)
μ	Mass of Plate per Unit Area (FT^2/L^3)
ν	Poisson's Ratio
ρ_o	Mass Density (FT^2/L^4)
σ	Liquid Surface Tension (F/L)
τ	Time Constant for Decaying Function to Reach 1/e of Original (T)
ω	Angular Velocity (1/T)

CHAPTER II

NOISE GENERATION

2.0 INTRODUCTION

The generation of noise by a platform is extremely important. Self-noise is one of primary sources of sonar performance degradation because it directly affects the signal-to-noise ratio (SNR). Radiated noise contributes to the source level of the acoustic signature of the ship and, thus, increases its detectability. Self-noise is undesirable because it decreases the capability of the ship to detect a target. The mechanisms that generate mechanical and hydrodynamic noise will be discussed in this chapter.

Ship noise arrives at the sonar transducer (hydrophone) via many paths, but the principal routes are the water and the structure itself. The air-to-structure-to-water path is also important in some instances. Major noise components are usually low frequency propeller and machinery sources that excite higher frequency modes. Figure 2.1 shows the near-field sound pressure level distribution for low frequencies and figure 2.2 shows that for high frequencies. Figure 2.3 illustrates the general trend of the sound spectrum with changing ship speed, and figure 2.4 shows how platform noise varies with location.

The general shape of the low frequency curve suggests that the ship is vibrating in free-free beam modes, as would be expected of a floating structure. These mode shapes tend to have their maximum amplitude at the free ends. The stern amplitudes are larger because the sources of the vibration are in that area.The shape of the high frequency band suggests that the source is also near the stern because the curve shows attenuation with distance away from the stern.

The frequency speed plots in figure 2.3 indicate that the general noise level increases with speed and increases faster at higher speeds. This is because more energy is generated by the

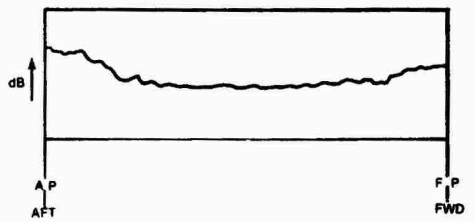

Figure 2.1. Low Frequency Near-Field Sound Pressure Distribution

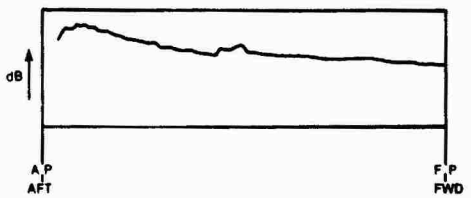

Figure 2.2. High Frequency Near-Field Sound Pressure Distribution

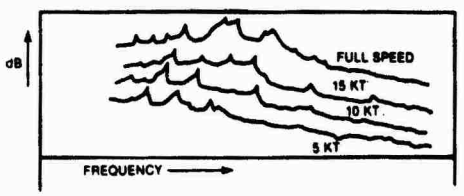

Figure 2.3. Sound Spectrum Variation with Ship Speed

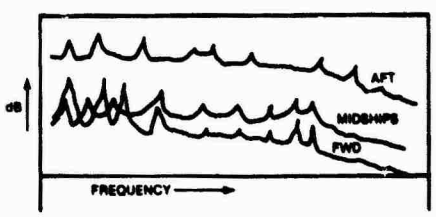

Figure 2.4. Platform-Noise Variation with Location

power plant and propeller and because the acoustic output increases as a high exponent of the speed. It also indicates that the lower frequencies have the most energy, which agrees with the concept that the majority of noise sources are at relatively low frequencies. The energy moves to the higher frequencies through mode conversion mechanisms in the structure. It can be seen that the intensity peaks at various modal frequencies.

Figure 2.5 categorizes the relationship between the machinery noise and the hydrodynamic noise radiated from the hull. The machinery noise is generated by unbalanced or pulsating forces. These pulses travel through the structure and excite structural members having the same modal frequencies. The structure, in turn, vibrates and generates other frequencies Also, human activities and flow noise from fluid systems create sound within the ship.

Water flowing by the ship causes eddies around the plating and sonar domes and creates pulsating forces that vibrate the dome windows or ship structures, especially when the frequency spectrum of the eddies overlaps that of the structure mode. The amplitude of the noise will depend on the mass and stiffness of the structure, damping of the plate, and how close the frequencies of the eddies are to structural resonances.

Water flowing around cylindrical structures causes pulsating vortices (the Karman vortex or Strouhal effect) that alternate from one side of the structure to the other. This effect is also present when streamlined structures and cables moving at right angles to the water are involved. In such cases, the structure or cable is tapered to provide a thin trailing edge.

Flowing water that reaches a pressure lower than its vapor pressure creates bubbles that produce noise when they collapse. This is known as *cavitation*. Also, water passing an opening in the hull (for example, when submarine ballast tanks are open to the sea through the flood holes) may cause a phenomenon known as *Helmholtz Resonance*.

Ships, especially surface ships, also vibrate in longitudinal free-free beams and such modes contribute to own ship noise either directly or by exciting higher frequency modes. They increase self-noise, reduce the SNR, and are sources for detection by opposing forces.

As mentioned earlier, sound may travel through the structure or enter the water and travel along the ship. In submarines, it may reflect from the water surface forward or, when the dome window is flow excited, pass directly into the hydrophone. Because the velocity of the steel plate bending mode may be equal, or higher, than the speed in water for some of the frequencies of interest, the acoustic energy may tend to travel along the skin of the ship. From there, it may be transmitted through the dome, diffuse around the baffles, and add to the received signal. Random phenomena, such as cavitation, produce broad continuous spectra,

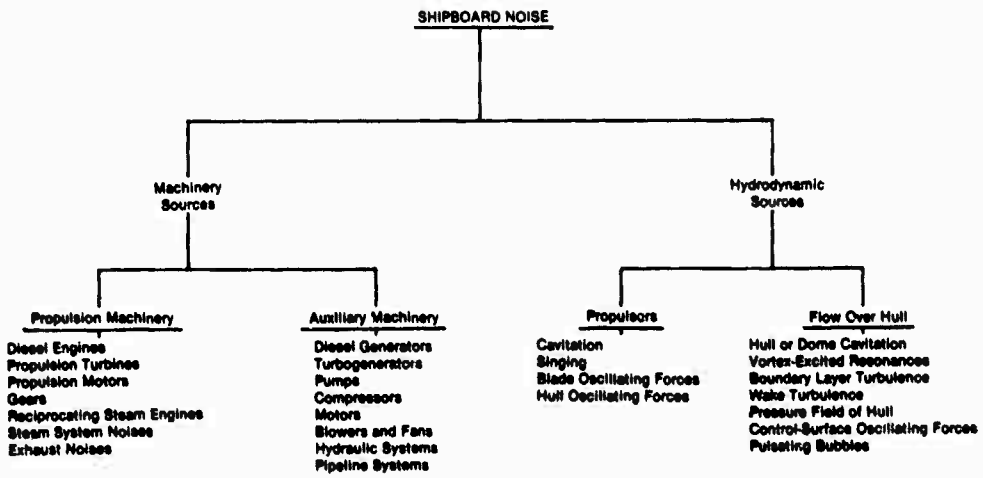

Figure 2.5. Relationship of Machinery Noise and Hull-Radiated Hydrodynamic Noise

whereas noise generated by constant speed rotating equipment is sinusoidal and tonal. Series impacts produce regular noise spikes over the higher frequency bands. Single frequency components are denoted *tonals* or *line frequencies*. Various phenomena may generate amplitude or frequency modulated noise.

2.1. MACHINERY NOISE

2.1.1. GENERAL

Machinery and fluid system noises are generally the major sources below 10 knots. They cause discrete line (or tones) and broadband (or distributed) noise and may be classified according to the basic physical mechanisms involved. These vibrations include

1. mechanical, hydrodynamic, and magnetic imbalances,
2. physical impact,
3. flow pulsations,
4. flow-excited structural resonances, and
5. cavitation.

Vibrations produced by machinery noise become underwater sound through

1. structural paths to the hull,
2. fluid paths directly to the sea,
3. fluid coupling of structures to the hull, and
4. airborne paths to the hull.

2.1.2. ROTATIONAL IMBALANCES

All rotating machinery is subject to slight dynamic imbalances. They are manifested as oscillating forces at the shaft-rotating frequency and transmitted through the bearings to the foundation, or support, the machine rests upon. The forces are transmitted to the hull and the resultant vibrational velocity radiates sound into the sea.

Since the sound pressure in the water, P, is proportional to the velocity of the vibration of the hull (which is, in turn, proportional to the force generated by the dynamic imbalance), it follows that the sound pressure is proportional to the force caused by the imbalance. Mechanical imbalances can usually be expressed in terms of an equivalent imbalance mass, m, rotating at a velocity, V, at a radius r. Thus, the imbalance force, f, is

$$f \approx \omega^2 mr$$

and

$$P \approx f \approx V^2.$$

Imbalance tones at rotational frequencies, therefore, increase by 12 dB each time the speed doubles.

Since mechanical power increases as the cube of the speed for rotating machinery,

$$W \approx P^2 \approx V^4 \approx W_{MECH}^{4/3},$$

where W is the acoustic power and W_{MECH} is the horsepower of the machinery. Underwater noises from a large number of machines correlate quite well according to

$$N = A + 10 \log W_{MECH}^{4/3}$$
$$= A + 13 \log W_{MECH},$$

where N is the noise level (in decibels), the coefficient A is, to some extent, dependent on the type of machine and its mounting arrangement, and W_{MECH} is the rated horsepower at the operating speed, not the delivered power.

2.1.3. HYDRODYNAMIC IMBALANCES

Hydrodynamic imbalances, inherent in any axial flow or centrifugal pump or blower, are caused by the blades and/or by asymmetrical flow paths; they generate tones at the blade-passage frequencies and their harmonics. Since the hydrodynamic forces are proportional to the square of the flow speed, the same 4/3 exponent dependence of acoustic power on rated mechanical power exists.

2.1.4. ELECTRICAL MACHINERY NOISE

Electrical machinery produces acoustic and electrical noise that can affect sonar system operation. Acoustic noise is caused by various imbalances in rotating equipment and magnetic forces generated by alternating currents. Magnetic forces are caused by periodic variations, which are proportional to the flux

density, in the gap between the stator and rotor, as well as by the differences in the number of slots in those components.

Such acoustic and electrical noise can be reduced by

1. making the rotor and stator as nearly circular and concentric as possible,
2. using skewed rotor magnets and/or stator slots, or closed rotor and stator slots, and the proper rotor/stator slot combinations,
3. minimizing permeance variations,
4. providing precision balanced rotors and precision electrical phase balance,
5. using low-noise anti-friction bearings,
6. designing for minimal harmonic distortion,
7. using damped rotor and stator structures,
8. providing quiet cooling systems, and
9. designing stators and rotors that reduce electrical and mechanical excitation and harmonics.

Harmonic distortion generated by electrical equipment may exist throughout the entire electrical system and can cause as much, or more, system degradation as can acoustic noise. The use of polyphase rectifiers onboard ship may be a principal cause of harmonic distortion. For example, the higher harmonics of 60 Hz power, i.e., the triplings, 3rd, 5th, 7th, 9th....., can be of such magnitude that they reflect back into the power bus and create torques in the ship's alternating current machinery. If the mechanical and electrical impedance of a system matches the triplings, there will be unwanted noise. Low harmonic distortion or electrical isolation of equipment can eliminate the problem. (See Paragraph 5.9).

2.1.5. PHYSICAL IMPACT

The impact of metal on metal generates a sharp noise spike, the duration of which is a function of damping, i.e.,

$$P(t) = P_o e^{-t/\tau},$$

where

$P(t)$ = sound pressure (time variant),
P_o = impact pressure,
t = time, and
τ = time constant of impact.

If these impacts are repeated at a regular rate, as when reciprocating machinery and reduction gears are operating, the series of exponential pulses results in a harmonic series of line components. The fundamental frequency of the series is the repetition rate of the impacts and the line components are roughly of equal amplitude out to a particular frequency, i.e.,

$$f_c \cong 1/2\pi\tau.$$

The spectrum decreases by 6 dB/octave above this frequency.

The impact of gear-teeth generates tones at the fundamental gear-tooth contact frequency and its harmonics. Generally, this frequency is so high that no more than one or two additional harmonics radiate at a significant intensity.

In the case of repeating impacts, the actual radiated noise spectrum is the superposition of the basic impact spectrum and the spectrum of the radiation efficiency of the hull. Thus, any resonances of the hull tend to amplify certain components of the impact spectrum.

2.1.6 RECIPROCATING MACHINERY NOISE

It might be expected that the dominant source of impulsive sounds from a diesel engine is the explosion and that other major sources are mechanical imbalances and pulsations generated in the intake and exhaust. (Intake and exhaust noises do dominate the spectra for automotive and rail applications but, in surface ships and submarines, remote intake and exhaust systems are used and the coupling of these sounds to the water is minimized.) However, a number of experiments have shown that the explosion is not the dominant source of impact sound in a marine diesel engine. That is,

1. motorized diesels are only a few decibels quieter than combustion-driven diesels,
2. radical changes in the firing cycle have little effect on the noise, and
3. reciprocating compressors have spectra similar to those of diesels.

The major source of structural vibrations and noise in the diesel engine, and other reciprocating machinery, is the impact of the piston against the wall of the cylinder as the direction of the side force reverses. The noise radiated in air by a large number of diesel engines having from 1 to 12 cylinders, 3 to 4200 HP, and 100 to 2000 rpm were measured and it was found that

$$L \text{ (at 50 cm)} = L_s + 10 \log HP + 18 \log N,$$

where

L_s = constant of 32 for 2-stroke and 34.5 for 4-stroke engine,
HP = horsepower, and
N = revolutions per minute.

The result, measured in dB//0.0002 dyn-cm², is in good agreement with theoretical analyses of the piston-impact mechanism and suggests some methods of reducing reciprocating engine noise. Such methods include

1. choosing the lowest possible rotational speed;
2. minimizing piston clearances;
3. using heavy, thick cylinders and radiating surface walls; and
4. applying vibration damping to plates and foundation structures.

2.1.7. FLOW PULSATIONS

Pulsations in the rate of flow in a sea-connected pipe, such as torpedo exhausts and sea-water pump intake and discharge lines radiate sound. For torpedo exhausts, which are essentially unbaffled pipes,

$$W = \varrho_o \omega^2 Q_o^2 / 8\pi c,$$

where

W = acoustic power (in Watts),
ϱ_o = mass density of water,
ω = angular frequency = $2\pi f$,
Q_o = volume flux or pulsating source strength vol/sec maximum amplitude,
c = sound speed in water.

For a pump intake or discharge line, the system is a pipe in an essentially infinite baffle and the radiated pressure is twice that of an unbaffled source. Thus,

$$W = \varrho_o \omega^2 Q_o^2 / 2\pi c.$$

The oscillating pressure is commonly measured in the pump inlet or outlet pipe. It is only an indirect measure of the sound because the radiation impedance of a pipe in an infinite baffle, for $ka < 0.25$, is given by

$$Z_{RAD} = \pi a^2 \varrho_o c[(ka)^2/2 + i(8/3\pi)(ka)] = R_{RAD} + iX_{RAD},$$

where

a = pipe radius,
Z = radiation impedance,
k = wave number,
R = resistance, and
X = reactance.

(Impedance, resistance, and reactance will be discussed in Chapter III.) The radiated power is given by

$$W = (3\pi/16)^2(\pi a^2)(p_i^2/\varrho_o c),$$

where p_i is the pressure of the pulsations measured inside the pipe within 1/8 wavelength of the end.

2.1.8. NONLINEAR VIBRATIONS

2.1.8.1 General

Nonlinear vibrations can sometimes be identified by one or more of the following characteristics:

1. subharmonics,
2. harmonics,
3. extremely stable frequencies, or
4. frequency dependence on driving force.

If a noise can be identified as originating from a nonlinear vibrating system, it can be the first step toward eliminating the problem. Some sample cases of nonlinear vibration are discussed below.

2.1.8.2. Chatter or Stick-Slip

Figure 2.6 illustrates a system that is subject to chatter or stick slip. If the belt is moving very slowly, the mass moves with it until the spring force breaks the static friction. The mass then snaps back until stopped by the spring and the dynamic friction on the belt; the process is then repeated. If the belt is moving rapidly, it reaches a speed above which the mass will not oscillate and it simply slides.

There are a wide range of belt speeds where the mass will vibrate at its natural frequency on the spring, i.e., where

$$f = (1/2\pi)(k/m)^{1/2}.$$

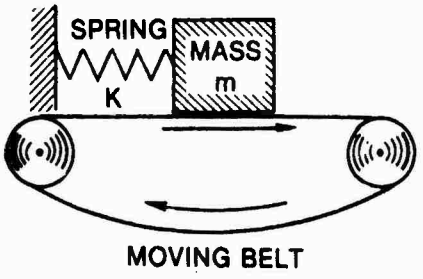

Figure 2.6. Chatter or Stick-Slip System

Figure 2.7 is a plot of the vibration spectrum versus time as the belt speed steadily increases from very slow to very fast.

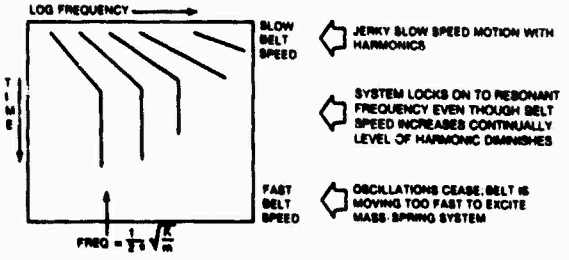

Figure 2.7. Vibration Spectrum Versus Time

Figure 2.8 shows a water-lubricated rubber spline bearing for a propeller shaft. For very low shaft speeds, there is a jerky movement. As shaft speed increases, there is a *lock-on* to a resonance frequency determined by the hull compliance (indicated by the two springs in the figure) and the rotary inertia of the structure holding the splines. The lock-on resonance will continue at a steady frequency as speed increases until it is too fast to excite vibration. The dynamics of this stick-slip case are influenced by the compliance of the rubber splines.

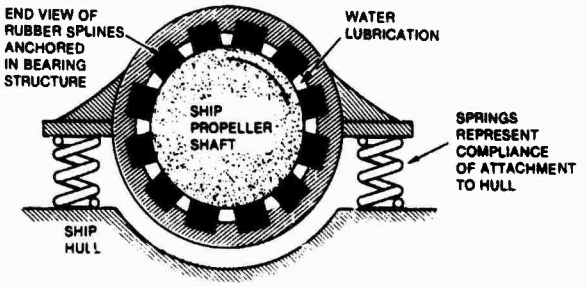

Figure 2.8. Water Lubricated Propeller Bearing

2.1.8.3. Flutter

Although flutter is a hydrodynamic source, it will be discussed here as a nonlinear vibration. It was once thought to be a problem only at high speeds (≈ 50 knots), but recent studies have shown that it can occur at speeds as low as 9 knots. Flutter is the flow-excited vibration of a strut that both deflects and rotates. The basic excitation force is vortex shedding; but flutter dynamics are a combination of hydrodynamic lift, vortex shedding, virtual mass of the water, mass of the member, and deflectional and torsional stiffness of the strut. The classic solution for the flutter problem is to greatly increase the torsional stiffness of the strut.

The phenomenon is subject to the same lock-on resonance frequency characteristics as is stick-slip. A frequency time plot of flutter for

continually increasing flow velocity is shown in figure 2.9.

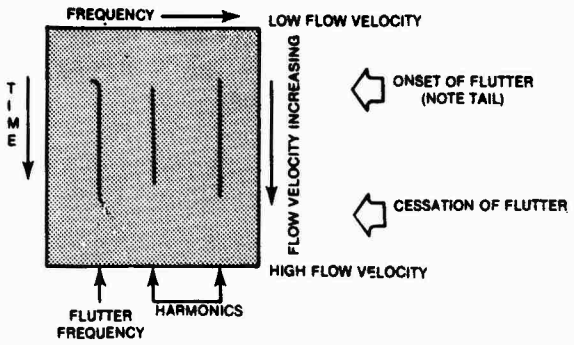

Figure 2.9. Flutter Frequency Time Plot

2.1.8.4. Bearing Oil-Whip

Figure 2.10 illustrates the bearing oil-whip effect produced by well lubricated sleeve journal bearings on vertical rotating shafts. Its characteristic frequency is 1/4 to 1/2 of the rotational frequency of the shaft.

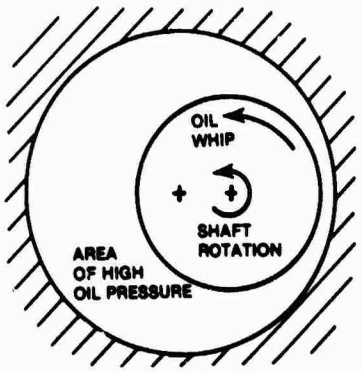

Figure 2.10. Bearing Oil-Whip Effect

2.1.8.5. Rattles

Rattles are caused by the vibration of equipment that has extremely nonlinear springs or restoring forces. They are characterized by either a random or relatively constant frequency of possibly intermittent occurrence.

Rattles are generally of a much higher vibration amplitude than other structural vibrations. They can be found by tapping suspect equipment with a rubber mallet and listening; the search for rattles should include the entire ship. Fittings should, of course, be designed to avoid rattles.

2.1.8.6. Belleville Spring

A Belleville spring (alternately, Belleville washer or spherical spring) can, at that same time, apply a high static force and be extremely compliant to low amplitude vibrations. Its load deflection curve begins steeply and then decreases as shown in figure 2.11. An example of the Belleville application is the spring under the stress rod retainer of a tonpilz hydrophone.

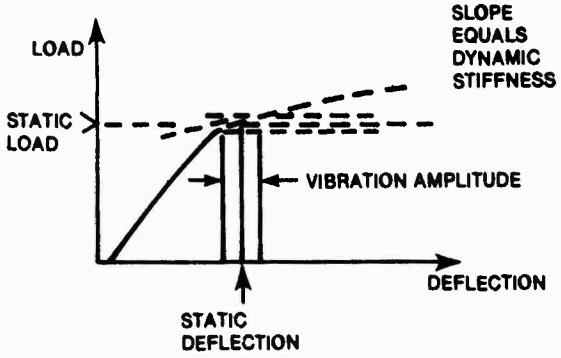

Figure 2.11. Belleville Spring Application

2.2. HYDRODYNAMIC NOISE SOURCES

Hydrodynamic noise, which is caused by ship motion through the water, and associated mechanisms, may result from a wide variety of sources. Some of the power required to drive a ship through the water is converted into acoustic energy. Although the energy radiated acoustically is very small, i.e., a negligible percentage, it can be impressive in terms of acoustic power. Therefore, an understanding of the mechanisms that convert such power into acoustic energy is important.

The variety of mechanisms is intriguing. They include the (1) impact of the rotating pressure field of the propeller on the hull (which can sound the same as a hammer beating on the hull plating), (2) rapid whirring of a strut being whipped by the water eddying around it, (3) high pitch of a singing propeller blade, (4) resonant *panting* of the sides of main ballast tank in a submarine, (5) rattle of a piece of loose

gear in the superstructure, or (6) snapping and crackling sound of cavitation. The mechanisms involved are grouped by theoretical acousticians into the classes of

1. monopole, or volume, sources that radiate sound by changing the size of the body in the water (an underwater explosion is an example);
2. dipole, or force, sources that create sound by the movement of a body normal to its surface (a vibrating plate surrounded by water is an example); and
3. quadrupole, or shear, sources that create sound by a movement of a body parallel to its own surface (a plate moving endwise through the water is an example).

Figure 2.12 illustrates these sources conceptually.

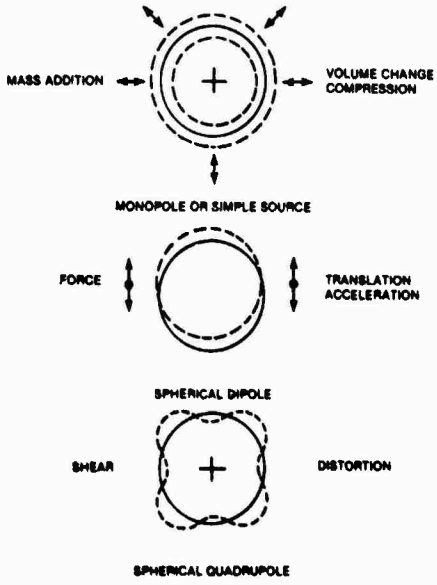

Figure 2.12. Hydrodynamic Noise Sources

The acoustic conversion efficiency is greatest for monopole sources and least for quadupoles. Hence, when monopole sources exist, they usually dominate the radiated spectrum. Dipole sources may be important when monopole sources are reduced or when the source is near a hydrophone. Quadrupole sources are unimportant in water.

2.2.1. MONOPOLE SOURCES

The monopole source (see figure 2.12) radiates sound by the mechanism of expanding and contracting. A simple treatment of such a source considers it to be a sphere having a sinusoidally varying radius: i.e.,

$$a_t = a_o + \xi e^{i\omega t},$$

where

a_t = radius at time, t,
a_o = mean radius,
ξ = amplitude of change in radius, and
ω = angular frequency.

This pulsation creates a time dependent movement of water into and out of the source. The radial velocity at the surface of the source, U_s, is the time derivative of the radius, i.e.,

$$U_s = da_t/dt = i\omega\xi e^{i\omega t}.$$

The volume flux, Q_o, of the water is the volume rate at which it moves into and out of the source: i.e.,

$$Q_o = 4\pi a_o^2 U_s.$$

Since the pressure variation with distance is equal to the mass multiplied by the acceleration,

$$-(dP/dr) = \rho_o(dU_s/dt) = (\rho_o/4\pi a_o^2)dQ_o/dt$$

where

P = pressure at distance, r,
r = distance from center of source, and
ρ_o = mass density of water.

When integrated and evaluated at $r = a_o$,

$$P = (\rho_o/4\pi a_o)(dQ_o/dt).$$

Hence, for the surrounding water, with the introduction of the spherical wave equation,

$$P = (\rho_o/4\pi r)[i\omega Q_o e^{i(\omega t - kr)}],$$

where k = wave number $= 2\pi/\lambda = \omega/c$.

2.2.2. DIPOLE SOURCES

The dipole source may be considered the net of two simple monopole sources a small distance apart and exactly 180° out-of-phase. That is, such that the water moves out of one source as it moves into the other (see figure 2.13). When the pressure fields of these two sources are calculated,

$$P = (\omega Q_o Q_o/4\pi r)(2ka_D \cos\theta)e^{i(\omega t-kr)},$$

where

a_D = 1/2 the distance between sources and
θ = angle from axis passing through sources.

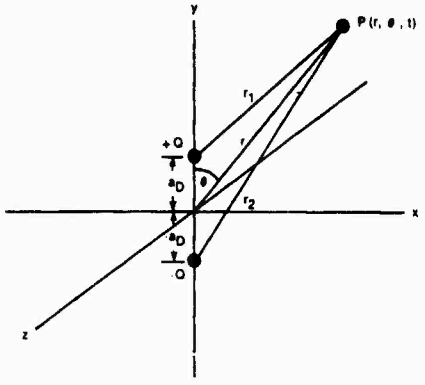

Figure 2.13. Dipole Source

2.2.3. QUADRUPOLE SOURCES

The quadrupole source may be considered to be four sources arranged such that there is no flux into the medium, half the sources are 180° out-of-phase with the other half, and there is no force applied along the coordinate axis. Lateral and longitudinal arrangements producing these results are shown in figure 2.14.

If the pressure fields from the four sources are added we have for the longitudinal and lateral cases, respectively,

$$P = i(\omega Q_o Q_o/4\pi r)(ka_Q)^2 \sin^2\theta\, e^{i(\omega t-kr)}$$

and

$$P = i(\omega Q_o Q_o/4\pi r)(ka_Q)^2 \sin\theta\cos\theta\, e^{i(\omega t-kr)},$$

where a_Q = 1/2 spacing between sources.

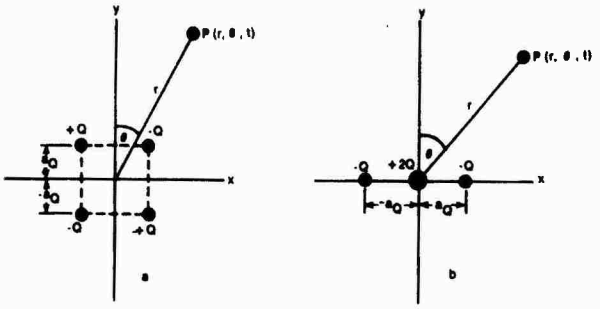

Figure 2.14. Quadrupole Sources

2.2.4. THE SOURCES SUMMARIZED

If we summarize the above discussion and add the expression for acoustic power, we have

MONOPOLE

Sound Pressure

$$P = i(\omega Q_o Q_o e^{i(\omega t-kr)})/4\pi r$$

Acoustic Power

$$W = \omega^2 \rho_o Q_o^2/8\pi c$$

DIPOLE

Sound Pressure

$$P = (\omega Q_o Q_o)(2ka_D)\cos\theta\, e^{i(\omega t-kr)}/4\pi r$$

Acoustic Power

$$W = \omega^4 \rho_o Q_o a_D^4 U_o/24c^3$$

QUADRUPOLE

Sound Pressure (Lateral)

$$P = i(\omega Q_o Q_o)(ka_Q)^2 \sin\theta\cos\theta\, e^{i(\omega t-kr)}/4\pi r$$

Acoustic Power (Lateral)

$$W = (\omega^2 \rho_o Q_o^2)(ka_Q)^4/120\pi c$$

Sound Pressure (Longitudinal)

$$P = i(\omega Q_o Q_o)(ka_Q)^2 \sin^2\theta\, e^{i(\omega t-kr)}/4\pi r$$

Acoustic Power (Longitudinal)

$$W = (\omega^2 \rho_o Q_o^2)(ka_Q)^4/40\pi c,$$

where

P = sound pressure,
W = acoustic power,

ϱ_o = mass density,
Q_o = volume flux, (maximum amplitude),
a = 1/2 distance between sources,
k = wave number = $2\pi/\lambda$,
λ = wavelength,
r = distance from source, and
c = sound speed.

When the acoustic efficiency, η_{ac}, is compared for the three modes on the basis of mach number, M, we have

$$\eta_{ac} \text{ (Monopole)} \approx M$$
$$\eta_{ac} \text{ (Dipole)} \approx M^3$$
$$\eta_{ac} \text{ (Quadrupole)} \approx M^5.$$

The speed of sound at MACH 1 is 5 kft/sec. Naturally, the speed of a ship or hydrodynamic disturbance ($M_v < 2 \times 10^{-2}$ M) is small in comparison. The low MACH values in water lead to the conclusion that the importance of a hydrodynamic source will depend on whether its basic radiation mechanism is monopole, dipole, or quadrupole. Typical causes of these hydrodynamic acoustic sources are as follows:

1. *Monopole Sources*
   a. cavitation,
   b. flow pulsations (e.g., torpedo exhausts, sea-connected pumps),
   c. pulsating bubbles, and
   d. vortex-excited cavity resonances.
2. *Dipole Sources*
   a. vortex shedding,
   b. blade oscillating forces,
   c. singing,
   d. control-surface oscillating forces, and
   e. boundary layer oscillating pressure.
3. *Quadrupole Sources*
   a. wake turbulence and
   b. free turbulence in boundary layer.

Sounds such as those radiated by nonrigid plates excited by oscillating pressures (e.g., rotating propeller pressure fields or turbulent boundary layers) are not as easily classified.

2.2.5. CAVITATION

2.2.5.1. Definition

Cavitation is defined as *the rupture of a liquid or of a liquid-solid contact*, where *rupture* is the formation of a macroscopic bubble. Generally, cavitation is associated with a local decrease of static pressure in the liquid.

The various types of cavitation may be classified according to

1. *Where the rupture takes place, i.e.,*
   a. at a surface or
   b. in the volume of liquid.
2. *Cause of reduced local static pressure, i.e.,*
   a. application of static tensile stress;
   b. flow of a liquid inside a conduit, e.g., a Venturi, valve, or pipe bend;
   c. flow of a liquid over a body, e.g., a propeller blade, strut, hull, or sonar dome;
   d. vortex motion of a liquid, e.g., vortices, turbulence; and
   e. acoustic field at a focal point in liquid or on the transducer face.
3. *Contents of the bubble, i.e.,*
   a. primarily gas or
   b. vapor.
4. *Pattern, i.e.,*
   a. transient (bubbles grow and collapse) or
   b. steady (large cavities).

The major areas of interest in relation to underwater acoustics are

1. propeller cavitation noise,
2. self-noise from sonar dome cavitation,
3. radiated noise from cavitating pumps, valves, and pipe lines,
4. limitations on active transducer output,
5. ambient noise from wave-produced bubbles.

2.2.5.2 Conditions For Cavitation Inception

Cavitation occurs when the local static pressure drops below some critical value. This value varies with the type of liquid, its temperature, surface tension, amount of dissolved gas and, most importantly, the size and distribution of residual nuclei. Also, cavitation usually occurs when the local static pressure approaches absolute zero. Most liquids are unable to withstand a tensile stress without rupturing because they usually contain numerous microscopic and submicroscopic

bubbles that act as nuclei in the formation of cavitation bubbles.

The surface tension of such a microscopic bubble will create a pressure difference between the internal forces and the surrounding fluid. If this pressure differential is defined as ΔP, then,

$$\Delta P = P_{in} - P_{out} = 2\sigma/r,$$

where

P_{in} = internal pressure,
P_{out} = external pressure,
σ = liquid surface tension, and
r = bubble radius.

The pressure difference is plotted in figure 2.15. Water without nuclei can sustain tensile stresses greater than 1000 atmospheres.

The gas content of a liquid provides the nuclei for cavitation and if it is close to saturation at the ambient static pressure, the bubbles will contain mostly gas. Such bubbles do not collapse with much force and, therefore, do not produce much noise or erosion.

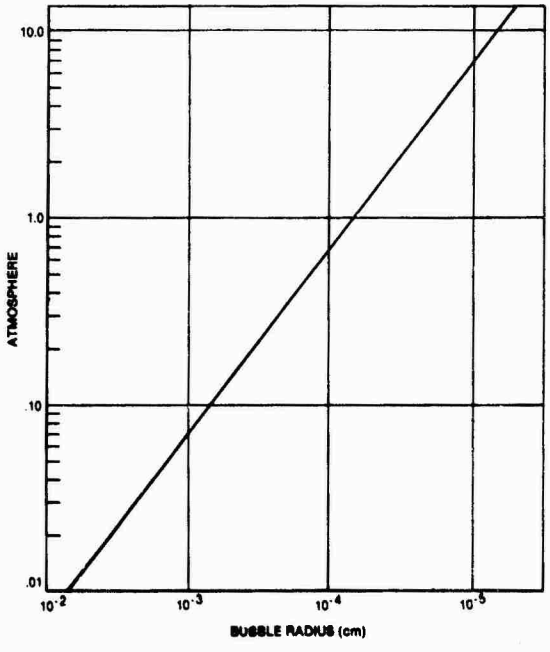

Figure 2.15. Internal Pressure from Bubble Surface Tension (Water)

Vaporous cavitation, however, is an important source of noise and erosion. It is initiated when the vapor pressure, P_v inside the bubble exceeds the internal pressure discussed above, i.e.,

$$P_v \geq P_{in} = P_{out} + \Delta P.$$

Hence, when P_{out} is less than the vapor presssure minus ΔP, the cavity will begin to form at the critical pressure, P_c, i.e.,

$$P_c \cong P_v - 2\sigma/r,$$

where r is the radius of the largest nuclei of sufficient abundance in the liquid. The dependence of P_c on the size of the nucleus explains the variability that results in cavitation inception experiments. (Repeatable values are found when the pressure is increased until cavitation disappears.) Generally,

$$P_c \cong P_v.$$

2.2.5.3. Cavitation Index

The most common cause of a reduction of local static pressure in a moving fluid is associated with an increase in the local flow velocity relative to the reference value. This concept is illustrated in figure 2.16. The equation for the relationship is

$$P_o + (\rho/2)V_o^2 = P_{min} + (\rho/2)V_{max}^2, \text{ i.e.,}$$

$$(P_o - P_{min})/(\rho/2)V_o^2 = (V_{max}/V_o)^2 - 1$$

$$\approx (A_o/A_c)^2 - 1,$$

where

A_o = area at point 0 and
A_c = area at choke section.

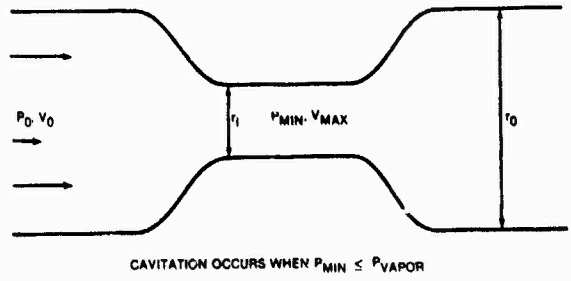

Figure 2.16. Reduction of Local Static Pressure in a Pipe

Since cavitation may occur when $P_{min} \leq P_v$, a dimensionless coefficient, that is primarily a function of geometrical factors and a measure of cavitation susceptibility, may be defined for each hydraulic system. This coefficient is the critical, or inception, cavitation index.

For the pipe construction considered here, we may choose K_i as the cavitation index, i.e.,

$$K_i \cong (P_o - P_{min})/(1/2)\rho V_o^2,$$

where cavitation occurs when $K_i = K_c$ and

$$K_c \cong (P_o - P_v)/(1/2)\rho V_o^2.$$

Figure 2.17 shows the pressure coefficient, C_p, for the type airfoil section such as might be used on a ships propeller. The minimum value of C_p is a measure of the critical cavitation index, K_c. The more susceptible the body or system is to cavitation, the higher the inception cavitation index.

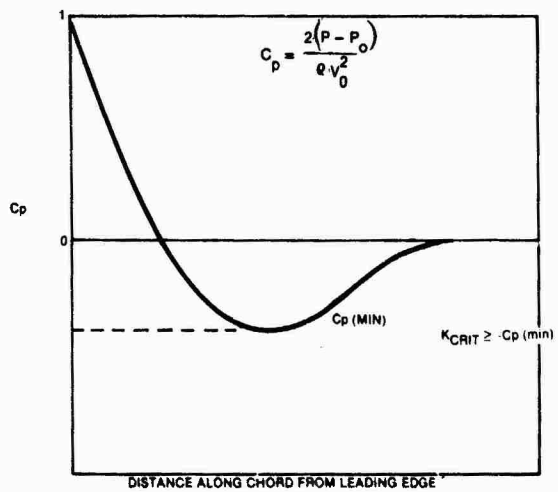

Figure 2.17. Pressure Coefficient for an Airfoil Section

The critical, or inception, cavitation index is a function of the geometry of the particular system. There is another cavitation index that is a function of the velocity and static pressure of the ambient flow. It may be defined in a manner similar to the cavitation index for the pipe, i.e.,

$$K_f = (P_o - P_v)/(1/2)\rho V_o^2,$$

where

K_f = flow cavitation index,
P_o = fluid pressure,
P_v = vapor pressure, and
V_o = speed of flow past body.

When $K_f > K_c$ cavitation does not occur and when $K_f < K_c$ it does occur. The lower the K_f of the flow, the more likely it is that high cavitation will occur.

If the water temperature and, hence, the vapor pressure and density are assumed to be a standard value, the water pressure becomes the important variable. In some instances the vapor pressure and density terms are omitted. Such is the case for a body moving in sea water at depth h and speed V, where the cavitation index caused by the flow, i.e., the operating cavitation index, K_o, is given by

$$K_o = P_o/V^2,$$

$$K_o \approx 64(h + 30\,ft)/V^2\,(in\ ft/sec),$$

or

$$K_o \approx 19.6(h + 9\,m)/V^2\,(in\ m/sec),$$

where

1 knot = 1.69 ft/sec = 0.515 m/sec.

To illustrate the use of the index consider a 15 knot submarine (a streamlined body) operating at a 400 ft depth. For this case

$$K_o = 64[430/(15)^2(1.69)^2] \approx 42.$$

Consider also a 40 knot torpedo at a 15 ft depth. For this case

$$K_o = 64[45/(40)^2(1.69)^2] \approx 0.63.$$

Generally, the operating critical cavitation index, K_{oc} = 0.2 to 0.5 for a streamlined object, 1.5 to 2.5 for a sharp protuberance, and 3 to 6 for a stalled airfoil section. It is apparent, then, that cavitation will not occur for the submarine and will occur for the torpedo in the examples given above.

2.2.5.4 Propeller Cavitation

Because the flow velocities of the propeller blades are higher than the forward speed of the

ship, the propeller usually cavitates first. The tip sections of a propeller move the fastest and are generally most susceptible to cavitation. Therefore, it is useful to define a special cavitation index for propellers, using the tip velocity as reference, i.e.,

$$K_{tip} = (P_o - P_v)/(1/2)\varrho V_{tip}^2,$$

where

$$V_{tip}^2 \cong V_o^2 + (\pi nD)^2$$
$$\cong (\pi nD)^2[1 + (J_o/\pi)^2]$$

and

V_o = speed of advance,
n = propeller rotational speed,
D = propeller diameter, and
J_o = advance ratio of propeller = V_o/nD.

The points where cavitation occurs on propellers are the

1. driving face;
2. back, or suction, surface;
3. tip vortex; and
4. hub vortex.

The point at which cavitation first occurs is a function of the angle of the flow relative to the blade, which is, in turn, a function of the advance ratio of the particular propeller.

Driving-face cavitation first occurs at high advance ratio values, whereas the other three types occur at low values. There is a value of J_o for which the critical index of the propeller is minimum and it increases sharply as the advance ratio deviates either side of minimum (see figure 2.18).

Propeller cavitation inception tests have been made in water tunnels that provide a uniform in-flow to the propeller. The critical cavitation index determined under nominal operating conditions has little relation to those measured because the wake of a ship is highly non-uniform; the propeller blade sees different in-flow conditions at each angular position. However, an approximate understanding of events can be developed if such variations are considered to be changes in advance ratio as the blade rotates. The critical cavitation index is then determined by the minimum or maximum value of J_o.

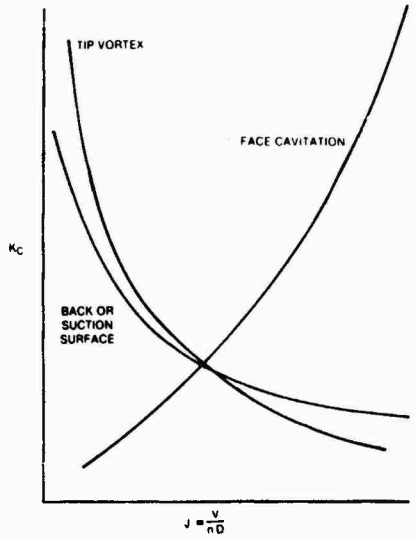

Figure 2.18. Critical Cavitation Index as a Function of Advance Ratio

The non-uniformity of the wake not only increases the critical index, it also causes the cavitation level to vary as the blade rotates. Near inception speed, the blade cavitates only during a small portion of each rotation and produces a clicking sound.

Figure 2.19 shows the degree of cavitation, as a function of the tip-cavitation index, that is likely to characterize ship and submarine propellers. It is apparent that as the index becomes smaller than 6, cavitation will be more severe.

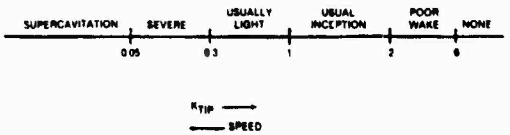

Figure 2.19. Cavitation as a Function of Tip-Cavitation Index

2.2.5.5 Production of Noise by Cavitation

A typical propeller blade cavitation bubble forms near the beginning of the cavitation region and grows until it arrives at the end of the negative pressure zone, where it collapses rapidly. If the bubble contains residual gas, it rebounds several times before disappearing as illustrated figure 2.20.

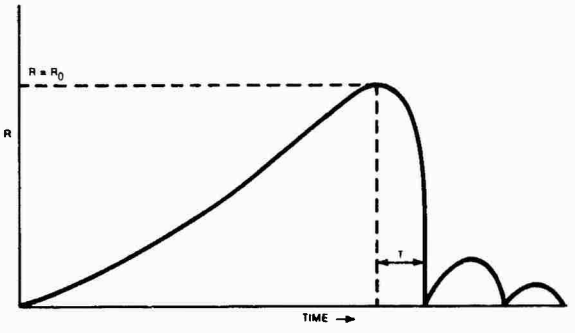

Figure 2.20. Cavitation Bubble Radius as a Function of Time

The energy radiated acoustically by each bubble collapse can be expressed as a fraction of the potential energy of the bubble before it collapses, i.e.,

$$E_A = \xi(4/3)\pi R_o^3 \Delta P = \xi V_o \Delta P,$$

where

E_A = acoustic energy,
ξ = function of R_o/R_f,
R_o = initial radius,
R_f = final radius,
ΔP = difference between internal and external pressure, and
V_o = volume of bubble.

Experimental ξ values of the order of 1/3 to 1/2 have been found for a ΔP of 1 to 2 atmospheres.

It appears that the acoustic energy radiated by each bubble is proportional to its maximum volume and the collapse pressure. Thus, the radiated sound power will be proportional to the number of larger bubbles produced per second multiplied by the volume of each, i.e., by the volume of cavitation bubbles produced per second. Therefore, the sound power is

$$W_{ac} \cong NE_A = \xi NV_o(\Delta P),$$

where

W_{ac} = acoustic power,
N = number of bubbles per second,
E_A = acoustic energy per bubbles, and
V_o = volume of bubble.

The acoustic power (expressing the volume in cubic centimeters and the pressure in atmospheres) is given by

$$W_A \cong (1/40)NV_o(\Delta P) \text{ Watts.}$$

Therefore, production of 40 bubbles per second, each having a volume of about 0.1 cm and collapsing under a pressure of 10 atmospheres, would produce about 1 W of acoustic power.

The radiated spectrum from cavitation bubble growth and collapse shows a 1 to 2 octave wide peak at a frequency that is somewhat less than the reciprocal of the collapse time. The spectrum rises steeply (12 to 15 dB/oct) at the lower frequencies; the peak may be estimated from

$$f_o \cong 1/2\tau \cong (1/2R_o)(\Delta P/\varrho)^{1/2},$$

which shows that the peak moves to lower frequencies as bubble size increases.

2.2.5.6. Noise Spectra from Propeller Cavitation

A cavitating propeller creates a random distribution of growing and collapsing bubbles. Peak frequencies vary from the order of 5 kHz for a small propeller near inception to less than 100 Hz for a large propeller that is cavitating vigorously. The lower peak frequencies are characteristic of surface ships and the higher ones are characteristic of deep running torpedoes and submarines.

Cavitation increases with increasing speed and constant depth and with decreasing depth and constant speed. The sequence of cavitation spectra are somewhat different, as illustrated in figure 2.21.

At constant depth, the increase in speed increases the amount of cavitation by creating larger bubbles. This increases the noise produced and lowers the peak frequency. At constant speed, increased depth (1) decreases cavitation and, thus, the size of the largest bubbles and (2) increases the collapse pressure. The pressure increase causes the peaks to move to the higher frequencies that are of concern to sonar operators and the cavitation produces more noise in the sonar band than it would at shallower depths. The result is the *anomalous*

depth effect, often observed at the higher frequencies, in which cavitation noise in the sonar band increases although actual cavitation decreases.

The amount of noncondensible gas in the cavitation bubble controls the final stages of collapse and, hence, the amount of noise produced. Significant noise reduction can be achieved by pumping air into the cavitation region of a propeller.

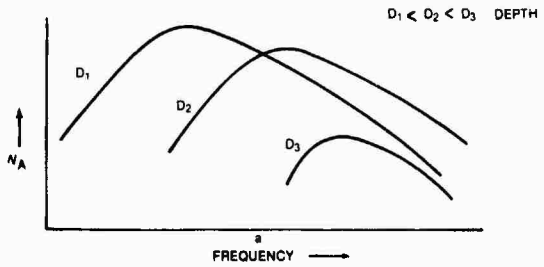

Figure 2.21a. Constant Speed, Variable Depth

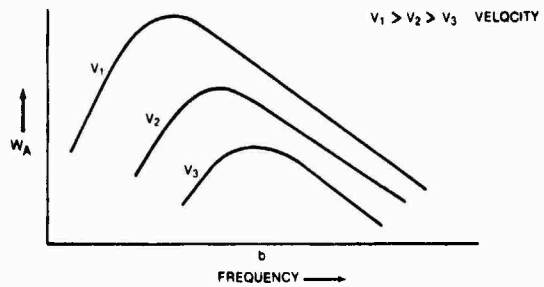

Figure 2.21b. Constant Depth, Variable Speed

Figure 2.21. Cavitation Spectra

2.2.5.7 Effects of Ship Wake on Propeller Cavitation Noise

The non-uniformity of the wake has an especially significant effect on the noise produced by a cavitating propeller. Because the cavitation index is determined by the most severe in-flow condition that the blade is subject to during rotation near inception speed, cavitation occurs only during part of each revolution. It may occur on only one blade, resulting in a clicking sound having the shaft-rotation-frequency repetition rate. As cavitation increases, all blades will cavitate and the pulses will occur at the blade-rate frequency. It is this modulation of the broadband cavitation noise that is used to detect and classify a cavitating target using passive sonar. (Even when all blades are cavitating, one will usually cavitate a bit more severely, which provides an accent that enables the sonar operator to calculate shaft revolutions per second.)

Cavitation varies as the in-flow conditions cause it to be more and then less severe. This periodic change in volume results in direct radiation of sound at the blade passage frequency and its harmonics.

2.2.6 OSCILLATING-FORCE NOISE SOURCES

2.2.6.1 Oscillating Hydrodynamic Excitation

When a rigid surface, which is small compared with a wavelength, is subject to an oscillating force, sound is radiated according to

$$P(t) = [F(t) \cos \theta]/4\pi rc$$

and

$$I = P^2/\varrho c = (F^2/16\pi^2 r^2 \varrho c^3) \cos^2 \theta,$$

where

I = acoustic intensity
$P(t)$ = time and spacial varying pressure,
$F(t)$ = time and spacial varying force,
r = distance from source,
c = sound velocity,
θ = angle from normal to the surface, and
ϱ = mass density of fluid.

If we express the oscillating force in terms of a dimensionless root-mean-square (rms) oscillating lift coefficient, then

$$F_{rms} = \omega(\varrho/2)V_o^2 A C_f,$$

where

ω = angular frequency,
V_o = fluid velocity,
A = surface area,
C_f = rms oscillating lift coefficient, hence

$$I = (\varrho V_o^3 A/16r^2)(f^2 A/V_o^2) C_f^2 M_o^3 \cos^2 \theta.$$

Total acoustic power equals the integral of the intensity at a surrounding surface, i.e.,

$$W = \int\int I ds$$
$$= (\pi/6)(\rho V_o^3 A/2)(f^2 A/V_o^2) C_f^2 M_o^3,$$

where

I = acoustic intensity,
f = frequency,
M_o = mach number = V_o/c,
Note: S = Strouhal number = fL/V.

Since the quantity f^2A/V_o^2 is directly proportional to the square of a Strouhal number (which is essentially constant) the equations presented above show that the acoustic intensity and radiated power are proportional to the sixth power of the speed of the ship. This is, of course, a direct result of the dipole nature of the oscillating force source.

2.2.6.2. Vortex Shedding as a Noise Source

Rigid bodies moving in a fluid are subject to oscillating forces caused by fluctuations of the flow and of the wake. Wake fluctuations are characterized by alternating vortices that produce alternating transverse forces. The acoustic efficiency of this process, based on experimentally determined values for the lift coefficient and Strouhal number for a steady flow past a cylinder, may be expressed as

$$\eta_{AC} \approx (3)10^{-3} M_o^3 (\ell/h_v)$$

where

η_{AC} = acoustic efficiency,
ℓ = correlation length of shed vortices, and
h_v = vortex shedding distance, i.e., distance between consecutive eddies.

(The correlation length, ℓ, is the length of vortex wake that is correlated. Therefore, the more uniform the eddy shedding, the more correlated the eddy wake and the longer the correlation length.)

The acoustic efficiency is thus directly proportional to the ℓ of the shed vortices and inversely proportional to h_v. It has been shown that when the body shedding the vortices is completely rigid, $\ell \approx 4 \times h_v$. When the body vibrates, *sings*, the motion tends to lock in the vortices and ℓ becomes much larger.

When the body is rigid, i.e., not *singing*, vortex shedding can become a significant source of sound for MACH numbers in excess of approximately 0.015 or 0.01. Although ship speeds are not high enough to create such values, propeller blade speed often is. The expression for rotating propeller blades yeilds

$$\eta_{AC} \cong 10^{-3} M_{tip}^3.$$

The spectrum of vortex sounds is generally broadband, covering approximately an octave.

2.2.6.3 Propeller Broadband Noise and Singing

Propellers generate substantial amounts of acoustic vibration energy. This noise, created by the turbulent wake flowing over the blades, is broadband in nature and increases with increasing speed. Because propellers are highly undamped structures, they are excited by the turbulent flow and radiate at natural frequencies in accordance with the efficiency of the radiating mechanism.

Singing occurs when the vortex-shedding frequency coincides with a resonance frequency of the blade for which a significant fraction of the trailing edge moves coherently. The oscillating force from the shed vortices causes the blade to vibrate. This, in turn, causes an increase in the coherent length of the vortices, with an attendant increase in the force and vibration. The sound is then radiated at the singing frequency. The intensity is greater than that for normal rigid-body vortex sounds because ℓ and C_f increase.

A singing propeller radiates sound by the

1. oscillating force that radiates as though the blade were not vibrating (the blade vibration serving to lock in the vortex pattern) and
2. vibration of the blade (if the blade is small compared with wavelength, its radiation is dipole).

It can be readily shown that the sound radiated at resonance by the vibrating blade can be Q

times as great as that radiated by the oscillating force, where Q measures the sharpness of the resonance. (See paragraph 3.1.2.).

Singing can generally be prevented by (1) altering the thickness of the trailing edge, so that shedding frequencies do not coincide with blade resonance frequencies; (2) scalloping the trailing edge, so that long vortices cannot form; and (3) damping the blades.

2.2.6.4. Propeller Sounds in a Non-Uniform Wake

A propeller blade in a non-uniform wake is subject to oscillating forces. It can be shown that sound is radiated at frequencies that are multiples of the blade-passage frequency, i.e.,

$$f_m = mnB = m(NB/60),$$

where

m = order of the harmonic,
n = revolutions per second,
N = revolutions per minute, and
B = number of blades.

This is a dipole (oscillating force) source.

2.2.7 FLOW NOISE

The flow over the hull of a ship and, particularly, over a sonar dome is an important sonar self-noise consideration. Such noise is caused by the turbulent flow of water across the exterior surface as the ship moves through the water. The flow contains pressure fluctuations that can produce vibrations in the structure of the sonar dome, which then radiate noise to the hydrophones. The noise is thus generated near the hydrophones and reaches them with little attenuation. Much effort has been given to the study of flow excited vibration of plates and structures. However, practical solutions to the problem remain difficult.

Flow noise may be considered to be composed of hydrodynamic, structural, or resonant; and acoustic components. The hydrodynamic component (associated with convective flow velocity, U_c, and wave number $k_h = \omega/U_c$), in which most of the energy exists, does not couple well to ship structures and is not usually a significant cause of dome or hull vibration. The acoustic component (associated with speed of sound in water, c, and wave number $k_a = \omega/c$), can contribute significantly, depending on the degree of structural mode coupling. The principal contribution is from the structural, or resonant, component (associated with resonant wave speeds in the structures, c_r, and wave number $k_r = \omega/c_r$). In this case, the frequency component may couple well with the hull structure, which provides an effective noise generation mechanism. Generally, $k_h >> k_r > k_a$ because U_c is so much slower than c.

The phenomenon is illustrated in figures 2.22 through 2.29. Figure 2.22 illustrates a model plate over which water is flowing. The vessel velocity is U_o and the dimensions of the plate are (a), long, and (b), wide. The depth of the cavity, e.g., the sonar dome, is d. Some turbulent wall pressure power spectra are plotted as a function of Strouhal number in figure 2.23, where

$\Phi(\omega)$ = pressure power spectral density,
U_o = flow velocity,
ϱ = mass density of fluid (water),
δ^* = turbulent boundry layer displacement thickness (i.e., the distance the undisturbed flow is moved away from the boundary by the lowered velocities in the boundary layer), and
ω = angular frequency.

It can be seen from the curve that the pressure spectrum remains reasonably constant at low frequencies and decreases rapidly at high frequencies.

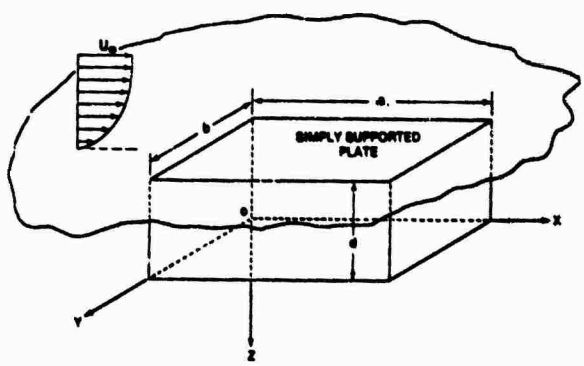

Figure 2.22. Model Plate over which Water is Flowing[1]

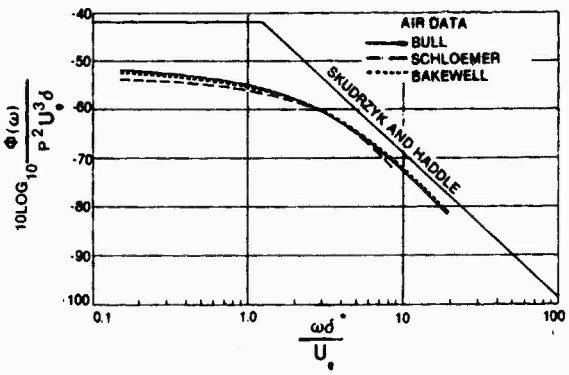

Figure 2.23. Turbulent Wall Pressure Power Spectra as a Function of Strouhal Number

The measured and computed ratios of plate displacement spectral density to turbulence spectral density are presented in figure 2.24. The greatest response of the plate is at the first modal resonance frequency. Although the other modal frequencies are missed, the overall envelope of the peaks agree with the measured values. Although this treatment does not include fluid loading on the plate, it does graphically illustrate the excitation phenomena.

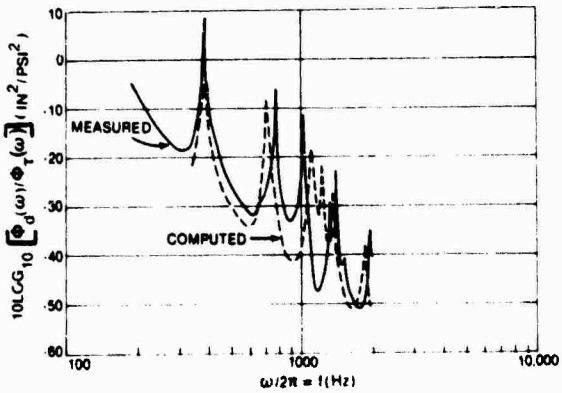

Figure 2.24. Ratios of Plate Displacement to Turbulence Spectral Density

Figure 2.25 shows the effect on the velocity peak spectrum (the envelope of the peaks in figure 2.2.4) of moving the point of interest to different locations in the central portion of the plate. Note that the effect is small.

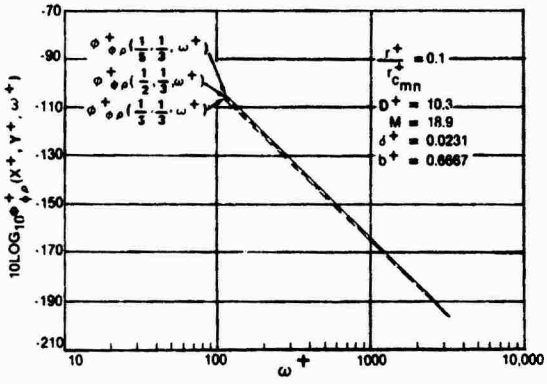

Figure 2.25. Plate Coordinate Effect on Dimensionless Plate Velocity Peak Spectrum

Figure 2.26 illustrates the decrease in the velocity peak spectrum as the plate damping factor is increased. The cross plot for $\omega^+ = 200$ in figure 2.27 shows the definite downward trend as damping increases and figure 2.28 shows the computed dimensionless plate velocity power spectrum at dimensionless coordinates 1/2 and 1/3.

Figure 2.29 shows that when plate stiffness is increased, the modal frequencies increase and the magnitude of the peaks decrease. Although the peak spectral density begins at a higher frequency, it changes little with increased plate stiffness.

The applicable equation (except in the portion a few wavelengths away from the edge of the plate) for frequencies of interest to determine the dimensionless plate velocity peak spectrum is

$$10 \log_{10} \Phi^+_{\phi_p}(\omega^+) = -159.9 - 20 \log_{10} [(100r^+)/(r^+_{c_{mn}})(\delta^+/M)] - [68.5 + \log_{10}(100r^+/r^+_{c_{mn}})] \times \log_{10}(\omega^+\delta^+/4.62),$$

where

$\omega^+ > \omega^+_{11}$,
$\omega^+ > 1.932/\delta^+$,
$\omega^+_{11} = \pi^2(D^+_\pi{}^{1/2})(b^{+2} + 1)/h^{+2}$,

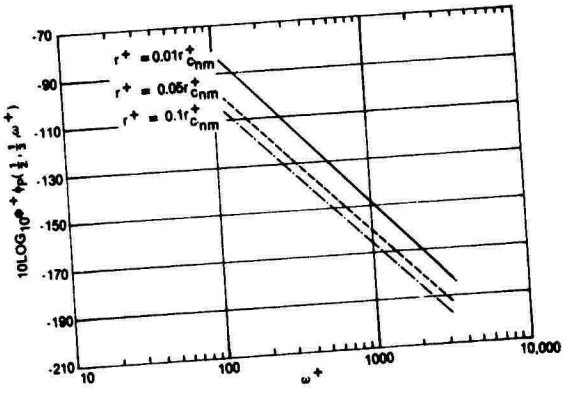

Figure 2.26. Plate Damping Effect on Dimensionless Plate Velocity Peak Spectrum

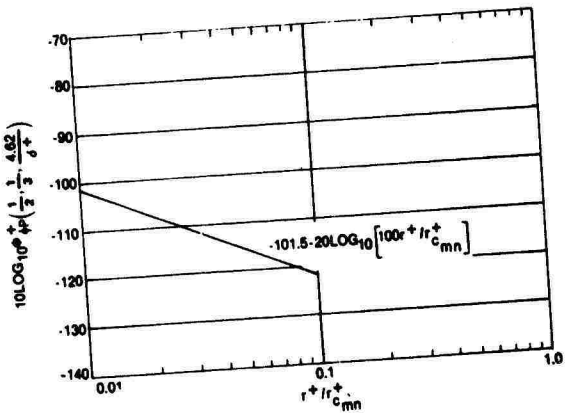

Figure 2.27. Plate Damping Effect on Dimensionless Plate Velocity Peak Spectral Density

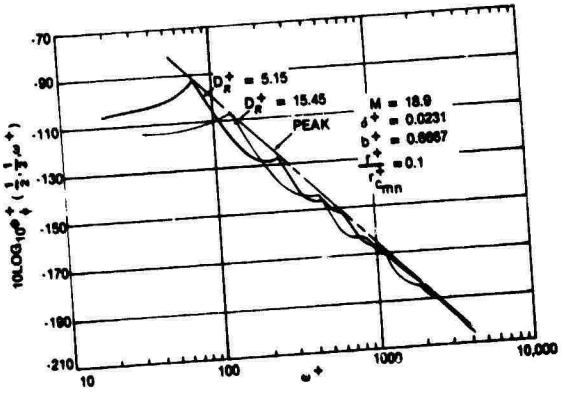

Figure 2.28. Computed Dimensionless Plate Velocity Power Spectrum at Dimensionless Plate Coordinates 1/2 and 1/3

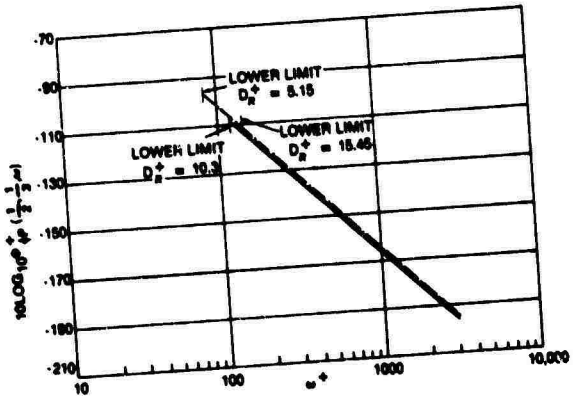

Figure 2.29. Plate Rigidity Effect on Dimensionless Plate Velocity Peak Spectrum

$r^+_{c_{mn}} = 2\omega^+_{mn}$,
$\Phi^+_{\phi_p} = (\phi_{\phi_p})a/\alpha^2\mu^2U_c^3$ = dimensionless plate velocity peak spectral density,
$\omega^+ = \omega a/U_c$,
$\delta^+ = \delta^*/a$,
$D^+_R = D_R/\mu U_c^2 a^2$,
$b^+ = b/a$,
$M = \varrho a/\mu$,
$r^+ = ra/\mu U_c$,
$r^+_c = r_{c(mn)}a/\mu U_c$,

and where

a = linear plate dimension (x coordinate),
b = linear plate dimension (y coordinate),
μ = mass of plate per unit area,
U_c = mean convection velocity of turbulent boundary layer, i.e., *speed of eddy along plate*,
δ^* = boundary layer (displacement) thickness,
D_R = plate flexural rigidity,
ω = angular frequency,
ϱ = mass density of fluid,
m,n = mode number,
r = plate damping coefficient per unit area, and
r_c = critical plate damping coefficient.

Figure 2.30 shows the agreement of this formula with a computed spectrum. Although the equation is quite complex, it does show that the acoustic pressure within the cavity is a function of frequency, cavity size, and bounding wall stiffness. For small cavities having stiff boundaries, the acoustic pressure will equalize throughout. The acoustic pressure drops rapidly for large cavities and cavities having resilient or acoustically absorbent boundary material. Surface roughness may be considered an additional source of flow noise because it creates turbulence and increases the forcing function on the plates.

Similar increases in noise occur if a sonar dome has been roughened by abrasion or the growth of marine organisms. These effects may be minimized by stringent quality control and by preventing fouling by marine growth. Various compliant coatings have not provided appreciable changes in the magnitude or spectrum of the turbulence. *However, excitation of viscoelastic surfaces is considerably different from that of the elastic plates discussed above.* (See Chapter 4).

2.2.8. TONAL GENERATION

Flow through, and across, hull openings or obstructions can often be responsible for conditions that produce very high noise levels at the resonance frequency. Typical examples are shown in figures 2.31, 2.32, and 2.33. They represent idealized configurations and, for the most part, are difficult to relate exactly to ship structures. However, such configurations can be used as guides to avoid resonant flow conditions. For example, cylindrical struts in a flow path should be designed such that their natural structural frequencies are outside the range of resonance frequencies for Karman vortex shedding.

The vortex shedding range (see figure 2.32) depends upon the strut diameter and the flow speed. When flow induced tones do occur, they can be eliminated by identifying the responsible tonal phenomena and making the necessary design alterations. Identification of the particular phenomena involved can be very difficult and time consuming.

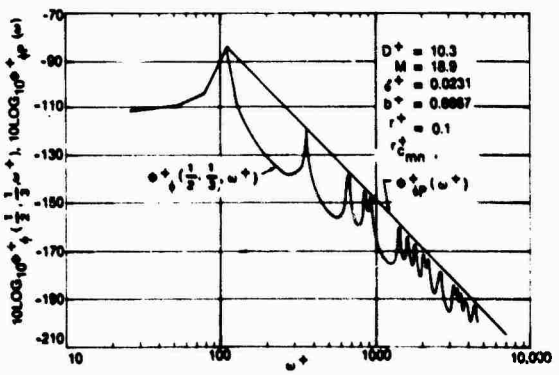

Figure 2.30. Comparison of Computed Dimensionless Plate Velocity Power Spectrum with Dimensionless Plate Velocity Peak Spectrum

PHENOMENON	DESCRIPTION OF MECHANISM	EFFECT OF FLOW VELOCITY	DIAGRAM OF MECHANISM TO GENERATE TONES	EQUATIONS WHICH GOVERN TONE FREQUENCY	TYPICAL FREQUENCY SPECTRUM OF TONE
ORGAN PIPE (CLOSED)	A closed organ pipe is a tube closed at one end with a jet of air (water, blown across the open end such that the jet impinges on the back edge of the pipe. This jet produces a "jet tone" which is dependent on the tube dimensions and jet velocity. When the jet oscillations correspond with the tube natural frequency a resonance occurs. The fundamental dominates, but odd overtones are present because jet oscillations are not purely sinusoidal. When the jet velocity is high the 3rd harmonic may couple better with the edge tone and become more intense. A closed organ pipe excited by a reed at its closed end has the same resonant frequencies as the closed pipe excited at its open end.	Fundamental tone dominates until jet tone velocity sufficiently high to cause tone to "jump" to 3rd harmonic	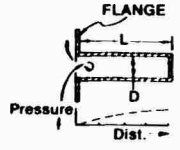 For Fundamental Resonance	For Air $f_n = \frac{cn}{4L_e}$ where: $L_e = L + \frac{8}{3\pi}\left(\frac{D}{2}\right)$ for large flanges $L_e = L + .6\left(\frac{D}{2}\right)$ for small flenges C = velocity of sound L = length of pipe n = 1, 3, 5 ...	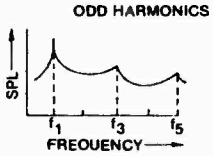
ORGAN PIPE (OPEN)	Same as for closed organ pipe, but all harmonics present.	Fundamental tone dominates until jet tone velocity becomes sufficiently high to cause tone to "jump" to 2nd harmonic	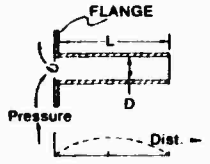 For Fundamental Resonance	For Air $f_n = \frac{cn}{2L_e}$ where: $L_e = L + \frac{16}{3\pi}\left(\frac{D}{2}\right)$ for large flanges $L_e = L + 1.2\left(\frac{D}{2}\right)$ for small flanges C = velocity of sound L = length of pipe n = 1, 2, 3 ...	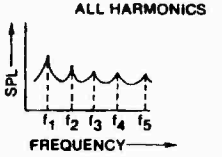
HELMHOLTZ RESONATOR	A Helmholtz resonator is a tank with connecting pipe whose dimensions are small compared with a wave length of sound in the fluid it contains. A jet blown across the pipe opening so that it impinges on the back edge creates an oscillating flow in and out of the pipe. The resonator is analogous to a simple spring mass oscillator in which the fluid in the pipe acts as a rigid mass and the main volume of the container acts as the spring. (For water the spring action may come from the compliance of the tank walls, rather than the compression of the fluid.) When the natural frequency of the tank and pipe coincides with the jet frequency oscillations, a resonance occurs.	Flow of jet must be such as to form oscillations in the pipe mouth which coincide with natural frequency of resonator High flow velocities appear to reduce the mass for resonators with small A which causes increase in resonant frequency	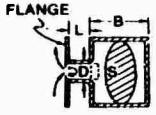	For Water $f_n = \frac{CD}{4\sqrt{\pi L_e BS}}$ where: A = area of opening = $\frac{\pi D^2}{4}$ $L_e = L + \frac{16}{3\pi}\left(\frac{D}{2}\right)$ for large flanges $L_e = L + 1.2\left(\frac{D}{2}\right)$ for small flanges C = velocity of sound S = cross sectional area of tank B = depth of tank L = length of inlet pipe D = diameter of inlet pipe	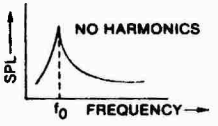
PLATE EDGE RESONATOR	A plate edge resonator consists of a flat plate the plane of which is perpendicular to flow. One, or more, edges of this plate form one side of a rectangularly shaped orifice. The other edge of the orifice can be a wall, etc, which parallels the flow. (Although not checked experimentally, the other orifice edge could probably consist of another similarly oriented flat plate. The flow through the orifice creates a vortex shedding condition, similar to a jet tone, which excites the resonances of the plate.	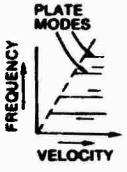	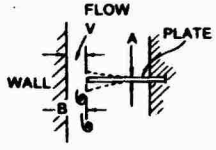	For Water f_n = determined by calculation of resonant frequencies of plate Frequency of forcing function is that of a jet tone f = KV K = Constant which is function of orifice geometry V = Flow velocity	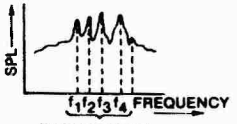 Plate Resonant Mode Frequencies

Figure 2.31. High Resonant Frequency Noise Levels from Organ Pipe (Closed and Opened), Helmholtz Resonator, Plant Edge Resonator

PHENOMENON	DESCRIPTION OF MECHANISM	EFFECT OF FLOW VELOCITY	DIAGRAM OF MECHANISM TO GENERATE TONES	EQUATIONS WHICH GOVERN TONE FREQUENCY	TYPICAL FREQUENCY SPECTRUM OF TONE
JET TONE	Periodic pressure fluctuations caused by periodic shedding of vortices from an orifice. As the vortices progress downstream, they tend to coalesce, producing subharmonics of the vortex shedding frequency. Harmonics of the fundamental also occur. Sometimes tones whose frequencies are the sum or difference of the fundamental frequency and its harmonics or subharmonics occur. Jet tones appear suddenly as flow velocity is increased and persists over a wide range of velocities.	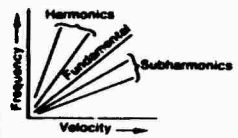	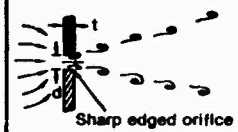 Tones are generally loudest when d = t	$\frac{fL}{w} = k$ = STROUHAL NUMBER where: f = jet tone frequency L = a characteristic dimension = d or t, whichever is smaller n = 1, 2, 3, for fundamental tone and harmonics n = 1/2, 1/3, etc., for subharmonics v = flow velocity through orifice k = a constant Test results show that k for water flow through a sharp edged orifice of t/d = 1 ranges from about 0.9 to 1.0	
PIPE TONE	Longitudinal cavity resonances of a fluid filled pipe, excited by periodic shedding of vortices from the pipe outlet. Periodic shedding of vortices at the outlet causes the effective outlet flow area to pulsate, producing periodic pressure fluctuations in the pipe. The pipe tones become apparent only when the vortex shedding frequencies (jet tone frequencies) approach the cavity resonance frequencies.	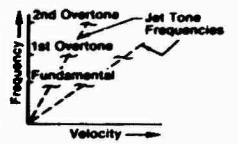	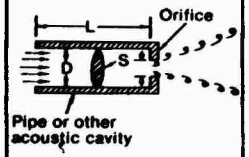	$\frac{2\pi fL_e}{C} \cot \frac{2\pi fL_e}{C} = -\frac{L_e D}{S}$ where: f = pipe tone resonant frequencies L_e = effective pipe length = L + 0.306D for pipe completely open at inlet C = speed of sound in the fluid S = cross-sectional area of pipe	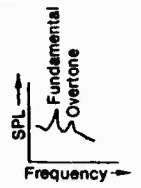
EDGE TONE	Caused by transverse oscillations of a jet impinging on an obstacle or "edge." The tone exhibits "stages," which occur between step changes in frequency as the flow velocity is changed. The various stages can also be produced at a constant flow velocity by varying the nozzle to edge distance. Two stages frequently are found to exist simultaneously. Sometimes, tone frequencies are observed which are equal to the sum or difference of the various stage frequencies.	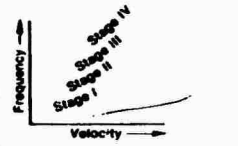 For air, four stages have been found to occur. For water, only two stages occur regularly, but sometimes three stages occur.	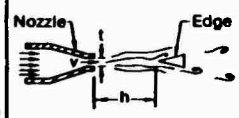	Various empirical relations have been developed for air $f = 1/2V \left\{ \frac{1+1/4}{h} - \frac{1}{3Qt} \right\}$ $f = AJ_n (V - a) \left(\frac{1}{h} - b\right)$ $f = AB_n \frac{t^{1/2}}{h^{3/2}}$ where: f = edge tone frequency V = jet velocity N = 1, 2, 3, etc for the various stages A . a . b = empirical constants (different for air and water) $B_n . J_n$ = constants for each stage For water, the following empirical relation has been used: $f = AJ_n (V - a) \left(\frac{1}{h} - b\right)$	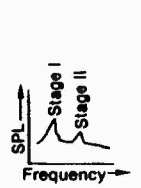
KARMEN VORTEX SHEDDING	Periodic pressure fluctuations produced by the alternate shedding of vortices from opposite side of an obstacle placed in a fluid stream.	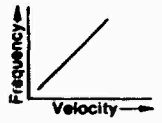		$\frac{fL}{v} = k$ where: f = vortex shedding frequency L = a characteristic dimension of the obstacle = diameter for a cylindrical body v = flow velocity approaching obstacle k = a constant, dependent on obstacle geometry = 0.22 for a cylinder	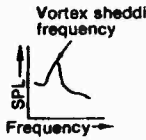
VORTEX WHISTLE	Mechanism not completely understood. Tones are thought to be generated due to an instability of the vortex as it exits from the tube. It has been postulated that the sound generated is caused by a circular distribution of dipoles whose phase angle varies around the periphery of the tube exit so that points diametrically opposed are always exactly out of phase.	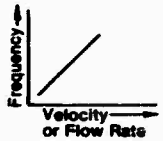	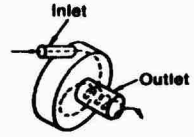	f = kQ where: f = tone frequency k = a constant depending on whistle geometry which must be determined experimentally for each case Q = flow rate	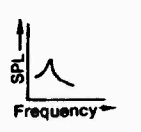

Figure 2.32. High Resonant Frequency Noise Levels from Jet, Pipe, and Edge Tones; Karmen Vortex Shedding and Vortex Whistle

PHENOMENON	DESCRIPTION OF MECHANISM	EFFECT OF FLOW VELOCITY	DIAGRAM OF MECHANISM TO GENERATE TONES	EQUATIONS WHICH GOVERN TONE FREQUENCY	TYPICAL FREQUENCY SPECTRUM OF TONE
SURFACE ROUGHNESS NOISE	Surface roughness noise is the noise generated when the roughness of a surface penetrates the laminar sublayer. Vortices are shed causing high frequency levels to increase over and above the levels due to ordinary boundary layer induced noise. This vortices shedding only occurs above a critical velocity, $V_{crit.} = 10^{-7}/h$ knots where, h = height of roughness in inches) when the laminar sublayer diminishes to the point where it is penetrated by the roughness of the surface.	A plot of SPL vs velocity shows a slope that varies between 18 dB/speed octave and 35 dB/speed octave depending on the roughness of the surface.	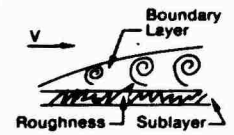	For Water critical frequency: where: $f_o = V/h$ where f_o = frequency (cps) V = stream velocity h = height of roughness	fo usually masked by boundary layer noise Slope ≤ −5 to −9 dB per octave 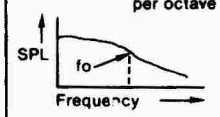
BOUNDARY LAYER INDUCED NOISE (TURBULENT BOUNDARY LAYER)	Boundary layer induced noise is produced by pressure fluctuations in the boundary layer around an object in a fluid. These pressure fluctuations are caused by velocity fluctuations within the boundary layer. Although these pressure fluctuations cause a near field only, they can produce far field radiation by exciting the surfaces in contact with this near field.	Below critical frequency (fo), slope of SPL vs flow velocity varies about 9 dB per speed octave Above critical frequency (fo), the slope of a SPL vs flow velocity follows the relation 60 log (Vel.) which is a positive 18 dB per speed octave.	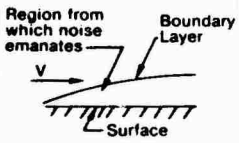	For Water critical frequency: where: f_o = V/J V = stream velocity J = boundary layer thickness For $f < f_o$ $SPL = K + 30\log_{10}V + 10\log_{10}J$ For $f > f_o$ $SPL = M_o + 60\log_{10}V - (20 \text{ to } 30)\log_{10}f - 20\log_{10}J$ where: M, K = amplitude constants	Slope = −6 to −9 dB per octave 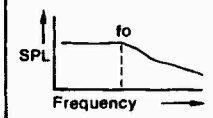
BOUNDARY LAYER INDUCED NOISE (LAMINAR BOUNDARY LAYER)	Same as boundary layer induced noise in turbulent boundary layer except for slope of SPL vs flow velocity curve above critical frequency fo.	Above critical frequency (fo), the slope of the SPL vs flow velocity curve is 15 dB per speed octave.	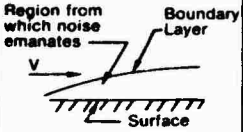	For Water Same as for turbulent boundary layer except velocity relation for $f > f_o$ is $53\log_{10}V$. rather than $60\log_{10}V$.	Slope = −6 to −9 dB per octave 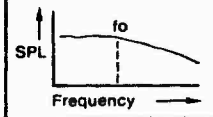
NOISE OF TURBULENT JET	Noise from a turbulent jet is a combination of a high and a low frequency source. The low frequency source comes from the mixing region of the jet and is due to a combination of boundary layer type noise and the turbulence in the mixing region. The high frequency noise comes from near the orifice and is probably due to boundary layer type noise alone. At large distances the combination of these two sources appear as a point source. This only occurs above a mach number of 0.3.	Acoustic power output varies as approximately V^8 where, V = jet velocity	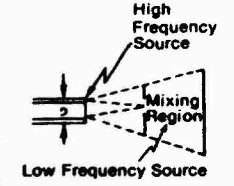	For Air $f_o = V/2D$ where V = jet velocity D = Orifice dia The above does not appear to hold for all cases There is some evidance that this noise, in general, is distributed as a broad peaked frequency spectrum	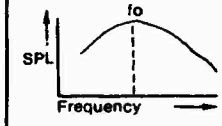

Figure 2.33. High Resonant Frequency Noise Levels from Surface Roughness, Boundary Layer (Turbulent and Laminar Boundary Layer), Turbulent Jets

ANNOTATED BIBLIOGRAPHY

Bakewell, H. P. et al., *Wall Pressure Correlations in Turbulent Pipe Flow,* U.S. Navy Underwater Sound Laboratory Report No. 599, August 1962.

Batchelor, G. K., "Pressure Fluctuations in Isotropic Turbulence," *Proceedings of the Cambridge Philosophical Society,* 47, 359-374, April 1951.

Blake, W. K., Wolpert, M. C., and Geil, F. E., "Cavitation Noise and Inception as Influenced by Boundary-Layer Development on a Hydrofoil," *Journal of Fluid Mechanics, 80, 617-640, May 1977.*

Provides measurements of noise from two-phase flow over hydrofoils.

Bull, M. K., Wilby, J. F., and Blackman, D. R., *Wall Pressure Fluctuations in Boundary Layer Flow and Response of Simple Structures to Random Pressure Fields,* University of Southampton, A.A.S.U. Report No. 243, July 1963.

Collier, R. D., *The Vibration and Acoustic Radiation of a Simply Supported Plate Excited by Turbulent Boundary Layer Pressure Fluctuations,* University of Connecticut, Ph.D. Dissertation, May 1966.

Corcos, G. M. and Liepmann, H. W., "On the Contribution of Turbulent Boundary Layer to the Noise Inside a Fuselage," *NACA Technical Memorandum,* 14 December 1956.

Corcos, G. M., "Resolution of Pressure in Turbulence," *Journal of the Acoustical Society of America,* 35, 192-199, February 1963.

Discusses two transducer applications to resolve the spatial details of a turbulent pressure field. One is an evaluation of the adequacy of contemporary measurements of the properties of turbulent pressure fields in laboratory shear flows. The other is a brief assessment of possible discrimination by a sonar receiver between sound and local turbulent pressure fluctuation acting as background noise.

Corcos, G. H., "The Structure of the Turbulent Pressure Field in Boundary Layer Flows," *Journal of Fluid Mechanics,* 18, 353-378, March 1964.

The problem of mapping a random function of several variables by a linear operator is examined. Contemporary measurements of turbulent pressure fields in their flow are evaluated.

Denhartog, J.P. *Mechnaical Vibrations,* 4th Edition, New York, McGraw Hill Book Company, Inc., 1956.

Dyer, I., *Sound Radiation Into a Closed Space from Boundary Layer Turbulence,* Bolt Beranek and Newman Inc., Report No. 602, December 1958.

The theory of noise generation by the action of boundary layer turbulence on an elastic system is developed. The resulting plate vibration and sound radiation is derived, taking into account coupling between the plate motion and sound field in the liquid.

Dyer, I., "Response of Plates to a Decaying and Convecting Pressure Field," *Journal of the Acoustical Society of America,* 31, 922-928, July 1959.

Analysis of the vibratory response of a plate to a random pressure field is made. Convection speed less than the speed of flexural waves in the plate and convection speed the same order as the flexural wave speed are considered.

El Baroudi, M. Y., Ludwig, G. R., and Ribner, H. S., *An Experimental Investigation of Turbulence-Excited Panel Vibration and Noise,* NATO Advisory Group for Aeronautical Research and Development Report No. 465, April 1963.

A study is made of the flexural motion and noise generated by 11 x 11 in. steel panels flush-mounted in the wall of a turbulent flow channel.

El Baroudi, M. Y., *Turbulence-Induced Panel Vibration,* University of Toronto, UTIAS Report No. 98, February 1964.

Eringen, A. C., "Response of Beams and Plates to Random Loads," *Journal of Applied Mechanics,* 24, 46-52, March 1957.

Generalized Fourier analysis is applied to vibrating beams and plates under stochastic loads and the problem is solved. Equations give cross-correlation functions for displacement, stresses, and moments in terms of the cross-correlation function of external pressure.

Fowcs, W. J. E. and O'Shea, S., "Sound Generation by Hydrodynamic Sources Near A Cavitated Line Vortex," *Journal of Fluid Mechanics,* 43, 765-688, October 1970.

The scattering properties of a cavitated line vortex when excited by line and point sources of sound is examined.

Gardner, S., *Surface Pressure Fluctuations Produced by Boundary Layer Turbulence,* Technical Research Group, Inc., Report No. TRG-142-TN-63-5, October 1963.

Harrison, M., *Correlation and Spectra of Pressure Fluctuations on Wall Adjacent to a Turbulent Boundary Layer,* David Taylor Model Basin Report No. 1260, April 1958.

Houghton, G., "Theory of Bubble Pulsation and Cavitation," *Journal of the Acoustical Society of America,* Vol. 35, 1387-1393, December 1962.

The theory of vibration-induced cavitation in which the Rayleigh equation is transformed into an equivalent Mathiew equation for small radial motion is presented.

Klein, E., "Underwater Sound and Naval Acoustical Research and Application before 1939," *Journal of the Acoustical Society of America,* 43, 931-947, 1968.

Discusses propeller singing.

Kraichnan, R. H., "Pressure Fluctuations in Turbulent Flow over a Flat Plate," *Journal of the Acoustical Society of America,* 28, 378-390, May 1956.

Qualitative features of the pressure flucutation structure associated with the boundary layer flow over a smooth flat surface are discussed. Some flow qualities whose experimental determination is important to the more accurate prediction of the pressure forces are presented. A formal method for further treatment of the problem is developed.

Kraichnan, R. H., "Noise from Boundary Layer Fluctuations," *Journal of the Acoustical Society of America,* 29, 65-80, January 1957

A theoretical study of noise spectra radiated by the vibration of thin, stiff, flat plates under the action of turbulent boundary layer pressrue fluctuations is presented. Radiated spectrum caused by transverse and longitudinal dipole excitation is discussed. Noise related to turbulent airflow over the skin of aircraft is emphasized.

Lighthill, M. J., "On Sound Generated Aerodynamically, I.-General Theory," *Proceedings of the Royal Society* (London) Series A, Vol. 211, 564-587, March 1952.

Lighthill, M. J., "On Sound Generated Aerodynamically, II. Turbulence as a Source of Sound," *Proceedings of the Royal Society* (London) Series A, Vol. 222, 1-32, February 1954.

Lilley, G. M. and Hodgson, T. H., *On the Surface Pressure Fluctuations in Turbulent Boundary Layers* NATO Advisory Group for Aeronautical Research and Development Report No. 276 (April 1960).

Maestrello, L., "Measurement of Noise Radiated by Boundary Layer Excited Panels," *Journal of Sound and Vibration,* 2, 100-115, April 1965.

Reports measurements of sound power radiated by panels excited by a turbulent boundary layer and investigates fluctuating forces produced by vibrating surfaces of flight vehicles. Fluctuating forces resulting from pressure flucutation in a turbulent boundary layer flowing over structural surfaces cause vibration; this motion becomes a source of noise.

Maestrello, L., "Measurement and Analysis of the Response Fields of Turbulent Boundary

Layer Excited Panels," *Journal of Sound and Vibration,* 2, 270-292, July 1965.

Presents results of wall pressure covariance on rigid wall, dynamic responses, and acoustic radiation characteristics of rigidly clamped panels excited by turbulent flow. Interior noise level and structural stresses induced by vibrating surface of flight vehicles excited by turbulent boundary layer are discussed, as well as the response of panels subjected on one side of turbulent layer excitation. Spectral and cross-correlation functions are used to analyze the structural response problem.

Neppiras, E. A. Coakley, W. T., "Acoustic Cavitation in a Focused Field in Water at 1 MHz," *Journal of Sound and Vibration,* 45, 341-371, April 1976.

Discusses transient bubbles that result from steady bubbles.

Powell, A., "On the Fatigue Failure of Structures Due to Vibration Excited by Random Pressure Fields," *Journal of the Acoustical Society of America,* 30, 1130-1135, December 1958.

A general analysis is made using the ideas of vibration theory and spectrum analysis in relation to aircraft. The power spectrum of any quantity depending linearly upon structural distortions is derived and a quantity concerning the spacewise structure of the pressure field and the geometry of the modes of vibration is investigated. It is shown that the result can be used to estimate fatigue life assuming cumulative damage.

Pretlove, A. J., "Forced Vibrations of Rectangular Panel Backed by a Closed Rectangular Cavity," *Journal of Sound and Vibration,* 3, 252-261, May 1966.

Discusses aspects of forced vibration of flexible panels with a backing cavity. The effect of mathematical combing is to modify both panel vibrations and cavity acoustics. The problem of modifying wall stress and displacement is treated for cases in which the system is excited by external random acoustic pressure. Sound transmission into a cavity is also treated.

Ribner, H. S., *Boundary Layer Induced Noise in the Interior of Aircraft,* University of Toronto, U.T.I.A. Report No. 37, April 1956.

Ross, D., *Mechanics of Underwater Noise,* Pergamon Press, 1976.

Discusses many types of noise phenomenon relative to ships.

Rusby, J. S. M., "The Onset of Sound Wave Distortion and Cavitation in Water and Sea Water," *Journal of Sound and Vibration,* 13, 257-267, September 1969.

The onset of sound wave distortion and cavitation in the acoustic field near a high power transducer element is discussed. Distortion and cavitation thresholds suggest two cavitation thresholds.

Schloemer, H. H., *Effect of Pressure Gradients on Turbulent Boundary-Layer Wall Pressure Fluctuations,* U.S. Navy Underwater Sound Laboratory Report No. 747 (July 1966)

Evaluates adverse and favorable pressure gradients effects on the properties and spectrum of wall pressure fluctuations.

Serafini, J. S., *Wall Pressure Fluctuations in a Turbulent Boundary Layer,* California Institute of Technology, Ph.D. Dissertation, June 1962.

Society of Naval Architects and Marine Engineers, 1978 Ship Vibration Symposium.

Society of Naval Architects and Marine Engineers, 1978 Propeller Symposium.

Skudrzyk, E. J. and Haddle, G. P., "Noise Production in a Turbulent Boundary Layer by Smooth and Rough Surfaces," *Journal of the Acoustical Society of America,* 32, 19-34, January 1960.

Predicts levels of boundary-layer noise and noise produced by surface roughnesses as a function of speed and frequency based on results obtained by flow-noise studies performed with a rotating cylinder. Analyzes small scale boundary-layer turbulence by means of flow-noise studies.

Sternberg, J., "A Theory for the Viscous Sublayer of a Turbulent Flow," *Journal of Fluid Mechanics*, 13, 241-272, June 1962.

Explains the laminar sublayer as the region where turbulent velocity fluctuations are directly dissipated by viscosity, the turbulent field between the wall, and the fully turbulent part of flow. Shows that large scale fluctuations containing most of turbulent energy are convected downstream with a middle boundary layer velocity characteristic. The linear pressure fluctuation field at edge of sublayer is calculated and the free-stream turbulence effect on laminar boundary-layer transition is examined.

Strasberg, M., "Response of Plates and Membranes to Pressure Fluctuations of a Turbulent Boundary Layer," (Abstract) *Journal of the Acoustical Society of America* 30, 680 (June 1958).

Calculates flexural vibrations of a flat plate excited by pressure fluctuations in the turbulent boundary layer of a fluid flowing on one side of vibrating surface in terms of measured value of spectral density.

Strawderman, Wayne A., *The Acoustic Field in a Closed Space Behind a Rectangular Simply Supported Plate Excited by Boundary Layer Turbulence*, USL Technical Report 827, May 1967.

Discusses plate excitation and flow noise (this document is the source of much of section 2.2.7).

Tack, D. N. and Lambert, R. F., "Response of Bars and Plates to Boundary Layer Turbulence," *Journal of the Aeronautical Society*, 29, 311-322 (March 1962).

Uberoi, M.S., "Quadruple Velocity Correleations and Pressure Fluctuations in Isotropic Turbulence," *Journal of Aeronautical Sciences*, 20, 197-204, March 1953.

Vaughn, P. W., "Investigation of Acoustic Cavitation Thresholds By Observation of the First Subharmonic," *Journal of Sound and Vibration*, 7, 236-246, March 1968.

Acoustic cavitation is studied using the lst peak of subharmonic generation as an indicator of the onset of cavitation in a liquid.

Wenz, G. M., "Review of Underwater Acoustics Research Noise," *Journal of the Acoustical Society of America*, 51, 1010-1024, 1972.

The purpose, problems, and progress of radiated noise, self-noise, and ambient noise research are reviewed.

White, F. M., *A Unified Theory of Turbulent Wall Pressure Fluctuations*, USL Technical Report 629, December 1964.

A unified theory of incompressible turbulent wall pressure fluctuations is developed by extending and revising a basic development proposed by Gardner. The theory leads to analytical results for the statistical properties of boundary pressure, such as power spectrum, longitudinal and lateral cross-spectra, diagonal correlations, convection speeds, and space-time correlations. The theoretical results are shown to be in good agreement with existing experimental measurements. Recommendations are made for critical experiments to test some of the new predictions of this unified theory. It is also recommended that the theory be extended to include an even broader range of problems in turbulent pressure fluctuations.

White, P. N., *Sound Transmission of Double Flexible Walls Excited by Random Pressure Fields*, University of California, Ph.D. Dissertation, January 1965.

Willmarth, W. W., *Wall Pressure Fluctuations in a Turbulent Boundary Layer*, Guggenheim Aeronautical Laboratory, California Institute of Technology Report, May 1956.

Some of the properties of wall pressure fluctuations in a turbulent boundary layer are measured. A few typical spectra are given for different values of Reynold's number and Mach number.

Willmarth, W. W. and Roos, F. W., "Resolution and Structure of the Wall Pressure Field Beneath a Turbulent Boundary Layer," *Journal of Fluid Mechanics*, 22, 81-94, January 1965.

Investigates the effect of a finite-size circular transducer on measurements of the wall pressure beneath turbulent boundary layer. The power spectrum of wall pressure that would be measured by a transducer of vanishingly small size and the correction to power spectra measured by finite-size transducers is determined from data measured by four transducers of different diameters.

Willmarth, W. W. and Wooldridge, C. E., *Measurements of the Correlation Between the Fluctuating Velocities and Fluctuation Wall Pressure in a Thick Turbulent Boundary Layer,* University of Michigan, College of Engineering Report 02920-2-T, April 1962.

Principles of Sonar Installation

CHAPTER III
VIBRATION AND ACOUSTIC PHENOMENA

GLOSSARY

A	Vibration Amplitude (L)
A_c	Accelerometer Output (mV)
A_i	Incident Wave Pressure (F/L^2)
A_r	Area (L^2)
A_n	Coefficient
a	Real Part of Vibration Amplitude (L)
a	Dimension (L)
a_c	Radius of Cylinder (L)
a_o	Bubble Radius (L)
B	Bulk Modulus (F/L^2)
B_1	Reflected Wave Pressure (F/L^2)
b	Imaginary Part of Vibration Amplitude (L)
b	Dimension (L)
C_1	Reflected Wave Pressure (F/L^2)
c	Speed of Sound (L/T)
c_D	Damping Coefficient (FT/L)
c_r	Rotational Damping (FTL)
c_c	Critical Damping Coefficient (FT/L)
c_p	Sound Speed (Compressional) (L/T)
c_f	Sound Speed (Flexural) (L/T)
c_s	Sound Speed (Shear) (L/T)
D	Dilational Modulus (F/L^2)
d	Dimension (L)
d	Standoff Distance (L)
d_e	Effective Standoff Distance (L)
E	Young's Modulus (F/L^2)
E_e	Effective Modulus (F/L^2)
E_{AVG}	Average Energy (FL)
E_m	Modal Energy (FL)
e	2.71828
F	Force (F)
F	Factor
F^2	Mean Square Force
F_x	Force in X Direction (F)
F_{COMP}	Compressional Force (F)
F_N	Oscillating Force (F)
F_{DISS}	Dissipation Force (F)
Δf	Frequency Band Increment (1/T)
f	Frequency (1/T)
f_R	Frequency at Resonance (1/T)
f_o	Frequency at Bubble Resonance (1/T)
G	Shear Modulus (F/L^2)
g	Acceleration of Gravity (L/T^2)
h	Plate Thickness (L)
I	Intensity (F^2/L^4)
I	Moment of Inertia (L^4)
I_R	Reflected Intensity (F^2/L^4)
I_I	Incident Intensity (F^2/L^4)
i	$(-1)^{1/2}$
J	Mass Moment of Inertia (FLT^2)
j_o	Bessel Function
K	Instrument Factor

K	Bulk Modulus (F/L^2)
K_T	Isothermal Bulk Modulus (F/L^2)
K_r	Torsional Stiffness (FL)
k	Spring Constant (F/L)
k	Radius of Gyration (L)
k	Wave Number (1/L)
L_X	Length in X Direction (L)
L_Y	Length in Y Direction (L)
L	Length (L)
l	Dimension (L)
M	Mass (FT^2/L)
m	Mass (FT^2/L)
m	Mass per Unit Area (FT^2/L^3)
m_L	Mass per Unit Length (FT^2/L^2)
N	Number of Modes in a Given Bandwidth
NIPTS	Noise Induced Permanent Threshold Shift (dB)
NITTS	Noise-Induced Temporary Threshold Shift (dB)
P	Sound Pressure (F/L^2)
P	Pressure (F/L^2)
P_i	Incident Sound Pressure (F/L^2)
P_R	Reflected Sound Pressure (F/L^2)
P_t	Transmitted Sound Pressure (F/L^2)
$P_{S\alpha}$	Sound Pressure Caused By Structure Having Infinite Impedance (F/L^2)
P_{SE}	Sound Pressure Caused By Elastic Structure (F/L^2)
Q	Quality Factor of Resonance
Q_o	Acoustic Source Strength (L^3/T)
R	Range (L)
R	Resistance Coefficient (FT/L)
R	Reflectivity
r	Frequency Ratio
r	Radial Distance to Point (L)
r	Polar Coordinate (L)
S_E	Energy Spectral Density (F^2L^2T)
S_A	Acceleration Spectral Density (L^2/T^3)
S_P	Sound Pressure Spectral Density (F^2T/L^4)
S	Shape Factor
S	Surface Area (L^2)
T	Torque (FL)
T	Temperature
T_F	Force Transmissibility
T_V	Velocity Transmissibility
TS	Target Strength (dB)
TTS	Temporary Threshold Shift (dB)
t	Time (T)
U	Velocity (L/T)
V	Volume (L^3)
V	Instrument Factor
v	Velocity ot Motion (L/T)
w	Cylindrical Coordinate (Radius) (L)
X_m	Mechanical Reactance (FT/L)
x_{RES}	Amplitude at Resonance (L)
x	Variable Distance (L)
x_{ST}	Static Deflection of Spring (L)

Y_m	Mechanical Mobility ($1/Z_m$) (L/FT)
Z_m	Mechanical Impedance (FT/L)
Z	Characteristic Impedance (FT/L)
α	Relative Damping Factor ($C_D/2M$)(1/T)
α_t	Transmission Coefficient
α_R	Reflection Coefficient
β	Material Coefficient
γ	Absorption Coefficient of Flexural Vibration at Panel Joints
γ	Ratio of Specific Heats (Gas)
δ	Loss Tangent
δ	Damping Factor Associated with Imaginary Part of Moduli
δ	Decay Rate (dB/T)
δ_o	Damping Constant at Bubble Resonance (1/T)
ζ	Critical Damping Ratio
θ	Polar Coordinate (Angle)
θ	Phase Angle
θ_i	Incident Angle
θ_r	Reflected Angle
θ_t	Transmitted Angle
θ_{im}	Angle of Intromission
θ_c	Critical Angle
θ_{cc}	Compressional Coincidence Angle
Λ	Logarithmic Decrement
λ	Wave Length
λ_f	Flexural Wave Length (L)
ν	Poisson's Ratio
ξ	Incremental Change in Dimension (L)
Π_s	Scattered Power (LF/T)
ϱ	Specific Mass (FT^2/L^4)
ϱ_s	Specific Mass of Structure (FT^2/L^4)
σ	Stress (F/L^2)
τ	Decay Modulus (Time for Amplitude to Decrease to 1/e of its Original Value) (T)
ϕ	Phase Angle
ϕ_s	Angle (Scattering)
ψ	Spherical Coordinate (Angle)
ψ	Phase Angle
Ω	Non-Dimensional Frequency
Ω	Angular Frequency (1/T)
ω	Angular Velocity (Frequency) (1/T)
ω_n	Angular Frequency of N^{th} Mode (1/T)
ω_o	Angular Frequency of Primary Mode (1/T)
ω_R	Angular Frequency at Resonance (1/T)
ω_c	Coincidence Frequency of Plate (1/T)

CHAPTER III
VIBRATION AND ACOUSTIC PHENOMENA

3.0 INTRODUCTION

Control of vibrational and acoustic phenomena is a major factor in managing acoustic signals and noise. The mathematical treatment of acoustics is closely related to that of vibration. Sound is caused by a vibrating body in contact with an acoustic medium, e.g., air or water. Concepts such as resonance and damping apply to both. This chapter will begin with a discussion of vibration and its propagation through the ship.

3.1 PROPAGATION OF VIBRATION

3.1.1 GENERAL

Vibrating structures in contact with air or water radiate sound. The audibility of the sound depends on its intensity and frequency. Intense low frequency shipboard vibration (e.g., that produced when heavy machinery is in operation on a steel deck) may add stress to the structure and be felt by the individual, but not be heard. On the other hand, minute movements of a cavitating valve in a high velocity fluid flow causes practically no stress and is not felt, but may produce an extremely loud sound.

Vibrations in a shipboard structure propagate from one component to the next, distributing the energy throughout the ship. Therefore, they cause sound to be radiated in the immediate vicinity of the source and, also, at remote locations. The manner in which vibrations travel through the structure may be explained by considering, first, the deflection of a structure under a static loading.

If a given static load is applied to any structural component, such as a frame, the component deflects different amounts at different points. The adjacent structural members influenced by the component also deflect. The ratios of the displacements of these deflections to the deflection under the static load, denoted *influence factors*, may be calculated by structural engineers. Since the influence factors are generally less than one, the amplitude decreases rapidly with distance from the point of application of the force.

A structure exhibits a similar displacement distribution when a low frequency fluctuating force is applied instead of a static load. However, the dynamic displacement distribution deviates more and more from that of the static distribution as the excitation frequency increases. When it reaches the modal frequency of a portion of the structure, that portion becomes excited. As shown on figure 3.1, the amplitude, which is limited by struc-

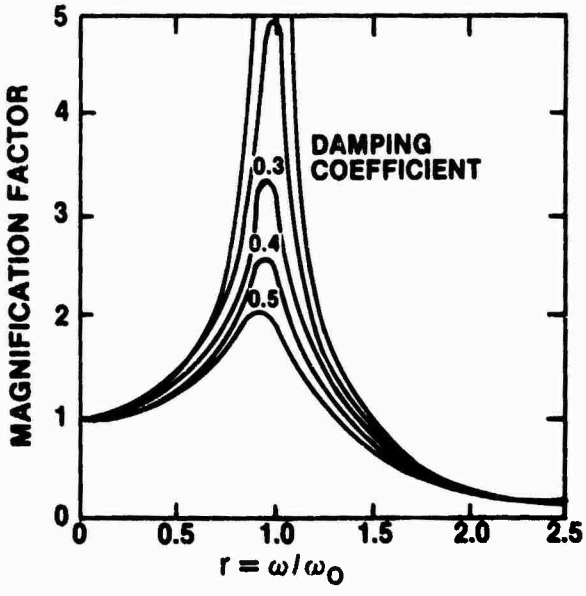

Figure 3.1. Magnification of Amplitude at Resonance and Other Frequency Ratios

tural damping, increases rapidly. Different modes of the structure become excited with increased frequency and then other portions reach high amplitudes.

In a ship, which is a complicated, extended structure, interactions involve torsion, shear, compression, and flexural deformations. Nodal points inherent in the structural arrangement cause mode changes, and some energy reflects back toward the source with phase changes.

As the vibration energy spreads through the structure, frequencies other than the forcing frequency are generated and various inherent mode shapes are excited.

If it assumed that the frequencies below the primary mode frequency of the structure are not of major concern, practically all the vibrational energy is in the resonant frequency bands. Therefore, if the energy input to the structure is known (e.g., by measuring the excitation source or estimating engine horsepower) and it is possible to distribute the energy among the various frequencies, a reasonable estimate of the vibration response of the structure can be obtained.

Although the deformation caused by a displacement of one member of a structure may appear to propagate instantly to another, the process requires an appreciable amount of time. While this factor is of little consequence for low frequency oscillations, it is important at high frequencies. Also, the vibrational behavior of structures that incorporate reasonable amounts of damping can be analyzed in terms of waves instead of modes when the frequencies are considerably above the fundamental resonance frequency. Such waves, which spread out from the excitation point, are subject to (1) attenuation by damping, (2) amplitude reduction by spreading, (3) absorption and reflection at the edges, (4) and discontinuities.

The situation is complicated because waves in structures are much more complex than sound waves in a continuous, generally isotropic medium such as air. Waves propagating along a one-dimensional structure, such as a beam, do not spread and are not subject to spreading attenuation; waves on plates or shells spread in two-dimensions, and those propagating in the interior of solid bodies spread three-dimensionally.

The frequency range of interest onboard a ship is from a little under 1 kHz to approximately 20 kHz, depending on the purpose of the sonar system. This is well above a 60 Hz hum, a propeller rpm of 200, or a blade rate of 1000/min. Such noises are of concern because they contribute to the ship's detectability. They also create harmonics of a higher order and excite structures at higher frequencies, which interferes with the ability of the sonar to sense signals. Since low frequency vibrations are generally subject to less attenuation than are high frequency ones, they most readily transmit energy through the ship.

3.1.2 VIBRATION OF A SINGLE MASS SYSTEM

The vibrating systems of interest here are characterized by mass and elasticity. They function through a continuing interchange of potential energy in a spring with the kinetic energy possessed by the mass as it moves. In addition, all vibrating systems are subject to damping that reduces the amplitude by imposing a retarding force that converts the energy of motion to heat. This limits the amplitude to the value at which the energy loss in the system equals the energy input. The equation of motion for a simple suspended mass system, such as that shown in figure 3.2, is

$$d^2x/dt^2 + \omega_n^2 x = 0$$

or

$$M(d^2x/dt^2) + kx = 0 \qquad (3\text{-}1)$$

the general solution of which is

$$x = A_1 \cos \omega t + A_2 \sin \omega t, \qquad (3\text{-}2)$$

which reduces to,

$$x = A \sin (\omega_n t + \psi),$$

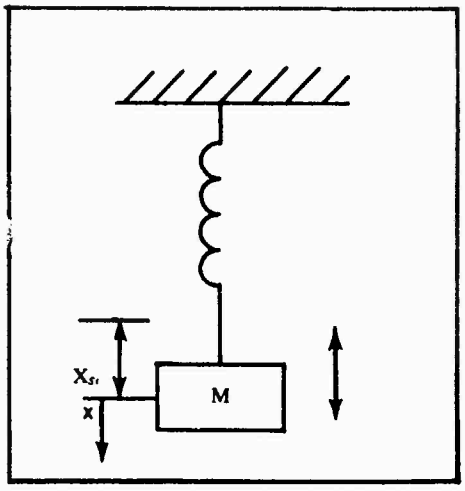

Figure 3.2. Simple Suspended System

where

A = vibration amplitude,
ω = angular frequency,
ψ = phase angle,
k = spring constant, and
$\omega_o = (k/M)^{1/2}$.

The frequency of this vibration is

$$f = \omega_o/2\pi = (1/2\pi)(k/M)^{1/2} = (1/2\pi)(g/x_{st})^{1/2},$$

where

x_{st} = deflection of spring by weight of mass
= weight/k

If damping is added, the equation becomes

$$M(d^2x/dt^2) + c_D(dx/dt) + kx = 0 \quad (3\text{-}3)$$

and, unless the damping is large, the frequency is not changed appreciably. The general solution is

$$x = e^{-\alpha t}\{[(dx_o/dt)/(\omega_o^2 - \alpha^2)^{1/2}] \sin(\omega_o^2 - \alpha^2)^{1/2}t + x_o \times [\cos(\omega_o^2 - \alpha^2)^{1/2}t + (\alpha/(\omega_o^2 - \alpha^2)^{1/2}) \sin(\omega_o^2 - \alpha^2)^{1/2}t]\},$$

where

$\alpha = c_D/2M$.

The value of damping at which the unforced system returns to equilibrium without oscillating is termed *critical damping ratio*, c_c. This occurs when $\omega_o^2 \approx \alpha^2$ or $(c_D/2M)^2 = k/M$, i.e., when $c_D = 2(kM)^{1/2}$. Other values of damping are sometimes given as a ratio to this value, such that $c_D = \zeta c_c$, where ζ denotes the critical damping ratio. Vibrating systems may be under-, over-, or critically damped. Examples of the displacement-time curves for each case are presented in figure 3.3.

If the vibration is harmonically forced, the equation becomes

$$M(d^2x/dt^2) + c_D(dx/dt) + kx = F \sin \omega t, \quad (3\text{-}4)$$

where

F = force amplitude.

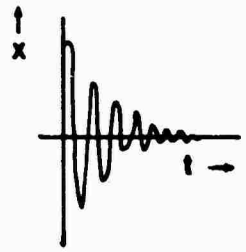

Figure 3.3a. Under Damped

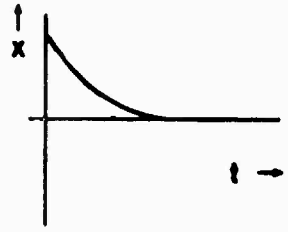

Figure 3.3b. Critically Damped

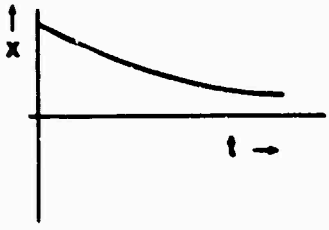

Figure 3.3c. Over Damped

Figure 3.3. Displacement Time Curves

From this equation, for steady state

$$x = A \sin(\omega t - \psi),$$

where

$$A = (F/k)/[(1 - \omega^2/\omega_o^2)^2 + c_D^2\omega^2/k^2]^{1/2} = (F/k)F_a$$

and

$$\tan\psi = c_D\omega/k(1 - \omega^2/\omega^2_o),$$

and, at resonance,

$$A = F/c_D\omega.$$

The second expression on the right of the amplitude equation is the *magnification factor*. This is plotted in figure 3.1 to show that as the frequency of the forcing vibration approaches the mode frequency of the system, the amplitude becomes very large. However, the value is inversely proportional to the damping factor, c_D, and decreases as damping increases. When the frequency of the forcing function is very low relative to the mode frequency, the system practically follows the force. When it is very high relative to the mode frequency, the mass has very little motion.

A second method of solving the differential equation is to assume a solution of the form

$$x = A_1e^{i\omega t} + A_2e^{-i\omega t},$$

since,

$$e^{i\omega t} = \cos\omega t + i\sin\omega t$$

and

$$e^{-i\omega t} = \cos\omega t - i\sin\omega t.$$

This equation becomes

$$x = A_1(\cos\omega t + i\sin\omega t) + A_2(\cos\omega t - i\sin\omega t)$$

or

$$x = (A_1 + A_2)\cos\omega t + i(A_1 - A_2)\sin\omega t.$$

Let

$$A_1 = a_1 + ib_1$$

and

$$A_2 = a_2 + ib_2,$$

where a_1, a_2, b_1, and b_2 are real numbers (A_1 and A_2 being complex).

Then

$$x = (a_1 + ib_1 + a_2 + ib_2)\cos\omega t + i(a_1 + ib_1 - a_2 - ib_2)\sin\omega t$$

or

$$x = (a_1 + a_2)\cos\omega t - (b_1 - b_2)\sin\omega t + i[(b_1 + b_2)\cos\omega t + (a_1 - a_2)\sin\omega t].$$

It is apparent from the physical constraints that the displacement, x, must be a real quantity. Therefore,

$$x = (a_1 + a_2)\cos\omega t - (b_1 - b_2)\sin\omega t$$

and, since

$b_1 + b_2$ and $a_1 - a_2$ must be equal to zero for the imaginary term to vanish, then

$$x = 2a\cos\omega t - 2b\sin\omega t,$$

which is the same form as the general solution to the differential equation (3-2).

If damping is considered, the solution becomes

$$x = e^{-\sigma t}(A_1e^{i\omega_a t} + A_2e^{-i\omega_a t}),$$

where

$$\sigma = c_D/2M.$$

A convenient form of this solution is

$$x = Ae^{-\sigma t}\cos(\omega_a t + \psi).$$

A decay modulus, defined as τ, is the time required for the amplitude to decrease to 1/e of its original value, i.e.,

$$\tau = 1/\sigma = 2M/c_D.$$

Increasing mass or decreasing damping in-

creases τ.

For the alternate solution to equation (3-4) for harmonically forced vibration, replace F sin ωt with its complex equivalent, $Fe^{i\omega t}$. The equation may now be written as follows:

$$\text{If } x = Ae^{i\omega t}$$

$$Fe^{i\omega t} = e^{i\omega t}(-A\omega^2 M + iA\omega c_D + Ak).$$

Now

$$A = F/(i\omega c_D + (k - \omega^2 M))$$

and

$$x = Fe^{i\omega t}/[i\omega c_D + (k - \omega^2 M)]$$

If we define a complex mechanical impedance, Z_m, as

$$Z_m = c_D + i(\omega M - k/\omega)$$
$$= c_D + iX_m = Z_m e^{i\psi},$$

where $X_m = \omega M - k/\omega$ = mechanical reactance, then

$$Z_m = (c_D^2 + X_m^2)^{1/2},$$

with phase angle Ψ, where

$$\Psi = \tan^{-1}(X_m/c_D).$$

The mobility of the system is defined as

$$Y_m = 1/Z_m.$$

Here, Z_m is analogous to the impedance of a series circuit, c_D to the resistance, M to the inductance, and k to the reciprocal of the capacitance.

Now in simplified form

$$x = -iFe^{i(\omega t - \Psi)}/\omega Z_m,$$

and the actual displacement is the real part of x or

$$x = F \sin(\omega t - \Psi)/\omega Z_m$$
$$= F \sin(\omega t - \Psi)/\omega[c_D^2 + (\omega M - k/\omega)^2]^{1/2}.$$

Mechanical resonance is defined as the frequency at which the mechanical reactance, X_m, vanishes, i.e., where

$$\omega_o = (k/M)^{1/2}.$$

The driving force supplies maximum power to the oscillator at this frequency, such that

$$x_{RES} = F(\sin \omega_o t)/\omega_o c_D.$$

However, this does not give the maximum displacement amplitude. That occurs when $\omega[c_D^2 + (\omega M - k/\omega)^2]^{1/2}$ is a minimum. The frequency for this case is

$$\omega = [\omega_o^2 - 2(c_D/2M)^2]^{1/2}.$$

As mentioned earlier, the amplitude peaks at resonance when there is low to moderate damping. If c_D is small, the amplitude rises and falls off rapidly and it is termed a *sharp resonance*. If it rises and falls off more slowly, it is termed a *broad resonance*. The sharpness of the resonance is measured in terms of the quality factor, Q, such that

$$Q = \omega_o/(\omega_2 - \omega_1),$$

where ω_o is the resonance frequency and ω_1 and ω_2 are the frequencies that are, respectively, below and above the resonance at which the power has dropped to 1/2 the resonance value. This occurs when $X_m = \pm c_D$, i.e.,

$$\omega_2 M - k/\omega_2 = c_D$$

and

$$\omega_1 M - k/\omega_1 = -c_D.$$

From the above, it follows that

$$\omega_2 - \omega_1 = c_D/M$$

and

$$Q = \omega_o M/c_D.$$

The factor $Q/2\pi$ is a measure of the ratio of the maximum energy of the driven oscillator at its resonant frequency to the energy dissipated per cycle.

A stiffness controlled oscillator system is characterized by a large value of k/ω for the frequency range over which the response is desired to be flat. In this range, ωM and c_D are

negligible compared with k/ω. In addition, Z_m is very nearly equal to $-i(k/\omega)$, so that $x \approx (F/k) \cos \omega t$ and $v \approx -(\omega F/k) \sin \omega t$. Hence, the displacement is independent of frequency.

A resistance (i.e., damping) controlled system is one for which c_D is large compared with the reactance X_m. This occurs when a highly damped oscillator operates in the vicinity of resonance. Then,

$$x \approx (F/\omega c_D) \sin \omega t$$

and

$$v \approx (F/c_D) \cos \omega t.$$

The velocity amplitude is independent of frequency, but the displacement amplitude is not.

A mass controlled system is characterized by a large value of ωM over the range of interest. In this case, k/ω and c_D are negligible, i.e.,

$$x \approx -(F/\omega^2 M) \cos \omega t$$

and

$$v \approx (F/\omega M) \sin \omega t.$$

Here neither the displacement nor the velocity amplitude is independent of frequency. The acceleration amplitude, $a = (F/M) \cos \omega t$, is however, independent of frequency.

ALGEBRA OF COMPLEX NUMBERS

Points in the complex plane can be expressed in the form $x + iy$, where x and y are real. Operations on these points are accomplished as follows:

$$\text{Addition: } (x_1 + iy_1) + (x_2 + iy_2) = (x_1 + x_2) + i(y_1 + y_2)$$

$$\text{Multiplication: } (x_1 + iy_1)(x_2 + iy_2) = (x_1x_2 - y_1y_2) + i(x_2y_1 + x_1y_2)$$

$$\text{Division: } (x_1 + iy_1)/(x_2 + iy_2) = (x_1x_2 + y_1y_2)/(x_2^2 + y_2^2) + i(x_2y_1 - x_1y_2)/(x_2^2 + y_2^2)$$

If two complex quantities are equal, their real parts are equal and the coefficients of their imaginary parts are also equal. The exponential function e^A or $\exp^A$ of any point, $A = x + iy$, is defined as the point whose distance is e^x and whose angle measured in radians, is y, i.e.,

$$e^{x+iy} = e^x(\cos y + i \sin y),$$

where $e = 2.718$. From this

$$e^A e^B = e^{A+B}, (e^A)^n = e^{nA}, e^{-A} = 1/e^A, e^1 = e, e^0 = 1.$$

The function e^A is a periodic function having a pure imaginary period $2\pi i$. Hence, $e^{A + k2\pi i} = e^A$, where k is any positive integer. Any point, A, can be expressed in the form $A = re^{i\psi}$, where r is the distance and ψ is the angle of the point. Therefore,

$$(r_1e^{i\psi_1})(r_2e^{i\psi_2}) = (r_1r_2)e^{i(\psi_1 + \psi_2)}; (re^{i\psi})^n = r^n e^{in\psi}.$$

If $x + iy = re^{i\psi}$ then

$$r = (x^2 + y^2)^{1/2}, \sin \psi = y/r, \cos \psi = x/r, \tan \psi = y/x.$$

If two complex quantities are equal, their distances will be equal and their angles will differ by some multiple of 2π. Thus, if $r_1e^{i\psi_1} = r_2e^{i\psi_2}$, then $r_1 = r_2$ and $\psi_1 = \psi_2$, or $\psi_2 \pm 2\pi b$. where b is a positive integer.

3.1.3 MULTIPLE MASS SYSTEMS

Figures 3.4 through 3.11 illustrate harmonic systems. Figure 3.4 summarizes vibrating system elements and figure 3.5 presents the equivalent stiffnesses for certain combined springs.

Figures 3.6 and 3.7 show the basic frequency formulas for some common systems. A log-log plot of the response of a simple-mass, damped system (system 1, figure 3.7) is presented in figure 3.8 and figure 3.9 shows the associated phase angle response. Figure 3.10 illustrates a log-log plot of the motion of a light-weight frame supporting a vibrating mass (system 2, figure 3.7) and figure 3.11 shows the phase relationship.

TRANSLATIONAL ELEMENTS

Element	Standard Symbol	Units	Impedance (F/V)	Symbol of Element
Mass	m_m	kilograms pounds	$i\omega m_m$	
Stiffness	K_m	kilograms/meter pounds/inch	$\frac{K_m}{i\omega}$	
Damping	c	kilogram seconds/meter pound seconds/inch (F = force, v = velocity)	c_D	

ROTATIONAL ELEMENTS

Element	Standard Symbol	Units	Impedance (T/Ω)	Symbol of Element
Rotational inertia	J	kilogram meter^2 pound foot^2	$i\omega J$	$J = mf^2$
Rotational stiffness	K_r	newton meter/radian pound foot/radian	$\frac{K_r}{i\omega}$	K
Rotational damping	c_r	newton meter second/radian pound foot second/radian	c_r	c

(T · torque, Ω = angular velocity)

Figure 3.4. Elements of Vibrating Systems

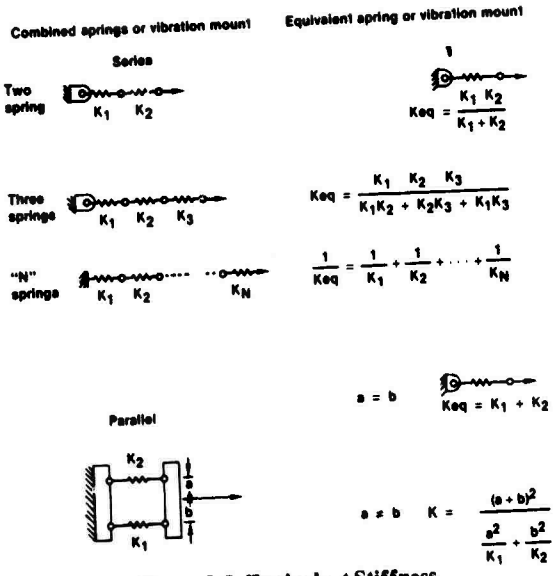

Figure 3.5. Equivalent Stiffness of Combined Springs

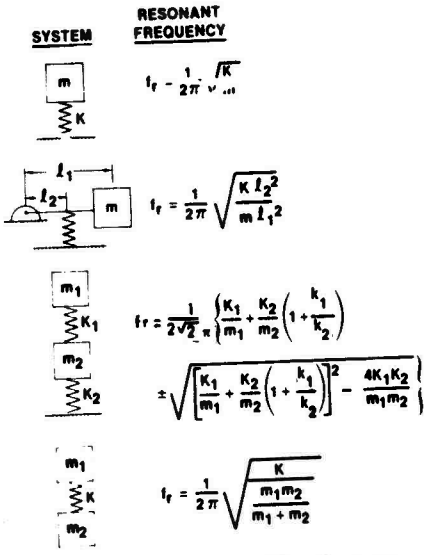

Figure 3.6a. Spring Mass Systems

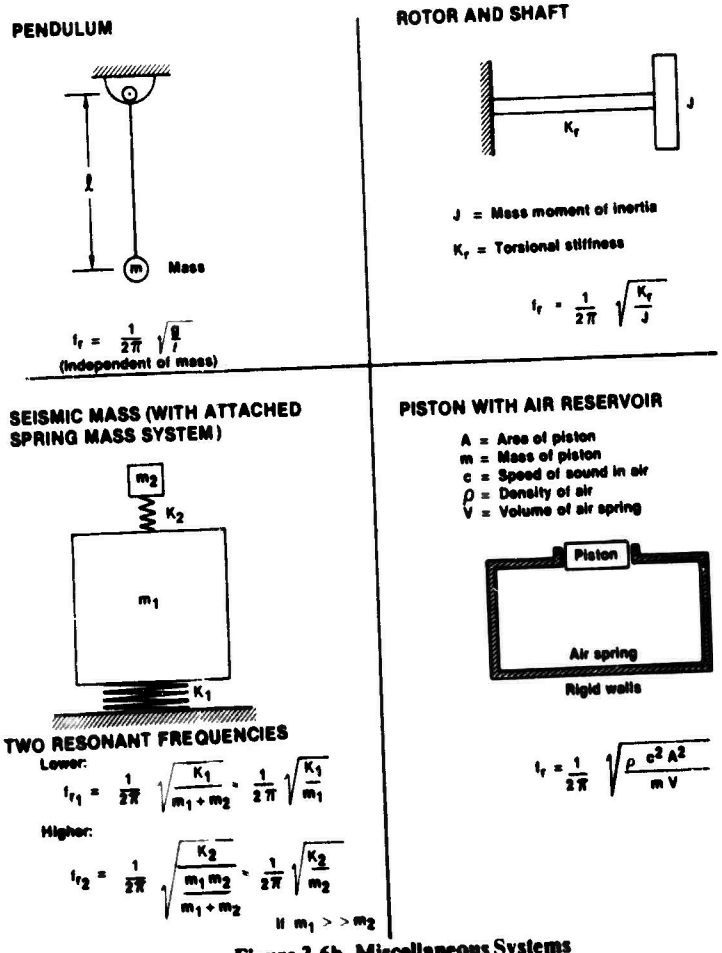

Figure 3.6b. Miscellaneous Systems

Figure 3.6. Natural Frequencies of Simple Vibrating Systems

SYSTEM 1 - DRIVEN MASS

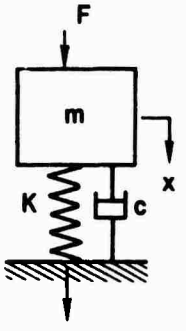

F_T = Transmitted force

Displacement response of system 1

$$X = \frac{F \sin(\omega t - \Theta)}{K\sqrt{(1-r^2)^2 + (2\zeta r)^2}}$$

Phase response of system 1

$$\Theta = \arctan\left(\frac{2\zeta r}{1-r^2}\right)$$

SYSTEM 2 - DRIVEN FOUNDATION

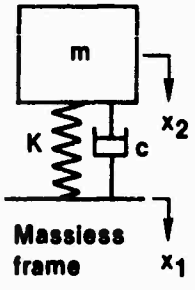

Force transmitted to foundation (F_T/F) of system 1 or displacement ratio x_2/x_1 of system 2

$$\frac{F_T}{F} = \frac{x_2}{x_1} = \sqrt{\frac{1 + (2\zeta r)^2}{(1-r^2)^2 + (2\zeta r)^2}} \sin(\omega t - \Psi)$$

Phase response of F_T/F or x_2/x_1 of system 2

$$\Psi = \arctan\left[\frac{2\zeta r^3}{(1-r^2) + (2\zeta r)^2}\right]$$

WHERE: $r = \omega/\omega_o$

Figure 3.7. Steady State Response of Simple Spring-Mass-Damper Systems

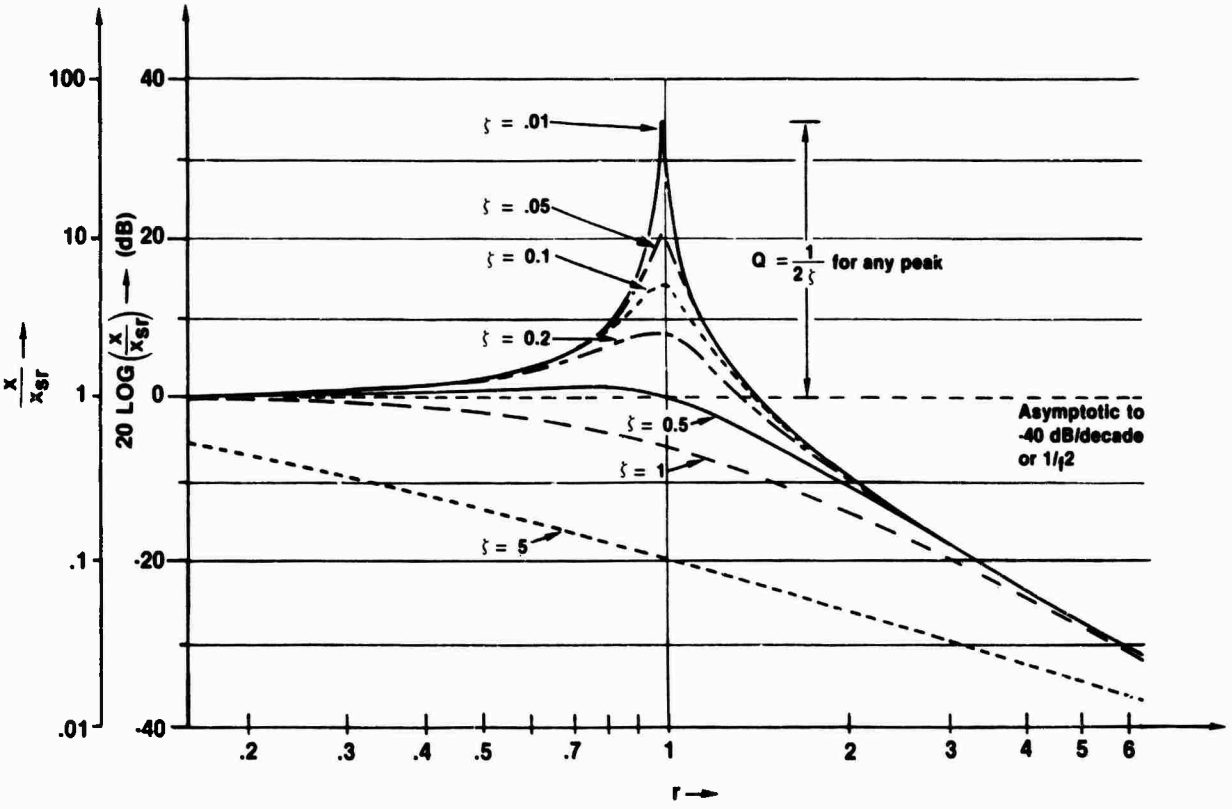

Figure 3.8. Displacement Response of Driven Mass

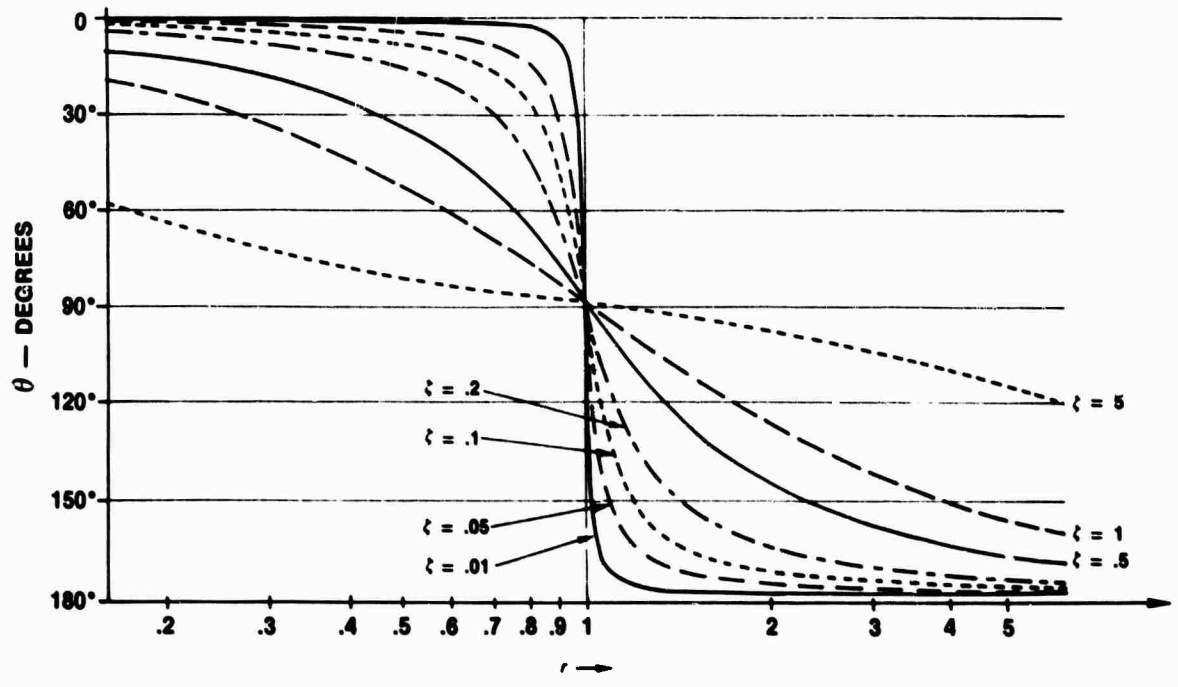

Figure 3.9. Phase Angle Response of Driven Mass

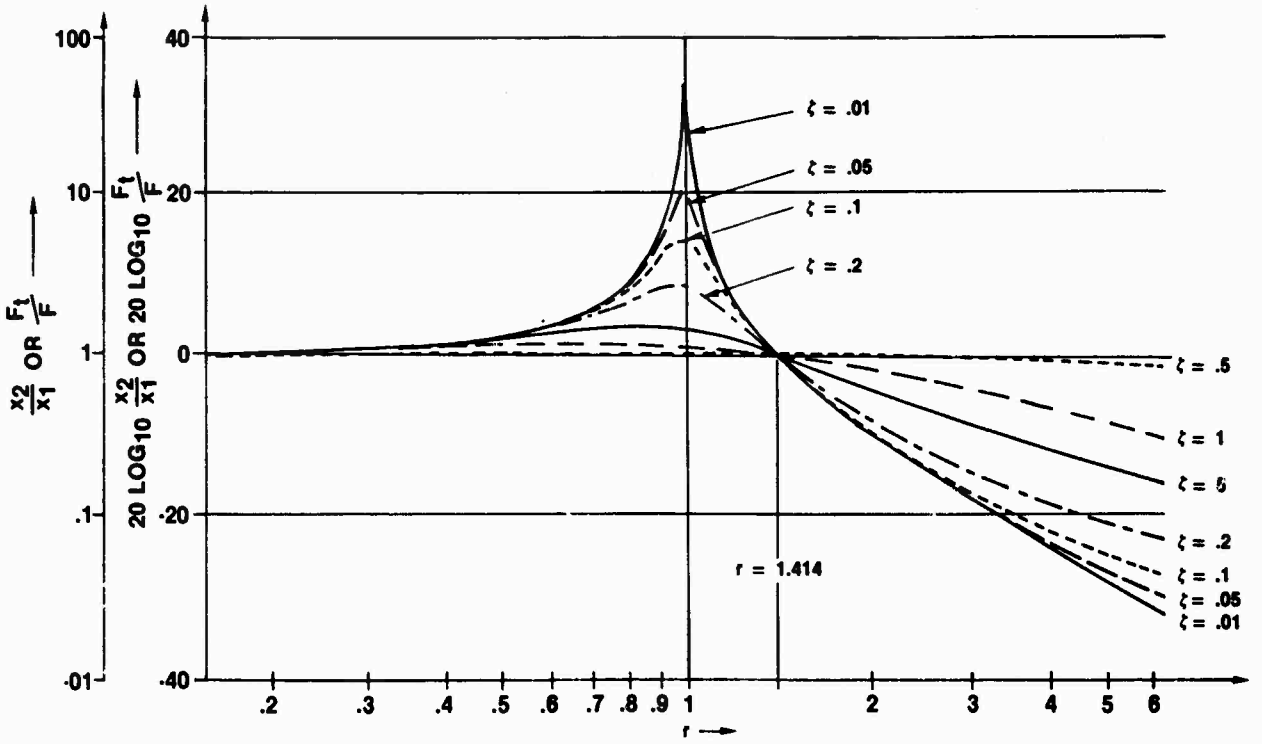

Figure 3.10. Displacement Response of Mass on Driven Foundation

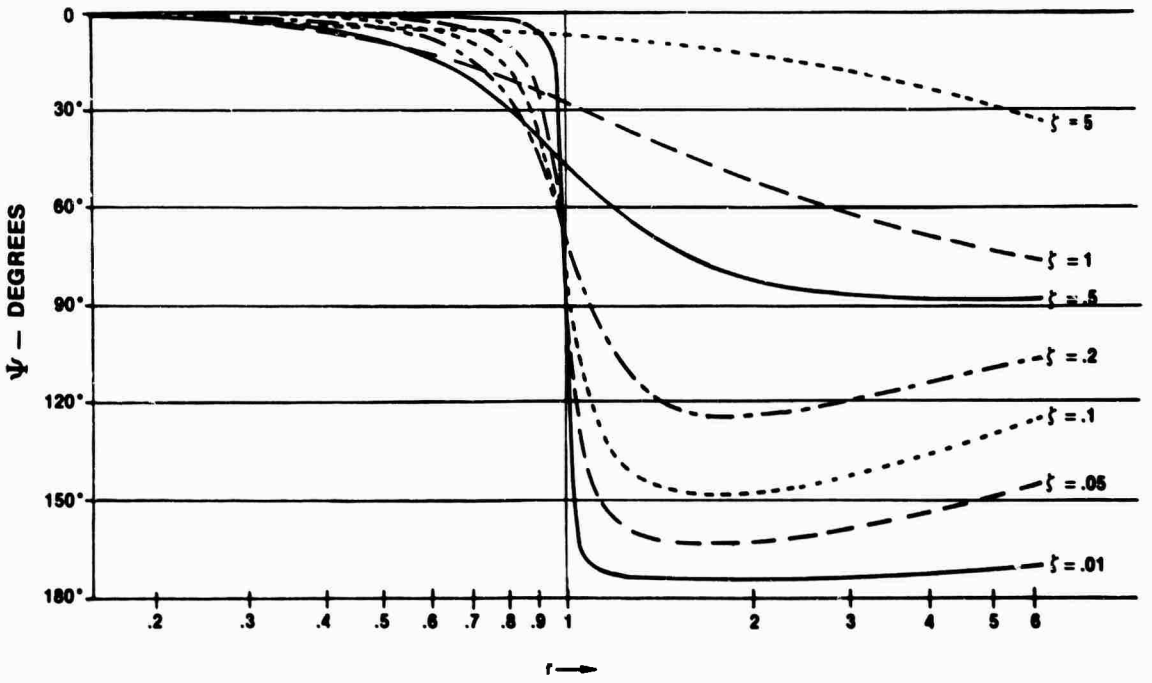

Figure 3.11. Phase Angle Response of Mass on Driven Foundation

3.1.4 DAMPING MEASUREMENTS

It is often necessary to measure the damping of a mechanical vibrating system to determine if additional damping will reduce vibrations. Damping is more difficult to model mathematically than mass or stiffness. Therefore, some of the measurement methods that apply to underdamped systems will be described below and the measurement parameters are presented in figure 3.12.

	Q No units	ζ No units	δ dB/sec	Λ No units
Q		$Q=\frac{1}{2\zeta}$	$\alpha=\frac{27.3f_r}{\delta}$	$Q=\sqrt{\frac{1}{4}+\left(\frac{\pi}{\Lambda}\right)^2}$
ζ	$\zeta=\frac{1}{2Q}$		$\zeta=\frac{\delta}{54.6f_r}$	$\zeta=\frac{1}{\sqrt{1+\left(\frac{2\pi}{\Lambda}\right)^2}}$
δ	$\zeta=\frac{27.3f_r}{\alpha}$	$\delta=54.6f_r\zeta$		$\delta=\frac{27.3f_r}{\sqrt{\left(\frac{\pi}{\Lambda}\right)^2+\frac{1}{4}}}$
Λ	$\Lambda=\frac{2\pi}{\sqrt{4Q^2-1}}$	$\Lambda=\frac{2\pi\zeta}{\sqrt{1-\zeta^2}}$	$\Lambda=\frac{2\pi}{\sqrt{\left(\frac{54.6f_r}{\delta}\right)^2-1}}$	

Q = Quality factor
ζ = Critical damping ratio
δ = Decay rate
Λ = Logarithmic decrement
f_r = Resonant frequency

Figure 3.12. Measurement Methods for Undamped Systems

3.1.4.1 Steady-State Damping Measurements

If a mechanical system is driven by a sinusoidal force, $F = F_o \sin 2\pi ft$, where f is near the resonant frequency, three frequencies are recorded. The recorded frequencies are designated f_r, the resonant frequency, and f_1 and f_2, the frequencies above and below f_r, where the response of the system is down 3 dB, as shown in figure 3.13. The expression for the calculation of Q, the quality factor, is

$$Q = f_r/(f_1 - f_2)$$

and, from that,

$$c_D = \omega_o M/Q = 2\pi f_r M/Q.$$

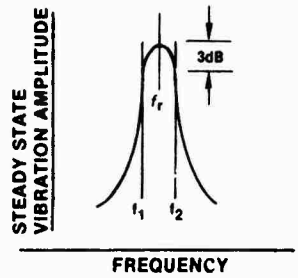

Figure 3.13. Quality Factor Method

If a system is characterized by one major resonance, it may be *bumped* to produce a decaying sinusoidal response at the resonant frequency. If there are many resonances, it may have to be excited at the exact frequency where damping is to be measured. Then, when the excitation is removed, the decay can be observed at the selected resonant frequency without interference from other resonances. A typical decaying signal is shown in figure 3.14. In any case, the decaying signal is $Ae^{-\alpha t} \sin 2\pi f_r t$, where α is a constant equal to $\zeta\omega_o$.

Among the methods to infer damping from a time plot of the decaying signal are logarithmic decrement and logarithmic decay rate.

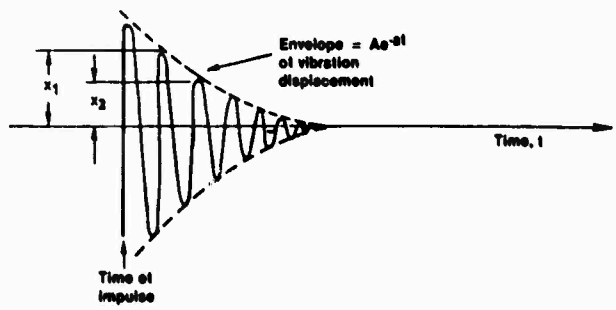

Figure 3.14. Decay Curve Envelope

3.1.4.2 Logarithmic Decrement

For this method, $\Lambda = \log_e (x_1/x_2)$, where x_1 and x_2 are any two successive peak amplitudes in the decay curve. For very light damping,

$$\Lambda \approx (x_1 - x_2)/x_1 = 1 - x_2/x_1.$$

3.1.4.3 Logarithmic Decay Rate

Many values must be averaged to minimize errors when determining logarithmic decrement. A simple method consists of converting the signal to decibels and recording the amount of decay on an oscilloscope having a memory cathode-ray tube. The decay envelope, $e^{-\sigma t}$, will be seen as a straight line and damping may be inferred from its slope using

$$Q = 27.287f/\delta,$$

where δ is the decay rate in decibels per second.

A nomograph that may be used to quickly calculate these factors is presented in figure 3.15 and the matrix for the relationship of damping parameters is shown in figure 3.12.

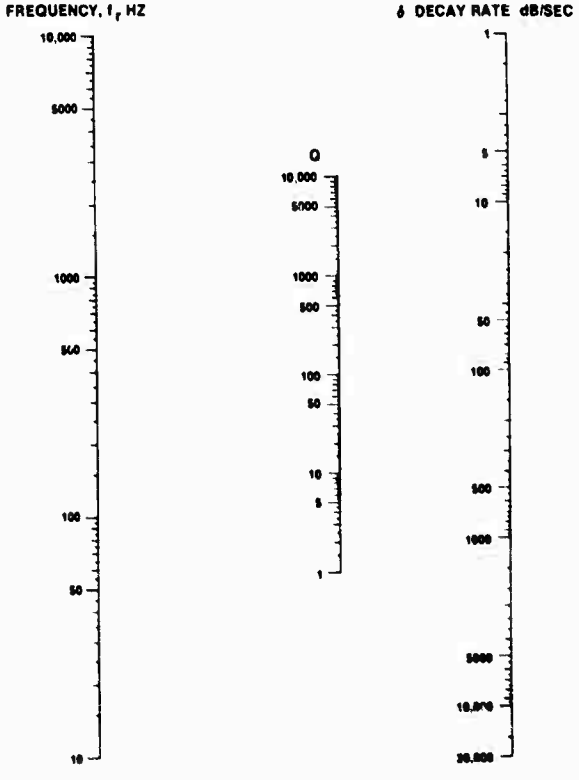

Figure 3.15. Nomogram to Obtain Q

3.1.5 COMPUTATION OF MECHANICAL IMPEDANCE

Mechanical impedance is measured by simultaneously measuring input force to a mechanical system and the resulting velocity. Mechanical impedance, **Z** is the resultant ratio, i.e., **Z** = F/V. The value **Z** consists of amplitude |Z| and a phase angle. The amplitude |Z| can be calculated from the following formulas using the output of a force gauge and velocity pickup,i.e.,

3.1.5.1. Velocity Pickup Method

$$|Z| = (F/V)K,$$

where

F = output of force gauge (mvolt),
V = output of velocity pickup (mvolt)
K = sensitivity of force gauge (mvolt/lb). divided by sensitivity of velocity pickup (mvolt/in.)

3.1.5.2. Accelerometer Method

$$|Z| = 2f\pi K(F/A_c),$$

where

F = output of force gauge (mvolt)
A_c = output of accelerometer (mvolt)
K = sensitivity of force gauge (mvolt/lb), divided by sensitivity of accelerometer (mvolt/K)
f = frequency (Hz).

The phase angle can be read directly from a phase meter or estimated from oscilloscope traces. Typical plots of impedance and mobility are shown in figure 3.16.

If a system has more than one attached impedance, the calculation depends on the number of *ports* or *points of attachment*. The one port system discussed above is illustrated in figure 3.17a. A diagram of a two port system and the applicable equations, which form a matrix, are shown in figure 3.17b. The matrix for an *N* port system is shown in figure 3.17c. The impedance and mobility matrices are the inverse of each other. Mobility matrix terms are easier to measure than the impedance matrix terms because the force values can be set to zero

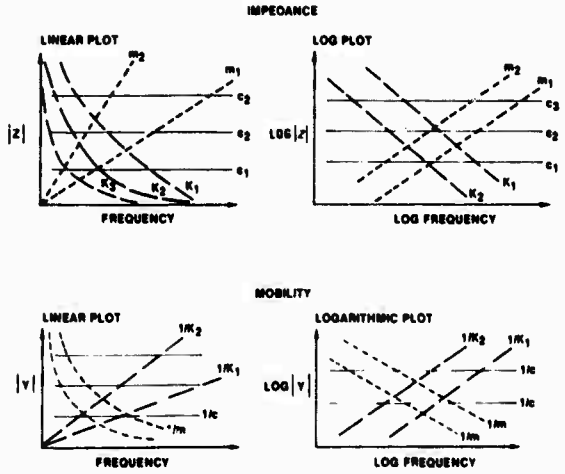

Figure 3.16. Plots of Impedance and Mobility of Masses, Springs, and Dampers

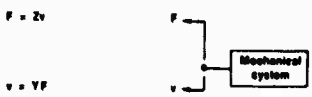

Figure 3.17a. One Port System

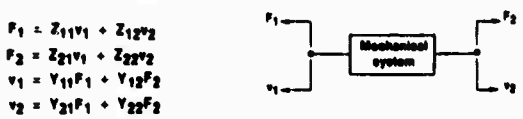

Figure 3.17b. Two Port System

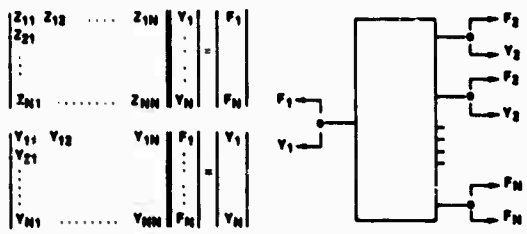

Figure 3.17c. *N* Port System

Figure 3.17. Computing Mechanical Impedance

easier than can the velocity values. Note that the phase of measured drive point impedance or mobility can never exceed $\pm 90°$.

It should also be noted that Z_{11} and Y_{11} are the driving point impedance and mobility, respectively, Z_{ij} and Y_{ij} are the transfer impedance and mobility, respectively, and Z_{NN} and Y_{NN} are the output impedance and mobility, respectively, Because of reciprocity, $Z_{12} = Z_{21}$, $Y_{12} = Y_{21}$, $Z_{21} = Z_{12}$, and so on.

For a one port system $Z = 1/Y$, but for two or more ports $Z_{12} \neq 1/Y_{12}$. For a two port system, the relationships between impedance and mobility are

$$
\begin{aligned}
Z_{11} &= Y_{22}/\Delta' \\
Z_{12} &= -Y_{12}/\Delta' \\
Z_{21} &= -Y_{21}/\Delta' \\
Z_{22} &= Y_{11}/\Delta' \\
Y_{11} &= Z_{22}/\Delta'' \\
Y_{12} &= -Z_{12}/\Delta'' \\
Y_{21} &= -Z_{21}/\Delta'' \\
Y_{22} &= Z_{11}/\Delta''
\end{aligned}
$$

where

$\Delta' = Y_{11}Y_{22} - Y_{12}Y_{21}$ and
$\Delta'' = Z_{11}Z_{22} - Z_{12}Z_{21}$.

3.1.5.3. Characteristic Driving Point Impedance of a Plate

If an infinite plate is driven at a point (or over a small area), its impedance, termed the *characteristic impedance*, is constant with frequency and easily calculated. Characteristic impedances for steel and aluminum are plotted in figure 3.18.

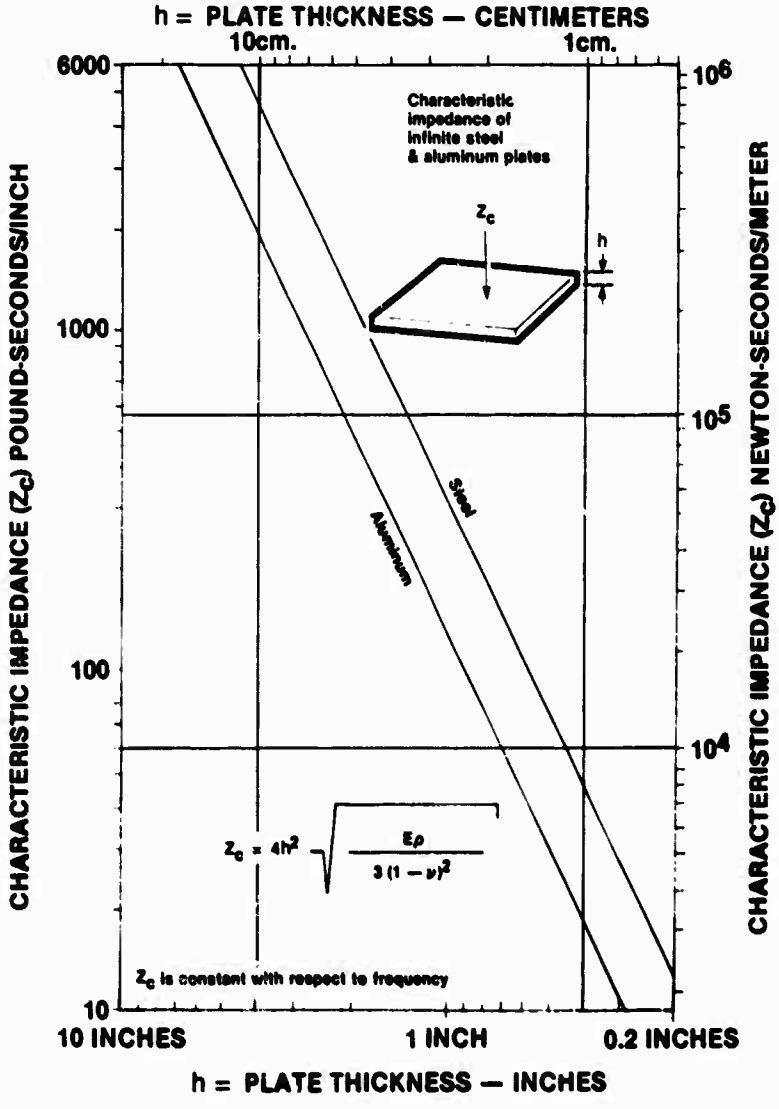

Figure 3.18. Characteristic Impedance of Infinite Steel and Aluminum Plates

Although calculated for an infinite plate, the characteristic for a finite plate is the geometric mean between impedance maxima and minima. Moreover, the maxima and minima tend to converge as frequency increases to the characteristic impedance. Thus, an estimate of the characteristic impedance of the infinite plate is an aid to determining the impedance of a finite plate. A plot of the impedance of a finite plate is provided in figure 3.19.

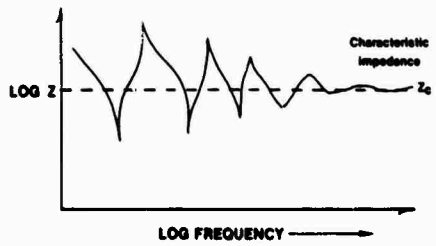

Figure 3.19. Impedance of a Finite Plate

3.1.6 VIBRATION DAMPING

Damping is one of the principal methods of attenuating acoustic energy in ship structures and the subject is, therefore, important to an understanding of sonar installations. Fundamentally, damping is a mechanism that converts vibratory energy into heat. However, because the energy associated with such vibration is so small, heat does not become a problem.

The three types of damping mechanisms are

1. viscous damping (damping force proportional to velocity),
2. dry friction or Coulomb damping (damping force proportional to weight), and
3. hysteresis, or material damping (damping force proportional to displacement).

The hysteretic damping of resonant structures by elastomers is the primary method used onboard ships.

All materials are characterized by some degree of inherent damping. Unfortunately, most structural materials, especially high tensile steels and bronze alloys, have very little. When excited, a structure responds at a frequency that depends on the mass elastic properties of the material.

Generally, damping is achieved by applying visco-elastic material to the plate and beam structures onboard ship. Sandfilled tubular foundations, and other dissipative means, are used to damp specific noise sources. Riveted and bolted joints are characterized by much more damping than are welded structures.

In the case of panel or plate damping, the application of a dissipative visco-elastic material to the surface provides a *dash pot* effect that absorbs a portion of the kinetic energy of vibration. Figure 3.20 shows a plot of the effect of damping materials on elastic plates and figure 3.21 shows the effect of sound damping material on a machinary foundation. The automobile *shock absorber* is an example of high-damping in which the viscous damping force is proportional to velocity.

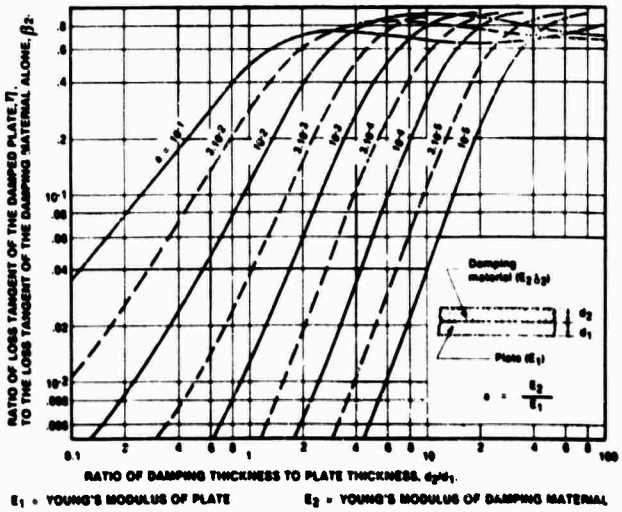

Figure 3.20. Effect of Damping Material on Elastic Plates

In distributed linear elastic structures there are numerous modes, natural frequencies, and resonances that contribute to the unwanted sound. The importance of resonance depends on the Q of the structure and the transmission of resonant vibrating energy through the hull to the sonar.

Some large plate and beamlike structures have higher Q values than others and, therefore, respond differently to the amount and type of damping applied. The wide spectrum of natural

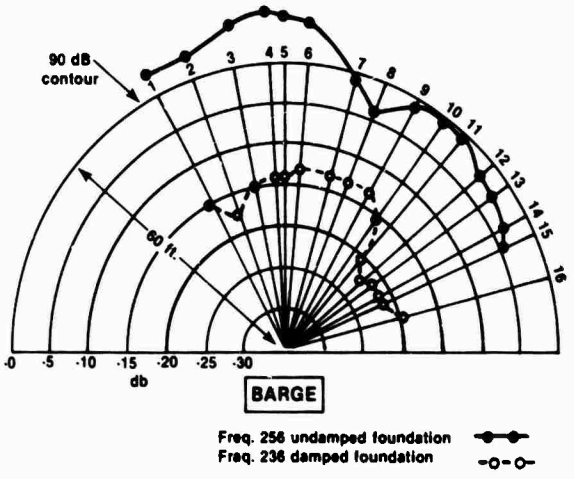

Figure 3.21. Effect of Sound Damping on a Machinery Foundation

frequencies can be heard when a ship structure is struck with a hammer while the vessel is in dry dock. Submarine propellers are particularly *live* and may effectively radiate sound. However, proper damping will eliminate the vibration, or *singing*, problem.

Figure 3.31, which will be discussed in detail in Section 3.1.7.7, shows a graph of cumulative structure modes versus frequency. As can be seen, there are numerous modes in the sensitive sonar bands where damping is effective for structures of the type used in submarines and surface warships.

Figure 3.22 shows the far field sound pressure and the inverse mechanical impedance of a foundation structure having 4 legs terminated in a 1/4-section cylindrical hull barge. Only the 200 to 500 Hz region is shown and it is clearly evident that the resonant regions, R_1 and R_2, control the sound radiation. Figure 3.21 shows the effect that damping had on the sound radiated at 256 Hz from such a structure.

Perhaps the most important areas where damping is effective are in

1. and around the acoustic environment of the sonar, e.g., adjacent bulkheads,
2. the transmission path between noise sources and the hull, e.g., bedplates and foundations,
3. non-pressure hull platings, e.g., ballast tanks, and
4. or on noise sources, e.g., fan housings.

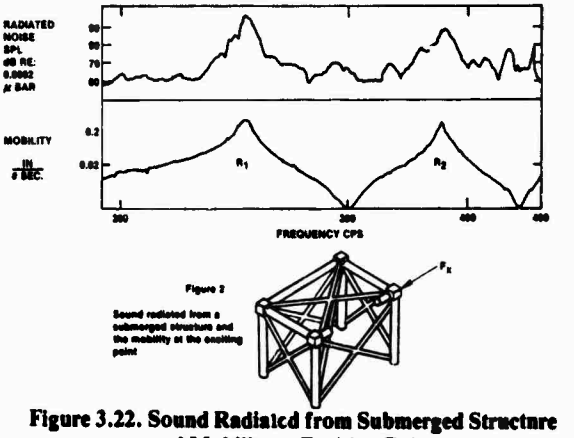

Figure 3.22. Sound Radiated from Submerged Structure and Mobility at Exciting Point

Note that in relation to 1 above, damping must not be located so that it causes an *acoustic opaque* situation in which the sonar cannot *look* at the desired field of view.

Unfortunately, damping cannot be used effectively on pressure hulls because their thickness relative to an effective damping treatment is prohibitive. The damping that could be applied would be in series with the resistive value of the acoustic impedance of the seawater. Adding a low value damping treatment to a pressure hull with a resistive impedance waterload of much higher value would not result in a measureable resonance reduction. This situation corresponds to the mass controlled system mentioned earlier.

Snubbers, or hard springs, are characterized by load/deflection curves that are opposite those for the Belleville spring. The resonant frequency of a mass on a snubber depends on the amplitude of the vibration. Typical response curves are presented in figure 3.23.

Damping is necessary for improved sonar operation, but it cannot be applied indiscriminately. This subject will be discussed further in Chapter 4.

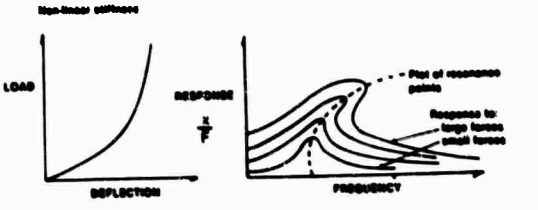

Figure 3.23. Load-Deflection and Response Curves for Elastomeric Snubbers

3.1.7 STATISTICAL METHODS OF VIBRATION ANALYSIS

3.1.7.1 General

The excitation of multiple modes of vibration causes the transmission of sound in ships to be highly complex. The flexural modes of a free-free bar will be used to illustrate this phenomenon because, when a ship vibrates as unit, the modes are similar. The primary mode, i.e., natural frequency, in a flexure, free-free bar is shown in figure 3.24a. This mode has two nodes, i.e., points of no displacement.

The second mode (see figure 3.24b) has three nodes and the third (figure 3.24c) has four. The frequency of each mode is different and, therefore, its damping will be different. These modes, and others, (see figure 3.25) can be concurrently excited and the resultant amplitude at each point is the summation of each.

Figure 3.24a. First Mode

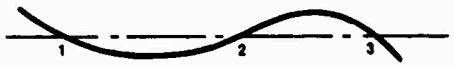

Figure 3.24b. Second Mode

Figure 3.24c. Third Mode

Figure 3.24. Modes of a Free-Free Bar

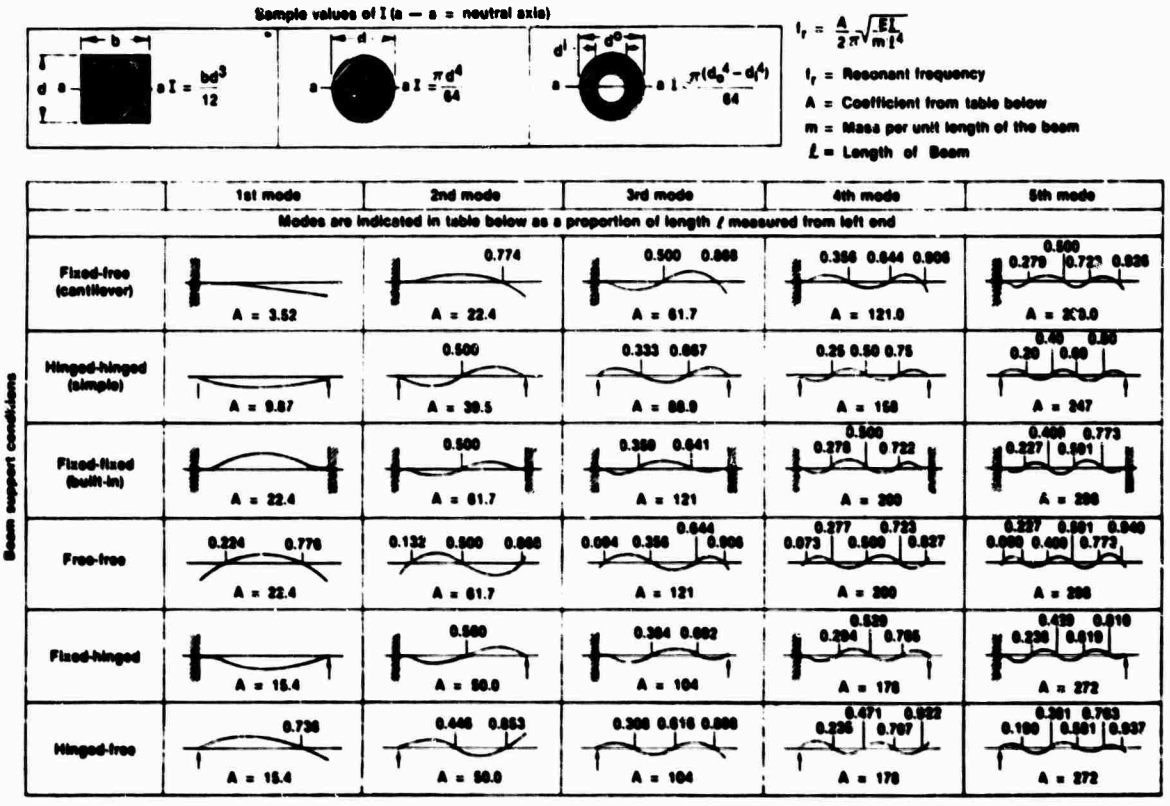

Figure 3.25. Resonance Frequencies and Modes of Simple Beams

Figures 3.26a and 3.26b show some of the many modes in which square and circular plates vibrate. The number of modes would be greatly increased, of course, if rectangular and oval plates were included. Figure 3.27, a cutaway view of a submarine bow, shows the many plates and structural members that can be excited by vibrations. The number of modes and modal frequencies such a structure is subject to is obviously very large. Because it is impractical to analyze each plate individually, statistical methods are employed.

The statistical analysis method for a steady state condition is based on the concept that, when the response is composed of many modes, it is easier to describe the behavior of the sum than of the individual. Architectural

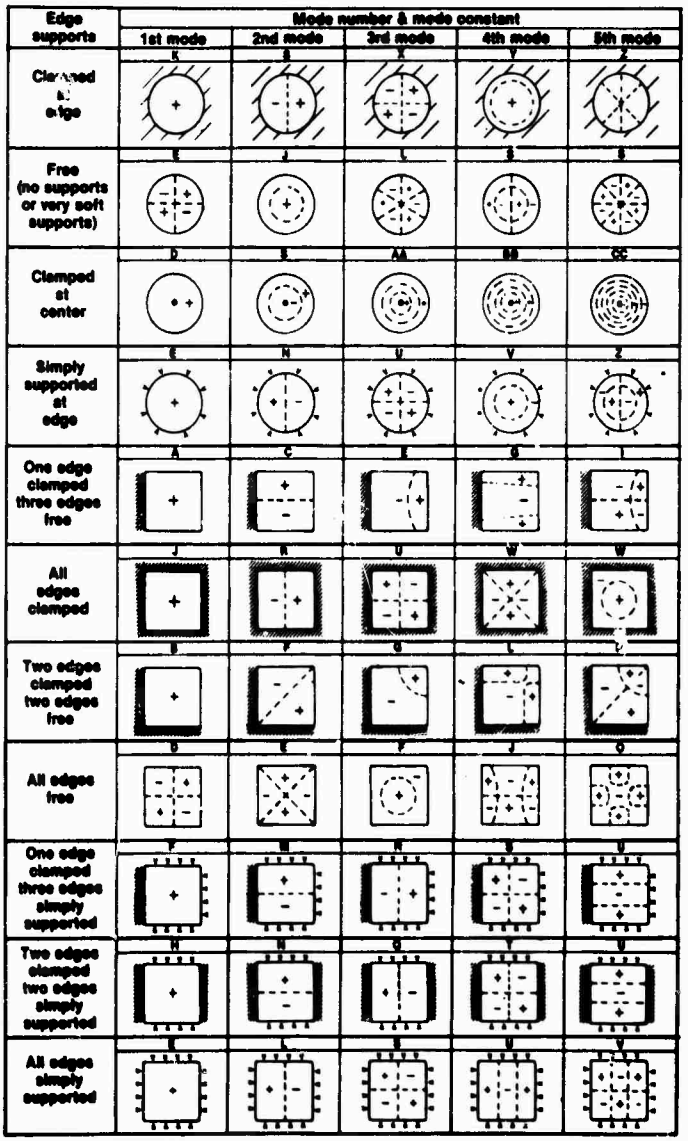

To find the resonance frequencies of each mode, select the mode constant (A,B,E,D,—BB,CC) for the appropriate edge supports to enter the graph on the next page together with plate thickness & either diameter or length of side as appropriate.

Figure 3.26a. Resonance Frequencies and Modes Shapes

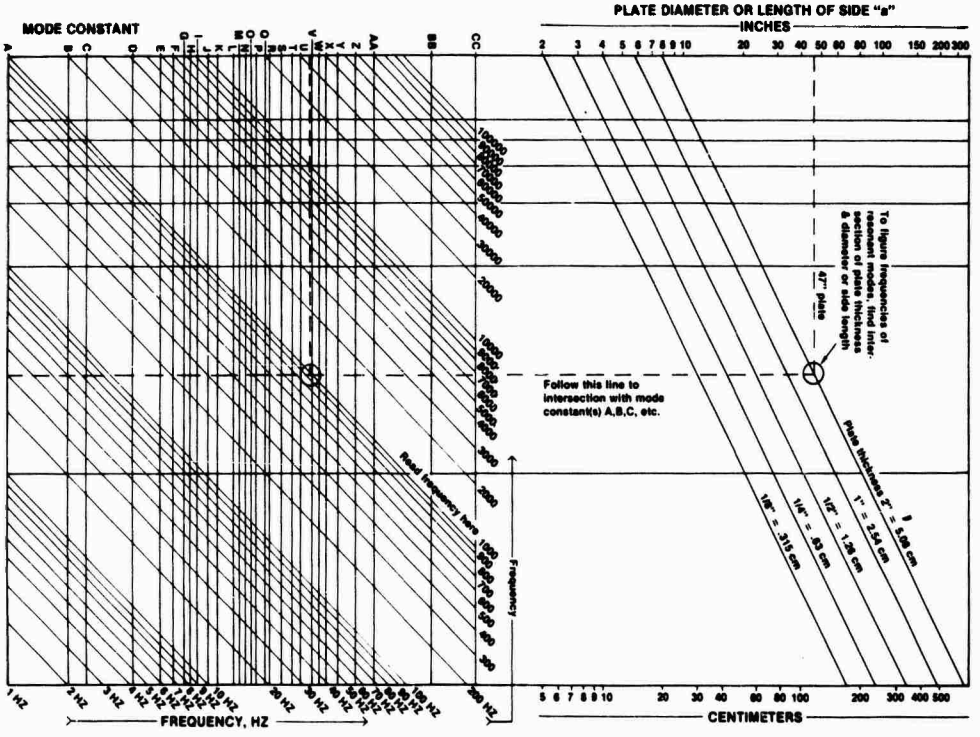

Figure 3.26b. Nomograph for Resonance Frequencies

Figure 3.26. Square and Circular Plate Characteristics

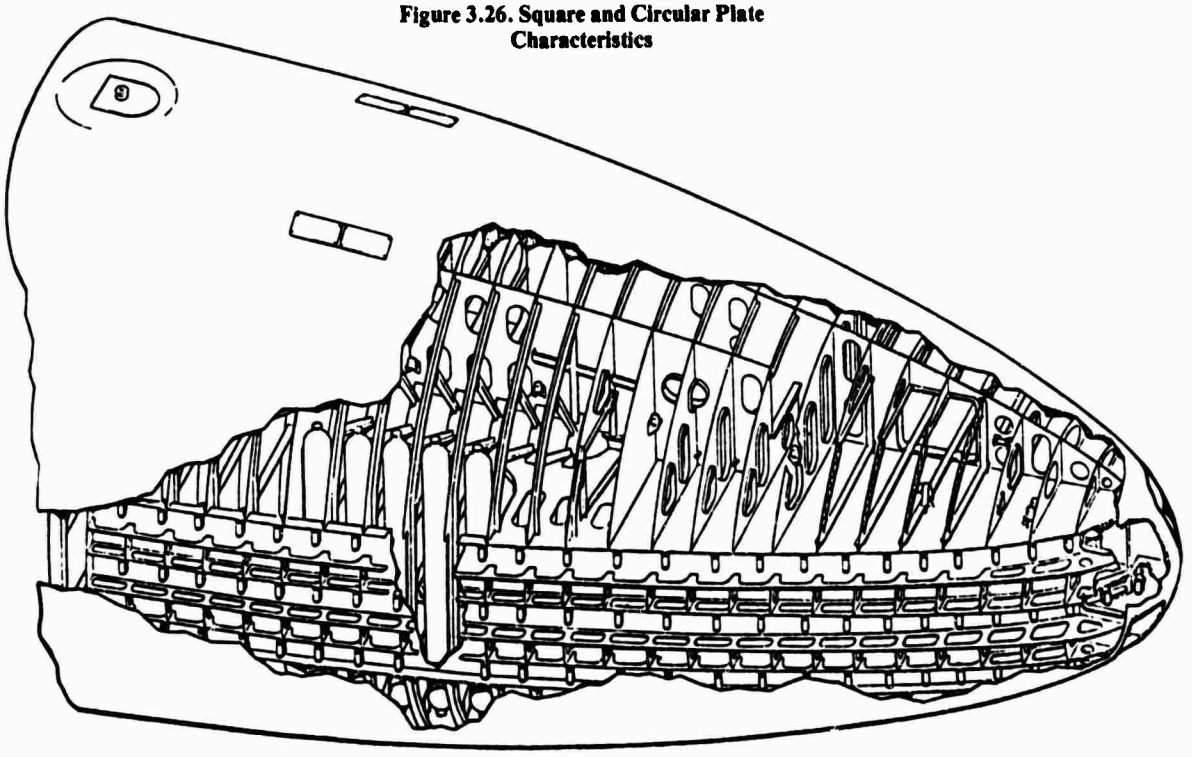

Figure 3.27. Cutaway View of Submarine Bow

acousticians design concert halls by using energy relations that follow from statistical concepts and not by solving wave equations. Any system supporting wave motion may be analyzed statistically when the system is large compared with a wavelength and the results sought are averages. Ships are in this category.

3.1.7.2 Resonance Amplitude of Modes

As discussed earlier, many modes may be excited simultaneously in ships. The amplitude of any one resonance is determined by structural damping and the external or exciting force. In particulai, the relevant external force for any given mode is determined by resolving or *weighting* the force according to the modal vibration pattern.

3.1.7.3 Forcing Function Spatial Pattern

If the spatial pattern of the external force, as a function of time, is very different from that of the mode of interest, the resolved force is much smaller than the total and the mode will not be excited strongly. On the other hand, if the spatial patterns of the force and mode are identical, or nearly so, the resolved force is equal or close to the total external force and the mode is excited strongly. Figure 3.28 represents a panel clamped at each edge and having two spatial pressure patterns above it. Both force fields have the same frequency as the modal frequency of the plates. However, the upper pattern will create a larger velocity amplitude because, at each point, the force field and the panel velocity *fit*, i.e., match closely.

In the bottom of the figure the pressure is uniform at any instant of time and the force over half the panel opposes the motion of this mode, thus inhibiting it. The amplitude is large in the first instance and small in the second, although both panels are in resonance.

For each mode, the resolved external or exciting force equals the internal or dissipation force.The flat plate excitation example discussed in Section 2.2.7 is an example of this phenomenon. The excitation peaks in the power spectra correspond to excited modal resonances in the plate.

3.1.7.4 Modal Energy

The energy in a mode is proportional to the mass multiplied by the square of the velocity. The velocity is, in turn, proportional to the external force divided by the structural resistance or damping. Thus the energy per mode is

$$\text{Modal Energy} \propto [\text{Mass}(\text{Resolved External Force at Resonance})^2]/(\text{Damping})^2 = MF^2/c_D^2.$$

If the exciting force is random, it will have a distributed frequency such as that shown in figure 3.29. It is expressed as a spectral density,

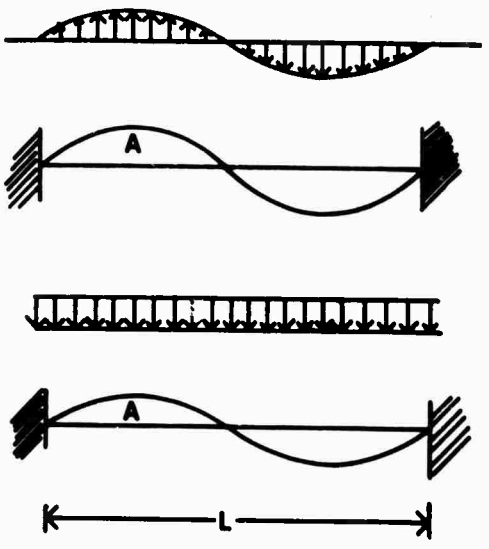

Figure 3.28. Modal Excitation

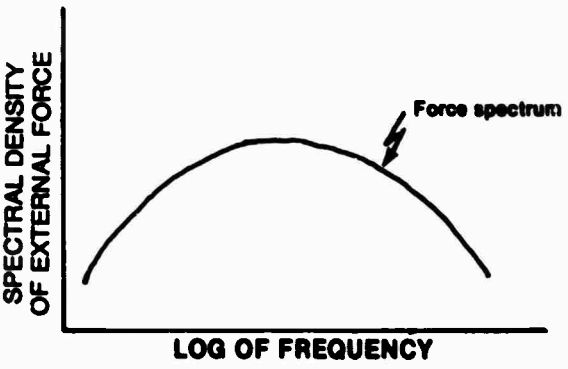

Figure 3.29. Forcing Frequency Spectrum

i.e., mean square force per unit frequency, $F^2/\Delta f$. The integration of the spectrum over all frequencies would yield the total mean square force acting on the structure. To obtain the modal mean square force, over the range of relevant frequencies, it is necessary to integrate over the modal bandwidth, which is proportional to the mode damping divided by the mass. The integration gives the mean square resolved force, which is

$$F^2 = (F^2/\Delta f) \times \text{Bandwidth}$$
$$\propto (F^2/\Delta f) \times \text{Damping/Mass}$$
$$= (F^2/\Delta f)(c_D/M)$$

and, substituting, we have

$$\text{Modal Energy} \propto (F^2/\Delta f)/c_D$$

or

Resolved Force Spectral Density/Damping.

Therefore, the modal energy depends on the damping and the resolved, or weighted, external force.

3.1.7.5 Average Energy

The resolved force spectral density and the damping are difficult to calculate. However, methods are available to calculate the average energy for various cases. For example,

$$E_{AVG} \propto (S_p/f^2)(hc_p/m)/\delta,$$

where

S_p = sound pressure spectral density,
m = mass per unit area,
h = panel thickness,
c_p = (Young's Modulus/Mass Density)$^{1/2}$
= compressional sound velocity,
f = vibration frequency, and
δ = absorption coefficient of flexural vibrations at panel joints.

The average modal energy obscures details, but permits easier calculation of the trends the designer desires.

The average energy, E_{AVG}, value can be used to calculate the total energy in each bandwidth of interest. If a number of modes, ΔN, occur in a frequency interval, Δf, the total energy in that bandwidth is $E_{AVG} \times \Delta N$ (see figure 3.30).

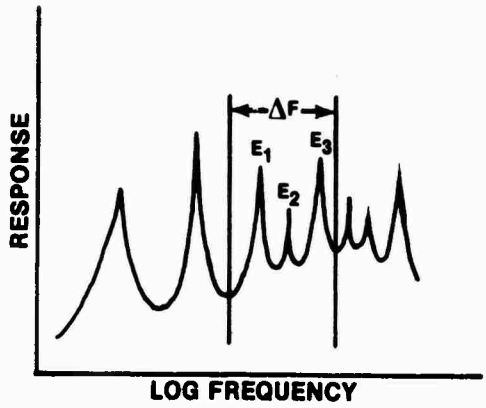

Figure 3.30. Calculation of Average Energy

3.1.7.6 Energy Spectrum

The energy spectral density, S_E, at each frequency is obtained by dividing the bandwidth energy, $E_{AVG} \times \Delta N$, by the bandwidth, Δf. Therefore,

$$S_E = \Sigma(E/\Delta f) = E_{AVG}(\Delta N/\Delta f).$$

3.1.7.7 Modal Density

The modal density, $\Delta N/\Delta f$, is usually a function of the properties of the structure. For a flat panel vibrating in flexure, it is proportional to the surface area divided by the mean thickness (see figure 3.31). Because the characteristics of most structures can be ap-

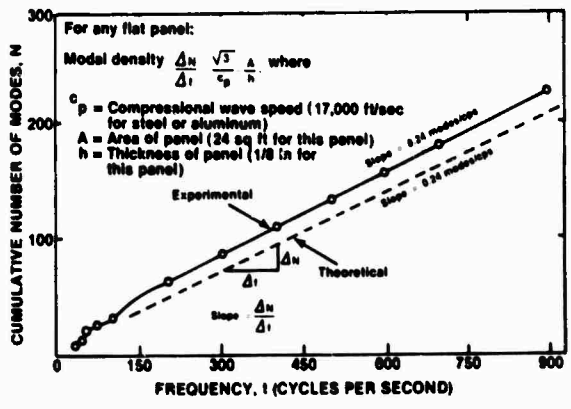

Figure 3.31. Modal Density

proximated in terms of an assemblage of panels or shells, the modal density is usually the sum of the densities of the structure's components.

Figure 3.31 presents the results of an experiment on a flat aluminum plate. The plate was shaken at increasing frequencies and the various resonances noted. The cumulative modes were then plotted and the modal density is the slope at any point. Since the result is a straight line, the modal density is constant.

3.1.7.8 Acceleration Spectra and Spectral Density

The acceleration spectral density, S_A, can be derived from the energy spectrum because the modal spectrum energy,

$$E_m \propto \text{Mass} \times \text{Velocity}^2.$$

Also, since

$$\text{Velocity} \approx \text{Acceleration/Frequency} \propto \text{Force/Resistance},$$

then

$$E_m \propto \text{Mass} \times (\text{Acceleration})^2/\text{Frequency}^2,$$

and, therefore

$$\text{Acceleration}^2 \propto E_m(f^2/M).$$

Now, if

m = mass per unit area of the structure,
A_r = total area, and
mA_r = Mass = M

then, since the frequency of interest is known, f^2/mA_r is known. Also,

$$E_m = E_{AVG}\Delta N$$

and, since,

$$S_A = \text{Acceleration}^2/\Delta f$$

then

$$S_A \propto E_{AVG}(\Delta N/\Delta f)(f^2/mA_r),$$

where E_{AVG} is the average energy in each ΔN mode over the Δf bandwidth.

Now (see figure 3.31), since

$$\Delta N/\Delta f \propto A_r,$$

$$S_A \propto E_{AVG}(f^2/m).$$

Specifically, for a flat panel the acceleration spectral density is independent of size factors, i.e.,

$$S_A \propto (S_p h c_p/\delta m f^2)(A_r/c_p h)(f^2/mA_r),$$

which reduces to

$$S_A \propto S_p(1/\delta m^2).$$

An acceleration spectral density curve is shown in figure 3.32 for two portions of a missile. The root-mean-square value of the acceleration in any given bandwidth can be obtained using the information in the figure.

Although difficult to apply to a whole ship, the statistical method develops valuable concepts that can be useful in solving particular problems.

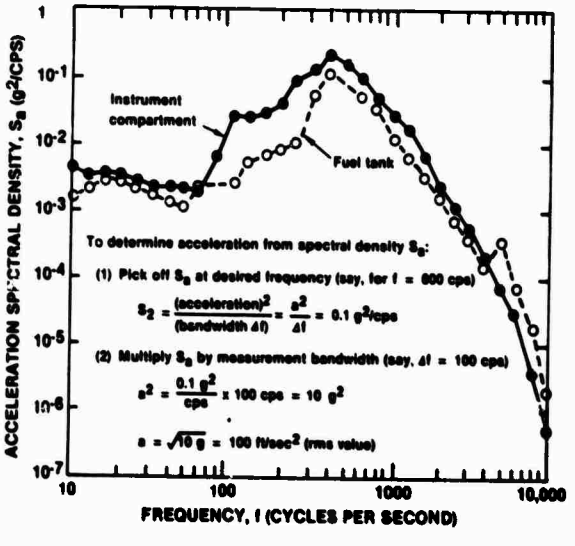

Figure 3.32. Acceleration Density Curve

3.2 TRANSMISSION, REFLECTION, AND DIFFRACTION OF SOUND IN MATERIALS

3.2.1 GENERAL

The vibrational nature of sound and the manner in which the energy is distributed through a ship was discussed in the previous section. This section will explore the nature of sound when the frequencies of interest are much higher than the primary modal frequencies, or when modal frequencies are not of concern. We will first consider the speed of propagation of sound in materials in terms of the basic modes of vibration, i.e., compression, shear, and flexure.

3.2.2 VELOCITY OF PROPAGATION

3.2.2.1 Longitudinal Waves

Consider a segment of material, dx, as shown in figure 3.33. When an elastic material is stressed, it either stretches or compresses. If A_r is any given area to which a force, F, is applied, the stress is

$$\sigma = F/A_r.$$

Applying Hooke's Law, i.e., Stress/Strain = Constant = E, we have

$$\sigma/(\delta\xi/\delta x) = -E$$

or

$$(F/A_r)/(\delta\xi/\delta x) = -E,$$

from which

$$F = -A_rE(\delta\xi/\delta x)$$

and

$$(\delta F/\delta x) = -A_rE(\delta^2\xi/\delta x^2).$$

For the dynamic case, if F_x represents the internal force at x, then $F_x + (\delta F_x/\delta x)dx$ represents the force at (x + dx) and the net force to the right is

$$dF_x = F_x - [F_x + (\delta F_x/\delta x)(dx)] = (-\delta F_x/\delta x)dx,$$

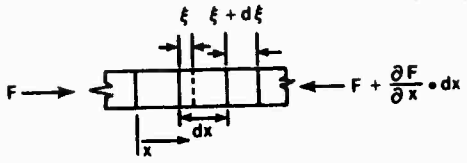

Figure 3.33. Speed of Longitudinal Waves

which, when we substitute for $\delta F_x/\delta x$, becomes

$$dF_x = -A_rE(\delta^2\xi/\delta x^2)dx.$$

Since the mass of the segment is $\rho A_r dx$, the equation of motion is

$$(\rho A_r dx)(\delta^2\xi/\delta t^2) = A_rE(\delta^2\xi/\delta x^2)dx.$$

If we let $c_p^2 = E/\rho$, we have

$$(\delta^2\xi/\delta t^2) = c_p^2(\delta^2\xi/\delta x^2),$$

which is the one dimensional longitudinal wave equation where the velocity of compressional wave propagation is

$$c_p = (E/\rho)^{1/2}.$$

The complete solution is

$$\xi = ae^{i(\omega t - kx)} + be^{i(\omega t + kx)},$$

where the values of a and b depend on the boundary conditions and k = wave number = $\omega/c_p = 2\pi f/c_p = 2\pi/\lambda$.

3.2.2.2 Shear Waves

The speed of propagation of shear waves is obtained in a manner similar to that for longitudinal waves (see figure 3.34). Consider

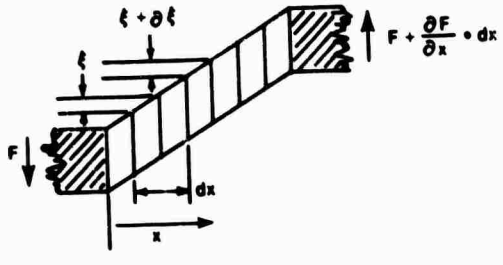

Figure 3.34. Speed of Shear Waves

the segment of material in shear, i.e.,

$$\sigma = F/A,$$

and we have

$$\sigma_s/(\delta\xi/\delta x) = -G,$$

where G is the shear modulus. Similarly, $c_s = (G/\varrho)^{1/2}$ = the velocity of wave propagation.

3.2.2.3 Flexural Waves

More complicated considerations for a plate in bending yield a wave velocity of

$$c_f = (\omega c_p k)^{1/2},$$

where

ω = angular frequency = $2\pi f$,
c_p = compressional speed = $(E/\varrho)^{1/2}$,
k = radius of plate gyration = $h/12^{1/2}$, and
h = plate thickness.

Figure 3.35 provides more exact versions of the bending wave and longitudinal plate velocities.

Bending wave velocity in an elementary plate

$$c = \sqrt[2]{2\pi f}\ \sqrt[4]{\frac{Eg^2}{12\rho(1-\nu^2)}}$$

Bending wave velocity in a Timoshenko-Mindlin plate

$$c = \sqrt{\frac{1}{\frac{\rho}{E}(1+\nu)\left[1.2+\frac{(1-\nu)}{2}\right]+\sqrt{\frac{12\rho(1-\nu^2)}{\omega^2 Eg^2}+\left\{\frac{\rho(1+\nu)}{E}\left[1.2+\frac{(1-\nu)}{2}\right]\right\}^2}}}$$

Longitudinal plate velocity $c = \sqrt{\frac{E}{\rho(1-\nu^2)}}$

Figure 3.35. Wave Velocity in Plates: Various Formulations

Figure 3.36 illustrates wave length versus frequency for steel plates in compression/tension, shear, and bending modes; it also shows those for air and water for comparison. The various wavelengths for a given frequency indicate that higher frequency vibrations in complex structures may be caused by vibrational energy transferring from one mode to another at discontinuities.

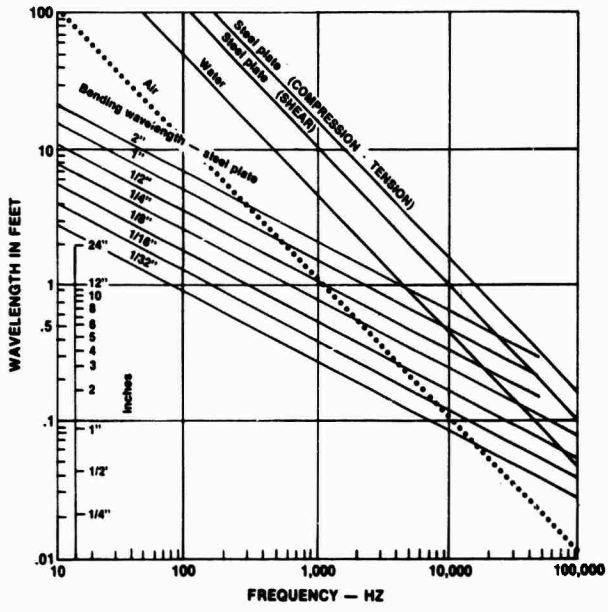

Figure 3.36. Wavelength versus Frequency

3.2.2.4 Velocity of Sound in Fluids and Bulk Solids

The sound velocities for fluids, i.e., air and water, are obtained in a manner similar to that for obtaining longitudinal waves, i.e., for

GASES

$$c = (\gamma P/\varrho)^{1/2},$$

where

γ = ratio of specific heats,
P = pressure, and
ϱ = mass density.

LIQUIDS

$$c = (\gamma K_T/\varrho)^{1/2},$$

where

γ = ratio of specific heats,
K_T = isothermal bulk modulus.

BULK SOLIDS

$$c = \{[K+(3/4)G]/\varrho\}^{1/2},$$

where

K = solid bulk modulus .

3.2.2.5 Summary

Equations to calculate the parameters of fluids are presented below. Those for wavelength and wave number are applicable to gases and liquids.

SPEED OF SOUND IN GAS

$$c = (\gamma P/\varrho)^{1/2} \propto T^{1/2}$$

SPEED OF SOUND IN A LIQUID

$$c = (K_T/\varrho)^{1/2}$$

WAVELENGTH OF SOUND

$$\lambda = c/f$$

WAVE NUMBER OF SOUND

$$k = \omega/c = 2\pi f/c = 2\pi/\lambda$$

3.2.3 WAVE EQUATIONS

The basic simple wave equation for a fluid medium without damping is

$$\partial^2 P/\partial t^2 = c^2(\partial^2 P/\partial x^2).$$

Figure 3.37 provides this equation, along with two and three dimensional versions and figure 3.38 provides solutions for five cases. Such equations are used extensively in the theoretical treatment of acoustics in fluids.

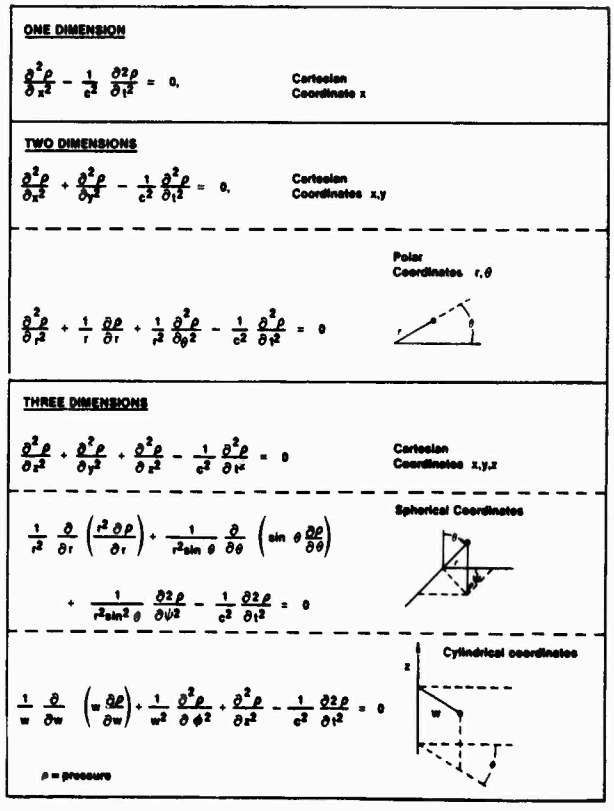

Figure 3.37. Wave Equations for a Lossless Acoustic Medium

3.2.4 TRANSMISSION AND REFLECTION AT MATERIAL DISCONTINUITIES

3.2.4.1 General

Material discontinuities in the acoustic path cause reflection, absorbtion, scattering, diffraction, and refraction. The proper treatment of such materials is required so the sonar installation has a quiet environment and a *window to the target*.

3.2.4.2 Interface Between Two Fluids

Figure 3.39 shows a simplified model of the situation at the boundary between two fluids, such as air and water. The sound wave moves from fluid to fluid and impinges at right angles to the interface, which is the normal incidence situation. Therefore if,

$$P_i = A_1 e^{i(\omega t - k_1 x)},$$

$$P_r = B_1 e^{i(\omega t + k_1 x)},$$

and

$$P_t = C_1 e^{i(\omega t - k_2 x)},$$

then

$$B_1/A_1 = (\varrho_2 c_2 - \varrho_1 c_1)/(\varrho_2 c_2 + \varrho_1 c_1),$$

where

	ACOUSTIC PRESSURE p	ACOUSTIC INTENSITY (DEPENDS ON DIRECTION) I	ACOUSTIC WAVE IMPEDANCE (DEPENDS ON DIRECTION) Z_a	ACOUSTIC POWER P
PLANE WAVE TRAVELING ALONG x AXIS 	$p = Ae^{i(\omega t - kx + \varphi)}$	$I_{x'} = \pm\frac{A^2}{2\rho c}\cos\theta$	$Z_x = \rho c$	POWER = INTENSITY X AREA
PLANE WAVE STANDING ALONG x AXIS x_0 = point on x axis	$p = A\cos[k(x-x_0)]$ X $e^{i(\omega t + \varphi)}$	$I_{x'} = \frac{A^2}{2\rho c}\sin[k(x-x_0)]$ X $\cos\theta$	$Z_x = i\rho c\,\mathrm{cotan}[k(x-x_0)]$	POWER = INTENSITY X AREA
CYLINDRICAL WAVE (SPREADING)	LINE SOURCE $p = \frac{A}{\sqrt{r}}e^{i(\omega t - kr + \phi)}$	$I_r = \frac{A^2}{2\rho cr}$	$Z_r = \frac{\rho c}{1 - \frac{i}{2kr}}$ ◇ ρc	POWER/UNIT LENGTH OF LINE SOURCE $P = \frac{\pi A^2}{\rho c}$
SPHERICAL WAVE (SPREADING)	POINT SOURCE $p = \frac{A}{r}e^{i(\omega t - kr + \phi)}$	$I_r = \frac{A^2}{2\rho cr^2}$	$Z_r = \frac{\rho c}{1 + \frac{1}{i\,kr}}$ ◇ ρc	POWER OF POINT SOURCE $P = \frac{2\pi A^2}{\rho c}$

NOTES 1. θ = ANGLE OF x' FROM THE x AXIS X = MULTIPLY
2 VELOCITY POTENTIAL ◆ = $p/i\omega\rho$

Figure 3.38. Basic Solutions to the Wave Equations

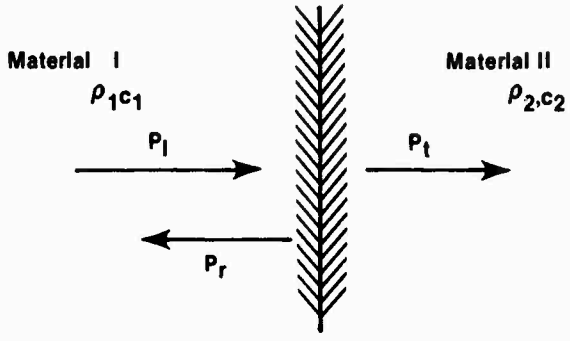

Figure 3.39. Interface Between Two Fluids at Normal Incidence

ϱ = mass density,
c = velocity of sound,
P_I = incident sound pressure,
P_R = reflected sound pressure, and
P_t = transmitted sound pressure.

Since the acoustic intensity is proportional to the square of the amplitude and the reflection coefficient, α_R, is the ratio of the intensities, we have

$$\alpha_R = I_R/I_I = B_1^2/A_1^2 = [(\varrho_2 c_2 - \varrho_1 c_1)/(\varrho_2 c_2 + \varrho_1 c_1)]^2.$$

Similarly, the sound transmission coefficient is

$$\alpha_t = 4(\varrho_2 c_2 \varrho_1 c_1)/(\varrho_2 c_2 + \varrho_1 c_1)^2.$$

It should be noted that whenever $\varrho_2 c_2$ and $\varrho_1 c_1$ have widely separated magnitudes, the sound power transmission coefficient is small. It is also apparent from the symmetry that the coefficient is the same if the sound goes from fluid 2 to fluid 1. This phenomenon provides an example of the ***Helmholtz Reciprocity Principle***, which states that the location of a source point and a field point may be interchanged without altering the pressure at either point. That is, the acoustic pressure change between points A and B will be the same whether the sound goes from A to B or from B to A.

Figure 3.40 is a plot of the value of α_t as the ratio $\varrho_1 c_1/\varrho_2 c_2$ varies. Since $\alpha_t + \alpha_R = 1$, most of the energy will be reflected if α_t is small. Therefore, a marked discontinuity of the values of ϱc for the two fluids will result in reflection of most of the energy.

If the wave impinges on the interface at an angle such as that shown in figure 3.41. Snells Law applies. Also, the angle of reflection equals the angle of incidence. Thus,

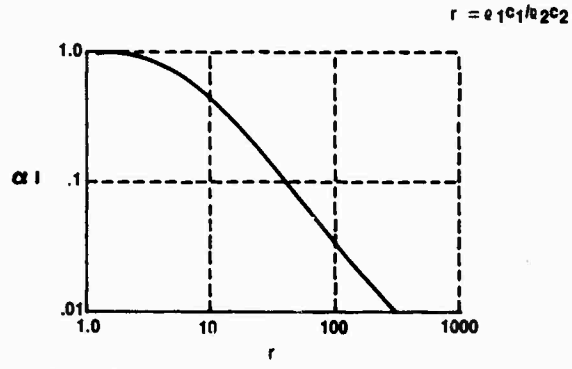

Figure 3.40. Transmission Coefficient as Function of Impedance Ratio

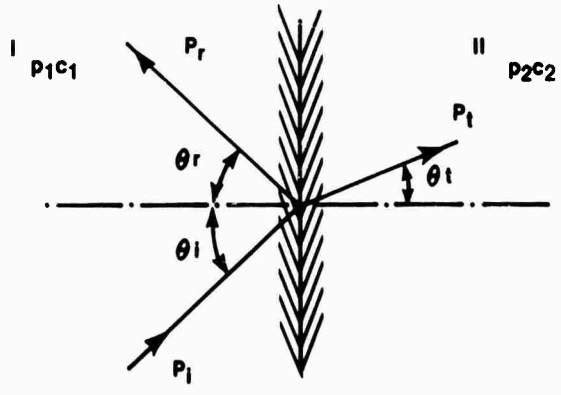

Figure 3.41. Interface Between Two Fluids with Incidence Angle

$$\theta_i = \theta_r$$

and

$$\sin \theta_i / \sin \theta_t = c_1/c_2.$$

Hence,

$$\alpha_R = [(\varrho_2 c_2 \cos \theta_i - \varrho_1 c_1 \cos \theta_t)/(\varrho_2 c_2 \cos \theta_i + \varrho_1 c_2 \cos \theta_t)]^2$$

and

$$\alpha_t = 4(\varrho_1 c_1 \varrho_2 c_2 \cos \theta_i \cos \theta_t)/(\varrho_2 c_2 \cos \theta_i + \varrho_1 c_1 \cos \theta_t)^2.$$

Although the conclusions for normal incidence apply to angles near normal incidence, other cases occur as the angle of incidence increases. When θ_i increases until $\varrho_2 c_2$ cos

$\theta_i = \varrho_1 c_1 \cos \theta_t$, the reflection coefficient is zero. This occurs when

$$\cot^2\theta_{im} = [(c_1/c_2)^2 - 1]/[(\varrho_2/\varrho_1)^2 - (c_1/c_2)^2].$$

Angle θ_{im}, the angle of intromission, will only occur if $\varrho_2/\varrho_1 > c_1/c_2 > 1$ or $\varrho_2/\varrho_1 < c_1/c_2 < 1$. An example of this is at the interface between fresh water and castor oil. The angle of intromission when going from water to castor oil is $\theta_{im} = 26.9°$ and when going from castor oil to water it is 28°.

Another special case occurs when $c_1 < c_2$ and for some critical angle of incidence, θ_c, the refracted ray makes an angle 90° to the normal. The critical angle is given by

$$\sin \theta_c = c_1/c_2.$$

For the case of air to water, the resultant angle is 13.2°. If the angle of incidence is equal to or greater than the critical angle, no acoustic energy is transmitted into the medium.

If θ_i approaches 90°, there is complete reflection because it approaches the grazing angle and $\cos \theta_i \rightarrow 0$. The equation for α_R then becomes

$$\alpha_R = (-\varrho_1 c_1 \cos \theta_t)^2/(\varrho_1 c_1 \cos \theta_t)^2 = 1.$$

Figure 3.42 shows how the transmission coefficient and angle vary with θ_i for sound waves traveling from oil to water, with oil defined in terms of $\varrho_1 = 900$ kg/m³ and

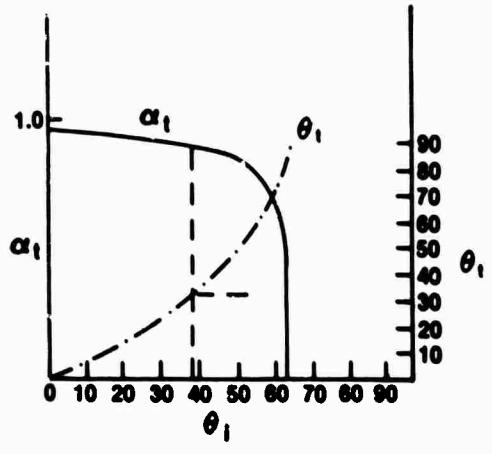

Figure 3.42. Transmission Coefficients and Angle of Refraction: Castor Oil to Water

$c_1 = 1300$ m/sec. Figures 3.43 and 3.44 summarize the above discussion and present it in a convienent form. The special case of the air-water interface is presented in figure 3.44.

3.2.4.3 Transmission and Reflection at an Interface Between Fluids and Solids

Continuity equations for the interface between fluids and solids must include the stiffness factor when calculating the impedance of the solid. The development of the formulas assume that the solid, as the fluid, is extensive in thickness as well as lateral dimension; such dimensions create many wavelengths. Assuming normal incidence, the sound power reflection coefficient (see figure 3.45) is

$$\alpha_R = B^2/A^2 = [(z/\varrho c) - 1]^2/[(z/\varrho c) + 1]^2.$$

where

z = the impedance of the solid.

Also,

$$\alpha_t = (1 - \alpha_R).$$

Figure 3.46 shows the reflectivity and phase angle for a water-solid interface; the impedance ratio of the solid to that of water is plotted on the complex plane. The imaginary portion of the ratio is plotted above and below the real axis, which is indicated at the center of the figure.

The point of perfect absorption (zero reflection) occurs when z has no imaginary part and equals the ϱc of water, i.e. it becomes an interface between water and water, or a material that has the acoustic properties of water. As noted earlier, a very thin plate (in terms of wavelength) backed by water acts in this fashion. The actual reflectivity of plates in water will be discussed later.

The shear, Young's, Bulk, and dilational moduli are useful constants. These and Poisson's ratio for materials are discussed in most text books concerned with the strength of materials and will not be discussed herein. Figure 3.47 is provided to summarize these moduli.

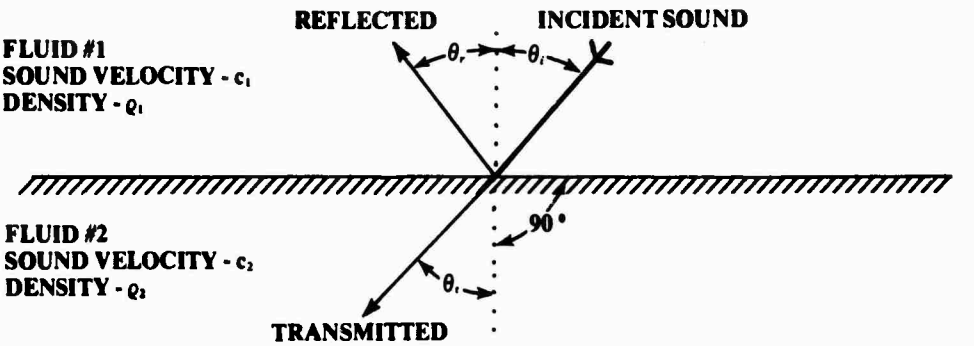

GOVERNING EQUATIONS FOR θ_t, θ_i, θ_r:

- **ANGLE OF REFLECTION EQUALS ANGLE OF INCIDENCE ($\theta_r = \theta_i$)**
- **SNELL'S LAW ($\sin\theta_t/c_1 = \sin\theta_i/c_2$)**

GOVERNING EQUATIONS FOR TRANSMITTED AND REFLECTED ACOUSTIC PRESSURE:

- **P_i = INCIDENT PRESSURE; P_t = TRANSMITTED PRESSURE; P_r = REFLECTED PRESSURE**

$$P_r/P_i = \{(\rho_2/\rho_1)\cos\theta_i - [(c_1/c_2)^2 - \sin^2\theta_i]^{1/2}\}/\{(\rho_2/\rho_1)\cos\theta_i + [(c_1/c_2)^2 - \sin^2\theta_i]^{1/2}\}$$
$$= (\rho_2c_2 - \rho_1c_1)/(\rho_2c_2 + \rho_1c_1) \qquad (\text{IF } \theta_i \to 0)$$

$$P_t/P_i = [2(\rho_2/\rho_1)\cos\theta_i]/\{(\rho_2/\rho_1)\cos\theta_i + [(c_1/c_2)^2 - \sin^2\theta_i]^{1/2}\}$$
$$= 2\rho_2c_2/(\rho_2c_2 + \rho_1c_1) \qquad (\text{IF } \theta_i \to 0)$$

CRITICAL ANGLE, θ_c (FOR ANGLES OF INCIDENCE GREATER THAN THE CRITICAL ANGLE REFLECTION IS TOTAL):

- **IF $c_2 > c_1$, THEN $\theta_c = \sin^{-1}(c_1/c_2)$**
- **TOTAL REFLECTION FOR $\theta_i \geq \theta_c$ (NO TRANSMISSION AT FLUID-FLUID INTERFACE)**

TRANSMISSION AND REFLECTION OF SOUND INTENSITY:

TRANSMITTED SOUND INTENSITY RATIO = TRANSMITTED INTENSITY/INCIDENT INTENSITY

$$= (\rho_1c_1/\rho_2c_2)[2(\rho_2/\rho_1)\cos\theta_i]^2/\{(\rho_2/\rho_1)\cos\theta_i + [(c_1/c_2)^2 - \sin^2\theta_i]^{1/2}\}^2$$
$$= (4\rho_1c_1\rho_2c_2)/(\rho_2c_2 + \rho_1c_1)^2 \qquad \text{(FOR NORMAL INCIDENCE)}$$

REFLECTED SOUND INTENSITY RATIO = 1 - (TRANSMITTED SOUND INTENSITY RATIO)

- **$\theta_c = \sin^{-1}(c_{AIR}/c_{WATER}) \approx 13.2°$**
- **120 dB//10^{-12} W ACOUSTIC SOURCE PRODUCES 109 dB//20 μPa (AIR, 1 m RADIUS) OR 171 dB//1 μPa (WATER, 1 m RADIUS)**

Figure 3.43. Sound Transmission and Reflection at a Fluid Interface

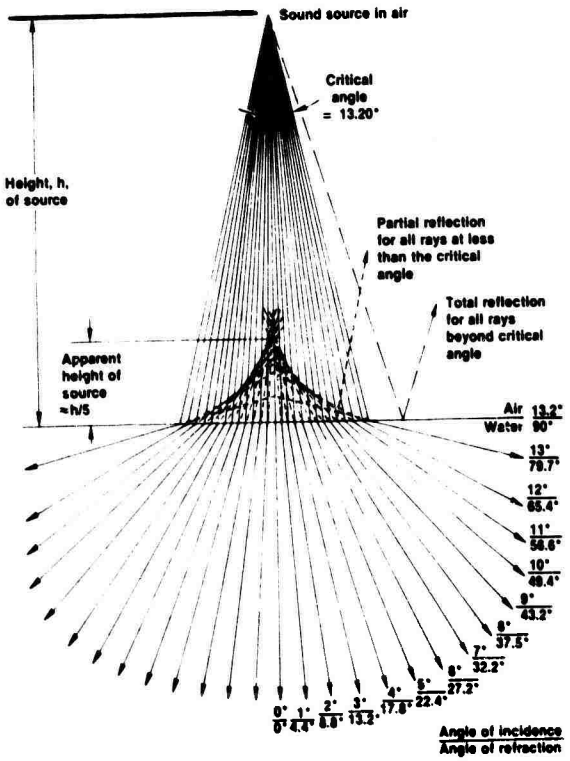

Figure 3.44a. Air-to-Water

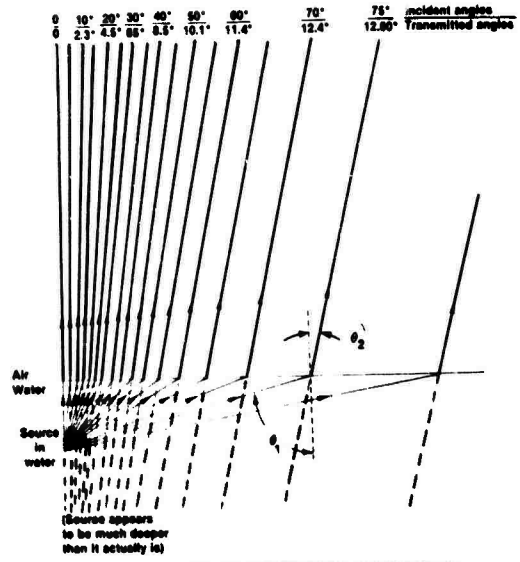

TRANSMITTED SOUND POWER RATIO, WATER-TO-AIR

(Water to air)	θ_1	Power ratio	dB	θ_2
	0°	.00111	−29.5dB	0°
	10°	.00111	−29.7dB	2.3°
	20°	.00098	−30.1dB	4.6°
	30°	.00104	−30.8dB	8.8°
	40°	.00085	−31.8dB	8.5°
	50°	.00047	−33.3dB	10.1°
	60°	.00029	−35.4dB	11.4°
	70°	.00014	−38.7dB	12.4°
	80°	.00004	−44.5dB	15.9°

Figure 3.44b. Water-to-Air

Figure 3.44. Ray Diagrams at Air-Water Interface

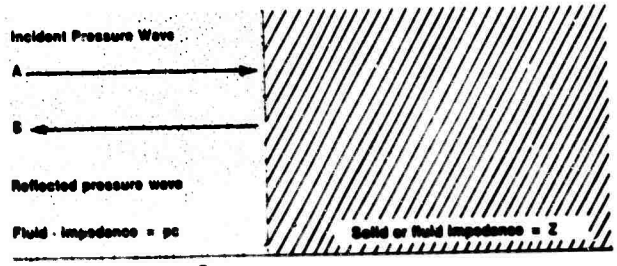

$$R, \text{ reflectivity} = \frac{B}{A} = \frac{\frac{Z}{\rho c} - 1}{\frac{Z}{\rho c} + 1} = R$$

$$z = r_m + ix_m \qquad r_m = \text{RESISTIVE COMPONENT} \qquad x_m = \text{REACTIVE COMPONENT}$$

Figure 3.45. Interface Between Solid and Fluid

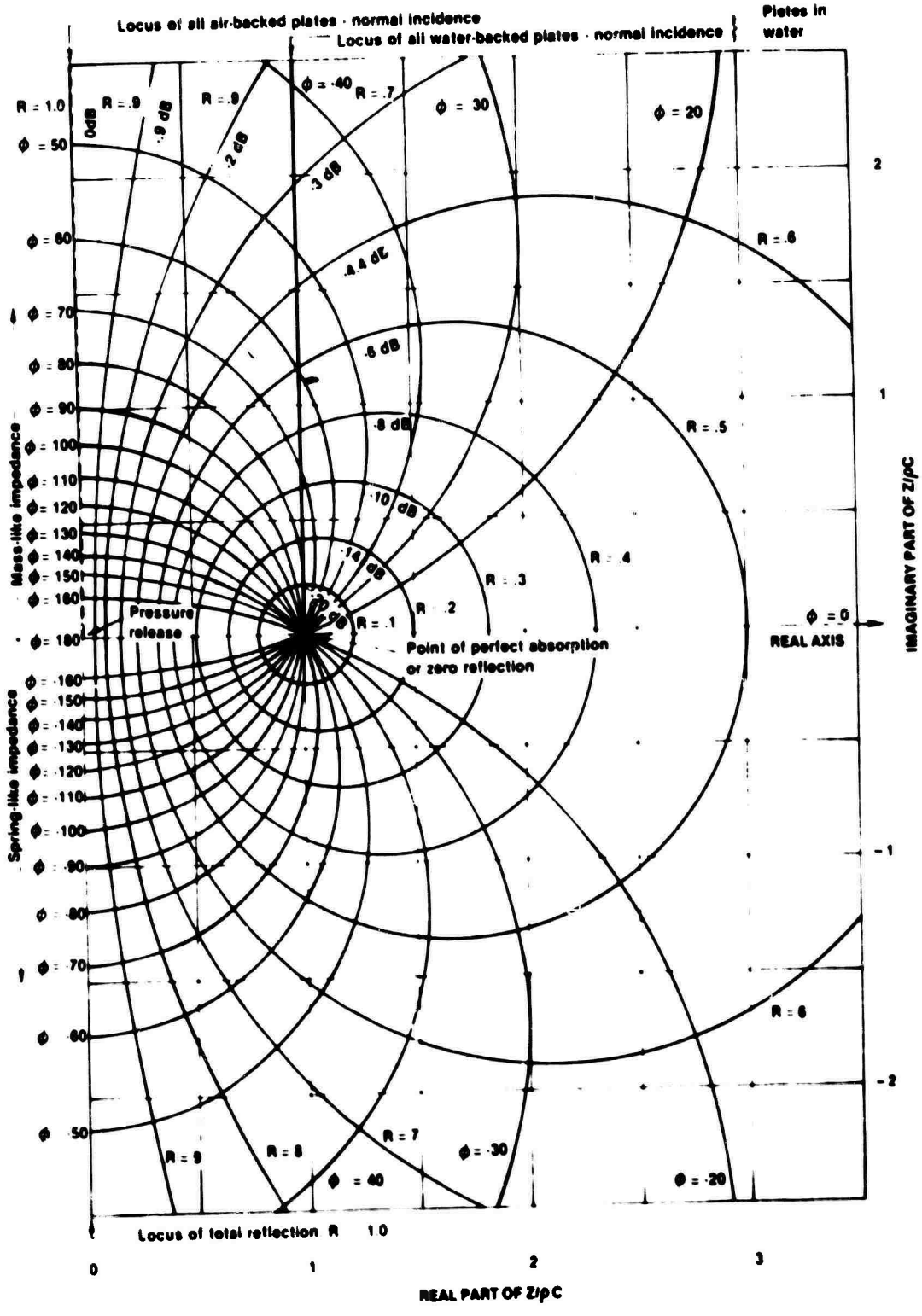

Figure 3.46. Relationship of Acoustic Impedance and Reflectivity

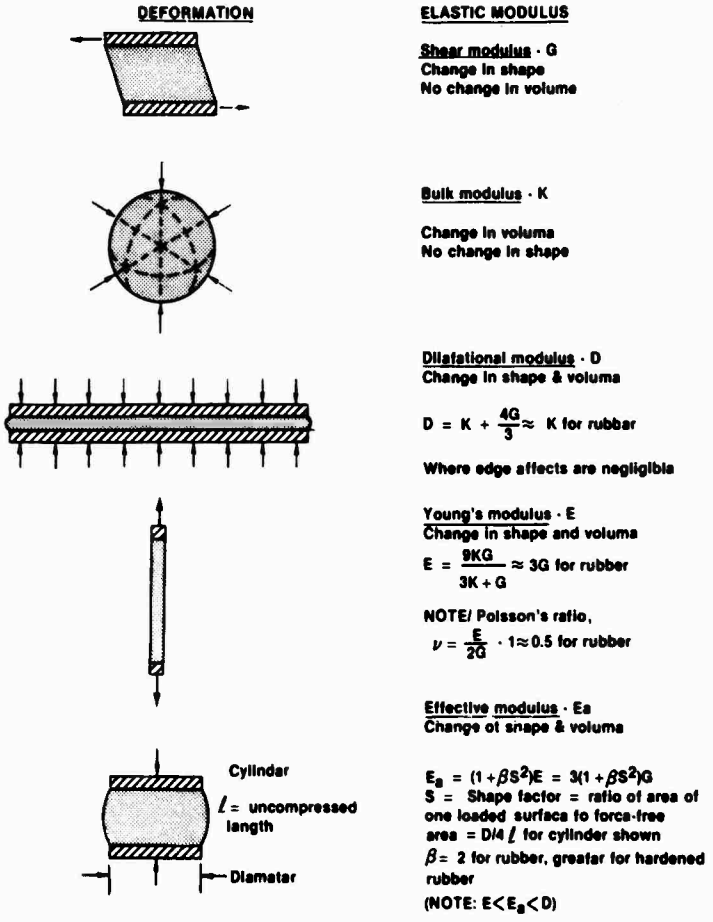

Figure 3.47.Types of Material Deformations and Corresponding Elastic Moduli

When damping is included, the moduli are designated *complex* and consist of a real and an imaginary part. The manner in which the complex moduli are formed and the inter-relationships between the elastic constants is shown in figure 3.48.

3.2.4.4 The Acoustic Field at an Interface

Incident and reflected waves contribute to the sound pressure at any point in the fluid from which the acoustic wave originates. This is illustrated in figure 3.49, which shows how these two waves are summed to yield the pressure at the field point, i.e.,

$$\begin{aligned} P_F &= P_i + P_r \\ &= A_r[e^{i(\omega t + kd)} + Re^{i(\omega t - kd - \phi)}] \\ &= A_r e^{i(\omega t + kd)}[1 + Re^{-i(2kd + \phi)}] \\ &= P_i \times F. \end{aligned}$$

Note that d is negative as shown in figure 3.49.

The amplitude factor, F, is plotted in figure 3.50, where the variable parameters are the phase angle-standoff, $2kd + \phi$, and reflectivity, R. It is apparent that phase change and standoff distance influence the same parameter. The effect of the reflected wave becomes smaller as reflectivity decreases until, at transparency, $R = 0$ and the amplitude becomes 1.

Figure 3.51 shows the amplitude factor versus standoff distance from a completely compliant, 100 percent reflective boundary. The returning reflected wave incurs a 180° phase shift at the surface. A wide range of frequencies is plotted. This has application if a hydrophone is located near a baffle. Because of the varying sound field, the location of the hydrophone may place it in either a low or high level signal field and effect the SNR.

GIVEN \ FIND	SHEAR MODULUS G	YOUNG'S MODULUS E	BULK MODULUS K	DILATATIONAL MODULUS D	POISSON'S RATIO ν
G, E			$\frac{EG}{3(3G-E)}$	$G\left(\frac{4G-E}{3G-E}\right)$	$\frac{E}{2G}-1$
G, K		$\frac{9KG}{3K+G}$		$K+\frac{4G}{3}$	$\frac{3K-2G}{6K+2G}$
G, ν		$2G(1+\nu)$	$\frac{2G(1+\nu)}{3(1-2\nu)}$	$\frac{2G(\nu-1)}{2\nu-1}$	
E, B	$\frac{3KE}{9K-E}$			$3K\left(\frac{3K-E}{9K-E}\right)$	$\frac{1}{2}-\frac{E}{6B}$
E, ν	$\frac{E}{2(1+\nu)}$		$\frac{E}{3(1-2\nu)}$	$\frac{E(\nu-1)}{(1+\nu)(2\nu-1)}$	
K, ν	$\frac{3K(1-2\nu)}{2(1+2\nu)}$	$3K(1-2\nu)$		$\frac{3K(1-\nu)}{1+\nu}$	

MATERIAL ELASTIC CONSTANTS MODIFIED TO INCLUDE DAMPING

G ➧ $G(1 + j\delta_G)$ complex shear modulus
E ➧ $E(1 + j\delta_E)$ complex Young's modulus
K ➧ $K(1 + j\delta_K)$ complex bulk modulus
D ➧ $D(1 + j\delta_D)$ complex dilatational modulus

δ = damping factor or loss factor corresponding to the appropriate strain — shear, dilatational, etc.
(For rubberlike materials $\delta_E \simeq \delta_G$)

Figure 3.48. Material Elastic Constants and Interrelationships

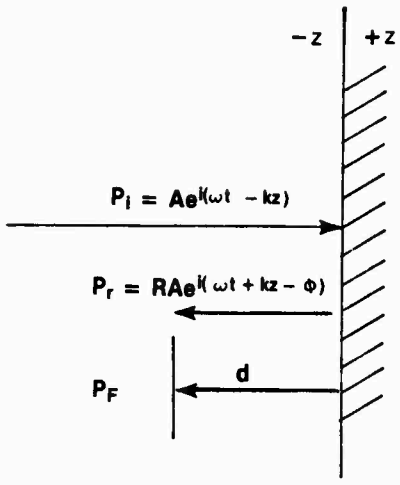

Figure 3.49. Acoustic Field Pressure in Water Near Boundary With Phase and Amplitude Change

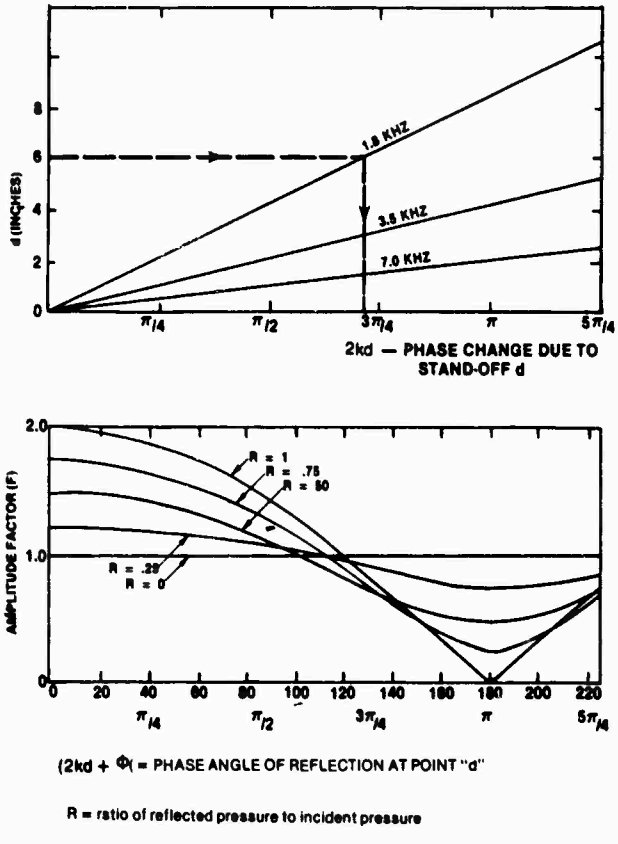

Figure 3.50. Amplitude Factor versus Standoff

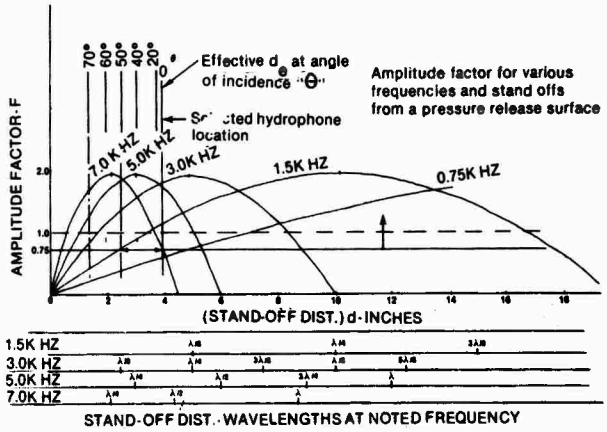

Figure 3.51. Amplitude Factor versus Standoff Distance For Various Frequencies (Compliant Surface)

It is apparent in figure 3.51 that if a signal pressure level of 75 percent of the incident level is acceptable despite the factor of almost five in frequency, there is a range of standoff distances at which an acceptable signal level exists. Figure 3.50 shows that when $R < 1$ for an imperfect reflector, F moves closer to 1. In some cases this reduces high values of F, but when F is less than 1, it will probably increase the value and the range of acceptable standoff distances.

The signal level is, of course, affected by the incidence angle (see figure 3.52). The effective standoff distance, d_e, is equal to the actual standoff multiplied by the cosine of the angle of incidence, i.e.,

$$d_e = d \cos \theta.$$

Therefore, as the angle of incidence increases, the effective standoff distance decreases until, at grazing, it becomes zero.

The effect of this phenomenon is shown in figure 3.51 where a selected standoff is indicated at 3.9 in. and the effective d and d_e for various angles of incidence are shown. It is apparent that for larger incidence angles the amplitude factor reduce at 1.5 and 3.0 kHz. For higher frequencies, however, the factor increases before decreasing.

Thus, hydrophones so located will be characterized by low responses at high angles of incidence. This may be a desirable characteristic because it discriminates against grazing angle noise such as that from machinery in the aft part of the ship. However, acceptable performance must be maintained to incident angles up to 60°

or 70° so that beams can be formed over a wide angle in azimuth.

It is interesting that, at low frequencies, heavier material may be substituted for the water standoff on an approximately mass basis. Therefore, 1 in. of steel can be substituted for approximately 7.7 in. of water. Figure 3.53 illustrates the response pattern for a hydrophone having the initial amplitude parameters discussed above.

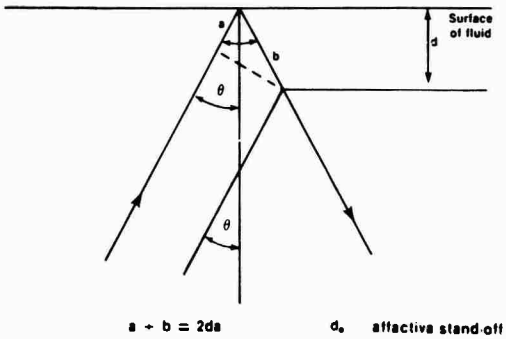

$a + b = 2d_e$ $\quad d_e$ effective stand-off

$$b = \frac{d}{\cos\theta} \qquad a = b\cos 2\theta$$

$$2d_e = b\cos 2\theta + \frac{d}{\cos\theta} = \frac{d\cos 2\theta}{\cos\theta} + \frac{d}{\cos\theta} = \frac{d}{\cos\theta}(1 + \cos 2\theta)$$

$$d_e = \frac{d}{2\cos\theta}(1 + \cos^2\theta - \sin^2\theta) = \frac{d(2\cos^2\theta)}{2\cos\theta} = d\cos\theta$$

Figure 3.52. Effect of Angle of Incidence on Standoff Distance

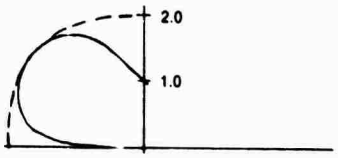

F = 1.0 (d on High Side)

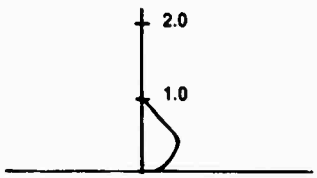

F = 1.0 (d on Low Side)

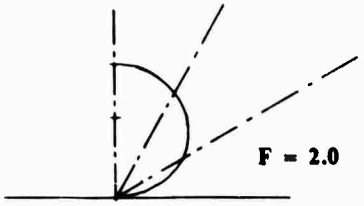

Figure 3.53. Hydrophone Response Patterns for Various Standoff Distances as Function of Incidence Angle

3.2.5 THE ACOUSTICS OF ELASTIC PLATES AND SHELLS

3.2.5.1 General

Ships are fabricated of flat and curved elastic plates and shells. Therefore, an understanding of the transmission and reflection by such structures is important to the sonar installation designer. The elastic, undamped situation common to most ships will be discussed in this section; the use of damping and its application to plates will be discussed later.

3.2.5.2 Air Backed Plate

The air backed and water backed plate are important when discussing flat plates. The coordinate system used for this discussion is presented in figure 3.54, where the incident pressure, P_i, arrives from side 1. For the air backed plate, the reflected pressure is

$$P_r = P_i \times \{ikh(\varrho_s/\varrho)[1 - (\omega/\omega_c)^2 \sin^4\theta] \times \cos\theta - 1\}/\{ikh(\varrho_s/\varrho)[1 - (\omega/\omega_c)^2 \sin^4\theta] \times \cos\theta + 1\},$$

where

P_i = incident pressure,

k = wave number of fluid (ω/c),

h = plate thickness,

ϱ_s = structure mass density,

ϱ = fluid mass density,

ω = angular frequency of incident wave,

ω_c = coincident frequency of plate,

θ = incident angle,

x,z = coordinates of field points, and

t = time.

For waves incident at the critical or coincident angle, $\theta_c = \sin^{-1}(\omega_c/\omega)^{1/2}$, the plate acts as a pressure release reflector, i.e., $P_r = -P_i$. For very thin plates, or low frequencies, at which $kh(\varrho_s/\varrho) \ll 1$, the plate also acts as a pressure release reflector and is independent of the in-

cidence angle. At the critical angle, the wave crests of the incident wave front (see figure 3.55) reinforce the flexural wave crests of the plate since they coincide. This occurs when

$$\lambda_f \sin\theta = \lambda.$$

Since $\lambda = c/f$, then, for a given frequency,

$$c_f \sin\theta = c.$$

When $\theta = 90°$, $c_f = c$. The frequency at which this occurs is the *critical* or *coincidence* frequency. The flexural wave velocity is

$$c_f = [\omega c_p h/(12)^{1/2}]^{1/2}.$$

Therefore, at ω_c, the coincidence frequency,

$$c_f = c = [\omega_c c_p h/(12)^{1/2}]^{1/2}$$

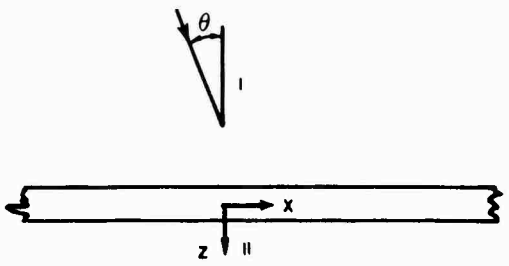

Figure 3.54. Pressure Field Coordinates at an Infinite Elastic Plate

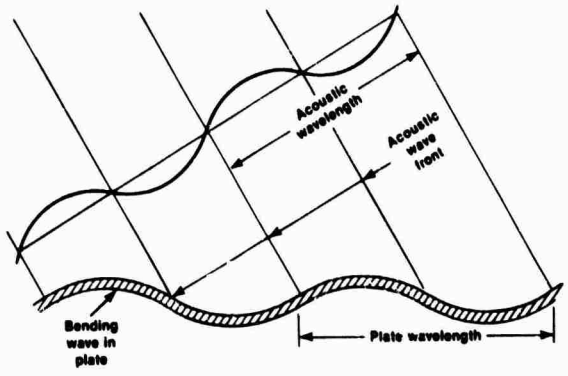

Figure 3.55. Coincidence Effect

and

$$\omega_c = c^2(12)^{1/2}/c_p h.$$

The above development is based upon classical plate analysis that is adequate in the frequency range of

$$\omega < 0.1(\pi c_s/h),$$

where c_s is the shear wave speed of the material.

For 1 in. aluminum or steel plates, the coincidence frequency is approximately 9.3 kHz. The frequency is lower for thicker plates.

3.2.5.3 Water Backed Plate

The reflected pressure for the water backed plate model is

$$P_r = \{iP_i kh(\rho_s/\rho)[1 - (\omega/\omega_c)^2 \sin^4\theta] \times \cos\theta\}/\{ikh(\rho_s/\rho)[1 - (\omega/\omega_c)^2 \times \sin^4\theta]\cos\theta + 2\}.$$

The transmitted pressure is

$$P_t = 2P_i/\{ikh(\rho_s/\rho) \times [1 - (\omega/\omega_c)^2 \sin^4\theta]\cos\theta + 2\}.$$

The transmitted pressure becomes equal to the incident pressure when $\theta \to \pi/2$, i.e., $\cos\theta \to 0$. It becomes equal for a wave incident along the critical direction when $\theta_c = \sin^{-1}(\omega_c/\omega)^{1/2}$ and when $kh\rho_s/\rho << 1$. This is true for low frequencies or thin plates whose inertial reactance per unit area, $\omega h\rho_s$, is negligible compared with ρc, i.e., when

$$\omega m = \omega h\rho_s << \rho c.$$

The transmission loss curves of steel plates in water (see figure 3.56) at 10 kHz graphically illustrates the above. The 2 in. plate exhibits a coincidence angle at about 42°, whereas the 1/2 in. plate does not. However, the thinner plate exhibits much less transmission loss than does the thicker one. The transmission loss would be even less for thinner plates and for lower frequencies.

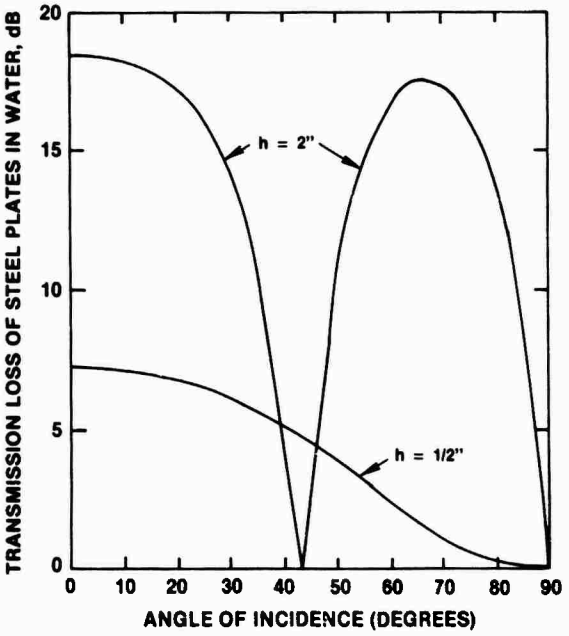

Figure 3.56. Transmission Loss Curves for Steel Plates in Water at 10 kHz

3.2.5.4 Summary

For the case of normal incidence at the surface of the plate, the expressions presented in the previous section may be simplified as follows:

AIR BACKED PLATE

$$P_r = P_i[ikh(\varrho_s/\varrho) - 1]/[ikh(\varrho_s/\varrho) + 1]$$
$$= P_i[(i\omega m/\varrho c) - 1]/[(i\omega m/\varrho c) + 1]$$
$$= P_i(\varrho c - i\omega m)/(\varrho c + i\omega m).$$

WATER BACKED PLATE

$$P_r = P_i ikh(\varrho_s/\varrho)/[ikh(\varrho_s/\varrho) + 2]$$
$$= P_i(i\omega m/\varrho c)/[(i\omega m/\varrho c) + 2]$$
$$= i\omega m/[2\varrho c + i\omega m]$$

and

$$P_t = -[2P_i]/[ikh(\varrho_s/\varrho) + 2]$$
$$= [-2P_i]/[(i\omega m/\varrho c) + 2]$$
$$= -2P_i\varrho c/(2\varrho c + i\omega m).$$

These and other formulas for the fluid plate-fluid case at normal incidence are shown in figure 3.57

Figures 3.58 through 3.63 provide curves derived from the equations shown in figure 3.57

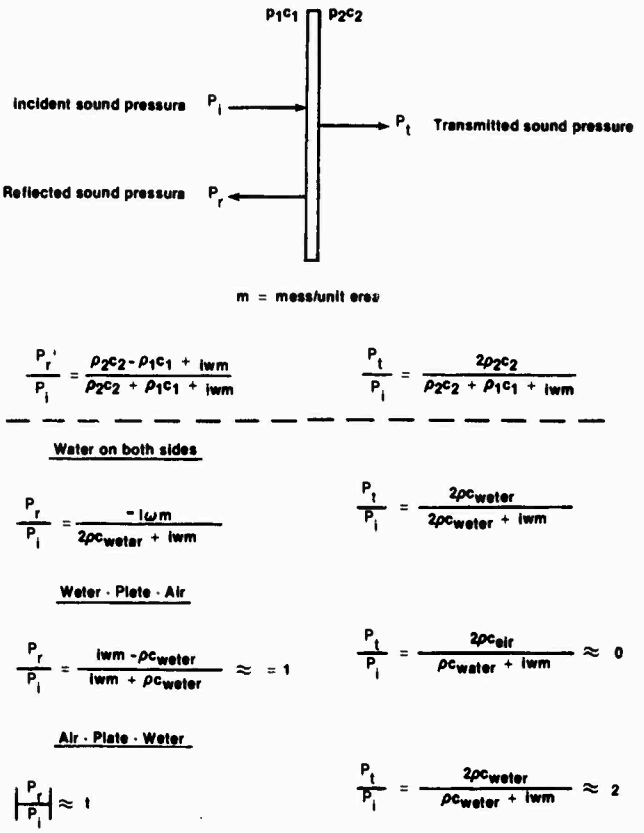

Figure 3.57. Sound Reflection and Transmission for Fluid-Plate-Fluid: Normal Incidence Acoustic Formulas

to illustrate the effect of frequency and plate thickness, or compliance, on reflectivity and transmissibility. For example, figure 3.58 shows the frequencies at which water backed plates of various thicknesses become totally reflective, i.e., where reflectivity is 0 dB.

Figure 3.59 presents the frequencies at which plates become transparent in water, i.e., where insertion loss is 0 dB. Figures 3.60 and 3.61 show these points for compliant material and figure 3.63 shows them for air backed plates; figure 3.62 illustrates the phase angle changes.

If the $2L_x$ wide, $2L_y$ long plate shown in figure 3.64 is considered, instead of the infinite plates considered above, the reflected pressure in the far field for a thick plate, $\omega m >>> \varrho c$, is

$$P_{s_\infty} = [-(i4kP_i/r)L_xL_y\cos\theta_i]$$
$$\times j_\infty[kL_x(\sin\theta_i\cos\phi_s + \sin\theta_s\cos\phi_s)]$$
$$\times j_\infty[kL_y(\sin\theta_i\sin\phi_s + \sin\theta_s\sin\phi_s)].$$

Fig 3.65 and 3.66 show the strength of the scattered field from steel plates, for normal

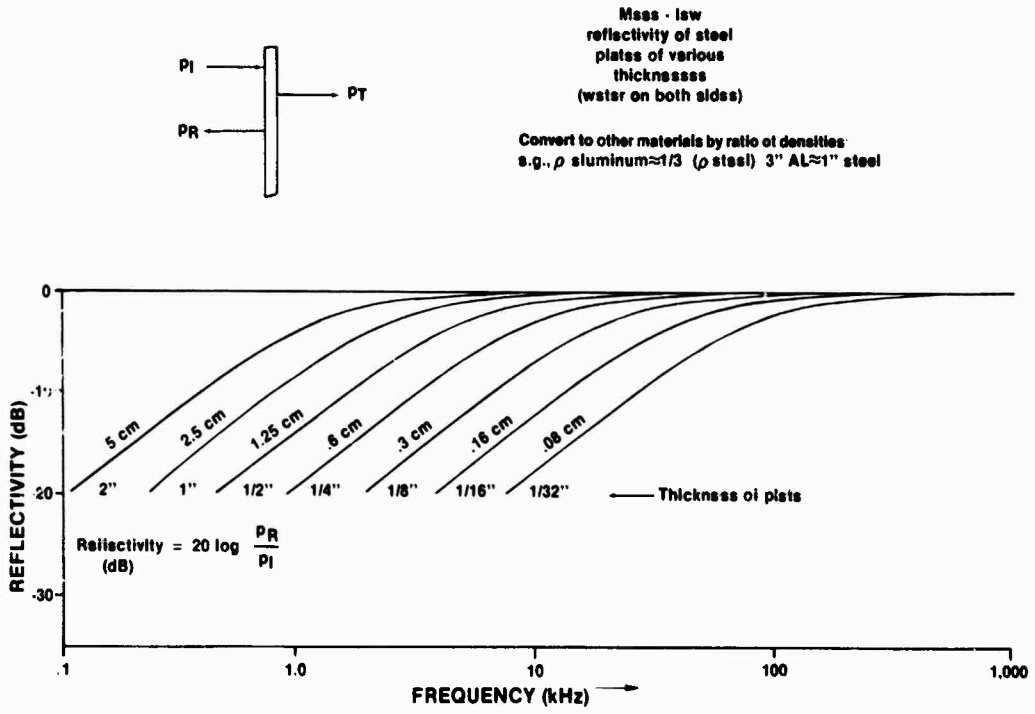

Figure 3.58. Sound Reflection: Water-Plate-Water

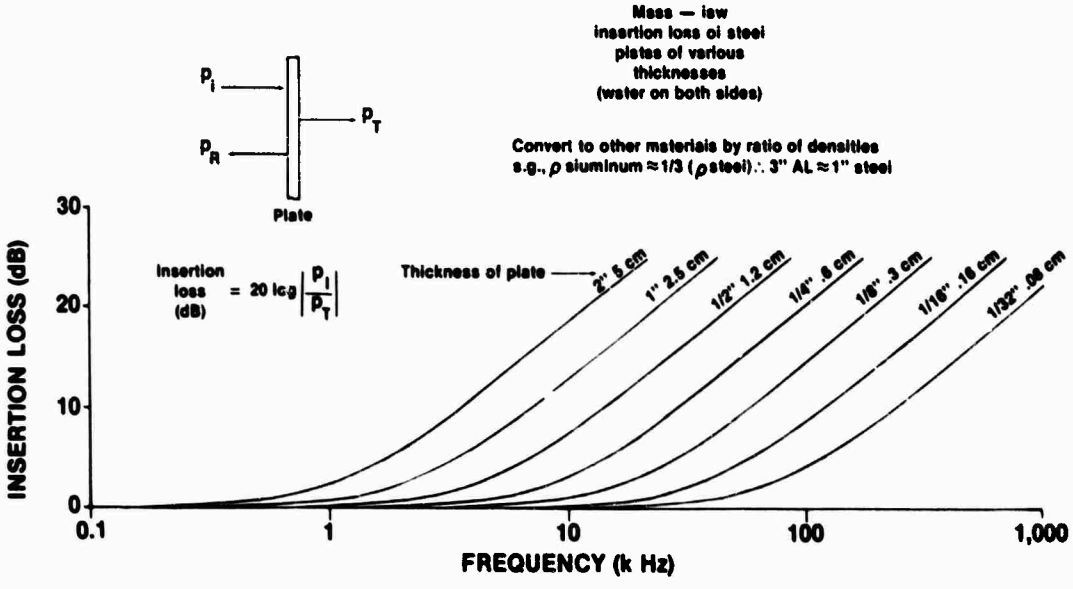

Figure 3.59. Sound Transmission: Water-Plate-Water

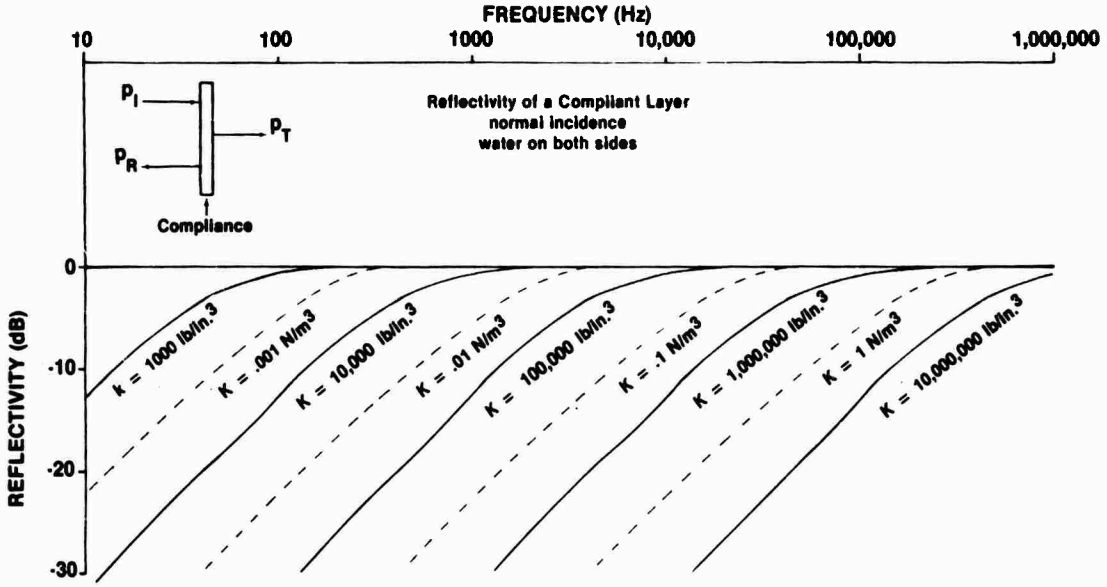

Figure 3.60. Sound Reflection: Water-Compliance-Water

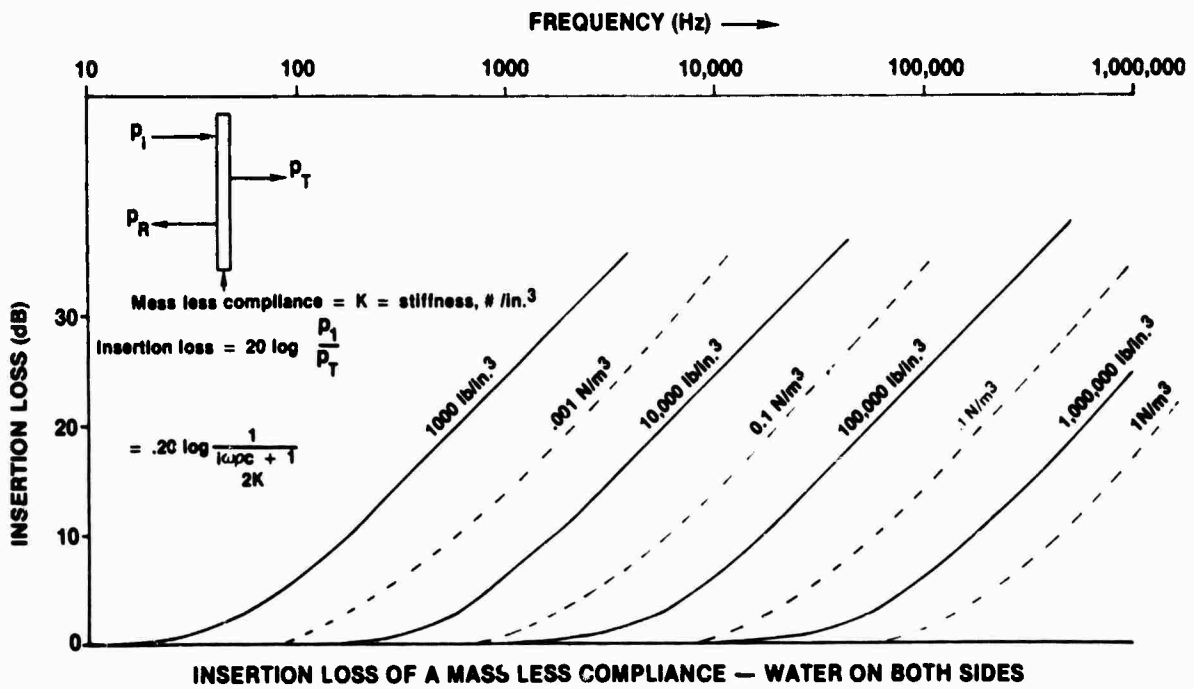

Figure 3.61. Sound Transmission:
Water-Compliance-Water

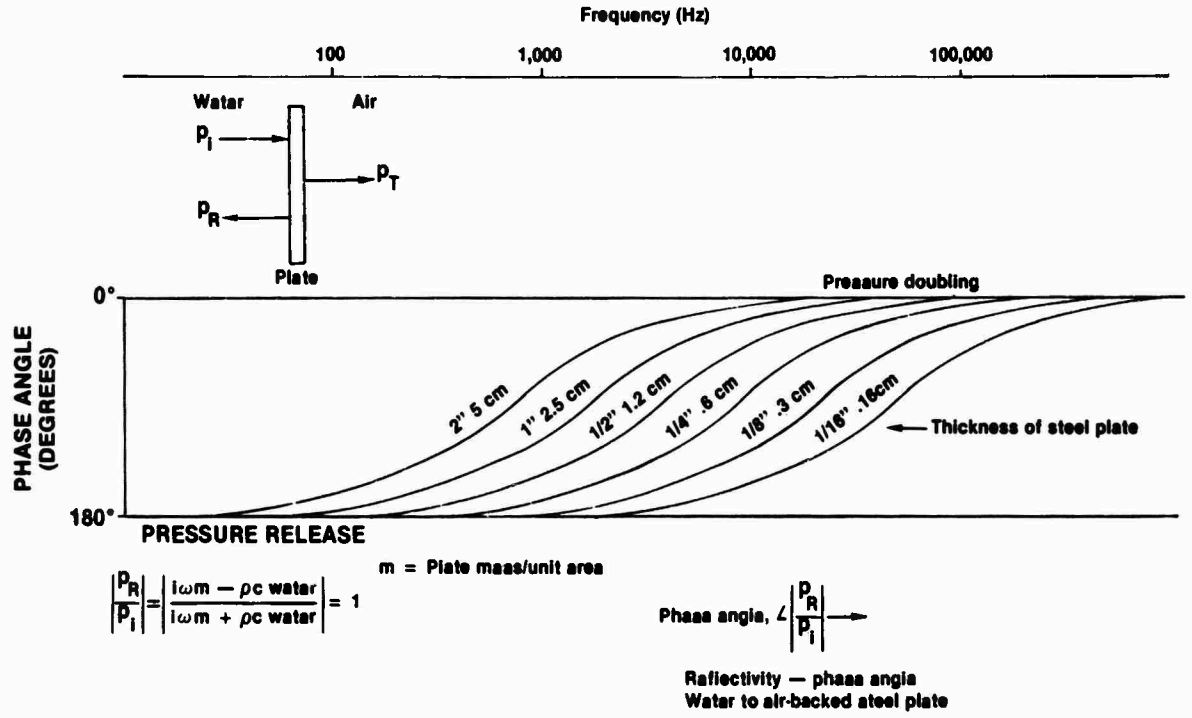

Figure 3.62. Sound Reflection: Water-Plate-Air

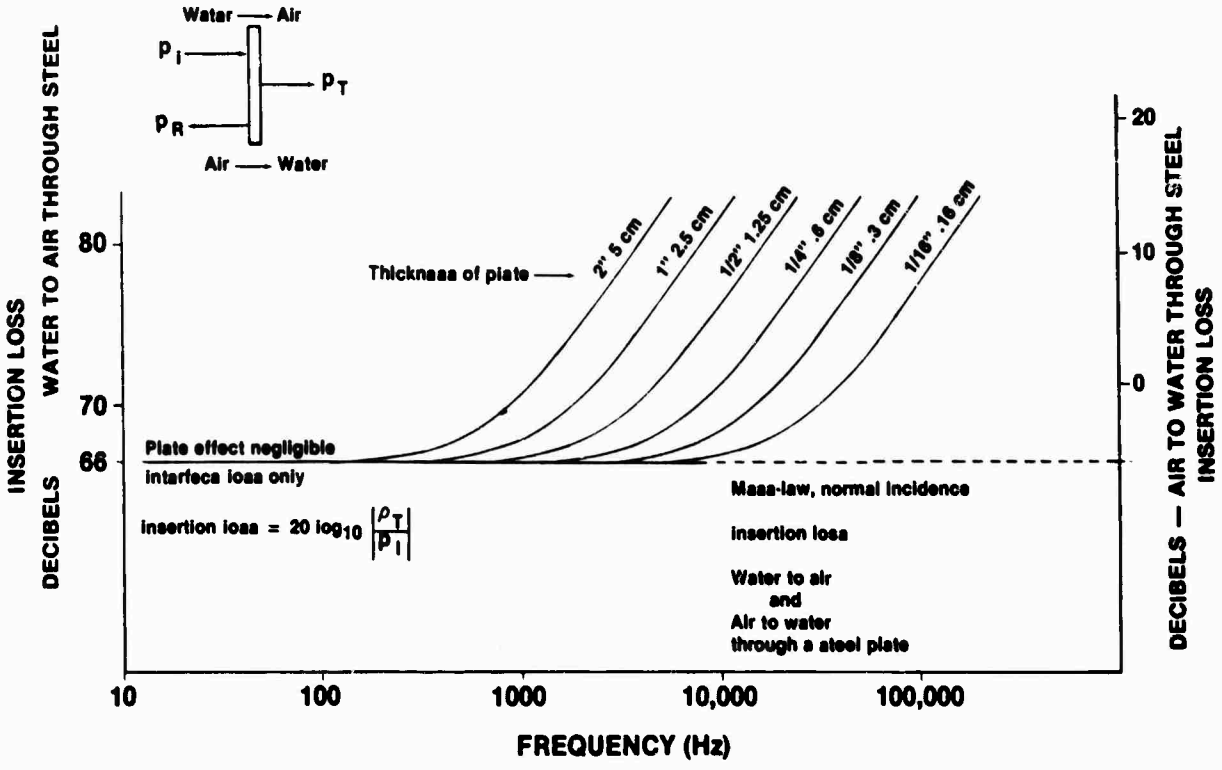

Figure 3.63. Sound Transmission: Water-Plate-Air or Air-Plate-Water

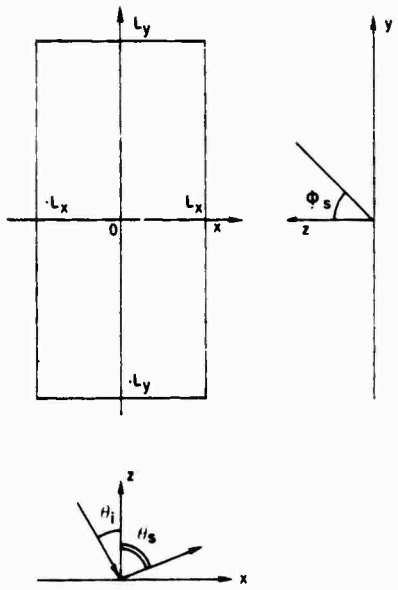

Figure 3.64. Coordinates for Pressure Fields at a Finite Plate

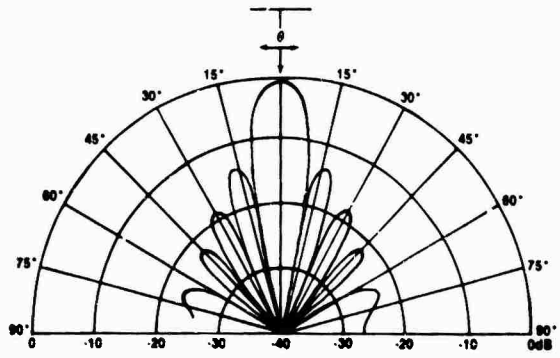

Figure 3.65. Sound Pressure Scattered From a Finite Plate ($kL_x = 4.8\pi$)

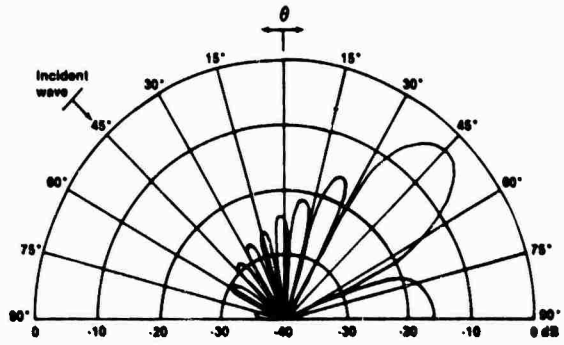

Figure 3.66. Sound Pressure Scattered From a Finite Plate ($\theta_i = 45°$)

incidence and angled incidence, and the complexity of the acoustic field radiated. For small plates, $kL < \pi$ the pattern becomes non-directive, i.e., the acoustic field scatters in all directions. However, as kL becomes large, the infinite case is approximated and scattering is specular.

Figures 3.67 and 3.68 provide two presentations of transmission loss data for a steel plate with water on both sides. They show that transmission varies greatly as the frequency-thickness product changes.

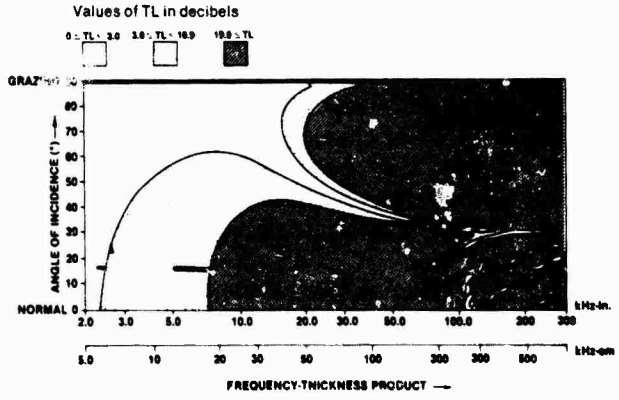

Figure 3.67. Transmission Loss for Infinite Steel Plate (Water on Both Sides)

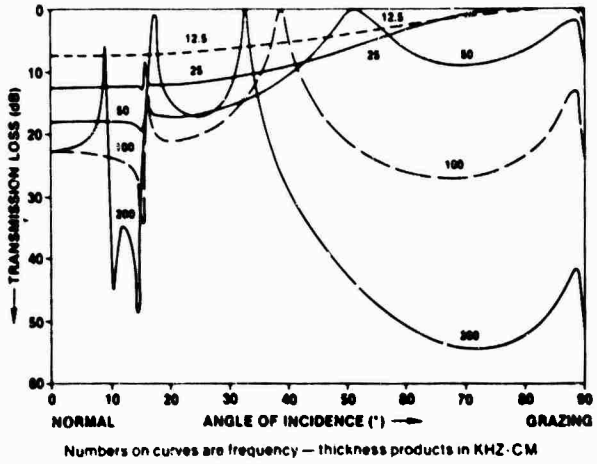

Figure 3.68. Transmission Loss versus Angle of Incidence for Infinite Steel Plate (Water on Both Sides)

3.2.5.5 Compressional Coincidence

When flat or nearly flat domes fabricated of steel, glass reinforced plastic, or other elastic material are used, a *compressional coincidence angle* may occur. This effect creates coherent noise that the beamformer *sees* as coming from an angle, θ_{cc}, where

$$\theta_{cc} = \sin^{-1} c/c_p,$$

and where

c = speed of sound in water and
c_p = compressional (membrane) velocity of sound in the dome material.

This effect is illustrated in figure 3.69, which shows a compressional wave moving along the dome shell (note the similarity to an incoming acoustic wave). The wave appears to arrive at the array from θ_{cc} when the acoustic pressure from the disturbance is summed with the time delays for that angle. Because compressional waves move through the dome shell in all directions, the coherent noise they propagate creates an apparent cone of noise having the apex angle θ_{cc}. Such noise is exhibited on the sonar display as a *spoke*.

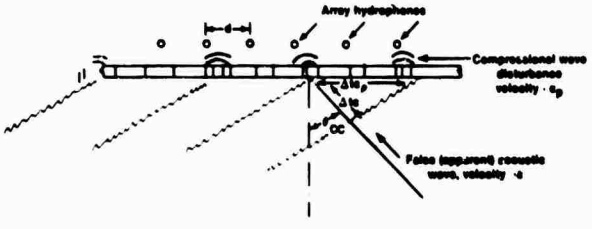

Figure 3.69. Compressional Coincidence Effect

The speed of sound, c_p, of most materials is independent of frequency and, therefore, compressional coincidence will also be independent of frequency, i.e., it will be the same for all. Since plate motion is primarily in its own plane (lateral motion at the interface is caused, principally, by Poisson's effect.) coupling between plate and water is weaker than for the

flexural coincidence case. However, because it is independent of frequency, it can cause persistent coherent noise at angle θ_{cc} over the entire frequency range.

For the water-steel case,

$$\theta_{cs} = \arcsin c_w/c_s = 17.3°$$

since $c_w/c_s = (1500 \text{ m/sec})/(5050 \text{ m/sec}) = 0.3$.

For the water-glass reinforced plastic case, c_{CG} varies over a large range and, therefore, θ_{CG}, varies, i.e.,

$$2500 < c_G < 5000 \text{ m/sec}.$$

Hence,

$$\theta_{CG} = \sin^{-1}(1500/2500 < c_w/c_s < 1500/5050)$$

or

$$17° < \theta_{CG} < 37°.$$

This indicates a possible problem in a monocoque structure; in a stiffened structure, however, the stiffeners will break-up the wave train. This effect, cannot occur in materials having sound speeds lower than that of water.

3.2.6 REFLECTION OF SOUND FROM HULLS

3.2.6.1 General

The general principles of sound reflection and how steel structures are excited are important to the designer of submarine hulls because they enable him to minimize the target strength (TS) to active sonar. Target strength, i.e., the echo reflected from the hull, is a measure of the magnitude of the reflected acoustic wave referenced to the magnitude of the wave impinging upon the reflector, or target. By definition then,

$$TS = 10 \log (I_R/I_I),$$

where

I_R = echo acoustical intensity 1 yd (arbitrary reference point) from acoustic center of target (i.e., where the echo appears to originate) and

I_I = incident acoustical intensity.

The larger the TS, the more detectable the target is by active sonar.

Sound is reflected from a target by a very complex process. The sound waves strike portions of the object in the order of arrival. Therefore, reflections may interfere or combine with one another. The strength of the echo also depends on the pulse length of the active wave and varies with target aspect, frequency, and range to the sound source.

The TS of an object in the water may be calculated with reasonable accuracy. Also, the effect on TS of changes to the structural design of a ship may be estimated. However, TS calculations for complicated structures, such as submarines, is difficult and subject to error.

3.2.6.2 Reflection from Water Backed Plates

Figure 3.67 shows that, for a plate with water on both sides and incident angles of 0° to 40°, the 3 dB contour line is between 2.3 and 3.0 kHz/in. A 3 dB transmission loss means that 1/2 the energy is transmitted and 1/2 reflected. It is, therefore, a convenient demarcation for separating cases in which most of the sound is reflected from those in which most is transmitted.

Large angles are not important to active sonar operation because the echoes scatter to other angles and do not return to the source. Therefore, the incident angles at, or near normal, incidence are of greatest concern. Figure 3.59 provides data for normal incidence. At 3 kHz and a plate thickness of 0.5 in. the frequency-thickness product is 1.5 kHz-in. The insertion loss is less than 1 dB, which means that over 80 percent of the energy is transmitted through the plate. A plate such as this in the ballast tank of a submarine would permit most of the energy to pass and be reflected from the pressure hull. If the plate were 1.5 in. thick, however, the frequency thickness product would be 4.5 kHz-in. and the values would be reversed; i.e., 80 percent of the energy would be reflected.

3.2.6.3 Reflection from Air Backed Plates

As shown in figure 3.63, insertion loss is never less than 66 dB for the air backed plate and, thus, the energy is almost completely reflected at all frequencies. Note, though, that the target strength is very small for very low frequencies (less than 50 Hz) where the diameter of the hull is small relative to a wavelength.

3.2.6.4 Target Strength Calculations

The equations necessary to calculate the TSs of different geometric shapes are presented in figure 3.70. The formulas are based upon 100 percent reflection. If there is reason to believe that a portion of the energy is transmitted through a plate, its TS should be reduced by that portion. Similarly, if some energy does not reach a structure, the TS should be reduced by the amount lost in the two-way travel. The total TS of a structure can be found by calculating the individual TSs of the portions and summing. However, because the energy is added, not multiplied, the decibel TS must be summed according to

$$TS_{TOTAL} = 10 \log[\sum_{n=1}^{j} \text{antilog}(TS_n/10)].$$

Note that the outer hull will reflect some energy and that its stiffened areas are better reflectors than the plate alone. The weight of the stiffeners adds impedance and the plate acts as though it were thicker.

Figure 3.71 shows the effect of increasing the incidence energy wavelength; note the loss of detail as wavelength increases.

3.2.6.5 Modal Frequencies of Cylinders and Spheres

In addition to understanding the specular reflection discussed above, it is important to understand the mode frequencies of cylinders and spheres because these shapes respond most readily and reradiate energy at such frequencies. The mode frequencies of a cylinder are given by

$$\Omega^2 = (1/2)(n^2 + 1)(1 + \beta^2 n^2) \times \{1 \pm \{1 - [4\beta^2 n^2 (n^2 - 1)^2/(n^2 + 1)^2 \times (1 + \beta^2 n^2)^2]^{1/2}\},$$

where

$\Omega = [\omega a_c / c_p]$,
n = modal number (positive integer), and
$\beta^2 = h^2/12a_c^2$

and where

$c_p = [E/\rho_s(1 - \nu^2)]^{1/2}$,
h = plate thickness, and
a_c = cylinder radius.

Figure 3.72 shows the discrete frequencies as a continuing curve versus mode number, n. The equation for the mode frequencies of a sphere is

$$\Omega^4 - [1 + 3\nu + \lambda_n - \beta^2(1 - \nu - \lambda_n^2 - \nu\lambda_n)]\Omega^2 + (\lambda_n - 2)(1 - \nu^2) + \beta^2 \times [\lambda_n^3 - 4\lambda_n^2 + \lambda_n(5 - \nu^2) - 2(1 - \nu^2)] = 0,$$

where

$\lambda_n = n(n + 1)$ and
ν = Poisson's ratio.

Two solutions for Ω are provided by the above equations, i.e., $\Omega_n^{(1)}$ and $\Omega_n^{(2)}$. Figures 3.72 and 3.73 show their variation as n varies.

3.2.7 DIFFRACTION

Diffraction brings sound energy into areas shadowed by an acoustically opaque object and becomes a problem when attempting to shield hydrophones from noise. In shipboard installations, the baffle size is constrained by hull lines and diffraction will bring sound around the baffle and into the shielded area. High frequency, short wavelength waves are subject to less diffraction than are low frequency, long waves. However, the diffraction pattern is the same when the geometry is scaled to the wavelength.

Early investigators, such as Huygens and Fresnel, developed theories applicable to

GEOMETRIC FORM	SYMBOLS	BACKSCATTERING TARGET STRENGTH T.S. = 10 log ($\sigma/4\pi$) $\sigma/4\pi$ IS TABULATED	VARIATION WITH ASPECT	CONDITIONS
Truncated circular cone 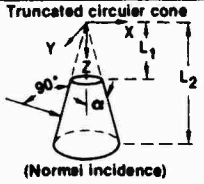 (Normal incidence)	L_1, L_2 as shown α is half angle of cone	$\frac{2}{9\lambda}\left[L_2^{3/2} - L_1^{3/2}\right]^2 \frac{\sin\alpha}{\cos^4\alpha}$	For an approximation for other than normal incidence, assume directivity of cylinder of same length	Dimensions large compared to λ
Uniform array of parallel cylinders 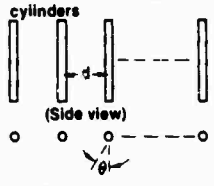 (Side view) (Top view)	N is number of cylinders d is separation	The product of the appropriate formula for target strength of single cylinder and the directivity function in next column	$\left[\frac{\sin(NKd\sin\theta)}{\sin(Kd\sin\theta)}\right]^2$	See conditions for individual cylinders
Cylinder (infinitely long) 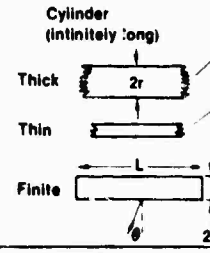 Thick Thin Finite	r is radius of cylinder R is range r is radius of cylinder R is range L is length of cylinder r is radius of cylinder θ is aspect $\beta = KL\sin\theta$	$\frac{\pi L^2}{2\lambda}\left(\frac{\sin\beta}{\beta}\right)^2\cos\theta$	Uniform / Uniform 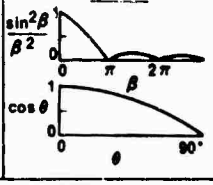	$Kr \gg 1$ $kr \ll 1$ $Kr \gg 1$ $R > L^2/\lambda$
Ellipsoid 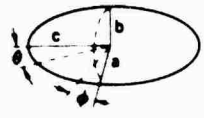	a,b,c are semiaxes of ellipsoid θ is horizontal aspect ϕ is vertical aspect	$\frac{\pi a^2 b^2 c^2}{\left(a^2\sin^2\theta\cos^2\phi + b^2\sin^2\theta\sin^2\phi + c^2\cos^2\theta\right)^2}$ (For prolate spheroid, a = b)		Ka, Kb, Kc $\gg 1$ R > a,b,c
Any smooth convex object (average overall aspects) 	S is total surface area	$\frac{S}{16\pi}$	Overall average	all dimensions large compared with λ
Ellipsoidal cylinder 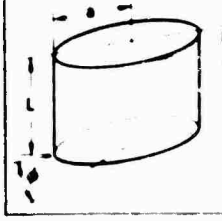	L is height of cylinder a,b are one-half the maximum and minimum dimensions of the ellipsoidal cross section ϕ is aspect $K = 2\pi/\lambda$	$\frac{(\pi a b L)^2}{2\lambda\left[(a\cos\phi)^2 + (b\sin\phi)^2\right]^{3/2}}$	Directivity in target strength pattern away from beam aspect depends on relative magnitudes of a and b	a > b KL, Ka, Kb > 1

Figure 3.70. Target Strength of Simple Geometric Figures (Measurements in Yards)

GEOMETRIC FORM	SYMBOLS	BACKSCATTERING TARGET STRENGTH T.S. = 10 log($\sigma/4\pi$) $\sigma/4\pi$IS TABULATED	VARIATION WITH ASPECT	CONDITIONS
Any convex surfaca 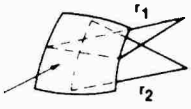	r_1, r_2 ara principsl radii ot curvatura R is ranga K is $2\pi/\lambda$	$\frac{r_1 r_2}{4}$	Detsrminad by $r_1.r_2$ at point ot tangsncy ot incident wavstront	Kr_1, $Kr_2 \gg 1$ R > r_1. r_2
Sphere (lerge)  (Rigid or pressura release)	r is radius ot sphere	$\frac{r^2}{4}$	Unitorm	Kr $\gg$ 1 R > r
(Small) (Rigid) 	V is voluma ot sphere	$61.7\ \frac{V^2}{\lambda 4}$	Unitorm	Kr $\ll$ 1 KR $\gg$ 1
(Pressure releesa) 	r is radius ot sphere	r^2	Unitorm	Kr $\ll$ 1
Spherical cep 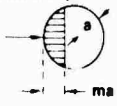	a is radius ot sphers m is detined in the tigure K = $2\pi/\lambda$ R is range	$\frac{a^2}{4}\left[4(1\cdot m)\sin^2(Kma) + m^2\left\{1-\frac{\sin(2Kms)}{(Kma)}+\left(\frac{\sin(Kma)}{Kma}\right)^2\right\}\right]$	Dspends on individual case	KR $\gg$ 1 Ka > 1
Inlinita plete (Plene surtaca) 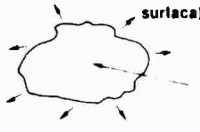	R is range	$\frac{R^2}{4}$	Unitorm	Nons
Finite plate (Any shape) 	A is araa ot plsta L is greatsst linsar dimension in plsne conteining normal, and incident ray ℓ is smallest linear dimansion β = KL sin θ	$\left(\frac{A}{\lambda}\right)^2\left(\frac{\sin\beta}{\beta}\right)^2\cos^2\theta$	Sea tinite cylindsr	R > L^2/λ K$\ell \gg$ 1
Rectangulsr ptate 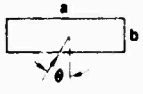	a,b ara sidss ot plsts β = Ka sin θ	$\left(\frac{ab}{\lambda}\right)^2\left(\frac{\sin\beta}{\beta}\right)^2\cos^2\theta$	Sea tinite cylindar	R > a^2/λ Kb $\gg$ 1 a > b
Circular plata 	r is radius ot plsta β = 2 Kr sin θ $J_1(\beta)$ is Bssel tunction	$\left(\pi r^2\right)^2\left(\frac{2J_1(\beta)}{\beta}\right)^2\cos^2\theta$	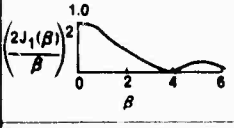	R > r^2/λ Kr $\gg$ 1
Dihsdral cornar rsttsctor 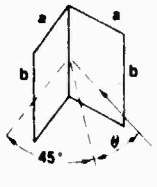	a,b ara isngths ot adgas ot rettector θ is angla ot incidencs with raspect to bisector ot dihadral angla	$\left(\frac{2sb}{\lambda}\right)^2\sin^2(45°\cdot\theta)$	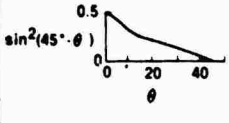	Dimsnsion is targa comparad to λ

Figure 3-70. (Cont'd) Target Strength of Simple Geometric Figures (Measurements in Yards)

High Frequency
Short Wavelength

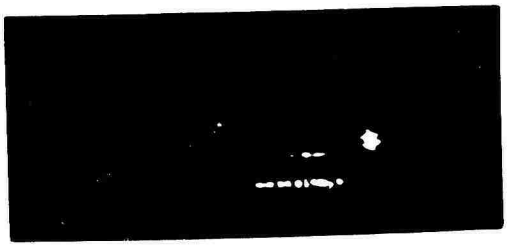

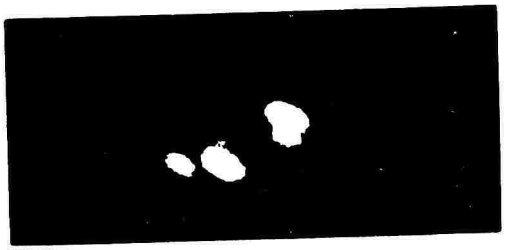

Low Frequency
Long Wavelength

Figure 3.71. Optically Simulated Acoustic Pictures of Submarine

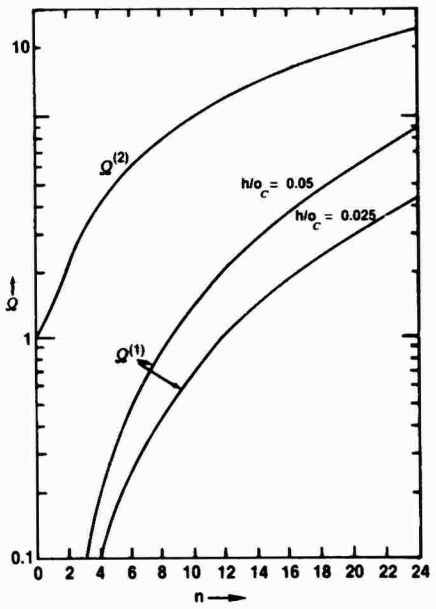

Figure 3.72. Resonant Frequencies of an Infinite Cylindrical Shell (ν = 0.3)

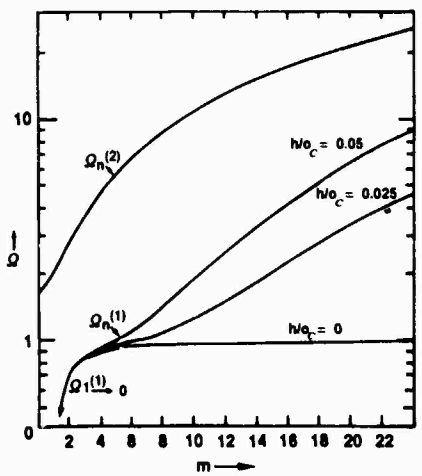

Figure 3.73. Resonant Frequencies of a Spherical Shell (ν = 0.29)

current problems, but, because of unique shipboard requirements, classic remedies are seldom adequate. Therefore, the problem must be discussed in terms of possible, instead of, definitive solutions. Note also that, for the geometries and wavelengths generally of interest, small wavelength approximations are useful only as guides. Full scale experimentation is required for accurate evaluations of particular cases.

Diffraction occurs whenever a wave flux passes the edge of an opaque barrier. Huygen's theory was that waves are propagated as though by *wavelets* formed at all points of disturbance and that the general field results when, considering their phase relationship, they are summed. When passing a barrier, the field is truncated and the wavelets propagate laterally (see figure 3.74). Figure 3.75, a depiction of an

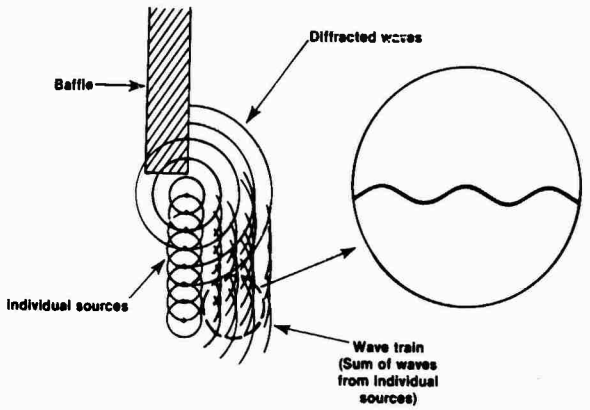

Figure 3.74. Wavelets Diffracting Around a Baffle

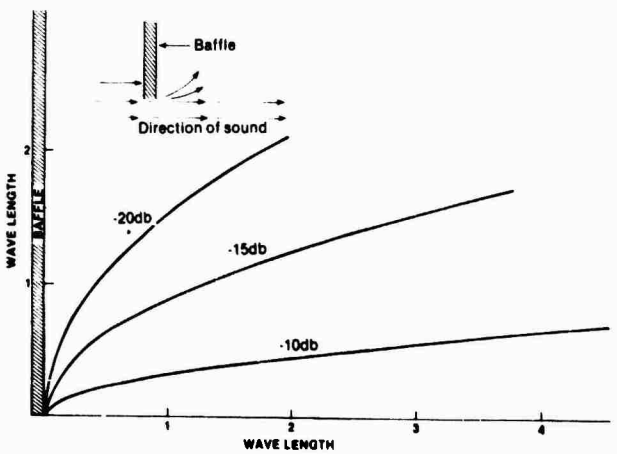

Figure 3.75. Acoustic Energy Diffracted Around a Baffle

experiment performed at the Naval Underwater Systems Center (NUSC), provides an example of diffraction around the edge of a shielding baffle. Because the data confirm general diffraction theory, they have been generalized for application to other wavelengths.

Diffraction also occurs around the slits and holes in baffles. Figure 3.76 shows data for the transmitted intensity through slits and holes. Spreading from the probe position shown, at 1λ, was spherical for the circular aperture and cylindrical for the slit.

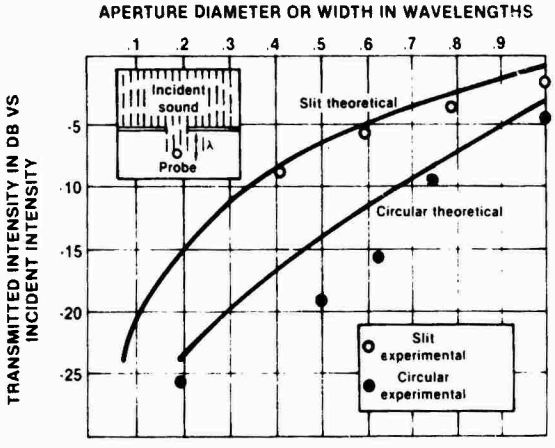

Figure 3.76. Diffraction From a Slit and Aperture in a Baffle

3.3 BUBBLE ACOUSTIC PHENOMENA

Small bubbles of air, or gas, in water create a resonant monopole frequency. The response is analogous to that of a typical vibrating mass and the resultant acoustic field can be described by treating the bubble as a simple sound source.

The scattering of sound by bubbles causes reverberation from the deep scattering layer. Bubbles may also cause *quenching*, or reduction, in transducer output when on, or near, the transducer. On the other hand, they can be used as a screen to quiet the radiated noise.

Consider an individual bubble, which is small compared with the wavelength of the impinging sound (assumed to be a plane wave). The instantaneous differential pressure on the bubble surface, P', is

$$P' = P_o e^{i\omega t}.$$

Hence the driving force is

$$F = 4\pi a^2 p' = 4\pi a^2 p_o e^{i\omega t}.$$

The air inside the bubble provides a restoring force, i.e.,

$$F_{COMP} = -(4\pi a_o^2)(3\gamma P_o/a_o)\xi_o e^{i\omega t} = k\xi_o e^{i\omega t},$$

where

a_o = radius,
γ = ratio of specific heats (of air),
P_o = static pressure in bubble,
ξ = change in radius = da_o, and
k = spring constant = $12\pi a_o \gamma P_o$.

The radial vibrations of the bubble move a mass of water, M, where

$$M = 4\pi a_o^3 \varrho$$

and ϱ is the mass density of water.

The dissipation of energy by radiation, thermal, and viscous losses, if assumed to be proportional to velocity, is

$$F_{DISS} = -R(d\xi/dt) = -c_D(d\xi/dt),$$

where $c_D = R$ = damping coefficient.

Now referencing paragraph 3.1.2.,

$$\omega_o = (k/M)^{1/2} = (3\gamma P_o/\varrho a_o^2)^{1/2}.$$

A convenient formula for calculating the natural frequency of air bubbles in water is

$$f_o = (3.3/a_o)(P_o)^{1/2},$$

where

f = frequency (kHz),
a_o = radius (mm), and

P_o = pressure in atmospheres (34 ft of water equals 1 atmosphere).

The scattered pressure is

$$P_s' = [-\omega^2 P_o(a_o/r)e^{i(\omega t - kr)}]/[(\omega_o^2 - \omega^2) + i\omega\delta],$$

where

k = wave number
r = distance from bubble and
$\delta = c_D/M = R/M$.

This expression yields

$$|(P_s/P_o)(r/a_o)| = 1/[(1 - \omega_o^2/\omega^2)^2 + \delta^2]^{1/2},$$

which is plotted in figure 3.77.

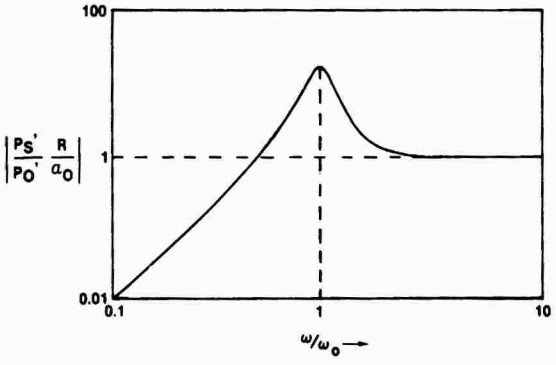

Figure 3.77. Scattered Pressure Factor for Bubbie as Function of Frequency

The scattering cross section of a bubble is a measure of the scattered sound power to the incident intensity, i.e.,

$$\sigma_s = \Pi_s/I_i,$$

where

Π_s = scattered power and
I_i = incident intensity.

For the bubble this becomes

$$\sigma_s = 4\pi a_o^2/[(1 - \omega_o^2/\omega^2)^2 + \delta^2].$$

Although the above treatment assumes that δ is constant, it is actually a function of frequency. The value of δ_o, which is the value of δ at resonance, is given in figure 3.78.

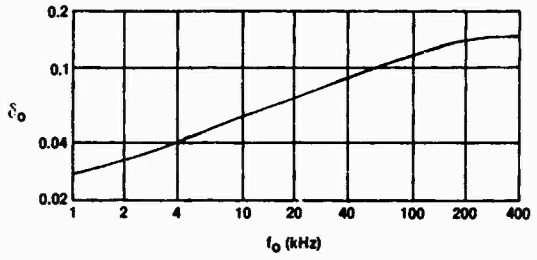

Figure 3.78. Damping Constant for Bubble at Resonant Frequency

The compliance of the air bubbles reduces the bulk modulus of the surrounding water, and therefore, reduces the speed of sound. The speed of sound in the mixture is

$$c_{mix} = c(1/(1 + 2.5 \times 10^4 F)^{1/2}$$

where:

c = speed in water
F = volume fraction of air in water.

The natural frequencies of air bubbles at the surface and at 35 ft in water are shown in figure 3.79. Figure 3.80 shows the theoretical attenuation of acoustic energy in decibels/inch of screen as a function of air volume concentration and frequency. (The assumption here is that all the bubbles are resonant at the frequency of interest.)

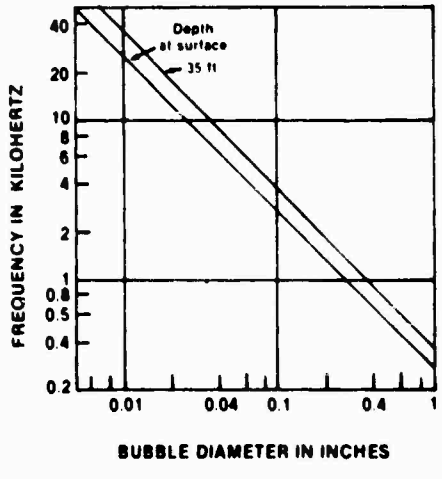

Figure 3.79. Natural Frequency of Air Bubbles in Water

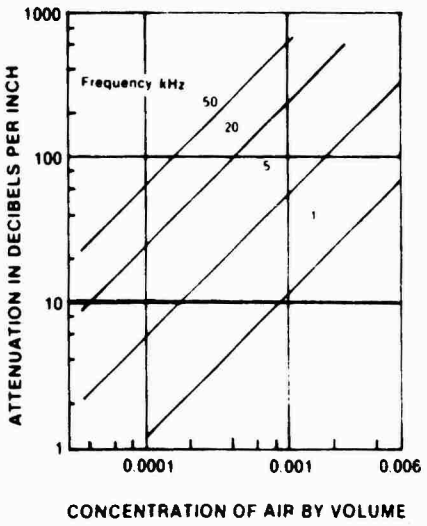

Figure 3.80. Theoretical Acoustic Attenuation of Air Bubbles

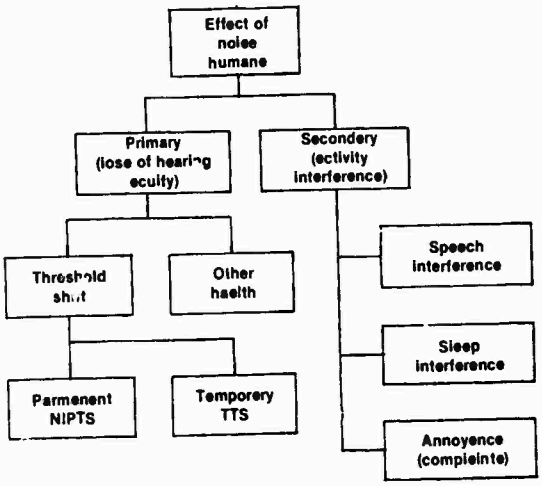

Figure 3.81. Noise Effects on Human Activities

3.4 NOISE LEVEL EFFECTS ON SHIPBOARD PERSONNEL

In general, because submarines rely on quietness to avoid detection, the active sonar is used sparingly. Some missions, however, require extensive operation of such systems. Also, surface ships employ active sonar systems for long periods.

The effects of noise on human beings are divided into the categories of primary, which results in loss of hearing acuity, and secondary, which interferes with normal activities (see figure 3.81). Primary effects include noise-induced temporary shifts (NITTS) or noise-induced permanent threshold shifts (NIPTS). Secondary effects include interference to aural communications and with recreational activites (radio, stereo, movies, or television).

Exposure to brief, intense sounds can, of course, cause immediate damage to the ear. More commonly, however, lower levels of intense sound for long periods reduces the ability to hear. Although some of this type of hearing loss is temporary, it can last for hours after the noise ceases. Also, prolonged exposure can cause chronic or even permanent hearing loss.

An example of noise-induced hearing damage is illustrated in figure 3.82. Three groups of workers, exposed for 8 hr a day, 5 days a week, 50 weeks a year to noise levels of 83, 92, and 97 dB were found, after approximately 10 yr to have an average NIPTS of from 11 to 45 dB. The threshold shifts were tested at 4 kHz, the frequency at which noise-induced hearing loss is most pronounced. Other studies have shown similar effects.

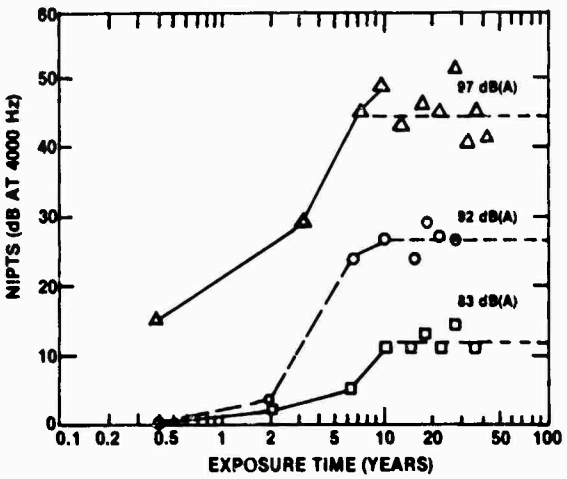

Figure 3.82. Noise-Induced Permanent Threshold Shifts versus Years of Exposure for 3 Noise Levels

The NITTS is not usually considered to be a health problem, except in cases where it is so severe that recovery is not possible after a few days away from the noise. Figure 3.83 summarizes the available information on NITTS for the 2.4 to 4.8 kHz range. Temporary threshold shifts greater than 35 to 40 dB at 4 kHz may become permanent threshold shifts. Weighted sound levels above 80 dB can contribute to ear damage if frequently encountered.

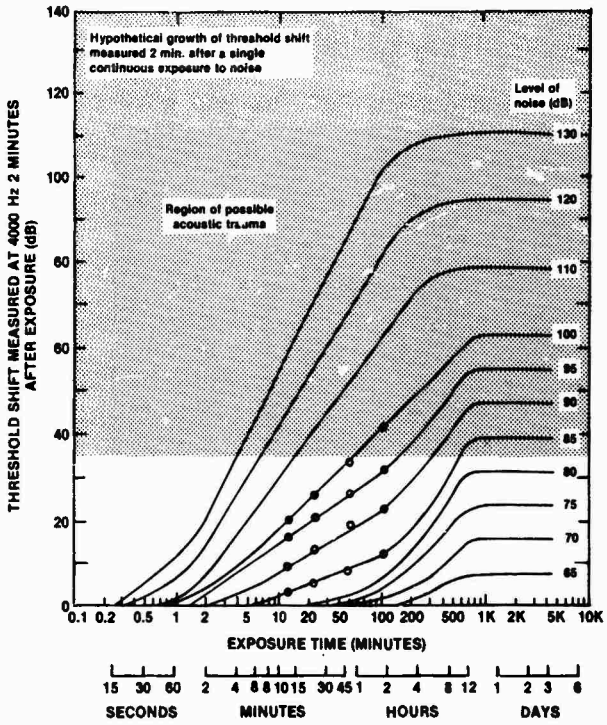

Figure 3.83. Hypothetical Threshold Shift for Single and Continuous Exposures

ANNOTATED BIBLIOGRAPHY

Amaral, J.E., *Dynamic Properties of Viscoelastic Materials,* General Dynamics, Electric Boat Division, IRAD Report P 440-75-144, December 1975.

Anderson, R.A., *Fundamentals of Vibrations,* The Macmillian Company, NY, 1967.

Azzi, V.D. and B. Celikkal, "Sound Scattering From Bubbles," *Journal of Sound and Vibration,* vol. 17, pp 143-148, July 1971.

Bansal, A.S., "Flexural Wave Motion in Beam-Type Disordered Periodic Systems: Coincidence Phenomenon and Sound Radiation," *Journal of Sound and Vibration,* vol. 62, pp 39-40, January 1979.

Bark, L.S., P.P. Ganson, and N.A. Meister, *Tables of the Speed of Sound in Sea Water,* Associated Technical Services, Inc., 1962.

Baumeister, T.H. and L.S. Marks, *Standard Handbook for Mechanical Engineers,* 7th edition, section 5, McGraw-Hill Book Company, Inc., NY.

Bell, T.G., "Underwater Sound Diffraction Around the Edge of a Shielding Baffle," NUSC Technical Memorandum 2040-168-70, August 1970.

Beranek, L.L., *Acoustic Measurements,* John Wiley & Sons, Inc., NY, 1949.

Beranek, L.L., *Acoustics,* McGraw-Hill Book Company, Inc., NY 1954.

Beranek, L.L., *Noise Reduction,* McGraw-Hill Book Company, Inc., NY 1960.

Beranek, L.L., *Noise & Vibration Control,* McGraw-Hill Book Company, Inc., NY, 1971.

Bishop, R.E.D. and W.G. Price, "A Note on Structural Damping of Ship Hulls," *Journal of Sound and Vibration,* vol. 56, pp 495-499, February 1978.

Brekhovsikh, L.M., *Waves in Layered Media,* Academic Press, Inc., NY and London, 1960.

Chalupnik, J.D., ed., *Transportation Noises, A Symposium on Acceptability Criteria,* University of Washington Press, WA, 1970.

Crandall, S.H., "The Role of Damping in Vibration," *Journal of Sound and Vibration,* vol. 11, pp 13-18,January 1970.

Damping mechanisms and amplitude and frequency effects are discussed.

Crandall, S.N. and W.D. Mark, *Random Vibration in Mechanical Systems,* Academic Press, NY, 1963.

Devin, C., Jr., "Survey of Thermal, Radiation and Viscous Damping of Pulsating Air Bubbles in Water," *Journal of the Acoustic Society of America,* vol.31, p.1654, 1959.

Dyer, I., "Statistical Vibration Analysis," *International Science and Technology,* August, 1963.

Gibbs and Cox Company, Inc., *Marine Design Manual for Fiberglass Reinforced Plastics,* McGraw Hill Book Company, Inc., NY 1960.

Graham, T., *A Handbook of Sound and Vibration Parameters,* General Dynamics, Electric Boat Division, 1978.

Harris, C.M. and C.E. Crede, *Shock and Vibration Handbook,* McGraw-Hill Book Company, Inc., NY, 1976.

Harris, C.M. *Handbook of Noise Control,* McGraw-Hill Book Company, Inc., NY, 1957.

A good generic text on vibration isolation fundamentals.

Heck, N. H. and J.H. Service, *Velocity of Sound in Sea Water,* Government Printing Office, DC, 1924.

Heuter, T.F. and R.H. Bolt, *Sonics,* John Wiley & Sons, Inc., NY, 1955.

The fundamentals of vibration, mechanical impedance, sound waves in fluids, and pressure reflectivity and transmissivity are discussed.

Junger, M.C. and D. Feit, *Sound, Structures and Their Interaction,* Massachusetts Institute of Technology Press, MA, 1972.

Keast, D.N., *Noise Control Needs in the Developing Energy Technologies,* Bolt Beranek and Newman Inc., Report 3717, March 1978.

Keast, D.N., *Measurements in Mechanical Dynamics*, McGraw-Hill Book Company, Inc., NY, 1967.

Keller, J., "Diffraction by an Aperture," *Journal of Applied Physics*, vol. 28, p.426, 1957.

Kinsler, L.E. and A.R. Frey, *Fundamentals of Acoustics*, John Wiley & Sons, Inc., NY 1962.

The fundamentals of vibration, underwater acoustics, and transmission phenomena are discussed.

Ko, S.H., C.H. Sherman, and W. A. Strawderman, "Baffling of Flexural Waves: Noise Reduction," NUSC Technical Memorandum TD12-80-74, 1974.

Kryter, K.D., *The Effects of Noise on Man,* Academic Press, Inc., NY, 1970.

Subjective responses including judgment of loudness, noisiness, and evaluation of environmental noise are discussed. Also, non-auditory responses to noise are covered.

Kryter, K.D., *Hazardous Exposure to Intermittent and Steady-State Noise,* NAS/NRC Report 86043, January 1965.

Langleben, M.P., "Reflection of Sound at the Water-Sea Ice Interface," *Journal of Geophysical Research,* vol. 75, pp. 5243-5246, September 1970.

Measurements of the specular reflection of water-borne sound at the water-sea ice interface are presented.

Libuha, J.J. and R.P. Radlinski, "Compliant Tube Baffles: Design and Development," *Journal of Underwater Acoustics*, vol. 25, no. 4, 1975.

Loeser, H. T., "Acoustic Tests of a Damped Signal Conditioning Plate," NUSC Technical Memorandum 801122, 11 September 1980.

Maidanik, M., "Acoustic Radiation from a Driven Plate Backed by a Parallel Infinite Baffle," *Journal of Acoustical Society of America,* vol. 42, p. 27, 1967.

Maidanik, M., "Acoustic Radiation from a Driven Coated Infinite Plate Backed by a Parallel Infinite Baffle," *Journal of Acoustical Society of America*, vol. 42, p. 32, 1967.

Mannheimer, M., "Velocity of Sound in Fluid Media," *Journal of Sound and Vibration,* vol. 10, pp. 343-349, September 1969.

Minorsky, N., *Non-linear Oscillations,* D. Van Nostrand Company, Inc., NJ, 1962.

Morrill, B., *Mechanical Vibrations,* The Ronald Press Company, 1957.

National Defense Research Committee on Propagation, *The Propagation of Radio Waves Through the Standard Atmosphere,* Summary Technical Report, vol. 3, chap. 8, *Diffraction by Terrain,* 1946.

Naval Sea Systems Command, *Navy Resiliant Mount Handbook 0900-LP-089-5010,* Naval Publication and Forms Center, PA., (Requistion No. DD1348).

Provides details of Navy approved sound isolation mounts.

Noise and Sound Transmission, Report of the 1948 Summer Symposium of the Acoustics Group, *The Physical Society,* 1949.

Transmission of sound by elastic panels, transmission of reverberant sound through single walls, and flexural waves are discussed.

Officer, C.B., *Introduction to the Theory of Sound Transmission,* McGraw-Hill Book Company, Inc., NY, 1958.

Pierucci, M., "Matched Asymptotic Expansion (MAE) Technique Applied to Acoustic Radiation from Vibrating Surfaces," *Journal of Acoustical Society of America,* vol. 62, 1977.

Peterson, A.P.G. and E.E. Gross, *Handbook for Noise Measurements*, General Radio Company, 1967.

Radlinski, R.P., "Modeling Predictions of Scattering from Planar Compliant Tube Arrays," NUSC Technical Memorandum TD12-40-74, 1974.

Randino, J.P., "Development of a Sprayable Vibration Damping Material for Low Frequncy Applications," NASL Technical Memorandum 44393-13, August 1966.

Shenderov, E.L. "High Frequency Asymptotic Behaviour of the Solution of the Problem of Sound Transmission Through an Elastic Shell," *Soviet Physics-Acoustics*, vol. 17, pp. 241-247, October-December, 1971.

Shertock, G., "Sound Radiated by Low Frequency Vibration of Slender Bodies," *Journal of the Acoustical Society of America*, vol. 57, pp. 1007-1016, 1975.

Skudrzyk, E., *Simple and Complex Vibratory Systems*, Pennsylvania State University Press, PA, 1968.

Snowdon, J.C. and E.E. Ungar, *Isolation of Mechanical Impact and Noise, a Colloquium*, American Society of Mechanical Engineers, NY, 1973.

Snowdon, J.C., *Vibration and Shock in Damped Mechanical Systems*, J. Wiley & Sons, Inc., NY, 1968.

Stanley, R. C., *Light and Sound for Engineers*, Hart Publishing Company, Inc., 1968, NY.

Longitudinal waves, velocity of sound waves, velocity of sound in liquids, and waves and vibration are discussed.

Timoshenko, S. and S. Woinowski-Krieger, *Theory of Plates and Shells*, McGraw-Hill Book Company, Inc., NY, 1959.

Trott, W.G. and R. Muise, "A Longitudinal Bottom Baffle for Surface Ship Self-Noise Reduction," *1970 Ship Silencing Symposium*, March 1970.

Tsai, S.C., E.C. Ong, B.P. Tan and P.H. Wong, "Applications of the z-Transform Method to the Solution of the Wave Equation," *Journal of Sound and Vibration*, vol. 19, pp. 17-20, November 1971.

Tucker, D.G. and B.K. Gazey, *Applied Underwater Acoustics*, Pergamon Press, NY, 1966.

Propagation of sound and longitudinal and shear waves are discussed

Winstanley, J.W., *Textbook on Sound*, Longmans, Green and Company, Inc., 1952, NY.

Sound caused by vibration and wave motion is discussed. Also, velocity and reflection of sound is covered.

Zavadskii, V.Y., "Critical Frequencies Associated with Sound Propagation in a Layerwise Inhomogeneous Fluid Half-Space Bounded by a Thin Elastic Plate," *Soviet Physics-Acoustics*, (in English), vol. 10, no. 2, 1964.

Principles of Sonar Installation

CHAPTER IV
ELASTOMERS

GLOSSARY

A	Area (L^2)
A_o	Constant
A_x	Solution to Wave Equation
ASTM	American Society for Testing Materials
a	Strain
B	Dynamic Bulk Compliance (L^2/F
c	Wave Speed
C_c	Sound Speed Correction Term
c_s	Shear Wave Speed (L/T)
C_α	Attenuation Correction Term
D	Dynamic Compliance L^2
d	Fractional Change in Lateral Dimension
E	Young's Modulus (F/L^2)
F	Force (F)
f	Frequency (1/T)
G	Dynamic Shear Modulus (F/L^2)
J	Dynamic Shear Compliance (L/F^2)
K	Dynamic Bulk Modulus (L^2/F)
k	Stiffness (FL/L)
k_s	Wave Number (Shear) (1/L)
L	Length (L)
M	Complex Wave Modulus (F/L^2)
M	Molecular Weight
m	Mass (FT^2/L)
N	Complex Wave Compliance (L^2/F)
n	Number of Molecules per Weight Class
p	Pressure (F/L^2)
s	Shear Stress (F/L^2)
T	Temperature
t	Time (T)
V	Volume (L^3)
v	Unit Volume Ratio
w	Total Molecular Weight per Weight Class
y	Dimension (L)
α	Attenuation Constant (1/L)
ν	Poisson Ratio
δ	Phase Angle
$\varkappa$	Dissipation Term (1/T)
Δ	Logarithmic Decrement
η'	Shear Viscosity
ω	Angular Velocity
*	Complex Quantity
'	Real Part (Storage)
''	Imaginary Part (Loss)

CHAPTER IV
ELASTOMERS

4.0. INTRODUCTION

Elastomers are effective materials in the control of acoustic energy onboard ship. Their mechanical, acoustic, and chemical characteristics will be discussed in this chapter. They are used increasingly in a variety of applications throughout the Navy because of their *non-mechanical* properties, such as low-loss dielectric, low water-absorption potting compounds, and low thermal-conductivity insulation. The importance of the mechanical properties in such applications are secondary. In other cases, plastic is used in primary or secondary structural applications, e.g., resin bonds (cements), safety glass, lock nuts, reinforced plastic gas tanks and plastic helmets, and mechanical properties are of chief interest.

In many instances, the *static* mechanical properties suffice to determine the applicability of a material. The ordinary static stress-strain diagrams, Young's modulus, modulus of rupture, and so on, are used in designing for a given application. Of course, certain negative factors such as creep, permanent set, brittle point, and strain rate intrude. But, generally, static (or quasi-static) stress-strain concepts and measurement techniques developed for elastic materials such as steel can be used for plastic materials.

However, many plastic materials have *dynamic* mechanical properties that make them uniquely suitable for acoustic, sonar, shock and vibration, and noise suppression applications. Here, the dynamic characteristics, which can depart markedly from the static properties, are important and specialized techniques must be used for measurement purposes.

4.1. DYNAMIC PROPERTIES

There are a number of specific areas in which the dynamic mechanical properties of plastic materials are of importance. One is in understanding the molecular structures of the plastics. The dependence of dynamic mechanical properties on temperature, frequency of applied stress, and other variables has been studied extensively during the last 20 years in an effort to understand the relationships between the molecular structure and macroscopic behavior of plastic materials.

Considerable progress has been made, qualitatively, in interpreting dynamic deformations in terms of various motions of segments of the large molecules that form the plastics. The results of dynamic measurements are important engineering data for the solution of structural design problems in which plastic material might be subject to vibrational stresses. The dynamic compliance, or modulus, of a plastic material can be tremendously different (by as much as 10 to 10^3) from the static compliance. Thus, a structure designed using static data might deviate considerably from its expected behavior under vibrational stress. In addition to the difference in magnitude between the absolute dynamic compliance and the static compliance, the dynamic loss must be considered because the energy associated with it is dissipated as heat and could affect the material.

Another problem of considerable importance is that of damping the vibrations of solid bodies to reduce noise. A plastic material having a large loss compliance (and, therefore, large damping) can effectively absorb energy that might otherwise be radiated as sound. Thus, if a

metal plate is coated with plastic, the rumbling, or rattling, caused by the periodic flexing of its surface is reduced. In this regard, the storage and loss moduli should be high for the most effective damping. Also, the amount of metal/plastic damping will be proportional to the mechanical loss tangent, tan δ, (i.e., proportional to energy loss/energy stored) of the plastic coating.

A plastic characterized by a large tangent loss over the entire audio-frequency range would be ideal but, in practice, such a material can only be developed by combining two or more materials, each having a high mechanical loss in one portion of the frequency range. The mechanical loss tangents of common construction materials are relatively small (about 0.0005 for metals, 0.005 for concrete, 0.01 for wood, and 2 for soft cork), whereas those of plastic materials may be relatively large (from 0.05 to 5) at certain temperatures and frequencies.

Plastic materials having high loss tangents are also applicable to vibration isolation mountings. They serve to isolate vibrating machinery from its support and to prevent vibrations of the supporting floor or other structure from being transmitted to the equipment.

Plastic material characterized by a narrow frequency range and high mechanical loss tangent may be useful in suppressing natural resonances that create large vibration amplitudes and subsequent rupture. In such cases, a material having a high loss region at the frequency of harmful resonance must be employed. A thorough knowledge of the dynamic mechanical behavior of various plastics is required for such a selection; correlation of macroscopic behavior and molecular structure would make it possible to synthesize a material having the desired properties.

The dynamic mechanical properties of plastic and rubber-like materials are of paramount importance in relation to underwater sound. The propagation of sound through plastic or rubber-windowed dome structures depends on the specific complex mechanical impedance of the composite structure instead of the idealized acoustical properties of an infinitely-extended plate. Non-reflecting coatings for submarines can be improved through a precise delineation of the dynamic mechanical properties of coating materials. Also, the self-noise levels of towed arrays depend on the effective damping of the composite construction of the array. Here again, it is possible to synthesize materials having increased damping by applying adequate dynamic measurements. Finally, knowledge of visco-elastic characteristics can result in more efficient transducer design and construction, particularly for low-frequency systems.

4.2. ENGINEERING PROPERTIES

Although no detailed quantitative theory exists to encompass the wide range of mechanical and chemical properties of elastomers, progress has been made in the qualitative understanding of basic mechanisms. The technology and engineering of elastomeric materials, however, are remarkably advanced and product applications are widely distributed throughout industry. Some pertinent engineering properties are summarized in the following discussion.

4.2.1. PHYSICAL STRUCTURE

The physical properties of rubbery polymers of high molecular weight are generally defined in terms of strong intermolecular coupling at widely separated points and depicted as being subject to topological entanglements. In certain time and frequency scale ranges, the network of entanglements behaves almost as the cross-linked network of a vulcanized rubber without entanglement slippage. Entanglement slippage dominates the elastic behavior in other regions, especially non-linear behavior at high strains or strain rates.

The topological entanglements remain when chemical cross-links are introduced into a rubbery polymer by vulcanization; some are trapped, others are on loose ends that can, to an extent, slip and relax. Viscoelastic losses tend to peak in a lightly cross-linked rubber at high frequencies, where local molecular motions fail to keep pace with changing external stresses, and at low frequencies, where the untrapped entanglements slip.

This low frequency loss mechanism can be exploited to reduce vibrations or self-noise. For example, if two polymers of nearly identical

chemical structure (except that only one is cross-linkable) are mixed and vulcanized, a low frequency loss mechanism is produced that is inversely proportional to the third power of the molecular weight of the (teptative) non-crosslinked species, but independent of its proportional amount. The magnitude of the loss peak, however, depends on this amount. Trapped and untrapped entanglements are important to dynamic viscoelastic properties and to mechanical properties such as tensile strength, abrasion, and tear resistance.

4.2.2. COMPOUNDING ELASTOMER STOCKS

Vulcanization occurs when natural rubber is mixed with sulphur, or other agents, and heated. According to current theories, the process causes the sulphur atoms to cross-link at approximately every 500 atoms in the long chain polymer, i,e., in the *back-bone*. The cross-links restrain the slipping of polymer chains over each other and impart elasticity and resilience to the rubber stock. Organic accelerators exert a profound effect on the vulcanization reaction; they increase the reaction rate and often improve physical properties and aging.

Principal among the reinforcing fillers added to elastomers for improved tensile strength and tear and abrasion resistance are the carbon blacks. Inert fillers do not enhance physical properties and can actually be deleterious. Other compounding ingredients may be used as antioxidants; they improve stock oil-resistance, sunlight resistance, and other characteristics.

4.2.3. STRESS AND STRAIN RELATIONSHIPS

Stress and strain properties such as modulus, tensile strength, and elongation are measured to evaluate elastomer quality. The resultant index is extremely sensitive; it is based upon the type of elastomer, compounding ingredients, cure, and temperature at which the measurements are made. Standard ASTM dumbbell shaped dimensions for tensile strength measurements are shown in figure 4.1.

Typical stress-strain curves for three natural rubber compounds, ranging from soft to relatively hard, are shown in figure 4.2. Figure

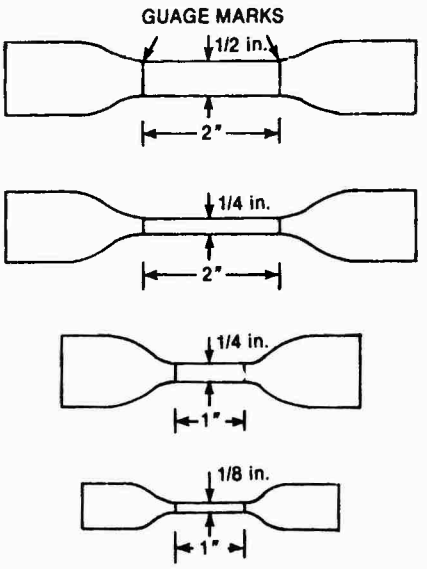

Figure 4.1. Standard ASTM Tensile Specimen

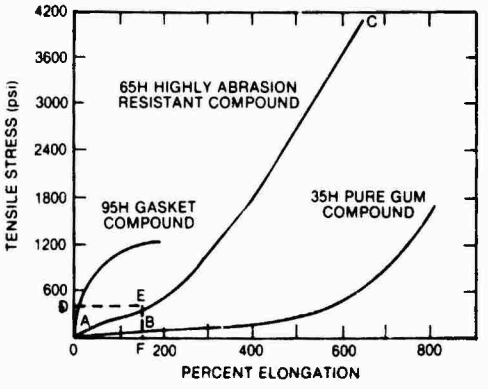

Figure 4.2a. Stress/Strain Curve

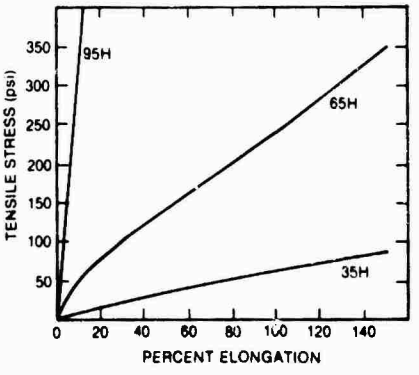

Figure 4.2b. Low Stress Region

Figure 4.2. Stress/Strain Curves for Typical Rubber Compounds

4.2a shows curves obtained by stretching dumbbell shaped samples at a standard strain rate of 20 in./min. Three regions can be differentiated using the middle curve. The initial portion, 0-A, is concave to the strain axis, the second, A-B, is nearly straight, and B-C is concave to the stress axis. Similar regions are shown for the compound having a Shore hardness of 35, but the curve for compound 95H does not have the last region. Figure 4.2b illustrates an enlarged portion of the initial region.

Young's Modulus is the ratio of tensile stress to the resultant extensional strain. This can be assumed to be the initial slope of a stress-strain curve, but it is limited to small strains for elastomers. Generally, therefore, the chordal slope from the original to a particular strain is specified.

The ultimate tensile strength of an elastomer is the unit force required to produce a rupture, based on the original cross section. Elongation at the rupture is also considered.

4.2.4. HARDNESS

Elastomer hardness is defined as relative resistance to surface indentation. The most commonly used instrument for such measurements, the Shore durometer, employs a spring-loaded truncated cone calibrated to indicate 0 for a 2 oz load and 100 for a 29 oz load; the linear scale is between 0 and 100.

The scale covers the range of practical elastomers and indicates differences in stiffness among compounds that correspond reasonably well with those that can be sensed by touch. The scale can be summarized as

1. 30 to 35 for ordinary, pure gum compounds,
2. 50 to 60 for tire tread compounds, near the center of the scale, and
3. 80 to 90 for compounds used for valves, stiff rolls, and so on.

4.2.5. TEAR RESISTANCE

Elastomer stock resistance to tear is important in tires and tubes, footwear, clothing, insulated wire, isolation mounts, and towed array hose. The standard ASTM test for tear resistance is based upon the model presented in figure 4.3. The tear begins at the nick and the maximum load is recorded. The results are computed in terms of the force per inch of thickness required to tear the material.

The compounding and curing of elastomers effect tear resistance, which decreases with increased temperature. Diluents and softeners lower tear resistance and reinforcing materials, particularly carbon black, greatly increase it. (This is also true of fabric reinforced composites.) Some fillers, such as magnesium carbonate or clay, create an area in which a tear can move with relatively little resistance. On the other hand, 28 volumes of carbon black per 100 of rubber in a GR-S compound raised the tear resistance from 27 lb/in. thickness to 265 lb/in.

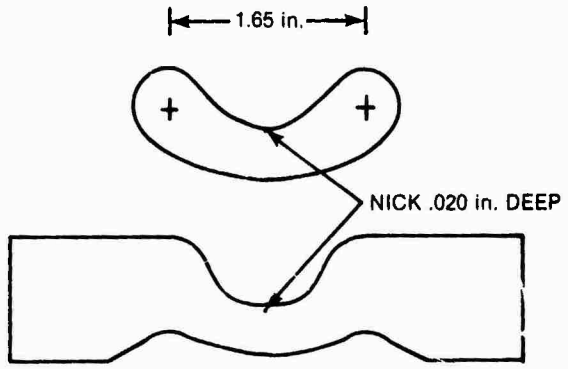

Figure 4.3. ASTM Crescent (Peanut) Tear Test Specimen

4.2.6. ABRASION RESISTANCE

The rate of abrasion for a given compound depends on the rate of slip, contact pressure, temperature, frequency and duration of frictional contact, and nature of the rubbing surfaces of the elastomer and abrasive surface. Although current knowledge concerning abrasion is limited, two mechanisms can be discussed. One, termed the *erosion mechanism*, is the mechanical removal of the surface layer by gouging, chipping, cutting, tearing, and shearing. The other is a *chemical mechanism*, in which the surface layer of the elastomer is degraded by oxidation or heating (i.e., pyrolisis) prior to the removal of material by mechanical means. When abrasion is extremely rapid, the erosion mechanism is generally primary,

particularly if there is no great temperature increase. This condition may exist during the *wet grinding*, or wear, of a towed array being dragged along the deck of a ship after recovery.

Chemical degradation results from exposure to sunlight, oxidation, and weathering. Also, dragging a dry towed array over the surface of a pier can cause enough frictional heat on the high stress contact points to melt or pyrolize the material to a semiliquid state. The abrasive rate can be severe in such cases and stone particles can become embedded in the hose wall. Because abrasion is complex and involves so many variables, it cannot be directly correlated with simpler physical properties. For this reason many abrasion tests have been developed. The commonly used techniques decribed in ASTM Method D 394 may require modification for particular Navy applications.

4.2.7. PUNCTURE RESISTANCE

There is no standard test for measuring the relative puncture resistance of an elastomer stock. One should be devised that is based upon the maximum force obtained when a section of a specimen is punctured by a standard penetrator. Measurements so obtained might be expected to correlate with the ultimate tensile strength and tear resistance of the stock.

4.2.8. SPECIFIC GRAVITY

The specific gravity of an elastomer is of minor importance in most applications. However, it is important to the reflectivity of the material for acoustic control and to the buoyancy design for towed arrays. The effective specific gravity of a particular stock depends upon the elastomer, the reinforcing filler and, when fabric reinforcement is involved, the type of fabric and number of plies. The specific gravity is, of course, temperature dependent and must be determined over the operational range of the application.

4.2.9. OTHER ENGINEERING PROPERTIES

Other engineering properties of elastomers that may be of interest include

1. compression modulus and permanent set,
2. shear modulus and permanent set,
3. fatigue and flexing,
4. resilience,
5. electrical resistance,
6. fluid resistance,
7. aging, sunlight, and ozone resistance, and
8. water absorption.

4.2.10. SUMMARY OF APPLICABLE ASTM TESTS

Standard test methods for most of the elastomer engineering properties discussed have been developed by ASTM. They are summarized in table 4.1.

4.2.11. SUMMARY OF ELASTOMER PROPERTIES

Elastomers of interest for sonar applications include the synthetic rubbers, i.e.,

1. GR-S (butadiene-styrenecopolymer),
2. Butyl (isobutylene-butadiene copolymer),
3. Neoprene(chlorprene polymer),
4. Nitrile (acrylonitrile-butadiene copolymer), and
5. Polyurethane (urethane linked polymers),

as well as the plasticized PVCs (e.g., polyvinyl chloride plasticized by dioctyl pthalate). Table 4.2 summarizes the general qualitative range of engineering properties that can be achieved using such elastomers. It should be emphasized, however, that elastomer properties depend greatly on, polymerization, compounding, and reinforcing fillers.

For example, all polyurethane elastomers are characterized by urethane links formed by the creation of an isocyanate and a compound containing hydroxyl groups. The polyurethane structure may also consist of urea groups, allophanates, and biurets produced by various side reactions. The resultant properties are useful in applications requiring rigid and flexible foams, elastomers, and coatings. Hydroxyl groups produced by polyesters and castor oil are most often used for elastomeric applications.

Polyurethane rubber can be developed to provide

1. tensile strengths from 3000 to 7000 lb/in.^{2}, at corresponding elongations of 200 to 700 percent;

Table 4.1. Physical Properties Test Methods

Hardness	ASTM D314, D531, D676 Federal Specification ZZ-R-601 Vanderbilt *Rubber Handbook*, pp. 404-418
Tensile strength elongation modulus permanent set	ASTM D412 Federal Specification ZZ-R-601
Compression Deflection (load deflection) (spring rate)	ASTM D573
Compression set	ASTM D395
Tear resistance	ASTM D624
Abrasion resistance	ASTM D394 Federal Specification ZZ-R-601
Resistance to fluids (oils, solvents, etc.)	ASTM D471, D314
Aging	ASTM D454, D572, D573, D865, D1206 Federal Specification ZZ-R-601
Staining and discoloration	ASTM D925
Low-temperature resistance	ASTM D736, D746, D797, D837, D1043, D1053
Fatigue and flexing tests	ASTM D430, D623
Resilience Tests	ASTM D945, D1054
Textiles test methods	ASTM Standards on Textile Materials (issued annually) Federal Specification CCC-T-191
Weathering resistance	ASTM D518, D749, D750, D1149, D1171

2. moduli from 250 to 5000 lb/in.^{2}, at 100 percent elongation,
3. hardness from 50 to 90, in terms of Shore durometer A, and
4. densities from 1.2 to 1.4 g/cm^3.

Urethane elastomers can be developed to provide improved

1. resilience,
2. tensile-to-elongation properties,
3. bearing-load capacity,
4. toughness,
5. abrasion resistance,
6. tear strength,
7. hardness range,
8. low temperature performance, and
9. resistance to oxygen, ozone, and various solvents.

There will be, however, a generally undesirable deterioration in properties over time and continuous service in air at temperatures in excess of 80° C.

4.3. DYNAMIC CHARACTERISTICS OF VISCOELASTIC MATERIALS

4.3.1. VISCOELASTIC MATERIALS

Classical deformation theory is concerned with the behavior of two idealized materials, i.e., the elastic solid and the viscous liquid. The theory of elasticity treats the mechanical properties of perfectly elastic solids in accordance with Hooke's law, i.e., stress is directly proportional to strain, but independent of strain rate. The theory of hydrodynamics deals with properties of perfectly viscous liquids in accordance with Newton's law; i.e., stress is directly proportional to strain rate, but independent of strain.

Actually, however, real solids exhibit some viscous properties and real liquids exhibit some elastic properties when subjected to time dependent stress. For many solids, such as metals and ceramics, elastic properties are predominant and viscous effects can be neglected. Similarly, elastic effects are negligible for many liquids given ordinary time variations of stress. On the other hand, most high polymers are intermediate materials in which appreciable elastic and viscous effects are present simultaneously at ordinary temperatures and stresses; for this reason they are said to be *viscoelastic* materials.

4.3.2. DYNAMIC MECHANICAL CHARACTERISTICS

Dynamic mechanical characteristics describe the deformation or strain of a material subjected to a stress that varies with time. Although the time variations of stress may be of different durations, it is convenient to describe the dynamic mechanical properties of a material in terms of the strain produced by a periodic stress of sinusoidal form and to consider the steady state. Periodic stresses of nonsinusoidal form, or transient stresses, can then be treated in sine or cosine terms.

Table 4.2. Relative Properties of Elastomers

Property	Natural Rubber	Grade R GR-S or Buna 5	Butyl	Grade SA Thiokol (GR-P)	Grade SB Nitrile (Buna N)	Grade SC Neoprene (GR-M)	Grade T Silicone
Composition	—	Butadiene-styrene	Isobutylene-Isoprene	Organic polysulfide	Butadiene-scrylonitrile	Chloroprene	Polysiloxane polymer
Tensile strength (psi)							
Pure gum	Over 3000	Below 1000	Over 1500	—	Below 1000	Over 3000	Below 1500
Black load stocks	Over 3000	Over 2000	Over 2000	—	Over 2000	Over 3000	—
Hardness range (shore durom A)	30-90	40-90	40-75	35-80	40-95	40-95	40-85
Specific gravity (base material)	0.93	0.94	0.92	1.34	1.00	1.23	—
Tear resistance	Good	Fair	Good	Poor	Fair	Good	Poor
Abrasion resistance	Excellent	Good to excellent	Good	Poor	Good	Excellent	Poor
Solvent resistance							
Aliphatic hydrocarbons	Poor	Poor	Poor	Excellent	Excellent	Good	Poor
Aromatic hydrocarbons	Poor	Poor	Poor	Good	Good	Fair	Poor
Acid resistance							
Dilute	Fair to good	Fair to good	Excellent	Fair	Good	Excellent	Excellent
Concentrated	Fair to good	Fair to good	Excellent	Fair	Good	Good	Fair
Oxygenated solvents (ketones, etc.)	Good	Good	Good	Good	Poor	Poor	Fair
Permeability to gasses	Fair	Fair	Very low	Low	Fair	Low	Fair
Oil and gasoline resistance	Poor	Poor	Poor	Excellent	Excellent	Good	Fair
Animal and vegetable oil resistance	Poor to good	Poor to good	Excellent	Excellent	Excellent	Good	Fair
Oxidation	Good	Good	Excellent	Good	Good	Excellent	Excellent
Sunlight aging	Poor	Poor	Very good	Good	Poor	Very good	Excellent
Heat aging	Good	Very good	Excellent	Fair	Excellent	Excellent	Outstanding
Resistance to swelling in lubricating oil	Poor	Poor	Poor	Excellent	Very good	Good	Fair
Resistance to water absorption	Very good	Good to very good	Very good	Fair	Fair to good	Good	Good
Resistance to lacquer solvents	Poor	Poor	Poor	Good	Fair	Poor	Poor
Flame resistance	Poor	Poor	Poor	Poor	Poor	Good	Fair
Cold resistance	Excellent	Excellent	Good	Fair	Good	Good	Excellent
Heat resistance	Good	Excellent	Excellent	Poor	Excellent	Excellent	Excellent
Ozone resistance	Fair	Fair	Excellent	Excellent	Fair	Excellent	Excellent
Rebound							
Cold	Excellent	Good	Bad	Fair	Good	Very good	Excellent
Hot	Excellent	Good	Very good	Fair	Good	Very good	Excellent
Dielectric strength	Excellent	Excellent	Excellent	Fair	Poor	Good	Good
Electrical Insulation	Good to excellent	Good to excellent	Good to excellent	Fair to good	Poor	Fair to good	Excellent
Compression set	Good	Good	Fair	Poor	Good	Fair to good	Fair
Vulcanizing properties	Excellent	Excellent	Good	Fair	Excellent	Excellent	—
Adhesion to metals	Excellent	Excellent	Good	Poor	Excellent	Excellent	—
Adhesion to fabric	Excellent	Good	Good	Fair	Good	Excellent	—

Thus, if a plastic material is under a dynamic shearing stress of the form $s = s_o \sin 2\pi ft$, a periodic strain of the same frequency, f, will be produced in the material. In general, this strain will be out of phase with the stress and described by $a = a_o \sin (2\pi ft - \delta)$, where δ is the phase difference or phase angle between the applied stress and the resulting strain (see figure 4.4). The ratio between the strain amplitude, a_o, and the stress amplitude, s_o, is the absolute dynamic compliance, J. Conversely, the ratio of s_o to a_o is the absolute dynamic rigidity, G (i.e., $a_o/s_o = J$ and $s_o/a_o = G$). The only quantities necessary to describe dynamic mechanical behavior of a material in shear are the combinations of G with δ or J with δ. The alternate quantities, J′ and J″, are often used in place of J and δ, respectively. Thus if the strain is divided into two parts, one of which is in phase and one of which is 90° out of phase with the applied stress, we have

$$a = s_o(J' \sin \omega t - J'' \cos \omega t),$$

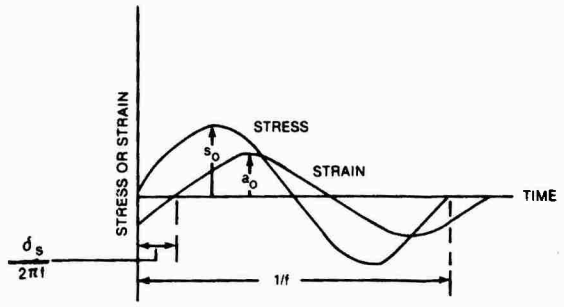

Figure 4.4. Stress/Strain Phase Relationship

which is equivalent to considering the compliance to be a complex quantity $J^* = J' - iJ''$, where $i = (-1)^{1/2}$. The storage compliance, J', is a measure of the elastic energy stored and recovered during each cycle of the deformation, whereas the loss compliance, J'' is proportional to the energy dissipated as heat during each cycle. The exact relationships between the various compliance quantities can be seen in figure 4.5.

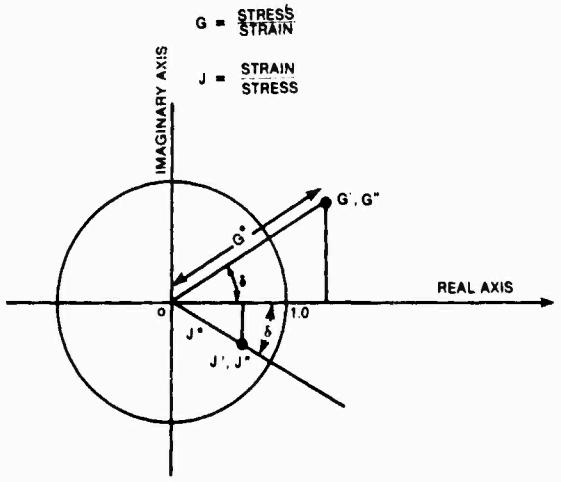

Figure 4.5. Vector Resolution of Modulus and Compliance in Sinusoidal Deformation

The complex shear rigidity is similarly defined as $G^* = G' + iG''$, where $G^* = 1/J^*$ and $G''/G' = J''/J' = \tan \delta$. It must be emphasized that because the quantities under discussion may vary with frequency and temperature, they should be termed *characteristics* instead of *constants* of a material. Therefore, in order to completely describe the mechanical properties of a material, the complex compliance (or modulus) must be known for various frequencies and temperatures.

The individual components are not reciprocally related, but are related by the following equations:

$$J' = G'/(G'^2 + G''^2) = (1/G')/(1 + \tan^2 \delta),$$

$$J'' = G''/(G'^2 + G''^2) = (1/G'')/[(1 + (\tan^2 \delta)^{-1}],$$

$$G' = J'/(J'^2 + J''^2) = (1/J')/(1 + \tan^2 \delta),$$

and

$$G'' = J''/(J'^2 + J''^2) = (1/J'')/[(1 + (\tan^2 \delta)^{-1}].$$

4.3.3. RELATIONSHIPS AMONG COMPLEX MODULI (COMPLIANCE)

From a physical standpoint, the two basic types of deformation of a material subjected to stress are (see figure 4.6) simple shear, which produces a change of shape with no change of volume, and bulk compression, which produces a change of volume with no change of shape. Other types of deformations produce combinations of shape and volume changes, e.g., tensile deformation.

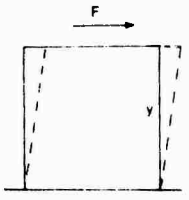

Figure 4.6a. Simple Shear

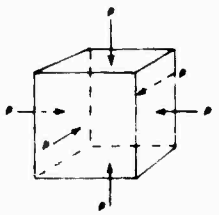

Figure 4.6b. Bulk Compression

Figure 4.6. Basic Stress-Induced Deformations

As we have seen, a viscoelastic material subjected to a sinusoidal shearing deformation can be characterized by a complex shear modulus, $G^* = G' + iG''$, or its complex reciprocal, $J^* = 1/G^* = J' - iJ''$. Analogous definitions apply to the complex bulk modulus, K^*, and its reciprocal B^*; the complex extension modulus, E^* (Young's Modulus), and its reciprocal D^*; and the complex wave modulus, M^*, and its reciprocal, N^*. These moduli, or compliances, are not independent and at least two are required to completely characterize a homogeneous, isotropic, linear, viscoelastic material.

Thus, consider a long, thin viscoelastic rod subjected to a sinusoidal tensile stress as shown in figure 4.7a. The longitudinal strain will be out of phase with the applied longitudinal stress, as is the viscoelastic shear deformation shown in figure 4.4, and we have

$$a_l = (s_o)_l(D' \sin \omega t - D'' \cos \omega t),$$

where

$D^* = 1/E^* = D' - iD''$ = complex extension compliance and $\tan \delta_l = D''/D'$.

Figure 4.7a. Thin Rod Under Sinusoidal Tensile Stress

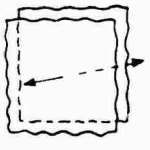

Figure 4.7b. Thin Plate Under Compression Stress

Figure 4.7. Viscoelastic Material Under Stress

The complex extension compliance is determined by the complex shear and bulk compliances, thus,

$$D^* = J^*/3 + B^*/9.$$

Similarly, the complex extension (Young's) modulus is a function of the complex shear and bulk moduli, or

$$E^* = 9G^*K^*/(3K^* + G^*).$$

If a thin flat viscoelastic plate of extended lateral dimensions (as shown in Figure 4.7b) is subjected to a longitudinal compression stress in the thin direction, an elemental volume experiences volume and shear strains because of surrounding medium constraints. The appropriate complex modulus for this case is

$$M^* = K^* + 4G^*/3,$$

which corresponds to a plane wave propagating in a medium whose dimensions are all large compared to the wavelength; this is termed the complex wave modulus.

4.3.4. COMPLEX POISSON RATIO

When the rod shown in figure 4.7a is stretched under an applied tensile stress, there is an associated lateral contraction. The ratio of this unit lateral contraction to the unit longitudinal extension is a semi-empirical characteristic of the material termed the *Poisson Ratio*, ν, and is defined as

$$\nu = (\Delta D/D)/(\Delta L/L) = d/a_l,$$

where

D = Diameter
L = Length

i.e., the fractional change in diameter divided by the fractional change in length. There is an accompanying increase in unit volume given by the relationship

$$v = \Delta V/V = (1 - 2\nu)a_l.$$

If s_l is the unit stress for an elastic rod then, by definition.

$$E \equiv s_l/a_l = (s_l/d)\nu.$$

As we have seen, the unit sinusoidal strain for the viscoelastic rod is out of phase with the unit

sinusoidal stress and the extension modulus becomes complex, i.e., $E^* = E' + iE''$. Hence, we can define the complex Poisson ratio for the viscoelastic case as

$$\nu^* = \nu' - i\nu''.$$

The storage Poisson ratio, ν', is that part of the lateral contraction that is in phase with the sinusoidal longitudinal extension. The loss Poisson ratio, ν'', is that part of lateral contraction that is 90° out-of-phase with the extension.

The complex Poisson ratio can also be expressed in terms of the fundamental moduli, i.e.,

$$\nu = (3K^* - 2G^*)/2(3K^* + G^*).$$

Table 4.3 summarizes the relationships between the various complex moduli.

Table 4.3. Relations Between Complex Moduli

	(G^*,E^*)	(G^*,K^*)	(E^*,K^*)	(G^*,ν^*)	(E^*,ν^*)	(K^*,ν^*)
E^*	—	$\frac{9G^*K^*}{3K^*+G^*}$	—	$2G^*(1+\nu^*)$	—	$3K^*(1-2\nu^*)$
G^*	—	—	$\frac{3E^*K^*}{9K^*-E^*}$	—	$\frac{E^*}{2(1+\nu^*)}$	$\frac{3K^*(1-2\nu^*)}{2(1+\nu^*)}$
K^*	$\frac{E^*G^*}{9G^*-3E^*}$	—	—	$G^*\frac{2(1+\nu^*)}{3(1-2\nu^*)}$	$\frac{E^*}{3(1-2\nu^*)}$	—
ν^*	$\frac{E^*}{2G^*}-1$	$\frac{3K^*-2G^*}{2(3K^*+G^*)}$	$\frac{1}{2}\left[1-\frac{E^*}{3K^*}\right]$	—	—	—

If the volume remains constant when a viscoelastic material is stretched, the absolute value of the Poisson ratio is 0.50. Liquids and soft, rubberlike materials approach this value. For most other materials, the static Poisson ratio is between 0.15 and 0.50, (e.g., plutonium = 0.15, uranium = 0.21, steel = 0.29, aluminum = 0.33, lead = 0.40 to 0.45, polystyrene = 0.31, cellulose acetate = 0.44, and rubber = 0.49). Table 4.4 shows the interrelationships between the absolute Poisson ratio values and those for various viscoelastic moduli as derived from table 4.3).

There are not very much experimental data concerning the dynamic complex Poisson ratio, particularly for high polymers. Apparently, in the rubbery region above the transition temperature, $\nu'' \cong 0$ and $\nu' \doteq 0.5$, for most high polymers and is independent of temperature. In the brittle region below the transition temperature the loss Poisson ratio also is approximately zero, i.e., $\nu'' \cong 0$ and $\nu' < 0.5$, but also tends to be independent of temperature. The Poisson ratio nominally depends on temperature, but in the transition region it becomes complex ($\nu'' \neq 0$) and frequency dependent.

Table 4.4. Poisson Ratio and the Moduli Ratios

Poisson Ratio $\lvert\nu^*\rvert$	$\lvert E^*/G^*\rvert$	$\lvert K^*/G^*\rvert$	$\lvert K^*/G^*\rvert$
0	2.00	0.333	0.667
0.20	2.20	0.417	0.917
0.25	2.40	0.556	1.334
0.30	2.60	0.667	1.667
0.35	2.70	1.111	3.000
0.40	2.80	1.667	4.668
0.45	2.90	3.333	9.666
0.50	3.00	∞	∞

4.3.5. APPROXIMATE RELATIONSHIPS

From table 4.3 we have

$$E^* = 9G^*K^*/(3K^* + G^*)$$
$$= 9G^*/(3 + G^*/K^*).$$

For rubber-like materials $|K^*|>>|G^*|$, such that the approximate relationship is

$$E^* \approx 3G^*.$$

Similarly, for the loss tangents, tan δ (tensile) = E''/E' and tan δ (shear) = G''/G' and we have

$$E''/E' = (G''/G')[1/(1 + G'/3K')].$$

Again, an approximate relationship results for rubber-like material, such that

$$E''/E' = G''/G'.$$

Thus, measurements of the dynamic complex shear modulus (or compliance) of a rubber-like material are sufficient to fully characterize the dynamic mechanical properties of the material. The significance of this, as will be discussed later, is that the complex shear modulus can be precisely measured over extended frequency (10 to 5000 Hz) and temperature ranges (-50° C to 150° C), and for loss tangents of from 0.01 to 5.0. This is in general not true for the other dynamic properties such as tensile, bulk and wave moduli, where experimental methods of only limited ranges exist.

Plane wave propagation in a viscoelastic medium is governed by the complex modulus

$$M^* = K^* + (4/3)G^*.$$

Again, if we have a rubber-like material where $|K^*|>>|G^*|$, the wave modulus becomes approximately equal to the bulk modulus, or

$$M^* \approx K^*.$$

4.3.6. LOSS TANGENT

The complex compliance, or modulus, is convenient because the storage compliance, J', is a measure of the elastic energy stored and recovered during each cycle, whereas the loss compliance, J'', is proportional to the energy dissipated by heat. Thus, if S is the root mean square (rms) value of a sinusoidal stress applied to a disc, we have

Energy stored per unit volume/cycle = $2S^2J'$.

Energy lost per unit volume/cycle = $2\pi S^2J''$.

(Energy lost per unit volume/cycle)
/(Energy stored per unit volume/cycle)
= $\pi J''/J' = \pi \tan \delta_s$.

The loss tangent is related to the mechanical Q by the simple relation

$$\tan \delta = 1/Q$$

and to the logarithmic decrement, Δ, by

$$\tan \delta = (\Delta/\pi)/(1 + \Delta^2/4\pi^2)^{1/2}.$$

For the case of small damping, this simplifies to the approximate relationship

$$\tan \delta \approx \Delta/\pi.$$

The damping in compression (K''/K') is generally much lower than that in shear (G''/G'), particularly for viscoelastic high polymers. In the brittle region below the transition temperature, shear damping is usually higher by a factor of 10 or more; in the rubbery region above that temperature, shear damping may be 50 to 100 times the compression damping.

Thus, it is possible to develop elastomers, or rubberlike materials, that exhibit high damping to vibrational deformations (involving the complex shear modulus) and low attenuation to an acoustic wave (involving the bulk modulus). This characteristic is important in reducing sonar dome and towed array self-noise.

4.3.7. COMPOSITE VISCOELASTIC ROD IN TENSION

4.3.7.1. Elastic Case

Assume that the concentric composite rod shown in figure 4.8 is subjected to a tensile force, F, and that the two materials composing the rod have the same deflection, ΔL. Then, if E_1, E_2, and A_1, A_2 are the moduli of elasticity and cross sectional areas of the respective materials, the elongation is given by

$$\Delta L = F_1L/E_1A_1 = F_2L/E_2A_2$$

and

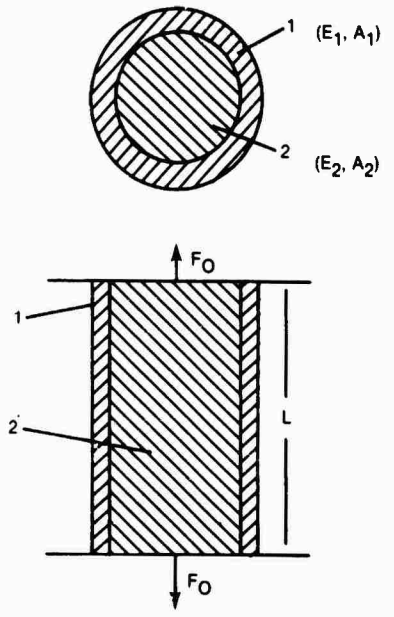

Figure 4.8. Composite Viscoelastic Rod

$$F_o = F_1 + F_2 = \text{Total Force},$$

$$A_o = A_1 + A_2 = \text{Total Area}$$

$$\Delta L = \Delta L_1 = \Delta L_2 = \text{Total Deflection.}$$

Hence, since $a = \Delta L/L$ = unit strain

$$F_o/aA_o = (E_1A_1 + E_2A_2)/(A_1 + A_2),$$

but

$$E_o = \text{Unit Stress/Unit Strain} = F_o/aA_o.$$

Therefore, the effective modulus of the composite rod is given by

$$E_o = (E_1A_1 + E_2A_2)/(A_1 + A_2).$$

4.3.7.2. Viscoelastic Case

For the case where the two materials comprising the composite rod are viscoelastic, we simply substitute the complex moduli, i.e.,

$$E^*_o = E'_o + iE''_o$$
$$= (E^*_1A_1 + E^*_2A_2)/(A_1 + A_2),$$

or, in another form

$$E^*_o = E'_o + iE''_o$$
$$= (E'_1A_1 + E'_2A_2)/(A_1 + A_2)$$
$$+ i(E''_1A_1 - E''_2A_2)/(A_1 + A_2).$$

Hence,

$$E'_o = (E'_1A_1 + E'_2A_2)/(A_1 + A_2)$$

and

$$E''_o = (E''_1A_1 + E''_2A_2)/(A_1 + A_2). \qquad (4.1)$$

4.3.7.3. Effective Loss Tangent

The effective loss tangent of the composite rod can be defined as

$$\tan \delta_o(L) = E''_o/E'_o$$

and

$$\tan\delta_o(L) = (E''_1A_1 + E''_2A_2)/(E'_1A_1 - E'_2A_2). \qquad (4.2)$$

In the foregoing equation, $\tan \delta_o(L)$ is the effective loss tangent of the composite rod to longitudinal vibrations and $E^*_1 = E'_1 + iE''_1$ and $E^*_2 = E'_2 + iE''_2$ are the complex modulus of the component materials.

4.3.7.4. Complex Unit Stiffness

The unit stiffness of an elastic rod in tension is given by

$$k = F/a = EA.$$

For the complex composite rod in question, we can define an effective dynamic complex longitudinal unit stiffness as

$$k^*_o = k'_o + ik''_o$$
$$= E^*_oA_o = E'_oA_o + jE''_oA_o.$$

Substituting from equation 4.1 and equating real and imaginary components we have

$$k'_o = E'_1A_1 + E'_2A_2 = k'_1 + k'_2$$

and

$$k''_o = E''_1A_1 + E''_2A_2 = k''_1 + k''_2.$$

Hence, we see from equation 4.2 that

$$\tan \delta_o(L) = (k_1'' + k_2'')/(k_1' + k_2') = k_o''/k_o'.$$

It is interesting to note that

$$k_o^*(L) = k_1^*(L) + k_2^*(L).$$

Thus, we see that the unit complex stiffnesses of the separate components of the composite system combine as complex vectors to yield the effective unit stiffness of the system shown on figure 4.9. The combining of complex stiffness of composite construction has important applications in towed arrays.

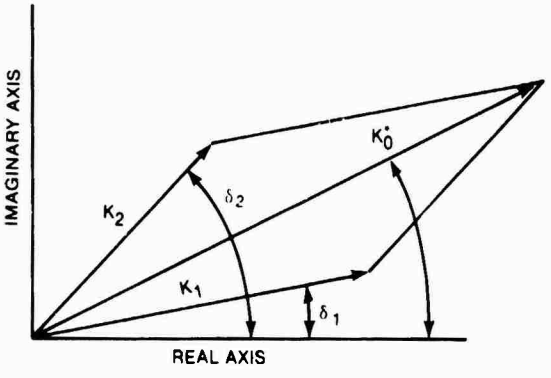

Figure 4.9. Vector Addition of Complex Unit Stiffness

4.3.8. WAVE PROPAGATION IN VISCOELASTIC MEDIA

4.3.8.1. Exact Solution

The characteristics of any system in relation to linear vibrations are generally described, with appropriate boundary values, by solving the wave equation, such that

$$\nabla^2\phi = (1/c^2)[(\partial^2\phi/\partial t^2) + \varkappa(\partial\phi/\partial t)],$$

where ϕ represents the deviation of a local value from the average and is the disturbance propagated. For example, ϕ may be the transverse displacement from equilibrium for a vibrating string, or it may be the excess pressure in an acoustic wave. In all cases some local property of the medium is perturbed and a force is created that restores the system to equilibrium. The factor c represents the velocity of propagation of the disturbance and $\varkappa$ is a dissipation term; c and $\varkappa$ then are the *propagation characteristics* of the medium and are directly related to the dynamic mechanical properties of the material.

Two solutions of the wave equation for a plane shear wave are

$$A_{x_1} = e^{-\varkappa_s t/2} f(x - c_s t)$$

and

$$A_{x_2} = e^{-\varkappa_s x/2c_s} f(x - c_s t).$$

The first equation represents a wave decaying exponentially with time and the second an exponential decay with distance. A progressive wave (of frequency $\omega/2\pi$) is then represented by

$$A_x = A_o e^{-i\omega(t - x/c_s)} e^{-\alpha_s x},$$

where α_s is the amplitude attenuation for the shear wave, $\alpha_s = \varkappa_s/2c_s$, and c_s is the propagation velocity. The two propagation constants can be combined into a complex characteristic

$$k_s^* = (\omega/c_s) - (i\alpha_s),$$

where k_s^* = the wave number (shear)

$$|k_s^*| = [(\omega^2/c_s^2) + (\alpha_s^2)]^{1/2}$$

and

$$\tan \delta_s = \alpha_s c_s/\omega = \alpha_s \lambda_s/2\pi,$$

from which equation 4.3 becomes

$$A_x = A_o e^{-i(\omega t - k_s^* x)}.$$

Now the propagation constants are directly related to the dynamic mechanical characteristics of the material as given by the complex shear modulus, i.e., $G^* = G' + iG''$ and $\tan \delta_s = G''/G'$, as described in the previous section. The exact relationships are

$$c_s = (G'/\rho)^{1/2}\{[2(1 + \tan^2\delta_s)] / [1 + (1 + \tan^2\delta_s)^{1/2}]\}^{1/2}$$

and

$$\alpha_s = (\omega/2) - (\rho/G')^{1/2} \tan\delta_s\{2[(1 + \tan^2\delta_s)^{1/2} - 1]/[\tan^2\delta_s(1 + \tan^2\delta_s)]\}^{1/2},$$

where ρ is the density of the medium.

4.3.8.2. Approximate Solution

For cases where $\tan\delta_s \ll 1$ (i.e., when losses are small) the expressions simplify to

$$c_s \approx (G'/\rho)^{1/2}$$

and

$$\alpha_s \approx (\omega/2)(\rho/G')^{1/2}(\tan\delta_s).$$

The exact relationship for velocity and attenuation can be written as

$$c_s \approx (G'/\rho)^{1/2}(C_c)$$

and

$$\alpha_s \approx (\omega/2)(\rho/G')^{1/2}(\tan\delta_s)(C_\alpha),$$

where C_c and C_α are correction terms given by

$$C_c = \{2(1 + \tan^2\delta_s)/[1 + (1 + \tan^2\delta_s)]^{1/2}\}^{1/2}$$

and

$$C_\alpha = \{2[(1 + \tan^2\delta_s)^{1/2} - 1]/\tan^2\delta_s(1 + \tan^2\delta_s)\}^{1/2}.$$

Values of C_c and C_α are given for various values of tan δ in table 4.5. As can be seen, appreciable errors in velocity and attenuation result for values of tan δ above 0.2 because small loss approximations are used. Since many plastics and elastomers have larger tan δ values, particularly those designed for high-damping properties, small loss approximations are generally unsuitable.

Although we have used only the shear wave and its complex shear modulus as an example, the foregoing relationships are true for other types of wave propagation, as long as the appropriate modulus is employed. The correction

Table 4.5. Velocity and Attenuation Correction Terms

Loss Tangent $\tan\delta$	Multiply Approx. Velocity by C_c	Multiply Approx. Attenuation by C_α
.10	1.004	.995
.15	1.008	.978
.20	1.015	.980
.25	1.023	.966
.30	1.033	.958
.35	1.044	.942
.40	1.057	.922
.45	1.071	.893
.50	1.086	.873
.55	1.103	.849
.60	1.119	.829
.65	1.119	.800
.70	1.160	.776
.75	1.178	.756
.80	1.199	.732
.85	1.220	.708
.90	1.243	.686
.95	1.264	.665
1.00	1.286	.643
1.05	1.309	.624
1.10	1.333	.603
1.15	1.357	.583
1.20	1.381	.565
1.25	1.404	.547
1.30	1.427	.531
1.35	1.451	.514
1.40	1.475	.498
1.45	1.499	.484
1.50	1.522	.469
1.55	1.545	.456
1.60	1.570	.442
1.65	1.593	.429
1.70	1.618	.415
1.75	1.641	.404
1.80	1.665	.393
1.85	1.689	.381
1.90	1.710	.371
1.95	1.734	.361
2.00	1.758	.352
2.05	1.780	.342
2.10	1.803	.333
2.15	1.826	.325
2.20	1.849	.317
2.25	1.872	.309
2.30	1.893	.301
2.35	1.916	.294
2.40	1.938	.286
2.45	1.959	.280
2.50	1.981	.273
3.00	2.191	.220

terms presented in table 4.5 are universally applicable.

4.3.8.3. Summary of Dynamic Mechanical Quantities and Propagation Constants

Table 4.6 presents terms commonly used in connection with shear wave propagation and mechanical vibration. The relationships between some of the characteristics are also included.

4.4. MOLECULAR STRUCTURE AND DYNAMIC MECHANICAL PROPERTIES

When considering the dynamic mechanical behavior of plastic materials, if only from the viewpoint of engineering applications, it is important to have some understanding of the molecular basis for typical variations of compliance (or modulus) with frequency and temperature. Such knowledge is important to the design engineer, for example, in relation to the inherent limitations of plastic materials and modifications available for particular applications.

4.4.1. MOLECULAR BONDING FORCE

The response of viscoelastic materials to stresses alternating with time are governed largely by the bonding forces and the detailed molecular structure. The forces between molecules listed in a decreasing order of strength are

1. hydrogen bonding,
2. dipole interaction, and
3. van der Waals forces.

The strongest force, hydrogen bonding, permits the development of strong materials such as nylon. When molecules possess permanent electric moments, i.e., *dipole interaction*, there is a strong electrostatic force between adjacent molecules. The high temperature characteristic of Kel-F, for example, is attributed to the highly polarized nature of the polytrifluorochlorethylene molecules.

The slightest bonding forces exist between molecules that have no permanent electric moments or are characterized by unsymmetrical geometric configurations, i.e., simple van der Waals forces. This force is about 1/2 to 1/3 as strong as the dipole force; it is directly proportional to the product of the molecular masses and inversely proportional to the sixth power of the distance between molecules. Although intermolecular forces in some polymers are relatively weak van der Waals forces, high crystallinities can result if the geometry of the individual chains is simple, as for polyethylene. In this case, the molecules are relatively closely arranged in a regular structure and provide a high strength material.

In addition to the forces listed above, there also exists a strong valence force between atomic constituents. This contributes to the overall mechanical properties of the material, particularly at low temperatures or high frequencies.

Generally, the response of a material to mechanical stresses is influenced by

1. viscous responses caused by slippage of chains past their neighbors,
2. elastic responses caused by deformation of valence bonds,
3. retarded elastic effects caused by cohesive forces between molecules, and
4. retarded elastic effects caused by mechanical uncoiling or disentanglement of the molecules.

4.4.2. CHEMICAL STRUCTURE OF PLASTICS

Plastics, rubbers, and fibers are characterized by extremely large molecules, thousands of times the size of those in ordinary substances. The large molecules usually consist of one or two structural units, i.e., *mers*, repeated throughout the entire molecule. The structural units of plastics may be connected in a number of ways that create straight chains, branched chains, or 3-dimensional (network) structures, depending on the chemical properties of the units involved. Thus, ordinary polyethylene consists of a number of molecular units formed by hydrogen and carbon atoms of the form

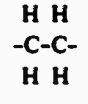

Table 4.6. Shear Wave Propagation and Mechanical Vibration Terms

Name	Usual Symbol	Definition	Relation to Other Characteristics
Shear Velocity	c_S	Velocity of Propagation of Transverse Disturbance Through a Medium	$c_S = (G'/\rho)^{1/2} C_C$
Shear Wave Attenuation	α_S	Logarithmic Decrement of Amplitude of Shear Wave per Unit Length Through a Medium	$\alpha_S = \omega/2(\rho/G^*)^{1/2} \tan\delta_S C_\alpha$
Mechanical Loss Tangent	$\tan\delta_S$	Tangent of the Phase Angle Between Strain and Stress	$\tan\delta_S = \alpha_S c_S/\omega = \alpha_S\lambda/2\pi$ $\tan\delta_S = G''/G' = J''/J'$
Velocity Correction Term for Visco-Elastic Media	C_C	Term by Which Elastic (or Small Loss Approximation) Velocity Must be Multiplied to Give True Velocity in a Viscoelastic Medium	$C_C = \left[\frac{2(1+\tan^2\delta_S)}{1+(1+\tan^2\delta_S)^{1/2}}\right]$
Attenuation Correction Term for Viscoelastic Media	C_α	Term by Which Small Loss Approximation for Attenuation Must be Multiplied to Give True Attenuation in a Viscoelastic Medium	$C_\alpha = 1/\tan\delta_S\left[\frac{2(1+\tan^2\delta_S)^{1/2}-1}{1+\tan^2\delta_S}\right]^{1/2}$
Absolute Shear Modulus	G	Magnitude of Shear Stress Divided by Magnitude of Shear Strain	$G = 1/J$
Complex Shear Modulus	G^*	$G^* = G' + iG''$	$G^* = 1/J^*$
Storage Modulus	G'	Component of Shear Stress in Phase with the Strain Divided by the Strain	
Loss Modulus	G''	Component of Shear Stress 90° Out of Phase with the Strain Divided by the Strain	$G'' = G' \tan\delta_S$ $G'' = \omega\eta'$
Absolute Shear Compliance	J	Magnitude of Shear Strain Divided by Magnitude of Shear Stress	$J = 1/G$
Complex Shear Compliance	J^*	$J^* = J' - iJ''$	$J^* = 1/G^*$
Storage Compliance	J'	Component of Shear Strain in Phase with the Stress Divided by the Stress	
Loss Compliance	J''	Component of Shear Strain 90° Out of Phase with the Stress Divided by the Stress	$J'' = J' \tan\delta_S$
Shear Viscosity	η'	Shear Stress Divided by the Time Rate of Shear Strain in Phase with the Stress	G''/ω
Angular Velocity	ω	2π x Frequency of the Propagated Wave or the Vibrating Sinusoidal Stress	$\omega = 2\pi f = 2\pi c_s/\lambda$
Wavelength	λ		$\lambda = c/f$

where branching occurs along the main stem, or chain, of the plastic molecule, such that

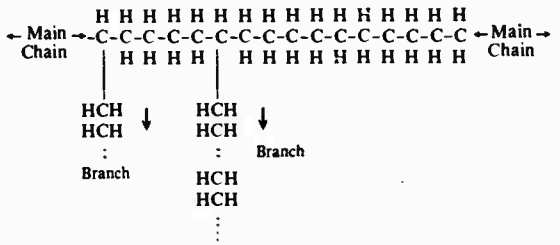

On the other hand, *linear polyethylene* has practically no side branches on the main chain and has mechanical properties different from those of the branched polyethylene.

The formation of a large chain molecule from its basic mer is termed *polymerization*; the resulting material is a polymer. Synthetic polymers can be classified, as addition or condensation polymers, according to the type of chemical reaction. One of the most common types of chain reactions is the free radical polymerization (addition) of vinyl monomers such as styrene, ethylene, vinyl acetate, vinyl chloride, and isobutylene. Such substances provide polymers that have a carbon-hydrogen chain as a backbone with some different element (or molecular group) substituted for a hydrogen on every other carbon atom. For example, for vinyl chloride,

$$\begin{matrix} H & H \\ C & = & C \\ H & & CL \end{matrix}$$

polyvinyl chloride (unplasticized Geon or Koroseal) of the form

$$\begin{matrix} H & H & H & H & H & H \\ -C & -C & -C & -C & -C & -C & - \\ H & CL & H & CL & H & CL \end{matrix}$$

is created. This repeating structure may be represented as

$$\left[\begin{matrix} H & H \\ -C & -C- \\ H & CL \end{matrix}\right]_X$$

where X, the degree of polymerization is the number of vinyl chloride units in a chain. A polymer has the same chemical composition as a monomer. Types of vinyl monomers have different elements, for example, fluorine substituted for hydrogen on the main chain or a group of atoms, such as the phenyl radical, substituted for one or more hydrogens. A summary of some of the many polymers is presented in table 4.7.

Condensation polymerization is different from the addition type because it involves the reaction of a group on one molecule with a different group on another to create a third molecule. For example, the condensation of hexamethylene diamine yields

$$\begin{matrix} H & & H \\ N-(CH_2)_6 & -N \\ H & & H \end{matrix}$$

with adipic acid $HOOC-(CH_2)_4-COOH$ under certain conditions produces water and polyhexamethylene adipamide (nylon), i.e.,

Table 4.7. Selected Addition Polymers

Monomer		Polymer	
Name	Formula	Name	Trade Name
Ethylene	$\begin{matrix} H & H \\ C=C \\ H & H \end{matrix}$	polyethylene	Polyethylene or Polythene, Alathon
Vinyl Chloride	$\begin{matrix} H & CL \\ C=C \\ H & H \end{matrix}$	Polyvinylchloride	Unplasticized Koreoseal or Geon
Vinylidene Chloride	$\begin{matrix} H & CL \\ C=C \\ H & CL \end{matrix}$	Polyvinylidene Chloride	Saran
Trifluoromono-Chlorethylene	$\begin{matrix} F & F \\ C=C \\ F & CL \end{matrix}$	Polytrifluoromono-Chloroethylene	Kel-F
Tetrafluoroethylene	$\begin{matrix} F & F \\ C=C \\ F & F \end{matrix}$	Polytetrafluoro-Ethylene	Teflon
Methacrylic Ester	$\begin{matrix} H & CH_3 \\ C=C \\ H & COOCH_3 \end{matrix}$	Polymethyl Methacrylate	Lucite
Styrene	$\begin{matrix} H & H \\ C=C \\ H & C_6H_5 \end{matrix}$	Polystyrene	Styron

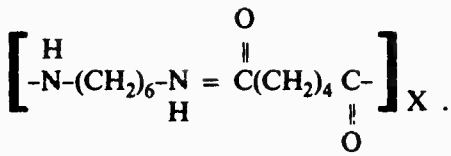

Other condensation polymers are the silicones (Silastic), pheonlic resins (Bakelite, Resinax, and so on), and polyethylene tetrasulfide (Thiokol).

4.4.3. MOLECULAR WEIGHT DISTRIBUTIONS

Most plastic materials are polydisperse, i.e., the number of monomer units in the molecules of a given substance is not the same, but varies over a wide range. Therefore, some of the molecules of a given amount of polyvinyl chloride may consist of only 5 or 6 monomers joined together; others may consist of 200 or 1000, and so on. The molecular weight of a polymer is, thus, an average that depends upon the experimental method used to determine it. Two of the most important molecular weights are the number average, M_n, and weight average, M_w.

$$M_n = (n_1M_1 + n_2M_2 + n_3M_3 + \ldots) /(n_1 + n_2 + n_3) = w_t/n_t$$

and

$$M_w = (w_1M_1 + w_2M_2 + w_3M_3 + \ldots) /(w_1 + w_2 + w_3 + \ldots),$$

where

w_t = total w;
n_t = total n;
n_1, n_2, n_3 = number of molecules of molecular weights M_1, M_2, M_3, respectively; and
w_1, w_2, w_3 = weight of all molecules of molecular weights M_1, M_2, M_3, respectively.

For a substance composed of molecules of identical size, $M_n = M_w$. For a typical high polymer, in which there is a wide range in sizes, however, M_w will be larger than M_n and the ratio M_w/M_n will increase as the disparity in size becomes greater. The number average, M_n, emphasizes small molecules and the weight average emphasizes the relative importance of large molecules. Measurements of osmotic pressure or freezing point depression give M_n because the results are affected only by the total number of molecules regardless of shape, size, or flexibility.

Conversely, light scattering or diffusion measurements yield M_w, under certain conditions, because the size and shape of the molecules becomes important. The actual distribution of molecule size has a significant effect on physical and mechanical behavior that is more important than molecular weight averages alone. As previously noted, however, the ratio is a measure of the relative narrowness or broadness of the size distribution and, therefore, of importance in relation to mechanical properties.

4.4.4. PHYSICAL STRUCTURE OF PLASTICS

As previously mentioned, the chemical nature and molecular weight of plastics affect mechanical properties. The structure has an even greater effect. Consider a polymer molecule composed of a string of mers joined end to end. Such a string will be flexible if adjacent atoms can rotate freely in relation to one another. This *free* rotation characterizes the carbon-carbon single bond and produces the flexible carbon chain of more than three atoms shown figure 4.10. Thus, although the shape of an ordinary small molecule is fixed, in so far as its relative position is concerned, polymer molecules may have a large number of shapes or configurations because of their extreme flexibility. If the carbon-carbon rotation were completely free, a long chain would be completely flexible and could assume any shape. Forces between atoms along the chain result in some restriction of the idealized free rotation shown in figure 4.10. Therefore, instead of an infinite number of possible shapes, a large but discrete number of configurations is possible for an isolated long chain molecule. Actually, of course, the different molecules of a plastic material impose external forces on one another, such that the possible configuration is further restricted by interaction between segments of neighboring chains.

If the molecular chains of a plastic are arranged in a random fashion, as shown in

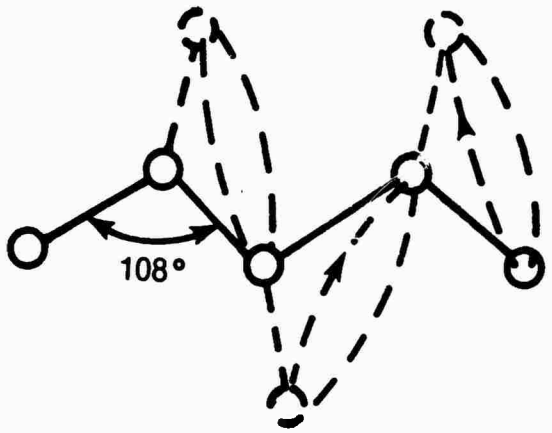

Figure 4.10. Flexibility of Carbon Chains Caused by Rotation Around Single Bonds

figure 4.11, the material is said to be amorphous. If the chains are arranged in some definite pattern, such as that illustrated in figure 4.12, the material is said to be crystalline. The distinction between an amorphous and a crystalline polymer is not always sharp and, in many cases, both occur. One portion of a single molecule may be in an ordered region and another randomly distributed (see figure 4.13) because the crystallite size is less than the molecular length.

A high polymer is probably never completely crystalline, consisting instead of regions of high order separated by amorphous regions (figure 4.13). In certain polymers, however (e.g., linear polyethylene), the crystallinity can be as high as 95 percent.

Generally, crystallinity produces a hard material that remains so until high temperatures melt the crystallites. Another factor that affects mechanical properties is the orientation of the crystalline regions. The crystallinity of a material may be enhanced by the stretching technique used for natural rubber,which is amorphous at room temperature but can be crystallized by an elongation of hundreds of percent. If crystallinity is produced by elongation, rubber crystallites will be oriented in the direction of applied stress, if it is produced by cooling (below 0° C) the distribution will be random.

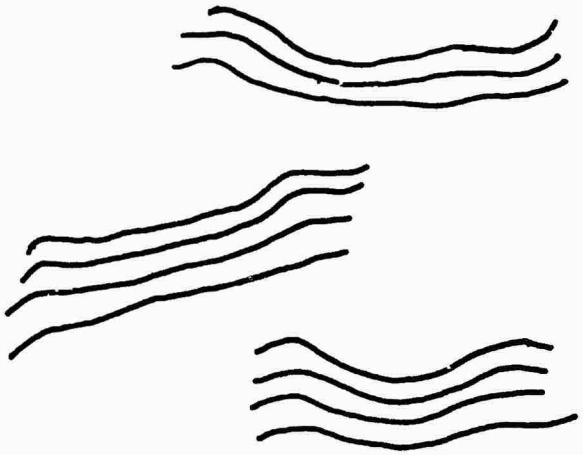

Figure 4.12. Ordered (Crystalline) Chain Configurations

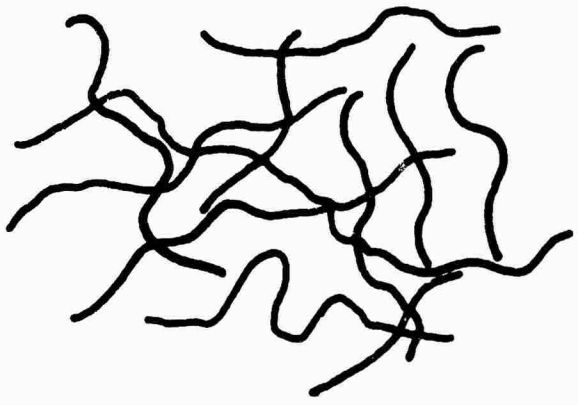

Figure 4.11. Random (Amorphous) Chain Configurations

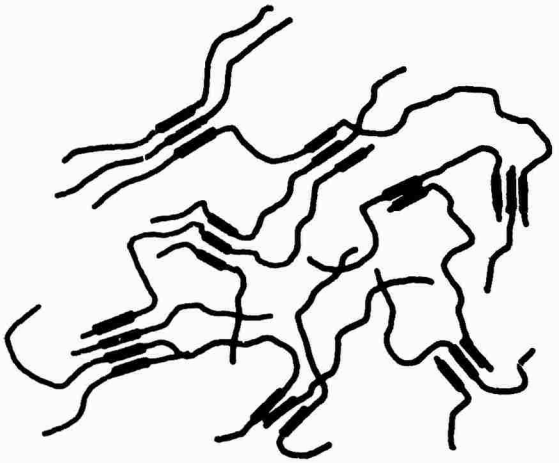

Figure 4.13. Unoriented Crystalline Polymer

A polymer structure is one in which various amorphous chains are joined at intervals along their lengths to form a three dimensional network structure (see figure 4.14). This *cross-linking* produces a more rigid material.

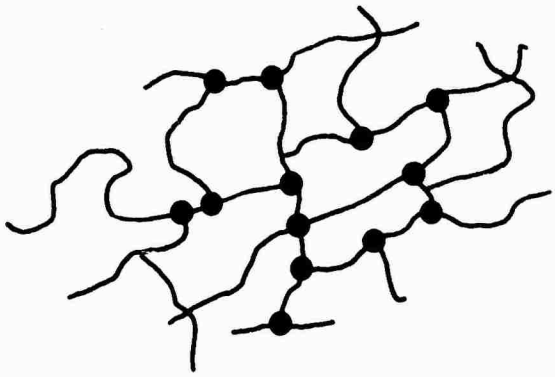

Figure 4.14. Cross-Linked (Network) Polymer

4.4.5. FREQUENCY DEPENDENCE

The dynamic properties of a plastic material vary with frequency. The following discussion uses the complex shear compliance characteristic, $J^* = J' - iJ''$, to describe dynamic behavior.

A high low-frequency storage compliance, J', will decrease slightly as the frequency is increased until a certain range, the *dispersion region*, is reached. It then decreases rapidly to a lower limiting value that remains constant with increasing frequency. The loss compliance, J'', decreases from a high value at low frequencies to a very low value at intermediate frequencies. It increases until the maximum region where the storage compliance begins to drop rapidly, then decreases at higher frequencies. The variation of compliance with frequency is shown in figure 4.15 and the corresponding modulus variation is illustrated in figure 4.16. This type of mechanical characteristic variation has been extensively investigated for linear amorphous polymers (these will be discussed in greater detail later as Type I plastics). The different behavior recently discovered for crystalline polymers (designated Type II) is illustrated in figure 4.17.

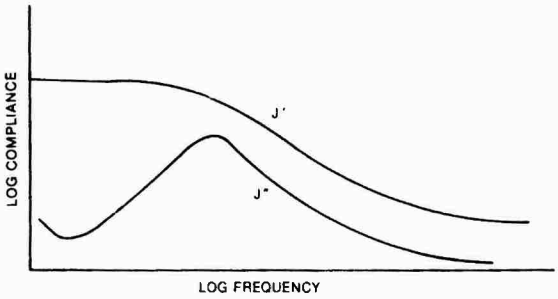

Figure 4.15. Dynamic Compliance Variation with Frequency for Type I Plastic

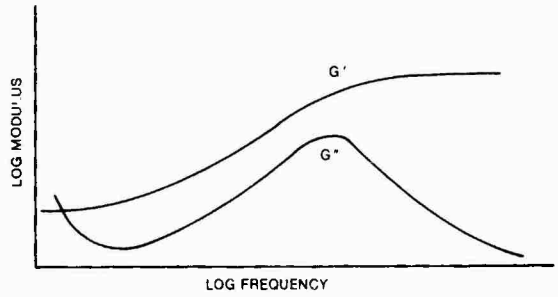

Figure 4.16. Dynamic Moduius Variation with Frequency for Type I Plastic

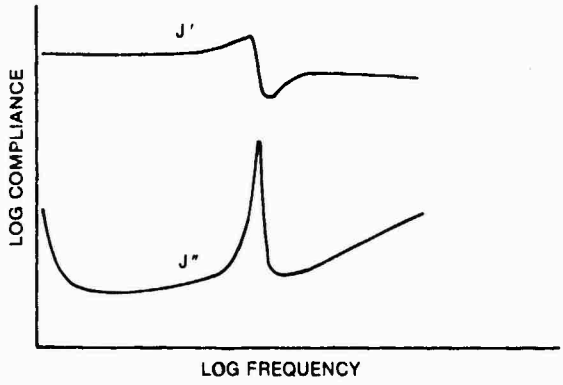

Figure 4.17. Dynamic Compliance Variation with Frequency for Type II Plastic

4.4.5.1. Relaxation Dispersion

A mechanical model approximating the behavior of a Type I plastic can be constructed using the four ideal units shown in figure 4.18,

where a spring of high modulus G_o, a dashpot of viscosity η_o, and a spring of modulus G retarded by a dashpot of viscosity η, are connected in series. The spring of modulus G_o represents an instantaneous and completely elastic response of the plastic, whereas the spring of modulus G does not respond instantly because it is retarded by the dashpot of viscosity η. The ratio η/G is the retardation time, τ. The dashpot of viscosity η_o corresponds to a possible permanent deformation, or flow of the plastic, under stress. The storage and loss compliances of the mechanical model when it is subjected to an alternating sinusoidal stress are, respectively,

$$J' = 1/G_o + (1/G)(1/1 + \omega^2\tau^2)$$

and

$$J'' = 1/\omega\eta_o + (1/G)\omega\tau/(1 + \omega^2\tau^2),$$

where $\tau = \eta/G$ and $\omega = 2\pi$ multiplied by the frequency of the applied stress.

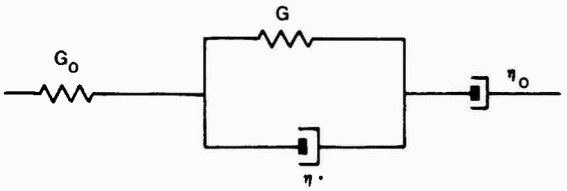

Figure 4.18. Mechanical Model for Dynamic Behavior of Type I Plastic

An examination of the above expressions reveals that they result in variations of J′ and J′′ that qualitativley resemble those actually measured (see figure 4.15). The chief difference is that this 4-parameter model predicts a much sharper transition from the low frequency value of $J' = 1/G_o + 1/G$ to the high frequency value of $1/G_o$ than that observed. The predicted maxima in J′′, based upon the model, is also higher than the observed. If we consider a model consisting of a number of retarded springs of varying retardation times in series as shown in figure 4.19, however, the actual frequency dependence of the complex compliance (or modulus) of a Type I plastic can be very closely approximated.

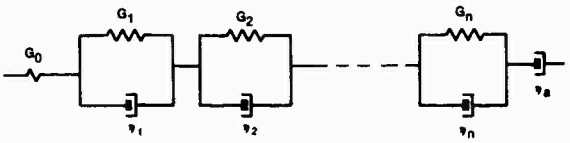

Figure 4.19. Generalized Mechanical Model for Dynamic Behavior of Type I Plastic

The storage and loss compliances of the generalized model in figure 4.19 are, respectively,

$$J' = 1/G_o + \sum_{i=1}^{n} (1/G_i)(1 + \omega^2\tau_i^2)$$

and

$$J'' = (1/\omega\eta_o) + \sum_{i=1}^{n} (1/G_i)$$
$$[\omega\tau_i/(1 + \omega^2\tau_i^2)].$$

4.4.5.2. Resonance Dispersion

The behavior noted in figure 4.17 for a Type II plastic under certain static loading conditions is qualitatively the same as that predicted for a mechanical model consisting of a retarded spring and a mass in series (see figure 4.20). When subjected to a sinusoidal stress of frequency, $f = \omega/2\pi$, the storage and loss compliances for the model in figure 4.20 are, respectively,

$$J' = (1/G_o) + (1/G)[(1 - \omega^2/\omega_n^2)]$$
$$/[(1 - \omega^2/\omega_n^2)^2 + \omega\tau^2]$$

and

$$J'' = (1/\omega\eta_o) + (1/G)\omega\tau/[(1 - \omega^2/\omega_n^2)^2$$
$$+ \omega^2\tau^2],$$

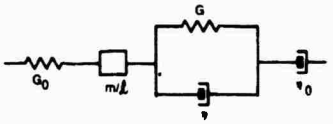

Figure 4.20. Mechanical Model for Resonance Dispersion of Type II Plastic

where $\omega_n = (k/m)^{1/2} = [G/(m/\ell)]^{1/2}$ is the resonant or natural frequency of the system $k = G\ell$ (where ℓ = the length of the spring) and m/ℓ can be considered the mass per unit length of the retarded spring. Also, $\tau = \eta/G$ is the retardation time and G_o and η_o have the same significance described for the model in figure 4.18.

The model predicts a maximum followed by a minimum in the J′ versus ω curve and that J″ will be a maximum in the vicinity of $\omega = \omega_n$. Such resonances have been attributed to the presence of momentum wave modes in crystalline lattice segments of micron (10^{-4}) end lengths. In particular, the frequency f_q of any such momentum-wave mode is given by

$$f_q = (h/8ms^2)q^2,$$

where

q = 1,2,3.....,
h = Planck's constant,
m = atomic mass (grams), and
s = length of regularly spaced lattice formed by the masses.

Resonance type dispersions have been observed in single inorganic crystals (e.g. sodium chloride, quartz, germanium), polycrystalline metals (e.g. lead, aluminum, plutonium), organic crystals (e.g. vinyl stearate, ethyl stearate, paraffin), and crystalline polymers (e.g. polyethylene, polytetrafluoroethylene, stretched natural rubber).

4.4.6. TEMPERATURE DEPENDENCE

Temperature dependent changes occurring in high polymeric materials include crystal melting, first-order crystalline, and first- and second-order glass transitions. The mechanical properties of the polymer are profoundly affected by such transitions. The glass transition is the primary one and is a characteristic of all elastomers. A polymer at a temperature above the glass transition temperature is a viscous liquid if the molecular weight is relatively low. If the molecular weight is high, or the molecules lightly crosslinked, the material behaves as a rubber. Below the glass-transition temperature, the elastomer behaves as a rigid plastic; the main difference between an elastomer and a rigid plastic depends on whether the glass transition temperature is above or below room temperature.

4.4.6.1. Transitions in Amorphous Polymers

Figure 4.21 shows the qualitative effects of various transitions on the elastic modulus for an amorphous, linear (uncross-linked) polymer. If the temperature is sufficiently high, the polymer chains slip past one another and the material flows as a viscous liquid. At lower temperatures, the thermal vibrational energy is sufficiently reduced so that the long chain molecules assume coiled configurations. When a stress is applied, the uncoiling of the molecules create large deformations in the direction of the stress and, upon release of the stress, the molecules coil again, which creates retraction. This process is the elementary mechanism underlying the highly elastic deformation in the *rubbery* region. A portion of this visco-elastic deformation energy is dissipated as heat and a portion is stored as the configurational free energy of the stretched molecule. The dynamic behavior of lightly cross-linked rubbers such as natural rubber gum-stock are similar except that some of the elastic energy is stored in the cross-linked bonds.

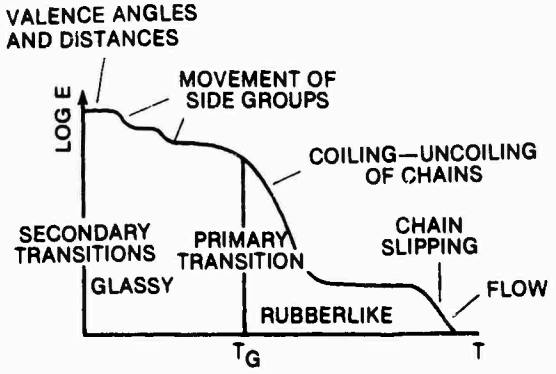

Figure 4.21. Modulus Variation with Temperature for Amorphous Uncross-Linked Polymer

If the temperature is further lowered (see figure 4.21) the glass transition temperature, i.e., the zone between glass- and rubber-like consistency, is reached. It is in this zone that the

dependence of viscoelastic properties is most important. As the polymer cools, the free volume and thermal energy become small and the structural units are unable to overcome the potential energy barriers for any mode of motion other than vibrational. Thus, the polymer segments and atomic groups are *frozen in*, as for an ideal solid, and the polymer is said to be in the *glassy* state.

4.4.6.2. Crystalline Polymer Transitions

As shown in figure 4.22, crystalline polymers are characterized by a modulus-temperature dependence different from that for amorphous polymers. The decrease in modulus is much smaller at low temperatures. The rubbery region between the glass transition temperature, T_G, and the melting temperatures of the crystallites, T_C, is much narrower and the polymer behaves as a tough leathery material instead of rubber. At the temperature where the crystallites melt and the strong intermolecular forces cease to exist, molecular slip occurs and the polymer abruptly changes into the flow region.

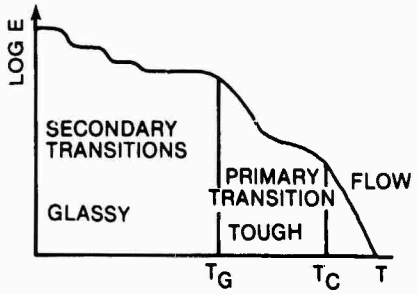

Figure 4.22. Modulus Variation with Temperature for Crystalline Polymer

4.4.6.3. Glass Transition Temperature

Figure 4.23 shows the measured temperature dependence of dynamic properties for an amorphous, uncross-linked polymer (in this case, a copolymer of styrene and butadiene) at 1Hz. The elastic component of the shear modulus, G′, of nearly all polymers in the glassy state are approximately 10^{10} dynes/cm². This

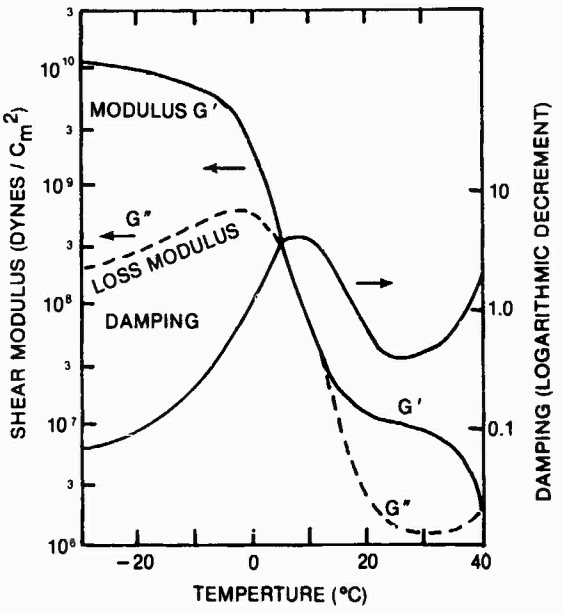

Figure 4.23. Dynamic Mechanical Behavior of Uncross-Linked Amorphous Polymer

value decreases slowly as temperature increases until the glass transition temperature is reached. Then, the modulus decreases rapidly by a factor of approximately 1000 with a temperature increase of only a few degrees. At temperatures above the transition region (i.e., in the rubbery region) the elastic component of the shear modulus is again relatively independent of temperature and has a value of approximately 10^7 dynes/cm².

The loss modulus, G″, is generally lower than the elastic modulus in the glassy region and increases as temperature increases. It peaks just before the transition region is reached and decreases rapidly through the transition region. The loss tangent, G″/G′, characteristically goes through a peak in the transition region and the temperature at which the peak occurs is usually taken to be the glass transition temperature ($T_g \approx 10^0$ C in this case) at low frequencies.

The temperature at which damping is a maximum depends on the frequency of measurement. For most polymers, an increase in frequency of a factor of 10 increases the temperature of maximum damping by approximately 7° C. Table 4.8 lists the glass transition temperatures at low frequencies (≈ 1 Hz) for selected polymers.

Table 4.8. Comparison of Polymers at Temperature Corresponding to Mid-Point of Glass Transition at Frequencies of 0.1 to 3 Cycles/sec (°C)

Polymer	Temperature of Mid-Transition	Frequency of Measurement
Natural Rubber	-50	1.2
Butyl Rubber	-50	1.1
Polyisobutylene	-48	1.0
Poly n-butyl acrylate	-34	1.25
Polyvinyl n-butyl ether	-32	0.8
Polyvinyl propyl ether	-27	1.1
Polyvinyl ethyl ether	-17	1.1
Polyvinyl methyl ether	-10	2.7
Polyethyl aerylate	- 5	1.6
Polyvinyl i-butyl ether	- 1	1.2
Polyvinyl propionate	12	1.5
Polymethyl acrylate	25	1.2
Polyvinyl acetate	33	1.9
Polyvinyl tert-butyl ether	83	1.7
Polyvinyl chloride	90	0.7
Polystyrene	116	0.9
Polymethyl methacrylate	120	0.12

4.4.6.4. Vulcanization

The effect of vulcanization (crosslinking) of natural rubber on the elastic shear modulus at 1 Hz is shown in figure 4.24. The glass transition temperature, T_G, is -50° C and the drop in the modulus is precipitous as this temperature is approached from the glassy state. For samples I and II, i.e., no vulcanization(0 percent sulphur) and negligible vulcanization (0.1 percent sulphur), respectively, the rubbery state above T_G is very narrow and the materials reach the flow state below 0° C. If 1.5 to 5 percent sulphur is added, enough cross-linking is formed in the vulcanization to extend the rubbery plateau to ≈ 160° C. The term *rubber-like* applied to other elastomers in the *rubbery zone* derives from the characteristic behavior of vulcanized (cross-linked) natural rubber.

In thermo-setting materials, such as phenolformaldehyde resins (hard rubber), the degree of cross-linking is such that there is no indication of glass transition below the decomposition temperature of the polymer.

4.3.6.5. Plasticizers

When plasticizers are incorporated into an elastomer, the glass transition and maximum

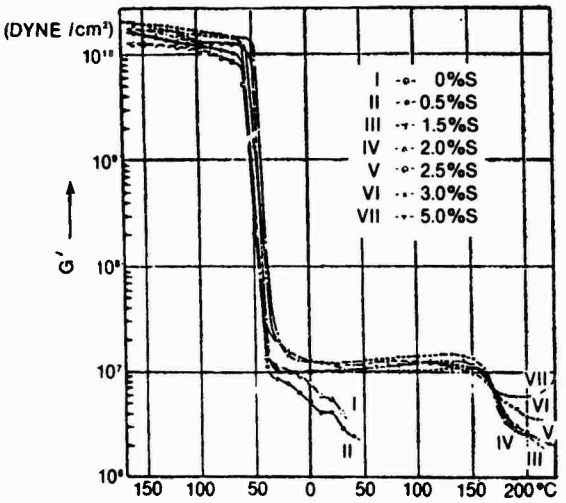

Figure 4.24. Complex Shear Modulus Variation with Temperature at ≈ 1 Hz

damping temperatures are lowered. The amount of the decrease depends upon the glass transition temperature of the material and the amount of plasticizer used. An effective plasticizer must be soluble in the polymer and, generally, a broadened transition zone should result. Figure 4.25 shows the effect of various plasticizers on polyvinyl chloride.

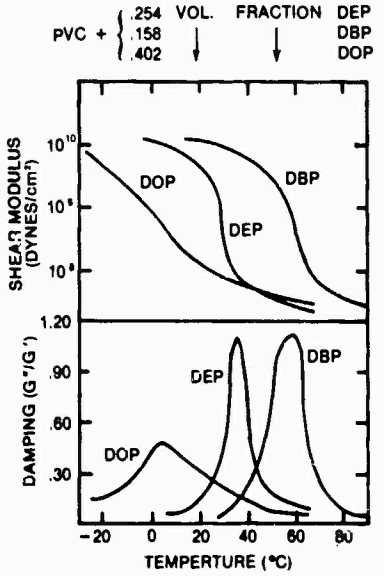

Figure 4.25. Dynamic Mechanical Behavior of Plasticized Polyvinal Chloride

ANNOTATED BIBLIOGRAPHY

Alfrey, T., Jr., Mechanical Behavior of High Polymers, *Interscience*, New York, 1948.

An early, useful account of the mechanical behavior of high polymers.

Cook, E. J., J. A. Lee, E. R. Fitzgerald, J. W. Fitzgerald, *Dynamic Mechanical Properties of Materials for Noise and Vibration Control,* Chesapeake Instrument Report, ONR Contract 2678(00), 1 January 1960.

Cook, E. J., J. A. Lee, E. R. Fitzgerald, *Dynamic Mechanical Properties of Materials for Noise and Vibration Control,* Chesapeake Instrument Report, vols. 1 and 2, ONR Contract 2678(00), 1 July 1962.

Ferry, J. D., *Viscoelastic Properties of Polymers,* Wiley, New York, 1961.

A careful and complete account of viscoelasticity, written by an authority.

Fitzgerald, E.R., *Particle Waves and Deformations in Crystalline Solids,* Wiley, New York, 1966.

The author, a student of Ferry, establishes a quantum mechanical basis for non-elastic resonances and demonstrates their applications.

Fitzgerald, E. R., "Dynamic Mechanical Properties of Stretched Natural Rubber," *Journal of the Acoustical Society of America,* vol. 33, no. 10, pp. 1305-1313, October 1961.

Fitzgerald, E. R. and J. D. Ferry, "Method for Determining the Dynamic Mechanical Behavior of Gels and Solids at Audiofrequencies, Comparison of Mechanical and Electrical Properties," *Journal of Colloid Science,* vol. 8, pp. 1-34, 1953.

Fitzgerald, E. R., "Mechanical Resonance Dispersion in Single Crystals," *Physical Review,* vol. 112, no. 4, pp. 1063-1075, 15 November 1958.

Fitzgerald, E. R., "Crystalline Transitions and Mechanical Resonance Dispersion in Vinyl and Ethyl Stearate," *Journal of Chemical Physics,* vol. 32, no. 3, pp. 771-786, March 1960.

Fitzgerald, E. R. and M. T. Watson, "Dynamic Mechanical Properties of Polyethylene from 25° to 150° C," *Journal of the Acoustical Society of America,* vol. 32, no. 5, pp. 584-593, May 1960.

Fitzgerald, E. R., J. W. Fitzgerald, A. E. Woodward, *Dynamic Mechanical Properties of Plastic Materials,* Cheasapeake Instrument Report, BuShips Contract 72108, 1 June 1957.

Hueter, T. F. and R. H. Bolt, *Sonics,* Wiley, New York, 1955.

A good reference for experimental methods of measuring dynamic mechanical properties.

McPherson, A. T. and A. Klemin, *Engineering Uses of Rubber,* Reinhold, New York, 1956.

A practical reference on the engineering uses of rubber.

Nielson, L. E., *Mechanical Properties of Polymers,* Reinhold, New York, 1962.

An excellent companion to Ferry's book; tends more toward the engineering aspects.

Snowden, J. C., *Vibration and Shock in Damped Mechanical Systems*, Wiley, New York, 1968.

An extensive account of the effects of damping on vibrating systems, using complex mechanical impedance methods.

Principles of Sonar Installation

CHAPTER V
SHIPBOARD SONAR SYSTEMS

CHAPTER V
SHIPBOARD SONAR SYSTEMS

5.0. INTRODUCTION

One of the first submarine acoustic detection systems is described by ADM C.A. Lockwood in *Down to the Sea in Ships*. This World War I technique required the search vessel to stop dead-in-the water before putting a hydrophone over the side. Prior to WW II, the passive capability was improved by the development of ASDIC, an active sonar that was further developed by the British and U.S. Navies. Active and passive sonars were developed for submarine applications during the same period.

Early sonar systems consisted of small rotatable sound heads operating in the 24 kHz range. Because a wavelength at that frequency is about 2 in., reasonably good directivity could be obtained using 1- to 2-ft transducer arrays. Sufficient fire control information could be obtained to target torpedoes at short ranges.

Post-WW II developments proved the advantages of submarines as ASW platforms. They are quiet, avoid the seaway motions of surface ships, and can change depth for best detection capability. A less tangible advantage is that a submarine crew *thinks submarine* and, thus, better understands *the game*.

Several *killer* submarines, featuring relatively large bow arrays, were built during the 1950s. During the same period, the development of nuclear powered submarines greatly increased the time the ships could remain submerged. Such advances improved submarine ASW capabilities.

Surface ships were fitted with variable depth sonars so that active sonar sensors could be lowered below the surface layer while underway and, thus, avoid the shadow zone effect surface sonars are subject to (see Section 1.3.7). They were also fitted with more powerful bow arrays and a quieting program was pursued. Long, linear towed arrays were developed for surface ships and submarines during the 1960s. Generally, emphasis in anti-submarine warfare (ASW) sonar systems has been to develop quieter platforms, lower self-noise, increased aperture size, and, when possible, towed sensors that avoid own ship noise and/or operate below the surface layer.

The most important requirements for ASW sonar applications (see Section 1.6.1.) are to reduce own ship noise, maximize detection capability, and reduce radiated noise. As a result, sonar system requirements increasingly affect ship design and great efforts are made to quiet machinery and other noise sources (see Section 2.1.). Acoustic projectors and sensors have been developed from the basic sound head into large, complex, hull-mounted, electrically steered arrays that influence the speed, size, personnel complement, and other ship design characteristics. Also, since operational usefulness depends heavily on sonar system performance for most U.S. Navy ASW vessels, the system may be the *raison d'etre* for a ship and determine its overall value.

A recent study showed that the combat system onboard a submarine, of which the sonar system was the heaviest, accounted for approximately 40 percent of the total displacement. Also, in addition to the main detection and fire control sonar system, most ships are equipped with auxiliary acoustic devices that serve many other functions.

Figure 5.1a shows surface ship sonar functions and figure 5.1b shows submarine sonar

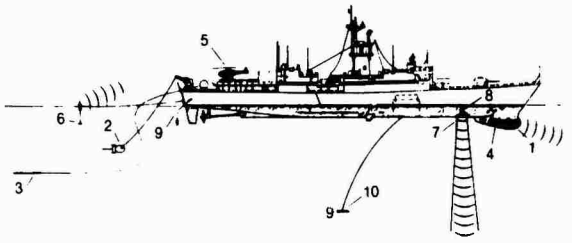

Figure 5.1a. Surface Ship

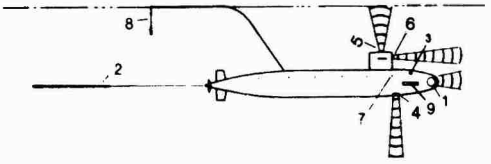

Figure 5.1b. Submarine

Figure 5.1. Surface Ship and Submarine Sonar System Functions

functions. They show more functions than a single ship could possess in order to illustrate the different types of sonar systems and their uses. Systems employed by surface ships are the

1. bow fire-control and detection array,
2. variable depth fire control and detection system,
3. towed detection array,
4. communication array,
5. helicopter-dipping sonar,
6. deployed sonobuoys,
7. depth sounder,
8. monitoring hydrophones,
9. XBT launcher, and
10. bottom search system.

Systems employed by submarines are the

1. bow fire-control and detection array,
2. towed detection array,
3. communication array,
4. depth sounder,
5. surface sounder,
6. under-ice navigation system,
7. monitoring hydrophones,
8. SSXBT launcher, and
9. conformal array.

5.1. SURFACE SHIP SONAR SYSTEMS

The bow array on surface ships is usually the active search device (see figure 5.1a) and generally provides wide azimuth coverage; only a small angle on the aft bearing is baffled against machinery and propeller noise. It is of sufficient vertical height to form depression/elevation (D/E) beams so that energy can be transmitted and received from vertical angles.

The array operates at frequencies that are high enough so there is a sufficiently large multiple of the wave-length to provide narrow beams for fire control. (The relationship between size and beamwidth is discussed in Section 1.9.) The operational advantage of the active sonar is that bearing and range can be determined from the echo received. Also, the Doppler effect, i.e., the frequency change caused by target motion, can also be detected. Such information defines the radial component of the target's motion and, combined with bearing and range data, yields course and speed estimations.

The surface ship bow array can also be used in the passive mode. However, the transducers are used to transmit as well as receive and their response characteristics over a wide band are non-linear because they must be tuned at or near the operating frequency for the transmission mode.

The array is located in the bow because it is the portion of the ship that is subject to the least self-noise. While acoustically desirable, the position is exposed to physical damage from debris, minor collisions, and the lowering and raising of the anchor. Hydrodynamically, the location is also a trade-off. That is, bulbous bows designed to match the maximum speed of the ship and reduce wave resistance may not be as large as the sonar designer requires.

The bow location also alleviates the ***bubble sweep-down*** problem. The sea surface contains bubbles created by white-caps, large waves, marine biota, and the wake of other ships. In addition, the ship's entrance and the bow wave create bubbles that sweep along the hull. Such bubbles lower the impedance of the water,

scatter energy, and, therefore, interfere with the transmission and reception of acoustic energy. Transducers located low and forward of the sweep-down area minimize this problem.

It is obvious that the size and shape of the bow dome influences ship motion. It may not be as obvious that ship motion influences sonar system performance, but it does. The system must be configured to compensate for roll and pitch angles and is subject to reception and transmitting problems when excessive pitch causes the bow to emerge from the water.

In many areas of the world, during certain seasons and particular weather conditions, variable depth sonar is employed by surface ships because the upper portion of the sea, down to as much as a few hundred feet, may be isothermal or have an inversion (see figure 1.9). That is, because of the increase in sound speed with depth, sounds originating in the layer either go down at steep angles or become trapped in the layer, or shadow zone. Similarly, sounds originating below the upper layer remain below it. This, of course, provides the submarine operating below the layer a tactical advantage over the surface ship. Variable depth sonars are weighted, low drag, stabilized *fish* lowered below the layer on a faired towline; they consist of an active source and a receiving array.

The towed array provides a large, linear aperture, sufficiently far from own ship noise to be unaffected. Such arrays are particularly suitable for low frequency detection at first or second convergence zone (CZ) ranges. The low operational frequencies increase the beam widths, but early detection provides a tactical advantage that may be used to vector other ships or a helicopter to the target area. Early detection also enables fire control sonar operators to search on an alerted basis. Such an array may be hundreds of feet long and the tow cable thousands. Long cable lengths are used to place the array outside the ship's acoustic field and for towing at optimum depth.

Underwater acoustic communications between a diver and ship or between ships can be accomplished at various frequencies and with various modulation techniques (including coded signals) depending on the desired range and data rate. Special transducers are sometimes used for this application; at other times existing transducers are used.

Helicopters, equipped with *dipping sonar* for active and passive detection, are assigned to operate from surface ships for the localization and destruction of enemy submarines. The range of the sonar is small, but that of the helicopter is large enough to investigate poor contacts and attack targets. The helicopters greatly increase the ASW capability of a ship, but the designer must consider a landing area, hanger, fuel supply (including tanks, pipes, and hoses), and room for additional personnel. All of these factors affect the arrangement, stability, and size of a ship.

Surface ship deployed sonobuoys are also used for detection and localization. Their transmission range is limited by the horizon but the capability can be extended if helicopters are available. The only effect sonobuoys have on ship design is the need to provide storage space.

Depth sounders are primarily used for navigation inside the 100 fm curve. Their range is very small, compared with ASW sonar systems, and their operating frequencies are high. Because the size and cost of such devices decrease as wavelength decreases, physically small, high frequency systems are most popular. Ships, especially oceanographic vessels, that require soundings at all depths use lower frequencies and larger transducers. Higher frequencies reflect readily from almost any type of bottom; lower frequencies penetrate soft bottoms and reflect a series of echoes at each material interface as ϱc changes (see Section 3.2.4). A continuous record of such soundings provides a cross section of the bottom structure.

The depth sounder transducer is usually mounted in a well located quarter of the length of the ship, aft of the bow. The placement ensures that it will remain below the water in violent seas and removes it from engine room noise. An intermittent problem with this configuration is that air bubbles are swept into the area around the transducer. The high operating frequency of the device means that very tiny bubbles, on the order of one-hundredth of an inch, will be in resonance with the transducer (see Section 3.3). Poor performance can result when bubbles are swept into crevices on, and around, the transducer.

Therefore, exposed surfaces should be as smooth as possible so the bubbles will be scoured away by the water flow. A method of removing and replacing the sound head without drydocking is sometimes provided for regular maintenance purposes.

Because radiated noise is of such great tactical importance, combat ships are often fitted with noise monitoring hydrophones that provide a record of spectrum levels at various points. Known noise levels are recorded and changes in level are used to alert the operator.

Although not an acoustic device, the expendable bathythermograph (XBT) (see figure 1.6 for a cut-away view) is important for effective sonar system employment. It is used to determine sound speed in the full depth of the water column below the ship. The XBT probe, or plummet, contains an open central tube that houses a thermister connected to the ship by a long, thin wire. The speed of descent of the probe is calibrated and synchronized with a recorder that plots depth versus sound speed. The sound speed profile (see Sections 1.3.5 through 1.3.9) determines the curvature of the acoustic rays and, therefore, local sound propagation. The profile provides tactically important information concerning surface ducts, convergence zones, and shadow areas.

Because XBTs are expendable, a ship must carry a supply sufficient to last the mission. They are deployed from a launcher permanently mounted in the stern and electrically connected to the recorder. When the expendable unit is inserted into the launcher, the breech door is closed, electrical contact is made, and the XBT is released into the sea. The launcher may be located on the weather deck or below deck.

The bottom search system is a device (a *fish*) containing a high frequency quasi-linear array of transducers that is towed near the bottom see (figure 5.2). The array insonifies a plane on one side, 0° from normal, and a similar array insonifies a plane on the other side. The two sides are separated by a baffle and, if necessary, by frequency separation to prevent mutual interference.

The arrays transmit short coded pulses that return when they strike an object. The echoes are recorded on a moving paper recorder scaled to the motion of the ship and the time delay is used to determine distance. The results provide an acoustic picture of the bottom presented as is a television picture; the raster rate is determined by the speed of the ship.

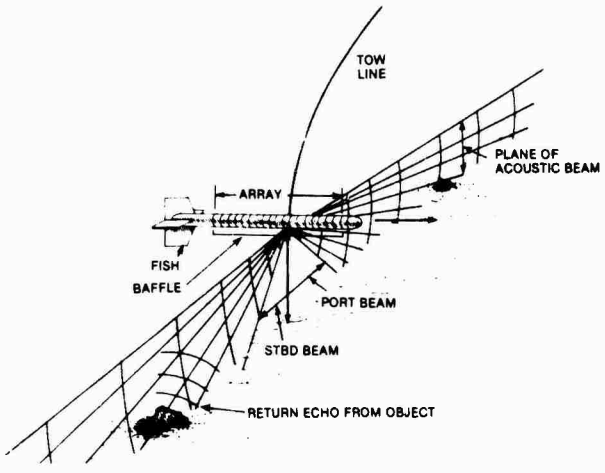

Figure 5.2. Bottom Search System

The high frequencies used by such systems provide good bottom surface definition, but detection range is short. Noise sources, such as small boat motors, create interference if the frequency band overlaps that being used. Also, passing ships may interfere with the picture of the bottom.

A summary of the types of sonar systems installed onboard U.S. Navy surface ships is presented in figures 5.3, 5.4, and 5.5. The figures are not intended to be accurate; they show only the general locations of external arrays and sensors. A detailed sonar equipment listing is provided in NAVSEA Instruction 0967-LP-560-8010.

5.2. SUBMARINE SONAR SYSTEMS

The bow array on submarines (see figure 5.1b) is usually the active search sonar. It is located to provide wide azimuth coverage and many installations are configured such that the hull acts as a stern baffle. The arrays also form beams in depression/elevation (D/E). Array size depends on the frequency of interest and the amount of space available.

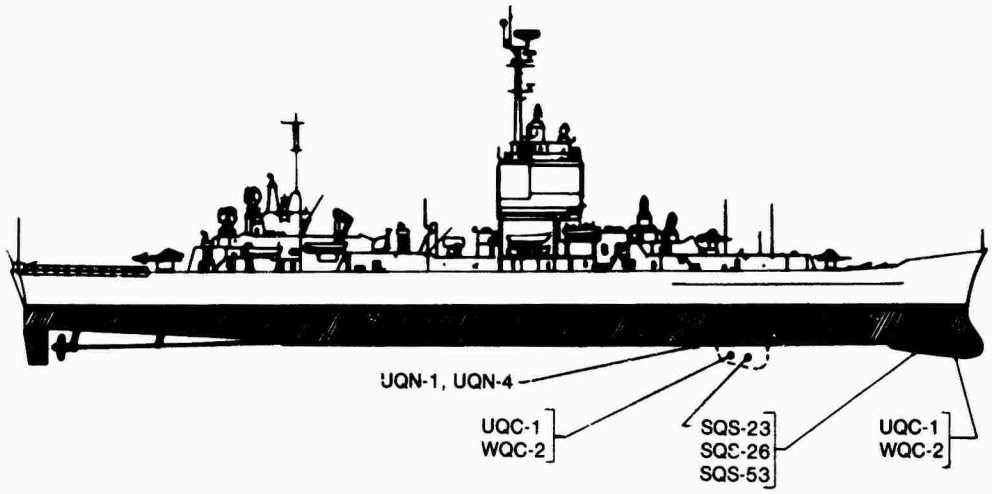

CRUISERS: NUCLEAR — NON NUCLEAR

CGN 9, CGN 35–40, CG 10, 11, CG 16–24, CG 26–34

Characteristics / System	Array Type[1,2]	Frequency (Khz)		System Function
		Active	Passive	
AN/SQS-23[3]	TA			ACTIVE DETECTING & RANGING
AN/SQS-26[4]	TA			ACTIVE DETECTING & RANGING
AN/SQS-53[5]	TA			ACTIVE DETECTING & RANGING
AN/UQC-1	T			UNDERWATER ACOUSTIC COMMUNICATION
AN/WQC-2	T			UNDERWATER ACOUSTIC COMMUNICATION
AN/UQN-1	F			DEPTH SOUNDING
AN/UQN-4	F			DEPTH SOUNDING

NOTES: 1. For further detailed information concerning specific sonar gear (e.g. hydrophones, transducers, etc.) refer to respective system technical manuals.
2. T — Transducer, TA — Transducer Array, F — Fathometer.
3. Bow–Mounted on CG 16–24 class.
4. Existing on CGN 35, 36 & 37, and CG 26 class only.
5. CGN 38, 39 & 40 only.

Figure 5.3. Sonar Sensor Locations Onboard Cruisers

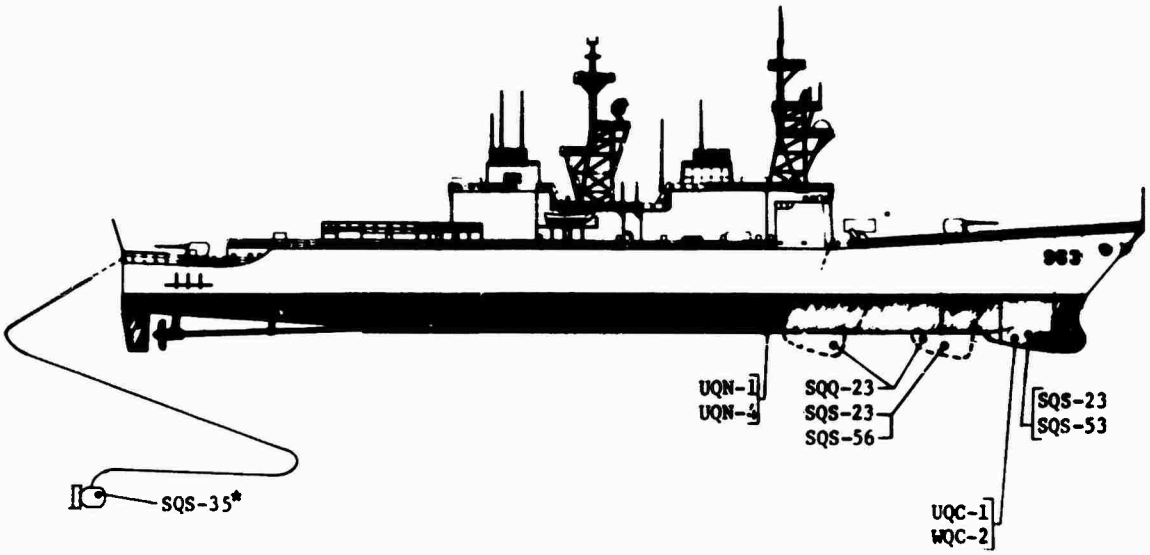

* TOWED FROM THE FANTAIL BY THE AN/SQA-13(V) HOIST

DESTROYERS/GUIDED MISSLE DESTROYERS

DDG 2-24, DDG 31-36, DD 37-46, DD 714-890, DD 931-951

DD 963-972

Characteristics / System	Array Type[1,2]	Frequency (Khz)		System Function
		Active	Passive	
AN/SQS-23[5]	TA			ACTIVE DETECTING & RANGING
AN/SQS-53	TA			ACTIVE DETECTING & RANGING
AN/SQS-35[3]	TA			ACTIVE DETECTING & RANGING/TOWED BODY
AN/SQQ-23[4]	TA			ACTIVE DETECTING & RANGING/TWIN DOMES
AN/SQS-56[6]	TA			ACTIVE DETECTING & RANGING
AN/WQC-2	T			UNDERWATER ACOUSTIC COMMUNICATIONS
AN/UQC-1	T			UNDERWATER ACOUSTIC COMMUNICATIONS
AN/UQN-1	F			DEPTH SOUNDING
AN/UQN-4	F			DEPTH SOUNDING

NOTES:
1. For further detailed information concerning specific sonar year (e.y. hydrophones, transducers, etc.) refer to respective system Technical manuals.
2. T - Transducer, TA - Transducer Array. F - Fathometer.
3. DD 933, 937, 938, 940, 941, 943, 948 & 950 only.
4. DDG 5, 6, 7, 11, 12, 15, 16, 17, 18, 19, 37, 45 & 46 only.
5. Bow mounted in DDG 20-24, & DD 933.
6. DD 821 only.

Figure 5.4. Sonar Sensor Locations Onboard Destroyers

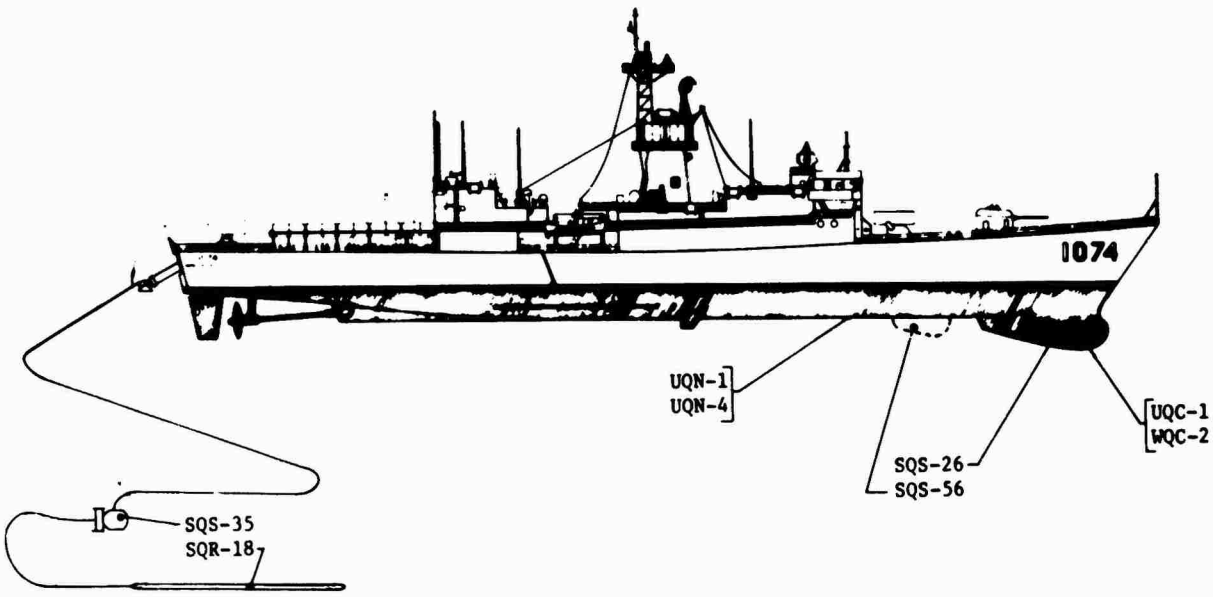

FRIGATES/GUIDED MISSLE FRIGATES

FF 1037, 1038, FF 1040-1051, FF 1052-1097, FFG 1-6, FFG 7-10

Characteristics / System	Array Type[1,2]	Frequency (Khz)		System Function
		Active	Passive	
AN/SQS-26	TA			ACTIVE DETECTING & RANGING
AN/SQS-56[5]	TA			ACTIVE DETECTING & RANGING
AN/SQS-35[3]	TA			ACTIVE DETECTING & RANGING/TOWED BODY
AN/SQR-18[4]	TA			PASSIVE-RECEIVING TOWED ARRAY
AN/UQC-1	T			UNDERWATER ACOUSTIC COMMUNICATION
AN/WQC-2	T			UNDERWATER ACOUSTIC COMMUNICATION
AN/UQH-1	F			DEPTH SOUNDING
AN/UQN-4	F			DEPTH SOUNDING

NOTES:
1. For further detailed information concerning specific sonar gear (e.g. hydrophones, transducers, etc.) refer to respective system technical manuals.
2. T - Transducer, TA-Transducer Array, F - Fathometer.
3. System is installed only on FF 1052 class with the exception of FF 1053-1055, FF 1057-1062, FF 1072 & FF 1077.
4. System is to be installed on FF 1052 class having the AN/SQS-35 system.
5. FFG 7 class only.

Figure 5.5. Sonar Sensor Locations Onboard Frigates

A submarine sonar array is subject to interference when own ship engine and propeller noise is reflected from the sea surface, so they must either be mounted low in the ship or protected by overhead baffles. Also, because submarine sonar arrays are operated at depth, high power per unit area may be projected without cavitation at the transducer face. In other respects, they operate much like active surface ship arrays.

Submarines naturally have no need for variable depth sonar systems but they do use towed arrays for detection purposes. The towed arrays may be permanently, or temporarily installed, self-deployable, retrievable systems. Submarine tow cables are usually shorter than those required for surface ships because the vessel can go below the surface layer to deploy the array. Also, since there is no reason to sink the array deeper than the submarine, the cable is made neutrally buoyant.

Submarines are often equipped with an underwater communications system and always with a depth sounder. Two navigational systems not required by surface ships are installed onboard submarines. One is a surface sounder used to accurately determine the distance to the surface; the other is a high frequency, forward looking sonar for under the ice navigation. They are also equipped with a platform noise monitoring system to detect own ship signature changes.

Operation of the submarine XBT (i.e., SSXBT) is more complicated than the surface version. The submarine ejects a unit that floats to the surface and drops a plummet. The SSXBT provides sound speed data for the complete water column that includes information concerning the existence of a surface duct.

5.3. TYPES OF SONAR

5.3.1. GENERAL

This section will deal with the generic types of sonar, i.e., with

1. active detection (hull mounted),
2. active detection (towed fish),
3. passive detection (hull mounted),
4. passive detection (towed array),
5. passive detection (expendable hydrophone or array sonobuoys),
6. fathometer and navigation sonars, and
7. self-monitoring systems.

5.3.2. ACTIVE DETECTION (HULL MOUNTED)

The active search mode employs an acoustic energy pulse that is projected from the array and reflects from the target. The transducers that transmit the pulses normally receive the echoes but other arrays can be used to sense the return signal. There are advantages to both approaches. If the same transducer is used as transmitter and receiver, the required aperture space is reduced and fewer cables and hull penetrations are required. When the functions are separated, the transducers can be optimized for active use without the requirement that they sense low level signals in the receive mode. In addition to being desirable to illuminate relatively wide sectors with active energy, it is also desireable to receive on small angle beams. Therefore, while the aperture for receiving signals should be large, that for transmitting need be only a fraction of the receive dimension.

Active transducers are far more expensive than receiving hydrophones and their size makes them difficult to isolate from self-noise in the receive mode. The most commonly used submarine transducer is the TR-155, but a wide variety is employed for various applications. They are used singly or in combinations configured as cylinders, spheres, or planes (current computer technology permits arrays of the more complicated shapes required by conformal arrays). The transducers vary in size from the dimensions of a twenty-five cent piece to arrays weighing hundreds of tons.

When used as projectors, transducers require only the sound isolation necessary to protect shipboard personnel. Because projected energy, and not signal-to-noise ratio (SNR), is the criterion for active projectors, they are usually equipped with a protective *window* for low transmission loss at the operating frequency. The transducers are packed closely in arrays so they act, effectively, as large monopoles, which improves radiation efficiency.

The transmitted pulse is acoustically coded so that the return echo can be easily detected and

Doppler information concerning the target can be readily obtained. The active pulse can be transmitted omnidirectionally or beamed into a selected sector as shown in figure 5.6. The concentration of energy in a beam permits the array to project a higher intensity signal and reduces reverberation from targets that are not of interest.

If there is more than one pulse in the water at a given time, detection and ranging difficulty increases. Therefore, it is standard practice to wait until the signal from one pulse has dissipated before transmitting another. The time delay between pulses depends on the range of interest; they are usually on the order of 10 to 30 sec. When sectors are illuminated sequentially, the sweep rate is reduced accordingly. The beamwidth of the active pulse is kept reasonably large in order to increase the search area. The received signal is sensed on much smaller beams for improved SNR and accurate target bearings. No time is lost in the receive mode because the beams can be formed and displayed simultaneously.

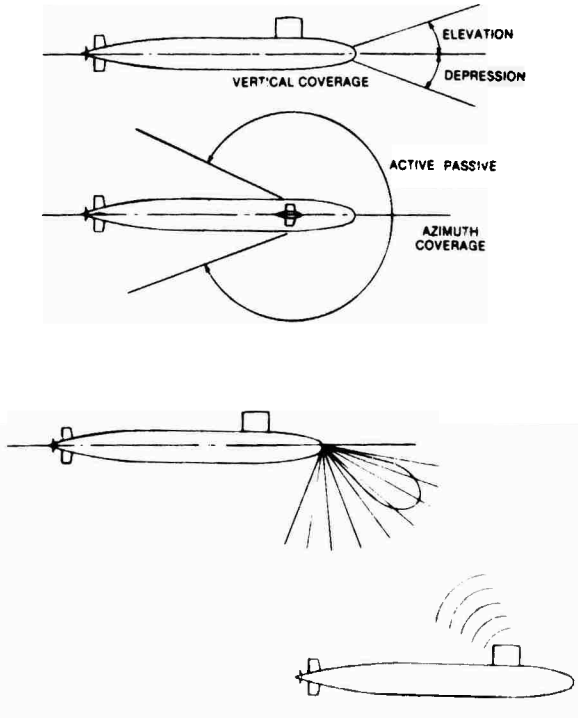

Figure 5.6. Submarine Sonar Coverage

Initial detection can be accomplished using the passive system (which is, of course, covert) when active and passive systems are used together. Once detection is made and fire control information is required, the target is illuminated by the active array for accurate range and bearing data.

The operating frequency of an active sonar is a function of the acoustic cross section of the target, ambient noise, reverberation levels, and propagation losses. The echo from an object is a function of its dimensions; e.g., a rigid cylinder will reflect well if the acoustic wavelength is less than πD. Thus, it is necessary to use high frequencies, i.e., short wavelengths, to detect small objects. It is also necessary to use high resolution beamforming, i.e., very small beamwidths, for the resolution required to classify such objects.

Achievable range decreases as frequency increases (see Section 1.3.3); so selection of optimum system frequency is a compromise between range and resolution. In addition (see figure 1.14), the ambient noise is less at the higher frequencies. The advantages of higher frequencies are that smaller objects are discernible, narrower beams are achievable, and ambient noise is lower. A disadvantage is that propagation loss is higher and, therefore, achievable ranges are lower.

As discussed in Section 2.0, the forward portion of a ship is quietest and forward and beam viewing the most important tactically. The acoustic pulse levels of sonar projectors are high and, in the far field (i.e., away from the hull), their location relative to the ship's noise is unimportant.

It is important, however, that noise at the receiving sensors be as low as possible. The detection equation

$$SL - 2(TL) + TS = NL - AG + DT$$

can be rearranged in the form

$$2(TL) = SL + TS + AG - DT - NL .$$

If all terms at the right of the equation remain unchanged, except for self-noise level (NL), system and ambient conditions remain the same and we change NL at the receive hydrophones

by (ΔNL), the allowable transmission loss (TL) decreases by $\Delta TL = -(\Delta NL/2)$.

If TL (see Section 1.3.3) is

$$TL = 60 + 20\log[r(10^{-3})] + \alpha[r(10^{-3})]$$

and the sonar system frequency is 5 kHz, then, from figure 1.3

$$\alpha = 0.25\ \text{dB/km}.$$

Now if

$$\Delta NL = 5\ \text{dB},$$

and, since,

$$\Delta TL = -(\Delta NL/2)$$

then

$$\Delta TL = -2.5\ \text{dB}.$$

If it is further assumed that r = 10 km, the initial permissible TL is

$$TL_o = 60 + 20\log 10 + 2.5 = 60 + 20 + 2.5 = 82.5\ \text{dB}$$

and, since,

$$TL_1 = TL + \Delta TL$$

then

$$TL_1 = 82.5 - 2.5 = 80\ \text{dB}$$

and

$$80\ \text{dB} = TL_1 = 60 + 20\log[r_1(10^{-3})] + \alpha[r_1(10^{-3})].$$

Hence, r = 7.95 km, the new range.

The result represents a reduction of 2.05 km from the original 10 km, i.e., an approximately 20 percent reduction for a 5 dB increase, or 3 to 4 percent reduction for each decibel.This is indicative of the importance of self-noise to sonar system range and the reason for locating hydrophones and passive transducers in low noise areas.

Because reverberation, especially from the bottom and surface, limits the detection capability by masking the target echo, the beam width of the active pulse is selected to be small enough to detect the target while avoiding echoes not of interest. Therefore, active arrays generally have the capability to beamform in azimuth and to change the D/E angle from slightly upward to slightly downward.

Machinery and propeller noise travels through the water and/or hull structure to the forward portion of the ship and interferes with the ideal 360° coverage in azimuth. Although kept to a minimum, such noise seriously degrades array performance. Since the aft bearings are inevitably degraded, the remaining bearings are protected by installing acoustic baffles behind the array. This is the reason a ship will periodically alter course, i.e., *clear baffles*, to search astern. Submarines also require baffles over and aft of the forward arrays for protection from machinery noise reflecting from the surface.

5.3.3. ACTIVE DETECTION (TOWED FISH)

The discussion of *layer* effects in Section 1.3.5 showed that when the water is agitated by wind or currents, a duct, or layer, of isothermal water may develop near the surface. Sound generated below this shadow zone tends to remain below it and sound generated in the layer tends to remain in it. This condition favors submarines because they can remain below the layer without being detected. For this reason, surface ships are equipped with towed sonars to penetrate the layer (see figure 5.7).

The system consists of an independent active sonar array lowered from the stern. The receiving array is protected by an upper baffle to reduce own ship noise. The towed *fish* may be equipped with a compass to determine heading.

The mechanical/hydrodynamic design of this system is more complex than it first appears. For example, if a body suspended from an unfaired cable is lowered from a moving ship, *strumming* results. Strumming, i.e., flow excited vibration (*Strouhal* or *Karman* vortex), is caused by the formation of eddies first on one side of the cable and then on the other (see figure 2.32). It results in broadband radiated noise and causes cable fatigue.

Fairing means that the cable is streamlined in shape, smooth, and has a small trailing edge. The disadvantage in handling faired cable is that it will not reel in layers and, therefore, requires a large reel.

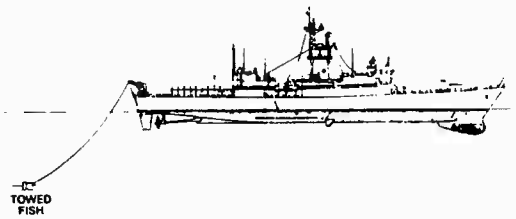

Figure 5.7. Variable Depth Sonar

Lowering and retrieving a body from a ship at sea requires continuous control from the time it leaves the cradle until it enters the water, and vice versa. Attempting to lift and lower by cargo boom would be extremely dangerous to personnel and, more than likely, damage the fish. The proper method is to *two-block* the fish and lower the boom beneath the water before releasing. The same method must be used for retrieval, i.e., two-block before raising.

The fish is designed with a low drag shape to deploy at a relatively vertical angle. If it did not have this shape, the force of the water would swing it aft and upward. However, even the best streamlining resembles an airfoil and, if the towing is improper, the body may become angled to the flow and the lift may *kite* it from one side to another.

The design, manufacture, and installation of such a system is a challenge. Consideration must be given to the available space, and the weight and stability of the winch, fish, and inboard electronics. Deployment of the system also imposes constraints on movement. For example, the ship cannot be backed down when the fish is in the water without the danger of snarling the tow cable in the propellers or rudder.

The AN/SQS-35 towed sonar is the primary system used onboard U.S. Navy vessels.

5.3.4. PASSIVE DETECTION (HULL MOUNTED)

Passive sonar arrays are used to listen for the radiated (acoustic noise) of a target. They are also located in the forward portion of the ship and own ship noise has a more detrimental effect than on active systems. The passive equation is

$$SL - TL = NL - AG + DT$$

or

$$TL = SL - NL + AG - DT.$$

If the only change to the terms on the right is that NL becomes ΔNL, then

$$\Delta TL = -\Delta NL.$$

It is apparent that the increase in TL is twice that for the active sonar system. In the example, the passive range is reduced from 10 to 6.25 km, or 37.5 percent compared with 20 percent for the active system.

Another concern about passive arrays is that the variation in self-noise over the length may negate the advantage of the large size. If this variation exceeds approximately 10 dB and the hydrophones are not shaded to reduce the noise input to the system, performance will be degraded (see Section 1.11.6). This provides the quantitative rationale for locating the array in a low noise area or baffling it so that the self-noise is of the order of magnitude of the ambient noise. The active array can be used for passive applications.

5.3.5. PASSIVE DETECTION (TOWED ARRAY)

The difficulty of siting large, quiet apertures onboard surface ships and submarines may be partially overcome by towing the array. Because such arrays are stored on large steel reels and are not constrained by the size of the ship, they can be made quite long. The length is generally determined by cost, handling difficulty, and the

acoustic improvement achieved. They are towed well behind so that distance attenuates own ship noise to approximately the ambient noise level. The long tow line provides a detection capability below the mixed surface layer. Also, the large aperture provides the beamforming capability to detect low frequency targets.

The arrays are subject to flow noise at high tow speeds and to damage or loss by collisions with obstructions in the water. Their beams are effectively conical (see figure 5.8) because they beamform in only one dimension. This can cause a right-left ambiguity and right-left-vertical ambiguity near end-fire. Also, the configuration and heading of the array are difficult to determine when the ship is maneuvering. The determination, in real time, of the location, configuration, and bearing of towed arrays during maneuvering requires considerable computer capacity and time. Therefore, simple approximations are generally used.

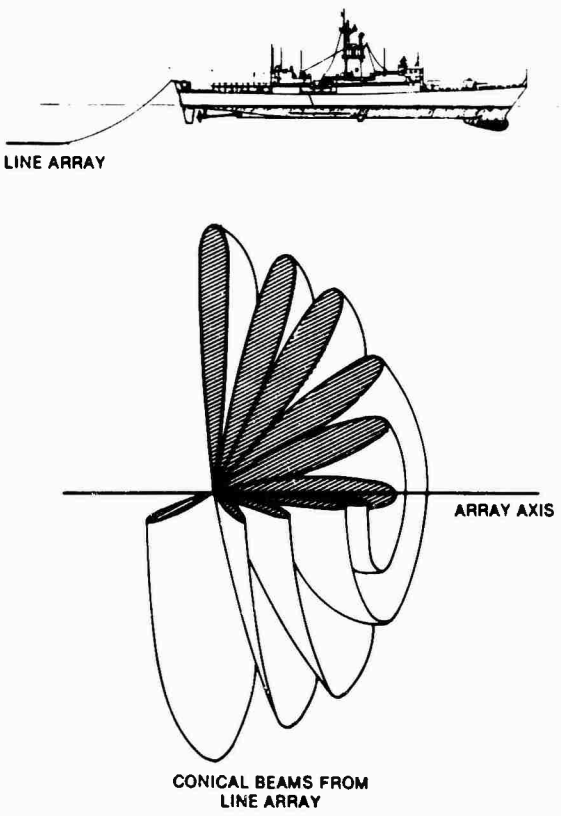

Figure 5.8. Conical Beams from a Line Array

When towed, the cable takes an angle with the horizontal, i.e., *the critical angle*, that is a function of ship speed and cable weight and diameter. The whole length of the cable is at approximately that angle and paying it out effectively makes it longer and lowers the array. If cable length remains constant, increasing ship speed causes the angle to become smaller and raises the array; decreased speed, of course steepens the angle and lowers. The deployment and retrieval of towed arrays is much simpler than for the variable depth sonar because array weight is distributed. Also, since it is neutrally buoyant, it weighs the same as an equal volume of water and it may be winched in and manhandled over the stern of a moving ship.

The same maneuvering constraints apply to towed arrays that apply to the variable depth sonar. In addition, course changes result in array configurations that are difficult to accurately track so performance is degraded until the ship is on a straight course.

Although the SNR is only slightly degraded by own ship noise, these arrays are affected by flow noise and noise in the cable caused by eddies and pulsations. The winch used to store the cable and array is the heaviest and largest item influencing ship design. An array maintenance area having a trough for holding and storing array modules is also needed.

5.3.6. PASSIVE DETECTION (EXPENDABLES)

The air-dropped sonobuoy is probably the most common expendable detection device. When dropped, it deploys a hydrophone and radio antenna and begins transmitting acoustic data to the monitoring aircraft via a radio link. Such sensors are not limited to a single hydrophone operation; they can consist of multi-hydrophone arrays of various shapes and configurations.

The buoys may also be deployed by surface ships to augment hull and towed array sensors. These senors are not affected by self- or flow-noises and there are no acoustic window losses. The deploying ship can move to a distance so that own noise does not interfere, and then vector a helicopter or ASROC to the target.

High performance SESs and hydrofoils that can not use hull mounted arrays or deploy towed arrays at speed can use these sensors to good advantage.

A hydrophone could, of course, be deployed on a payout system similar to the XBT, which would lay out a thin connecting wire from the phone to the ship over which the data are telemetered. Since the period of deployment is limited by the length of the data link and ship speed, use of this type of device would be for specific tactical situations.

5.3.7. FATHOMETER AND NAVIGATION SYSTEMS

The fathometer is used more than any other hydroacoustic device. Its basic operating principle is very simple. An acoustic pulse is projected in a beam to the bottom and reflected back. The time between the pulse and its reception is divided by two and multiplied by the speed of sound, which yields the distance to the bottom. The basic active sonar equation applies to this device. Therefore, source level, array configuration, and the detector may be designed accordingly.

Although the fathometer is subject to self-noise, it operates at a relatively high frequency in a narrow band. The transducer is located forward, to avoid machinery noise, and aft of the bow; so it is in the water at all times. It is located to avoid areas of bubble sweep-down. Since it is near the keel it must be shown on the docking plan. No keel or bilge blocks should be located nearby.

The frequencies used for the device will vary depending on its use. For shallow depth sounders, the frequency may be between 100 and 200 kHz. For deep water fathometers it may be as low as 20 to 30 kHz. Commercial systems tend to use high frequencies because the transducers are small and inexpensive.

5.3.8. SELF-MONITORING SYSTEMS

Hydrophones are located at points around the exterior of ships to detect changes in radiated self-noise. Such systems are installed throughout submarines and near the bow sonar dome on surface ships. If there is a change in noise level, the cause is investigated using the frequency, periodicity, and other characteristics as clues.

If the cause is apparently equipment related, machinery is operated and secured until the source is found. If the cause is apparently a rattle, a rubber mallet is used to pound the hull throughout the ship. Vibrations travel through the ship and are difficult to locate.

5.3.9. BOTTOM TOWED SEARCH SYSTEMS

The bottom towed search system is installed only on ships that require detailed bottom information. Such information is obtained using an array located near the bottom. This is because very high frequencies, i.e., short wavelengths, are needed for detailed information and the attenuation is too high when operating from the surface.

Figure 5.2 depicts a bottom search system being towed. It transmits a narrow beam, high frequency(> 100 kHz) coded pulse of acoustic energy that reflects back from objects on the bottom. The time delay of the return provides a depiction of the bottom; each pulse is equivalent to one raster line. Raster spacing is determined by the speed of the ship .

Bottom survey systems for deep water require long cables, large winches, and are frequently deployed from a bottom well. They are useful for detailed surveys before emplantment.

5.4. DESIGN CONSIDERATIONS

5.4.1. GENERAL

The major considerations involved in installing sonar systems onboard combat ships will discussed in this section. It should be apparent from previous discussion that good SNR is the most important factor in acoustic warfare. Therefore, it is not suprising that practically every part of the ship is designed for maximum quiet.

Propellers are designed to operate quietly without cavitating or singing, rotating machinery is balanced to avoid pulsating forces, and electric motors and generators are designed to minimize pulsating magnetic fields. Fluid

flow velocities in pipes and ventilating systems are limited to avoid the generation of flow noise and cavitation. Turbines are designed for quietness. Sound isolation mounts are used to interrupt acoustic paths and pumps and fans are designed for quietness.

The shape of the hull is also affected by sonar considerations. The large bow transducer array is housed in a bulbous bow on surface ships. The seakeeping design maximizes immersion so that the bow remains in the water as much as possible; when it is out of the water during high sea states, it can not send or receive.

Towed arrays, variable depth sonars and, to some extent, helicopters are all used in the constant search for better SNR. Wire-way configurations, cable shielding, electrical connectors, junction boxes, and the design of alternating current systems are chosen to eliminate electro-magnetic noise.

The information presented in the first four chapters is intended to provide the engineer with the basic tools to understand the relatively general discussions that follow. It should be noted that quietness is generally compatible with good design; noise mechanisms are usually also wear mechanisms.

5.4.2. INSTALLATION OBJECTIVES

Among other functions, acoustic warfare sonar systems are designed to sense sound at an array and project it from transducers, present sonar information to CIC, and protect shipboard personnel from high level acoustic signals. The installation must ensure that all such functions are possible. It should be possible, then, to receive acoustic signals over the frequency band of interest with minimum interference and to project undistorted, wide azimuth signals while protecting the crew from excessive acoustic levels. Internal cabinets and other equipment must be designed for the thermal environment and existing ship services. Sonar operators must be provided a comfortable, quiet area suitably located in relation to other combat system operating areas. Electromagnetic interference must be minimized.

To accomplish these and other objectives, the design should

1. minimize system weight and space requirements,
2. locate arrays for large azimuth and D/E coverage,
3. provide passive arrays with large apertures,
4. provide active arrays with apertures consistent with sector scan requirements,
5. protect personnel against active transducer output,
6. locate hydrophones in quiet areas and/or provide baffling,
7. locate equipment near arrays to reduce cable runs,
8. minimize cable penetrations,
9. minimize electromagnetic interference,
10. locate sonar operators in a quiet, comfortable space,
11. locate sonar equipment where it is accessible for maintenance and repair,
12. provide readily available utilities, and
13. locate hydrophones and transducers where they are not subject to reflections or refractions.

5.4.3. ACTIVE DETECTION (HULL MOUNTED)

Active transducers are usually the heaviest single item in a sonar system. Associated requirements, such as sonar dome water and recesses for arrays are also heavy and occupy much space. Transducer arrangement is essentially a sonar system design problem but ship design is also influenced. Because large arrays are sometimes built in the shipyard, it is important that the builders follow good practice.

The center-to-center and relative location is very important because a transducer influences others in an array and changes the effective impedance. The structure must be such that no air pockets exist. Air reduces the impedance at the face of the transducer and prevents radiation of full power.

Because transducers must be replaced and inspected, they must be located in accessible areas. Large domes usually have sufficient room for a man to enter. Small domes must either be removed completely or entered through an access plate. When changing transducers housed

in protruding domes, it is necessary to break and remake electrical connections. Connectors for this application have a history of poor performance. Therefore, good design and workmanship are necessary when using connectors. Good practice is to use a continuous length of cable between the transducer and hull penetrator. If necessary, a splice can be made.

The *field of view* of the array must be clear of opaque material. This requires engineering drawings of the array and structure in the immediate vicinity to identify interference. Clearances of 30° are desireable (see figure 5.9a). The sonar system designers should be informed if such a clearance cannot be provided. Also, reflecting surfaces (see figure 5.9b) result in interference.

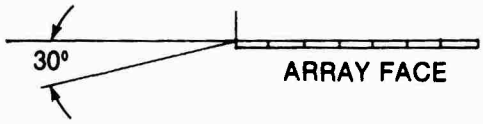

Figure 5.9a. Thirty Degree Clearance

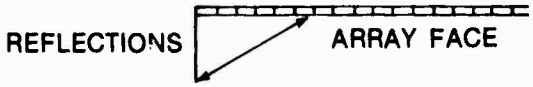

Figure 5.9b. Reflecting Surfaces

Figure 5.9. Array Aperture Requirements

5.4.4. ACTIVE DETECTION (TOWED FISH)

Design considerations for the variable depth sonar system consist mainly of space and weight allowances for the stowage and deployment. A deck installation is shown in figure 5.10. As mentioned earlier, deploying a fish is an involved process. The rolling and pitching motions require rugged launch/retrieval equipment that is sophisticated enough not to damage the fish. Because of the danger of corrosion of the equipment, a combination crane and winch, is located below decks on the most current combat vessels. These units require protected operating areas that have watertight doors through which the fish is deployed and retrieved. The doors must open wide enough to permit the handling unit to move aft and close with only an opening for the tow cable. The tow cable opening is fitted with a fingered rubber fairlead to prevent spray from entering. The doors provide complete watertight integrity when the unit is not in use.

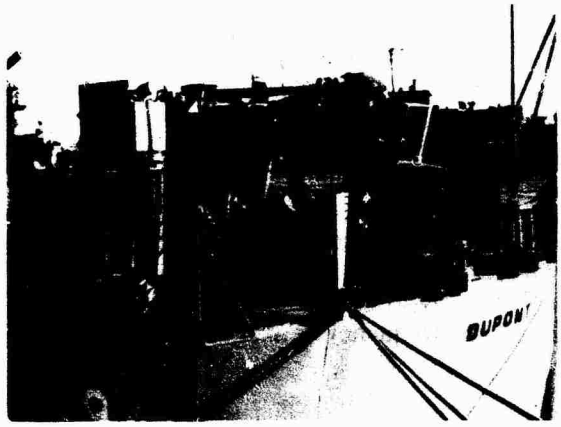

Figure 5.10. Variable Depth System Deck Installation

Fish have been towed from an *A* frame projecting from the side of the ship, but it is more efficient to tow from the stern because maneuverability is enhanced. The towing unit and its foundation must meet the shock and vibration requirements of the general specifications for the particular ship. Intermittent power to operate the winch and continuous power to operate the acoustic system while the fish is deployed is required. The active towed fish system requires a (1) winch room to house the handling gear and fish, (2) sonar equipment room to house receivers, amplifiers, beamformers, and other data handling equipment; and (3) presentation space in CIC.

5.4.5. PASSIVE DETECTION (HULL MOUNTED)

Passive detection systems require large arrays because they operate at low frequencies and form small beams. They are also sensitive to low intensity noise because they are designed for

maximum range and SNR. Such requirements make the installation design very difficult.

The hydrophones must be protected from hull borne noise, usually by baffles. The location of the baffles must be precise to avoid placing the hydrophone in a null (see Section 3.2.4.4). Figure 5.11 shows a pressure release material that is angled away from the line of hydrophones. It is certain in such a situation that one hydrophone is partially nulled at almost any frequency or azimuth angle.

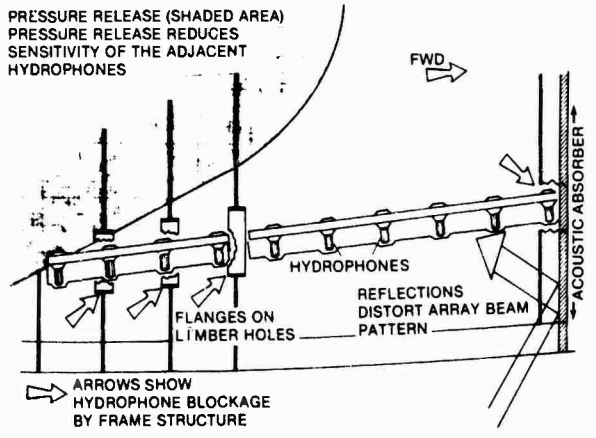

Figure 5.11. Various Degradation Sources

Also, hydrophones should be located in areas that are free from structural reflections. Miscellaneous reflections from nearby flanges or structural frames create out-of-phase, partially coherent interference that degrades SNR (see Section 1.11.8).

If a structure blocks acoustic energy from the hydrophones, the energy will diffract around it, be attenuated, and, because it takes a slightly longer path, the refracted energy may be out-of-phase with the direct path energy. If two parallel reflective surfaces are in the vicinity of the array, the sound reverberates between them and causes a perturbed sound field that degrades hydrophone performance.

Therefore, the design objectives for a hull-mounted passive array are to

1. locate it in a quiet area,
2. provide a large horizontal aperture and reasonably large vertical aperture ($A_h/A_v \approx 7$),
3. provide extensive coverage in azimuth ($\approx 160°$ port and starboard, $\approx 20°$ port and starboard stern baffle to screen propeller noise),
4. provide reasonable D/E coverage from $\approx 15°$ up angle (for submarines) to $\approx 40°$ down angle, and
5. baffle array from hull noise.

The array should be noise isolated from the hull so that shipboard sound is not directly transmitted to the hydrophones. It should also be protected from flow noise turbulence by an acoustic window that is unresponsive to frequencies in the flow noise spectrum (see Section 2.2.7). Since this is not entirely possible, the hydrophones should stand back several inches from the outer surface to attenuate flow noise and cause it to lose its coherence. The outer hull should be made as smooth as possible by using an anti-fouling material, such as impregnated rubber.

5.4.6. PASSIVE DETECTION (TOWED ARRAY)

It is far easier to deploy a passive towed array than it is a variable depth sonar because, effectively, it is deployed a little at a time. The mechanical portions of the system on surface ships consist of a winch, a maintenance area, and a spare unit stowage area.

The towed system is deployed manually by unreeling the drum and feeding the end of the array through the after clamp and fairlead until there is sufficient drag from the forward motion of the ship to provide tension on the winch. The speed and the water depth required for deployment depend on the system being used and the particular project.

The after clamp is used to hold the deployed portion of the array when a section must be replaced during an operation. If a spare reel is available, the sections aft of the one to be replaced are reeled in. A maintenance trough that is as long as the longest array section is usually provided.

Submarine towed array installations differ considerably from those onboard surface ships because the integrity of the pressure hull must be maintained. Such arrays are deployed either external to the pressure hull or by bringing the array and cable in through a watertight penetration. Installation details vary and are supplied with the interface information.

5.4.7. EXPENDABLE SONOBUOYS

Expendable sonobuoys are deployed from surface ships, aircraft, helicopters, and submarines. Their weight and space requirements are negligible and their value depends entirely on the tactical situation. They may be used, for example, to screen the escape route of a target submarine or to increase search capabilities during poor sonar conditions.

5.4.8. DEPTH SOUNDER AND NAVIGATION SONARS

Design considerations for depth sounder and navigation sonars emphasize transducer location and the high (usually ultrasonic) operating frequencies used to obtain narrow beams. The transducers for such systems must face in the direction of interest, i.e., depth sounders face downward and navigation sonars face forward. Because the water depth is usually less than 5.4 km, except in the deep trenches where it reaches 11 km, there is no need for navigation sonars to range more than 5 to 6 nmi. The continental shelf areas, where depth information is most valuable, is only about 180 m deep; high frequencies are adequate for such applications (see figure 1.5).

Figure 3.79 shows that the bubbles resonant at ultrasonic frequencies are very small (from 6 to 10 thousandths of an inch in diameter). They collect on the transducer face and in crevices on the mounting and can cause large changes in the impedance the transducer sees; this seriously degrades system performance. To alleviate the problem the depth sounder is located where the down flow of surface water is a minimum and its window and the surrounding area is made as smooth as possible. The transducer is sometimes recessed behind a window so there will be a bubble-free volume and sufficient loading impedance.

Submarines are equipped with navigation sonar systems to help avoid ice and small craft when surfacing. They also have problems with bubbles, except that the accumulation is on the vertical surface instead of the horizontal one.

High frequency arrays are usually very small and relatively unsophisticated if multiple heads are substituted for a complex beamformer. A typical commercial transducer for a short range depth finder is approximately 2 in. in diameter. The installation criteria are a function of the bubble problem and high operating frequency. The operating frequencies cause even very thin steel to be opaque (see figures 3.58 and 3.59), so fiberglass and rubber are used for the windows. The rubber is impregnated with antifouling compounds and remains free of marine growth for years; when used, it should have an impedance near that of water.

5.4.9. SELF-MONITORING SYSTEM

The installation criteria for self-monitoring systems are hydrophone location and frequency band. The hydrophones will be sensitive over a wide band of frequencies, especially the low ones that radiate great distances. Their function is to record changes in the acoustic signature; so they must be located throughout the length of the submarine and concentrated in areas where noise is likely to be generated. It is also useful to locate one near each array to provide data if the sonar signal becomes abnormal. The hydrophones are located away from structures and baffles for the widest monitoring area.

5.4.10. TELEMETRY

The telemetry system should facilitate the transmission of hydrophone signals to the data processing system with minimum distortion, attenuation, and cross-talk between channels (see Section 1.12). It is part of both the *wet* and *dry* ends of the sonar system. The wet end is that portion outboard of the watertight hull and the dry end is the inboard portion. The primary design constraint on the wet end is that it must operate in a conductive liquid medium characterized by strong corrosive properties.

Therefore, the wet end must be watertight and constructed of material capable of withstanding salt water corrosion for the projected life of the

system. Materials subject to electro-potential differences, such that small areas are cathodic to large areas, must be avoided. Note also that the conductive water surrounding cables will effect the impedance and attenuate the signal unless sufficient impermeable insulation is used.

The telemetry system must be designed to accommodate the hull penetrator, which usually requires a pin connector on the outboard side and one on the inboard side (see figure 5.12). The resistance and associated voltage drop related to pin connectors must be considered in the design.

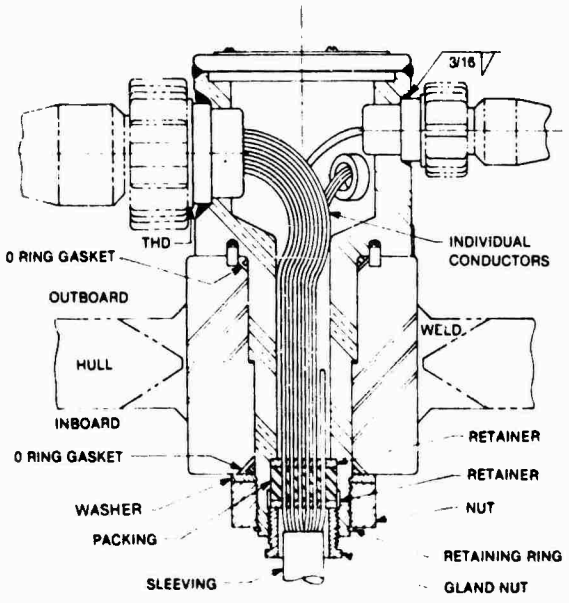

Figure 5.12. Hull Penetrator

The inboard signal is subject to interference from other electrical equipment. Encapsulated preamplifiers installed at the hydrophone end can be used to increase the signal level to reduce the effect of such factors. The wet end electronics can also include an encoder to digitize the signal.

Fiber optic electronics has advantages, especially for large arrays having numerous sensors. They are physically small, operate across a large bandwidth, and are not sensitive to electromagnetic interference.

5.5 ACOUSTIC CONTROL METHODS

5.5.1. ASW APPLICATIONS

There are three major objectives in controlling shipboard acoustic energy. One is to reduce the energy radiated from the ship into the environment, i.e., the radiated noise signature. Another is to reduce the own ship noise to the sensors, i.e., the self-noise. The third is to reduce active sonar levels in personnel areas. Radiated noise increases the detectability of the ship and the self-noise reduces its ability to detect. In this section we will be concerned with methods to decrease the acoustic and vibrational energy that reaches the ship structure and, in particular, that in and around sensor arrays.

The acoustic energy levels are minimum at low ship speeds and the energy influencing the sonar detection equipment is primarily machinery noise. Ambient environmental, electrical system noise, and some low level flow noise may also be present.

Self-generated acoustic energy dominates at midrange speeds and flow, propeller and machinery noise increase. This range is of concern because it is here that sonar system performance can become degraded to unacceptable levels.

Propeller noise dominates at high speeds. Cavitation may be a problem and flow noise is also very high. Machinery noise is,of course, highest at the high speeds but the other sources predominate.

The main acoustic energy paths at the various speeds are

LOW

From machinery to hull causing vibrations; then from hull to sonar sensors by mechanical or acoustic transmission.

MIDRANGE

Flow generated vibrations in hull plates or domes to sensor system by mechanical or acoustic transmission; flow generated acoustic frequencies through array window to sensors.

HIGH

Propeller noise and vibration to hull causing vibrations then transmitted to sensors; waterborne noise to sensors through array window.

Although tuned-elastic supports and baffles are sometimes used to control acoustic energy, elastomers are generally used. Elastomeric coatings can be broadly classified into the categories of damping treatments, decoupler coatings, and anechoic coatings. A coating that fits one of these classifications will probably also have some performance capability that is in the other categories.

Damping treatments damp vibrations in structural members. It is necessary to attenuate such energy to reduce the structural contribution to self-noise. Decoupling coatings create a compliant impedance mismatch in the path of energy and reflect it back in the direction from which it originated (see Section 3.2.6). Such coatings may also prevent a vibrating plate from coupling to the water and transmitting energy into it; they are used to reflect energy away from sensors.

Anechoic coatings absorb sound. They have a reasonably close impedance match to water, which permits the energy to enter the coating and be absorbed. Anechoic coatings can be designed to resonate at selected frequencies, for which they they will provide maximum absorption. The performance will, however, decrease at other frequencies.

The type of suitable material for a given application will depend on the objective and the location for which it is intended. Table 5.1 illustrates a general approach for selecting materials.

Coatings that depend on voids or air cells to perform their function are influenced by external pressure and frequency. The performance of decouplers and anechoic coatings varies over a wide range as depth and frequency change; damping materials remain essentially unaffected. A candidate coating must be tested at the frequency, pressure (depth), and temperature of the environment in which it will be used.

Figure 5.13 provides an example of the distribution of types of coatings for quieting the

Table 5.1. Selection Of Coating Material

Objective	Treatment
Reduce structural vibration	Damping treatment
Reduce waterborne radiation	Decoupler (water side)
Reduce structural vibration and waterborne radiation	Decoupler (water side) Damping reverse side
High transmission loss through plate in water	Decoupling coating on one or both sides
Reduce structural vibration with low transmission loss through plate in water	Damping treatment (Acoustically transparent type)
Echo Reduction on watertight hull	Anechoic coating (water side)
Echo reduction on plate in water	Anechoic coating on incident side decoupler on reverse side.
High transmission loss from one side with echo reduction on other side.	Decoupling coating and anechoic coating

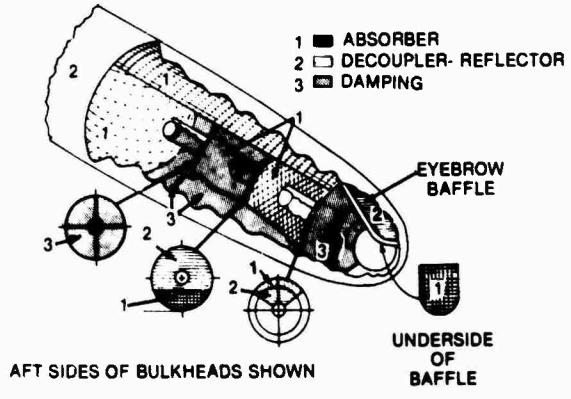

Figure 5.13. Acoustic Control Materials

area around the sonar dome. The coatings shown in the figure absorb, or otherwise dissipate, structurally radiated sound, reflected acoustic energy arriving from the ship, and acoustic energy arriving at a structural surface from the array.

Because steel structural members are elastic and have little inherent damping, they resonate (see Section 3.1.2) to vibrational or acoustic energy at modal resonant frequencies. The complex nature of the structure permits almost any frequency to find a corresponding mode (see Section 3.1.7). Hence, there is a high

statistical probability that the steel structure will vibrate at frequencies that will interfere with the sonar system. The value of a particular damping treatment must be determined by testing. Figure 3.20 plots the theoretical effect of damping materials on elastic plates. It is apparent that the combined loss tangent will be very low unless a thick, high modulus, high loss factor damping material is used.

Acoustic decoupler material is put on the source side of bulkheads and other structures to reflect noise away from the array. An *eyebrow* baffle is installed over the array for protection against surface reflections.

Absorber material is used on the array side of baffles to reduce the amplitude of the sonar signals reflected back to the array. Such signals, i.e., coherent noise, are more destructive to SNR than is incoherent noise (see Section 1.11.8).

The combination of an absorber and reflector on structural members is illustrated in figure 5.14. The noise toward the array from the rear of the baffle is efficiently reflected and that passing through the structure is attenuated by the absorber. Also, acoustic energy leaving the array toward the baffle is partially absorbed; then the portion of energy reflected is again partially absorbed for further attenuation.

The decoupler on the exterior hull reduces radiated energy and, therefore, the passive signature. If the coating includes an absorption capability, target strength is reduced for active sonar operation.

Acoustic coatings also prevent the high energy levels produced in the active mode from reaching living quarters and working areas. The treatment is such that the energy is significantly reduced as it passes through several acoustically treated bulkheads before penetrating into the living areas. Energy that diffracts arround bulkhead baffles is the most difficult to control and is a major contributor to internal noise levels.

Figure 5.14 also shows the use of this arrangement for passive arrays. An acoustic reflector and absorber are tailored to the frequencies of interest for a hydrophone array. The absorber decreases the ratio of reflected to incident pressure, R, at the hydrophones. This extends the frequency range for acceptable signal levels without decreasing the effectiveness of the reflector.

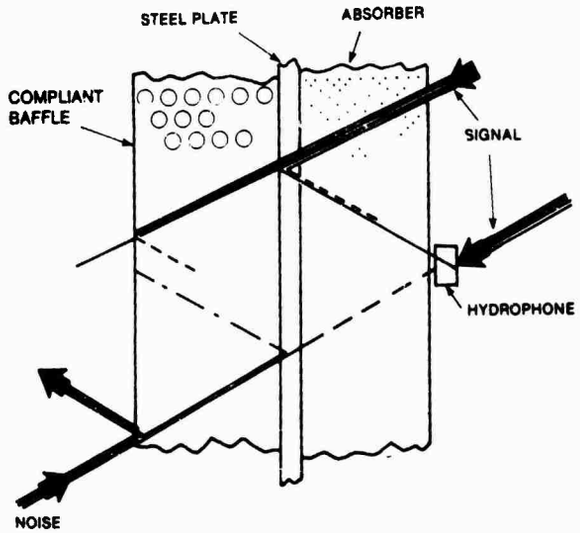

Figure 5.14. Acoustic Control at Sensor

5.5.2 STRUCTURAL DAMPING (PLATE PANELS)

The general subject of damping was discussed in Sections 3.1.2, 3.1.4, and 3.1.6. This section is concerned with the materials and methods for structural panel damping.

The excited modes of an extended structure such as a ship are varied and numerous (see Section 3.1.7) and, as figure 3.27 shows, there are extensive areas in which structural panel vibrations may contribute to self-noise. Such areas include ballast tank plating, bulkhead plating, and smaller plating on deep frames that resonate in various frequency ranges. The primary vibration addressed by damping is flexural vibration (see figure 5.15). Flexural vibration in the hull creates acoustic waves in the medium at attachments and discontinuites. The usual damping method involves adding an elastomer to the plate, with or without a sep-

Figure 5.15. Flexural Vibration of Hull Structure

tum, as is shown in figure 5.16. This adds a complex modulus to the plate and damps the vibrations.

To illustrate the effect of damping on flexural waves, consider a straight crested wave traveling in the x-coordinate direction along a panel in the absence of damping as described by

$$v(x,y,z) = v_o R_e[e^{i(\omega t - kx)}],$$

where

$k = (\omega^2 h \varrho_s / D)^{1/4} \approx (3.46\omega/hc_p)^{1/2}$ denotes the flexural wave number and where

$k = 2\pi/\lambda$,
ϱ_s = plate mass density,
D = flexural rigidity = $Eh^3/12(1 - \nu^2)$,
ω = angular frequency,
h = plate thickness,
$c_p = (E/\varrho)^{1/2}$ = longitudinal (compressional) wave velocity.
ν = Poissons ratio
λ = flexural wave length

If the damping effect is introduced by replacing E with $E^* = E(1 + i\eta)$, the complex wave number $k \approx k(1 + i\eta/4)$, and the result is

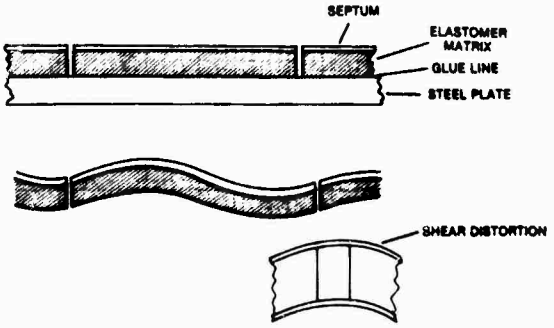

Figure 5.16. Plate Damping

$$v(x,y,z) = v_o e^{-k\eta x/4} \cos(\omega t - kx),$$

where k is now complex which represents a propagating wave whose amplitude decreases with distance. As the propagation distance, x, increases by one wavelength, i.e., by $\lambda = 2\pi/k$, the amplitude changes by $e^{-\eta\pi/2}$ and the decay per wavelength becomes

$$\Delta_\lambda = -20 \log_{10}(e^{-\eta\pi/2}) = 10(\log_{10} e)\pi\eta = 13.6\eta.$$

where

Δ_λ = decibels/wavelength and
η = loss tangent at frequency of interest.

The decay rate, Δ_t, of the vibration is directly proportional to the loss tangent and the center frequency of the band or mode, i.e.,

$$\Delta_t = 27.3\eta f \text{ (dB/sec)}.$$

The loss tangents of most commonly used ship structural materials are relatively independent of amplitude, if stress amplitude remains well below the fatigue limit; temperature, if it remains well below the melting point; and frequency. These loss factors are also relatively low.

On the other hand, elastomers, such as plastics and rubbers, are characterized by stiffnesses (moduli of elasticity), and loss factors that vary greatly with frequency and temperature and are relatively high. Figure 5.17 shows how the shear modulus, G (which for plastics and rubbers is nearly equal to 1/3 the modulus of elasticity), and the loss factor, β, in shear vary with frequency and temperature for a typical plastic. At low frequencies and high temperatures, the material is soft and mobile enough so the strain follows an applied stress without much phase shift and the energy losses and β are relatively small. At high frequencies and at low temperatures, the material is relatively stiff and lossless and its behavior resembles that of an elastic material; this is termed the *glassy* region. Damping is greatest at intermediate frequencies and temperatures.

If one or more layers of a material having high inherent damping are added to a lightly damped panel, the resulting composite is characterized by higher damping. Bending a

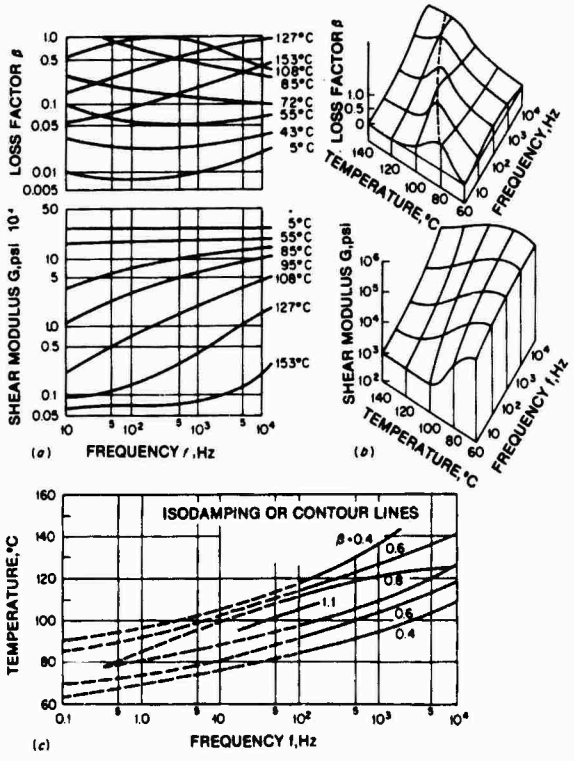

Figure 5.17. Variation of Shear Modulus and Loss Factor with Temperature and Frequency

laminated panel causes each laminate to bend, extend, and deform in shear and strain energy is stored and then dissipated with each type of deformation. The action is similar to a series/parallel array of springs. If K_i is the stiffness of the i^{th} spring, the stored energy is $W_i = K_i X_i^2/2$ and the dissipated energy is $D_i = 2\pi\eta_i W_i$. Therefore, the loss factor for the array is

$$\eta = (\Sigma D_i)/2\pi\Sigma W_i = (\Sigma\eta_i W_i)/\Sigma W_i = (\Sigma\eta_i K_i X_i^2)/\Sigma K_i X_i^2.$$

If the i^{th} spring is to make a significant contribution to the loss factor, $\eta_i K_i X_i^2$ must be a significant fraction of the sum in the numerator. This means the i^{th} spring must have a large loss factor, a large stiffness, and be arranged such that there will be a large deformation, X_i, when the array is displaced. If only one spring has a loss factor, i.e., if the others have insignificant loss factors, then

$$\eta = \eta_1 W_1/\Sigma W_i = (\eta_1)/[1 + (W_2 + W_3 + \ldots)/W_1].$$

Thus, η is always smaller than η_1 but may approach it if the stiffness is such that the stored energy, W_1, using mechanism 1 is a large fraction of the total.

If a viscoelastic layer is attached to a panel that otherwise has a very small loss factor (see figure 5.18), bending will flex both layers. Shear usually has little effect on energy storage in such situations. The loss factor for the combined panel is

$$\eta = \beta_2/\{1 + [\varkappa^2(1 + \beta_2^2) + (r_1/H_{12})^2 [(1 + \varkappa)^2 + (\beta_2\varkappa)^2]/[\varkappa(1 + r_2/H_{12})^2(1 + \varkappa)^2 + (\beta_2\varkappa)^2]\},$$

where

β_2 = visoelastic layer loss factor,
$\varkappa = K_2/K_1 = E_2H_2/E_1H_1$ = extensional stiffness ratio,
$r_1 = H_1/(12)^{1/2}$ = radius of gyration elastic layer,
$r_2 = H_1/(12)^{1/2}$ = radius of gyration viscoelastic layer,
$H_{12} = (H_1 + H_2)/2$ = distance between neutral planes,
E_i = modulus of i^{th} layer, and
H_i = thickness of i^{th} layer.

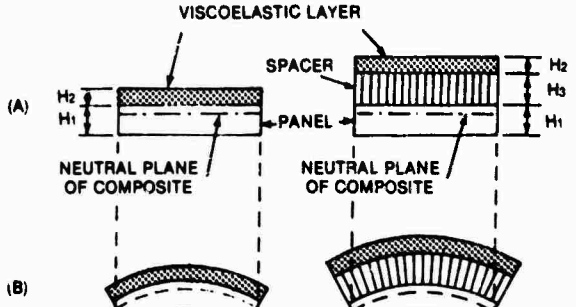

Figure 5.18. Flexing of Viscoelastic Layer (with and without Spacing Layer, (a) Undeformed and (b) Deformed)

Figure 3.20 shows a plot of η/β_2, assuming that $\beta_2^2 << 1$.

In most cases, the added layer is less stiff than the basic panel and $\varkappa << 1$. For useful materials, β_2 seldom exceeds unity and $\varkappa\beta_2 << 1$. Hence,

$$\eta = (\beta_2)/[1 + (E_1/E_2)$$
$$[(H_1^3/H_2)/(H_2^2 + 12H_{12}^2)]$$
$$= (\beta_2)/[1 + [1/e_2h_2(3 + 6h_2 + 4h_2^2)],$$

where

$e_2 = E_2/E_1$ and
$h_2 = H_2/H_1$.

This shows that η depends on both the properties and geometry of the material. It also shows that η for the composite is proportional to β_2 for the viscoelastic material and increases with increasing e_2 and h_2.

If $e_2h_2(3 + 6h_2 + 4h_2^2) << 1$, then

$$\eta = \beta_2e_2h_2(3 + 6h_2 + 4h_2^2)$$
$$= (E_2'H_2/E_1H_1[3 + 6(H_2/H_1)$$
$$+ 4(H_2/H_1)^2],$$

where $E_2' = \beta_2E_2$ is the imaginary part of the complex elastic modulus. Because viscoelastic materials have much smaller moduli than steel, e_2 is generally less than 10^{-2}. Hence, the above equation applies for thickness ratios up to approximately 1.5.

If a viscoelastic layer is applied to each side of a structural panel, the loss factor of the composite will be approximately twice the value of each layer. However, if both layers are applied to one side, the loss factor is four times the value for one layer.

Other damping configurations, such as the addition of a septum to the outer surface of the layer, can be used. This arrangement is shown in figure 5.19, where the loss factor of the composite panel is

$$\eta = \beta_2YX/[1 + (2 + Y)X$$
$$+ (1 + Y)(1 + \beta_2^2)X^2],$$

where Y is a stiffness parameter defined by

$$1/Y = [(E_1H_1^3 + E_3H_3^3)/12H_{31}^3]$$
$$(1/E_1H_1 + 1/E_3H_3)$$
$$= (1 + e_3h_3^3)(1 + 1/e_3h_3)/12h_{31}^3),$$

and where

E_1, E_3 = modulii of two elastic layers,
H_1, H_3 = thickness of two elastic layers,
$H_{31} = H_2 + (H_1 + H_3)/2$ = distance between neutral axes,
$X = (G_2/k^2H_2)(1/E_1H_1 + 1/E_3H_3)$,
G_2 = real part of complex shear modulus,
k = wave number $2\pi/\lambda$, and
λ = flexural wavelength of composite.

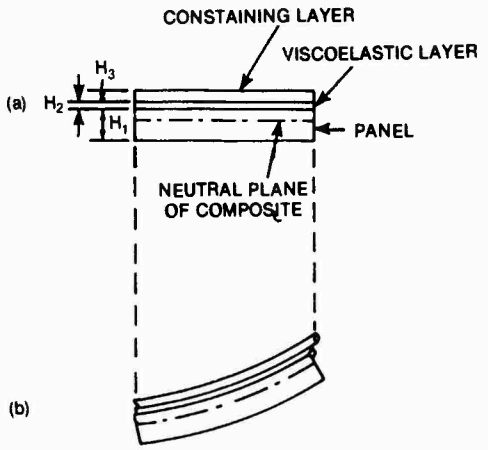

Figure 5.19. Constrained Viscoelastic Layer (with and without Spacing layer, (a) Undeformed and (b) Deformed)

Figure 5.20 shows the curve that results when η is plotted against X, using β and Y as parameters.

In many cases, especially where the weight factor is important, damping of a part of the plate can be nearly as effective as the full treatment. Strain energy storage in a simple viscoelastic layer occurs mainly by extension, which is greatest at the antinodes and least at the vibrating plate nodes. If continuous lengths of damping material are long enough to be significantly flexed, i.e., by approximately 40 percent of the flexural wavelength, the loss factor will be approximately 80 percent of that for a fully covered panel.

5.5.3 DECOUPLERS AND REFLECTORS

When a soft material is placed in water between a sound source and a sensor, the high compliance, i.e., low relative impedance, of the material prevents the sound energy from going through the barrier. Instead, it is reflected back in the direction of arrival.

The *soft* material may consist of an elastomer, such as rubber, having holes or voids to capture air; this makes the material soft

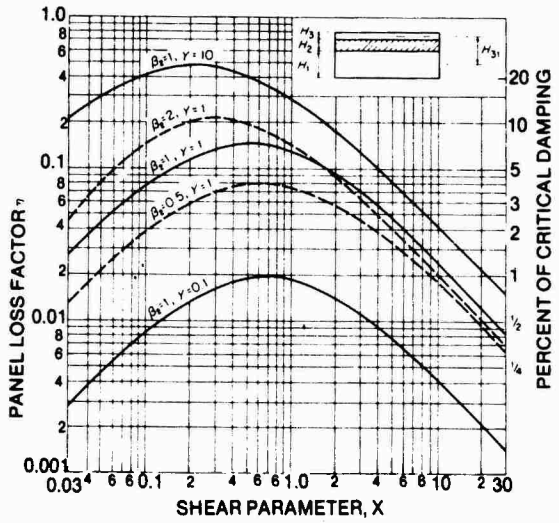

Figure 5.20. Constrained Viscoelastic Layer Loss Factor

compared with water. Another method is to separate two plates by a series of springs to make the unit compliant. The elastomer coating approach will be the principal concern here. The design or selection of such coatings is contingent upon the pressure, temperature, and frequency at which it must be effective.

Anechoic coatings were developed by German engineers during WW II. Current performance requirements for decouplers are, of course, more stringent because they must operate at lower frequencies and over larger bandwidths. Decoupler materials must be more dynamically compliant than those that were effective at typical WW II sonar frequencies.

Decoupler material behavior often depends on a complicated coherent interaction between different modes of vibration. The effectiveness of the material can be quantified in terms of the impedance mismatch between it and the uncoated hull. Important factors are the equivalent stiffness, K_c, and the loss factor, η_c. By definition,

$$K_c = E/h.$$

The relationship shows that there are two methods of increasing the dynamic compliance. The first is to use thicker coatings, which increases h.The second is to reduce the stiffness, or storage modulus.

Reducing the modulus by introducing air into the elastomer increases the compliance and decreases the weight of a given thickness. Although this enhances performance, sensitivity to increased depth increases. The greater pressure makes the air cells smaller and reduces their compliance; the reduced thickness that results also degrades performance.

Increasing the thickness of the blanket increases the effective frequency range. A coating that performs well at 10 kHz would have to be ten times as thick to perform equally at 1 kHz. The emphasis in decoupler design is increased dynamic compliance while maintaining static stiffness. One method is to mix two materials, one to support the static load and the other to provide compliance.

The performance of rubber-air cell materials depends greatly on the size and geometric arrangement of the cells in the matrix. The air cells create resonances and provide coupling mechanisms that absorb energy or divert it to a mode that does not radiate sound.

The decoupling and reflecting material categories are

1. rubber-air cell (compliant rubber with air cavities),
2. air-compensated (air-sandwich of two pressure compensated sealed plates),
3. composite (one forming a matrix, the other a binder),
4. compliant-element (flexible plates or tubes to reflect incident sound through induced flexural waves in plates or tubes).

5.5.3.1 Rubber-Air Cell Materials

Rubber-air cell material acts as a spring, in which the compliant element is low modulus rubber being deformed in the thickness dimension. The compliance, which is a measure of acoustic performance (i.e., the higher the compliance the higher the radiation reduction), is a function of the effective softness of the rubber in the thickness dimension. The softness is caused by compression, bending, and shear in the rubber matrix surrounding the air cells and by compression of the air.

The coating may be a uniform layer having a pattern of cavities that reduces the effective

modulus (see figure 5.21). Such coatings are available commercially (see table 5.2 for a listing of this and other materials). Increasing the thickness of rubber-air cell materials improves their performance by further reducing transmitted energy and increasing the effective bandwidth on the low side.

Uncompensated coatings are attractive because of their mechanical simplicity but acoustic performance decreases with depth. Such performance degradation is the result of pressure compressing the air cell volume and the tendency of the air to diffuse after extended periods of being submerged.

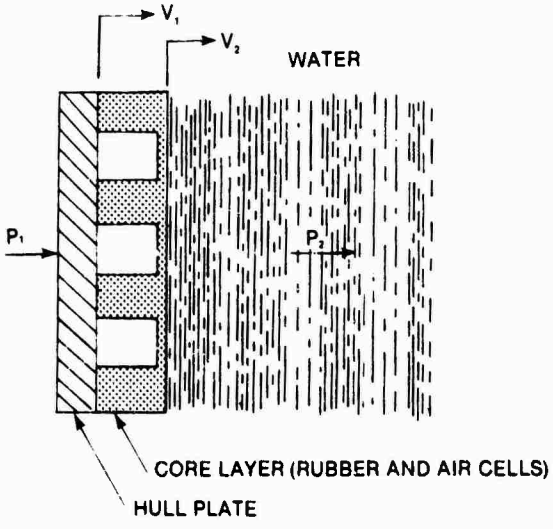

Figure 5.21. Rubber/Air Cell Material

If the rubber-air cell coating is approximated by a massless spring, the effective coating stiffness per unit area, K_c, is

$$K_c = \gamma(P/h),$$

where

γ = specific coating design constant,
P = hydrostatic pressure, and
h = layer thickness.

Compliance is defined as the reciprocal of coating stiffness, $C = 1/K_c$. The layer thickness, h, varies as 1/P unless the air cells are pressure compensated. Thus, the stiffness of the uncompensated air cell increases as P^2. Expressing K_c in terms of depth and of the air cell thickness at the surface yields

$$K_c = (9\gamma/h_o)[(33 + D)^2]10^2,$$

where D is expressed in feet, h_o is expressed in centimeters, and γ is 1.4 for an air layer. The stiffness of the matrix is not included.

Table 5.2. Summary of Some Elastomeric Sound Treatments

Designation	Source
Type II Damping Tile	MIL-P-23653
MIRL-3 Damping Tile	MIL-T-24487
RAL Absorber Tile	MIL-R-23074
RAL-1 Absorber Tile	MIL-R-23074
AA-4 Absorber Tile	MIL-A-24486
A-80 Absorber Tile	—
SAPER D Absorber	Goodrich
ISOPER Reflector	Goodrich
SOAB Absorber	Goodrich
RA Reflector	MIL-R-23074 (without lead shot)
AD-1 Decoupler-Reflector	MIL-T-24180
AR-1 Reflector	MIL-A-24485
R-81 Reflector	—
ML-D2 Damping Tile	—

The equation for velocity reduction in a fluid filled pulse tube, where the decoupler material is attached to a hull plate attached, in turn, to an acoustic piston radiator, is

$$VR = 10 \log \{[(\rho_o c_o \omega/K_c) + \eta_c]^2/(1 + \eta_c^2) + 1\},$$

where

$VR = 20 \log |V_1/V_2|$,
V_1 = hull plate velocity, and
V_2 = velocity of fluid particles adjacent to coating.

The total stiffness of a coating is obtained by adding that of the rubber matrix to that of the air layer. Because the stiffness of the rubber

predominates, depth sensitivity is less than that given in the above equations. The reduction, however, is usually large.

If air compensation is desired, the design becomes complicated and such coatings are seldom used. The equivalent relationship for the stiffness of compensated air cell material is

$$K_c = (3\gamma/h_o)[10^4(33 + D)],$$

where h_o is held constant by the pressure compensation system. Here again, the rubber matrix stiffness is important to the overall coating stiffness.

Decoupler coating performance depends on its compliance at the desired operating depth and temperature; the performance level can only be determined by testing. It requires ingenuity to develop a composite material that is compliant at the frequencies of interest and sufficiently stiff to resist the ambient water pressure.

5.5.4. ABSORBERS

Anechoic coatings are applied to reduce the detectability of the ship by an active sonar, i.e., to minimize the acoustic energy reflected back to the active sonar. This is done by diverting the reflected wave away from the receiver (through the design of the shape of the ship) and using a coating to absorb incident sound.

The two basic methods of absorbing sound use the characteristics of the sound wave. An acoustic wave has a pressure, P, that is equal to $P_o e^{i\omega t}$, superimposed on the ambient pressure and an associated particle velocity, V, that is equal to $V_o e^{i\omega t}$. In order to attenuate an acoustic wave, a mechanism that dissipates energy when P and/or V fluctuates must be operative. The two factors are physically different and, when appreciable attenuation occurs, one will predominate.

Pressure absorption occurs when the stress on any element of the material is out of phase with the strain during an acoustic pressure cycle. Hysteretic loss results and acoustic energy is converted to heat energy. A substantial loss of this type occurs when elastomeric materials undergo a time-varying shear deformation.

Velocity absorption occurs when propagation takes place in a liquid or gas within a rigid matrix. Viscous losses result as particles are forced through the interstices of the matrix.

The effectiveness of the absorbing mechanisms depends on the rigidity of the surface on which they reside. If a plane progressive wave is incident normal to an acoustically hard surface, i.e., its ρc is much larger than for water, the acoustic pressure will be maximum at the water-material interface and minimum at the quarter wavelength. If the reflecting surface is soft, i.e., its ρc is much smaller than for water, the situation is reversed and there will be a pressure node at the surface and a maximum at a quarter wavelength from the surface. Velocity nodes in such a situation will be pressure anti-nodes, and vice-versa.

In most cases of interest, the thickness of the coating is much less than a quarter wavelength. Hence the coating will be operating in a region of high pressure fluctuation and low velocity fluctuation if it is on the hard surface of a submarine. An hysteretic-type absorber which functions best in a pressure field should be used in this case. A thin, viscous absorber would have to be mounted against a soft backing or be located a quarter wavelength from a hard surface. If the coating is several wavelengths thick, the type of mechanism may be either or both.

5.5.4.1 Simple Homogeneous Anechoic Coating

Figure 5.22 shows a simple homogeneous anechoic coating with the rays depicted obliquely so that they can be distinguished individually. The ratio of reflected to incident sound pressure, P_R/P_i, is given by

$$P_R/P_i = |P_R/P_i|e^{i\theta} = (Z - \rho_o c_o)/(Z + \rho_o c_o),$$

where θ is the phase shift at the interface; the other terms are defined in the figure 5.22. If the input impedance of the coating, Z, is complex, $Z = R + iX$, the absolute value of the ratio, is given by

$$|P_R\ P_i| = [(R - \rho_o c_o)^2 + x^2]^{1/2} / [(R - \rho_o c_o)^2 + X^2]^{1/2},$$

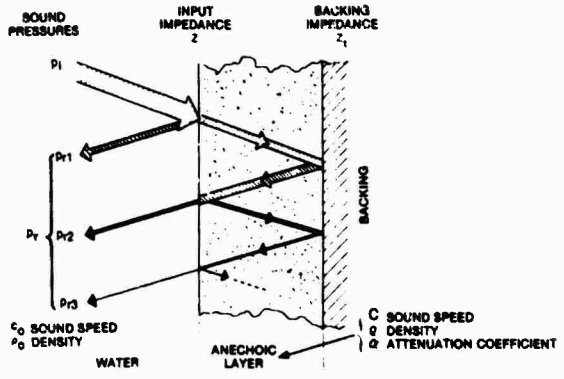

Figure 5.22. Anechoic Layer with Sound Ray Structure

where

$|P_R/P_i|$ = pressure coefficient.

It is customary to express this ratio by the negative of the logarithm of its square, i.e. by $-20 \log |P_R/P_i|$, or the *echo reduction*.

When selecting an anechoic coating there must be a sufficiently good acoustic match at the water-material interface to permit most of the incident sound energy to enter the material. Hence, P_{r1} in figure 5.22 is negligible. There must also be sufficient attenuation so that the vector sum of the rays emerging after passing through the material one or more times, i.e., $P_{r1} + P_{r2} + \ldots$, is negligible.

The input impedance, Z, is determined by the density, sound speed, and attenuation in the coating material, and by the thickness and impedance of the backing material, Z_t. Although the input impedance can be calculated for any value of Z_t, it is convenient to consider the case for $Z_t = 0$ or ∞. The expression for impedance when there is infinite impedance backing is

$$Z = [\rho c/(1 - i\alpha c/\omega)] \coth(\alpha + i\omega/c)d.$$

If the backing impedance is zero, tanh is substituted for coth. Here, α is the decrement per unit distance in the natural logarithm of the amplitude of the pressure or particle velocity for the wave in the material. It is convenient to represent the loss parameter, i.e., $\alpha(c/\omega)$ or $\alpha(\lambda/2\pi)$, by the symbol r. The corresponding decrement in the natural logarithm of the pressure or particle velocity in one wavelength then is $\alpha\lambda$, i.e., $\log (P_x/P_{x+\lambda}) = \alpha\lambda$. It is customary to describe the rate of attenuation with propagating wave distance in terms of the rate of decrement of the decimal logarithm of the intensity. Thus, if intensity decreases by a factor of 10 in 1 m, then, $\alpha' = -10$ dB/m. Hence, $\alpha' = 0.868\alpha$.

When the attenuation is attributable to the loss factor (loss tangent), η, of the material, r and η are related by $\eta = 2r(1 - r^2)$. The input impedance with infinite impedance backing can be calculated using a table of hyperbolic functions with complex arguments or by using

$$\rho c/(1 - ir) = (\rho c)/(1 + r^2) + ir\rho c/(1 + r^2)$$

where $r = \alpha c/\omega$

and

$$\coth(\alpha d + ikd) = (\sinh 2\alpha d - i \sin 2kd)/(\cosh 2\alpha d - \cos 2kd),$$

which results in

$$Z = [\rho c/(1 + r^2)]\{[(\sinh 2\alpha d - i \sin 2kd)/(\cosh 2\alpha d - \cos 2kd)] - i[(r \sinh 2\alpha d - \sin 2kd)/(\cosh 2\alpha d - \cos 2kd)]\} = R + ix.$$

It is convenient to present the above two equations as curves in the complex plane where ρc and r are constant for each curve and kd is the running variable ($k = \omega/c$). The result is a spiral that starts with small kd at $R = +\infty$ and $X = -\infty$, and spirals to an asymtotic point whose coordinates are $R = \rho c/(1 + r^2)$ and $X = r\rho c/(1 + r^2)$.

Sample spirals for a fairly high-loss material ($r = 0.618$) and a comparatively low-loss material ($r = 0.224$), where $\rho c = \rho_0 c_0$, are shown in figure 5.23. As thickness and/or frequency is increased, the spiral approaches the asymptotic point where the layer is effectively infinitely thick. This point is on a line having slope r. In this case, the only ray reflected is P_r (see figure 5.22). The line for decreasing kd asymptotically approaches the line through the origin and has slope $-(1 - r^2)/2r$.

Note that the curves of constant echo reduction are circles centered on the real axis. Some reference circles are shown in figure 5.24.

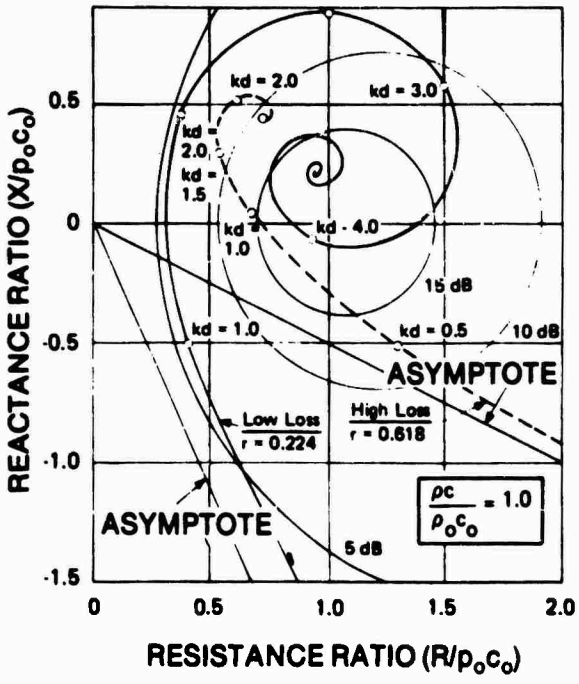

Figure 5.23. Impedance Spirals for Two Loss Parameters

The spirals are similar in shape and proportional to ϱc, which is a factor of both the real and imaginary parts of the impedance.

The value R - $\varrho_o c_o$ can be eliminated by the appropriate choice of ϱ, c, and r. However, the X term will always have a finite value if there is any loss present. A perfect acoustic match for a simple, infinite thickness coating cannot be made regardless of how the parameters are adjusted.

For a given loss parameter, r, the value of ϱc that will yield maximum echo reduction for the infinite thickness case can be obtained (see figure 5.24) from

$$\varrho c = (1 + r^2)^{1/2} \varrho_o c_o .$$

Curves of the echo reduction of an *infinite thickness* layer as a function of ϱc for various loss parameters are shown in figure 5.25. The maximum echo reduction that can be obtained using a simple layer absorber under these conditions depends on the loss parameter .

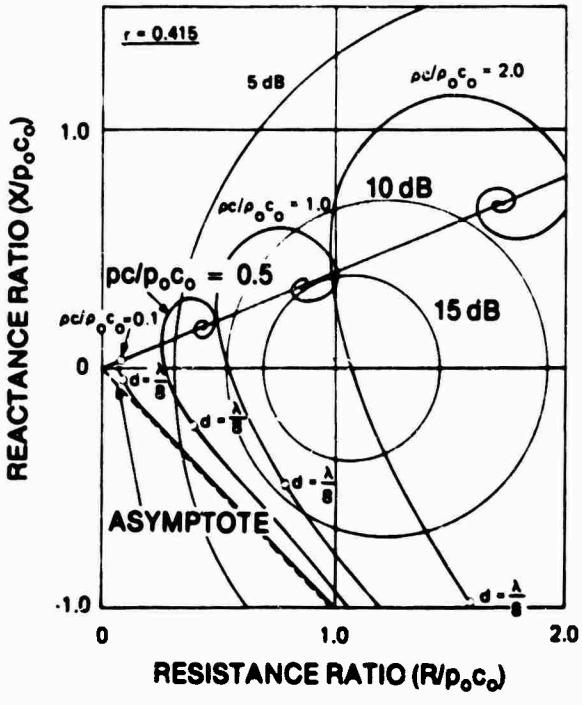

Figure 5.24. Impedance Spirals for the Same Loss Parameter But Different ϱc/$\varrho_o c_o$ Values

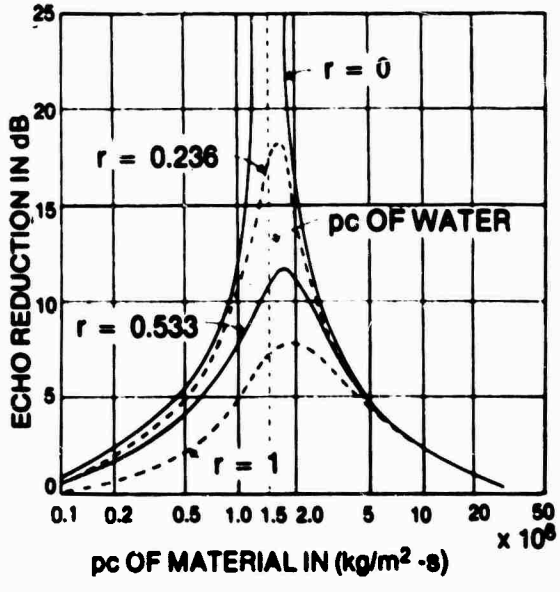

Figure 5.25. Echo Reduction of An Infinite Thickness Layer versus ϱc for Various Loss Factors

Variations of maximum echo reduction with r are illustrated by the impedance spiral in figure 5.23, where the asymptotic point is on a line passing through the origin and having slope r. The location of the point on this line depends on the value of ϱc. The low-loss curve spirals down to approximately 17 dB and the curve for the high-loss material approaches 11 dB.

The above discussion applies only to simple coatings; those containing air bubbles or other variations require more complicated treatment. The acoustic impedance can be computed readily from measured echo reduction and phase shift values at the interface using the equation for P_R/P_i.

5.5.4.2 Broadband Absorbers

For an anechoic structure to operate well over a broad band of frequencies, the thickness of the absorbing layer must be such that it is, effectively, infinitely thick, i.e., the only appreciable reflection is from the water-material interface. This means that the operating region is in the vicinity of the asymptotic point of the spiral (see figure 5.23). To achieve this objective while maintaining a reasonable thickness, it is necessary that high attenuation and a good acoustic-water match exist. Although an elastomer filled with air holes is a high attenuation material, its ϱc is much lower than that of water and (see figures 5.24 and 5.25) will provide only mediocre echo reducing performance. The only remedy would be to add a transition layer characterized by slightly different acoustic properties, but it would have to be of a thickness approaching the wavelength of sound at the lowest frequency of interest.

A transition material can be obtained by using small layers of slightly different properties, but the procedure is difficult. A more feasible method is to use wedges, or pyramids, mounted such that the apexes are pointing toward the incident sound and water fills the spaces between them. The construction is economical, but the irregular outer surface makes it an unlikely candidate for coating submarines. It is, however, useful for lining the sides of anechoic test tanks.

The absorber shown in figure 5.26 is constructed of thin, sound absorbing wedges. Figure 5.27 shows the effect varying the tapered

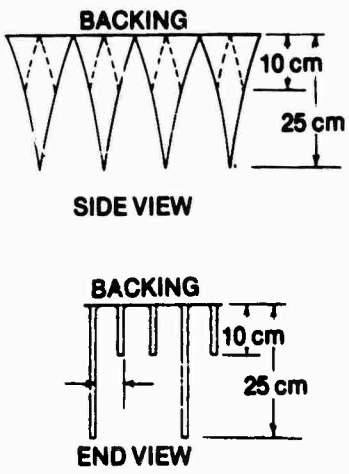

Figure 5.26a. Mounted

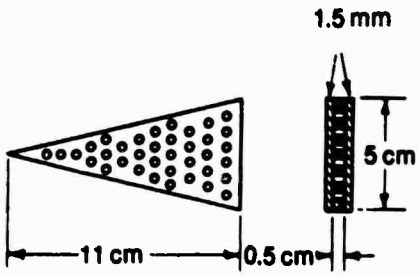

Figure 5.26b. Hole Pattern

Figure 5.26. FAFNIR Wedge

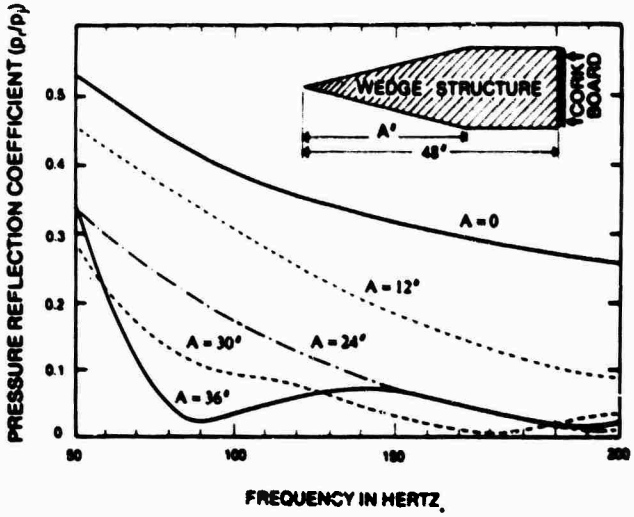

Figure 5.27. Gradual Transition Matching

length of the wedges has on frequency range. The design of this *FAFNIR* coating is relatively simple. A lossy material is cut into wedges sufficiently long for the low frequency range and then arranged with varying spacing for the high frequency range.

5.5.4.3 Resonance Absorbers

A good example of a resonance absorber is the *ALBERICH* coating, which consists of two 2 mm thick layers of rubber cemented together. The inboard layer has a pattern of macroscopic air-filled holes of 5 and 2 mm diameter and the outer layer, which has no holes, acts as a cover plate (see figure 5.28). The coating was designed for the 9 to 18 kHz octave range and is made of Buna S rubber with 40 parts carbon black.

The ALBERICH can be explained in terms of two resonant circuits, one associated with the 5 mm holes and the other with the 2 mm holes. The construction, air filled holes in rubber, is a logical approach to the design of anechoic coatings mounted on rigid walls. The most serious problem is the sensitivity to pressure, which reduces the size of the holes and, thus, the resonant qualities.

5.6. DOME DESIGN

The term *dome* refers to a vaulted structure. It probably originated when rounded projections were first installed to protect protruding hydrophones. Today the term encompasses any structure housing arrays or hydrophones, whatever the shape, and sometimes even describes the supporting structure and array. Domes may now comprise the whole front portion of a submarine or the bulbous bow of a surface ship. They are either conformal domes, i.e., conforming to the general shape of the ship, or appendage domes, i.e., protruding into the water flow around the ship.

A stationary hydrophone or projector needs no protection from water flow or wave action. However, when it is mounted on a ship and moved rapidly through the water, it is subject to physical damage and to flow and own ship noise.

Hydrophones and projectors are protected from such forces by enclosing them in a dome

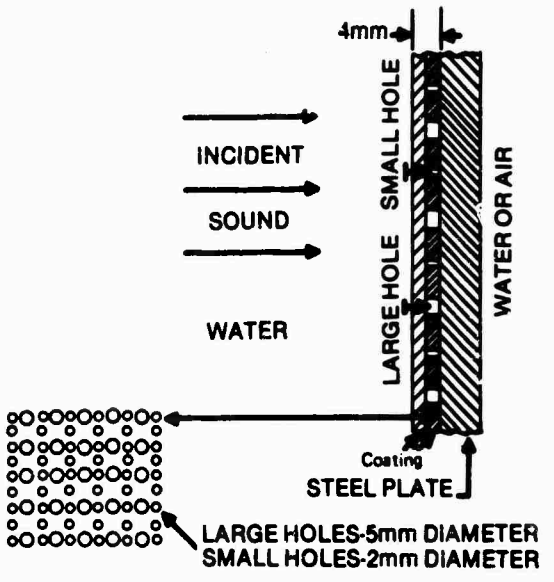

Figure 5.28. Hole Arrangement for ALBERICH Coating

that either protrudes from the shell of the ship or is part of the faired hull shape. Unfortunately, even the best dome cannot provide the acoustic performance level of a stationary hydrophone in a quiet sea.

When designing and installing sonar domes, the emphasis is on protecting the transducers and minimizing the negative aspects of this action. The interposition of the dome, or window, reduces the signal level because it reflects from the dome surface and there is attenuation of the sound in the material. The attenuation is not particularly objectionable because external noise is also attenuated at particular frequencies. However, if the hydrophones hear unattenuated self-noise at the same frequencies, SNR is reduced.

The window should be made of tough, hard to damage, material because hydro-elastic excitation or flutter around a damaged portion can cause noise. It can also be excited by the flow of water past its surface and radiate to the hydrophone if it is constructed of an elastic material, i.e., steel or fiberglass. A highly damped, low modulus material, such as rubber, reduces flow noise problems.

The fluid inside the dome may not have the same speed of sound as the external water. This results in refractions and focusing, which

confuses the beamformers and gives erroneous bearings. Also, the continuously changing temperature of the sea water causes problems.

The hull of the ship *masks* some bearings and the sonar system is blind in those directions. For example, the bow sonars of some submarines and surface ships are blind astern.

The dome may be equipped with baffles to reduce the effect of own ship machinery noise on the sonar array, thus increasing the SNR. However, the baffles will mask some aft bearings. Flat or curved surfaces inside the dome also reflect sound, especially if the construction is such that echos reverberate within it. This creates spurious signals that make detection and bearing determination difficult.

Dome design depends, to a great extent, on the frequencies of interest. For example, a material and thickness that is satisfactory for 3 kHz operation could be unsatisfactory at 20 kHz because the loss might be 4- to 5-dB higher. Similarly, materials that are highly absorbent at 4 kHz may have little value at 1 kHz. The same is true of the transmission and reflection properties.

At low frequencies, where large arrays and domes are required, the wave lengths are large and attenuation through the material is low. The thicker windows required for mechanical strength do not, therefore, cause unacceptable attenuation losses at these frequencies. Thus, design becomes a compromise between acoustic hydrodynamic and structural requirements and on the location, size, operating frequency, and shape of the array.

Protection for an acoustic projector or active element is, in some ways, simpler than for a receiving array. Relatively low level interferences, such as self and flow noises, do not affect their performance because the source intensity is so high. However, signal distorting reflections are a major concern.

5.6.1 DOME LOCATION

The location of an acoustic antenna-dome system is the first concern in sonar system design. It must be located in the quietest area of the ship because SNR is the most important consideration in total system design. For most ships, self-noise in the sonar system band of interest is lowest forward because most acoustic sources are located aft.

The next consideration is azimuth and D/E coverage. Generally, depression angles of 20° to 30° and elevation angles of 10° are acceptable. In azimuth, 360° coverage is desired for detection, fire control, and communication purposes.

The azimuth coverage is achieved by locating the arrray low enough so that after bearings having a slight depression angle will clear the hull. *Chin* mounts on submarines and low bulbous sonar domes on surface ships are the result. However, machinery noise in the aft bearings greatly reduces their value. Moreover, noise on the aft beams reaches all of the hydrophones and reduces the SNR of the entire array. An acoustic baffle aft of the array to attenuate the noise will improve the performance somewhat. Generally, the loss of some aft-looking azimuth angles is accepted as the tradeoff for better overall system performance.

Surface ship bow arrays are also located low in the ship to ensure that they remain submerged as much as possible. Current submarine domes are located on the axis of the hull.

An *eyebrow*, or horizontal baffle above the antenna on a submarine protects the forward array from the own ship noise reflected back from the surface of the water. Bottom reflections when operating in shallow water also present a problem.

5.6.2 DOME SHAPE

When the general location for the array has been determined, the dome configuration is investigated. At this time, consideration of hydrodynamic shape is important. For a submarine, drag is basically a function of wetted surface so the dome should be designed to minimize that surface.

At high speeds, surface ships are limited primarily by ***wave making resistance***. Bulbous bows may be used to reduce such drag. However, the drag may increase at cruising speeds so the design should be the result of a well considered compromise.

5.6.3 DOME ACOUSTICS

The most serious acoustic considerations in dome design are illustrated in figure 5.29. They are

1. transmission through dome wall material,
2. compressional and flexural coincidence angles in dome wall,
3. flow excitation,
4. refraction,
5. internal reflection,
6. structure-borne noise,
7. waterborne noise,
8. reverberation
9. cavitation
10. bubbles, and
11. fouling.

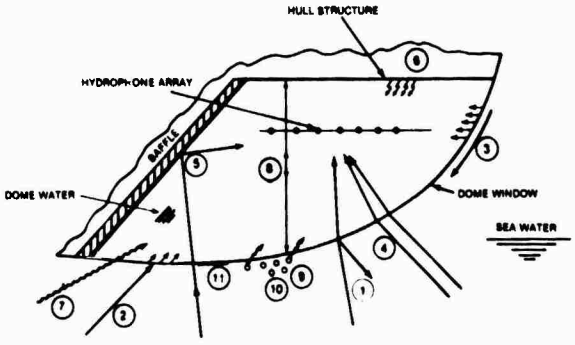

Figure 5.29. Acoustic Problem Areas in Dome Design

5.6.3.1 Transmission Through Material

Dome materials have included bronze, stainless steel, carbon steel, glass reinforced plastic (GRP), and reinforced rubber.If the acoustic frequency-material thickness product remains small (see Section 3.2.5), reflection losses remain small and most of the energy is transmitted through the dome. However, a small thickness will probably create structural problems. For example (see figure 3.67), if it is desireable for the transmission loss at normal incidence to be below 3 dB, the frequency-thickness product (kHz/in.) of a steel dome must be below 2.3. Then, because sonar systems should be useful up to 10 kHz, the thickness of the plate should be less than 0.6 cm. Since dome dimensions may be on the order of tens of meters, the plate would have to be supported by frames spaced to provide adequate support, which would present problems in terms of signal distortion, radiation from hard points, and local attenuation.

If GRP is used instead, the frequency thickness product at 3 dB is 9.75. This means that the GRP thickness can be four times thicker, i.e., 2.5 cm. Because the plate stiffness varies as the cube of its thickness in proportion to its modulus, the stiffness ratio of the windows is

$$E_s I_s / E_g I_g = E_s t_s^3 / E_g t_g^3$$
$$= 30{,}000{,}000(0.23)^3/2{,}200{,}000(1)^3 = 0.166,$$

assuming that

E_s = steel = $30(10^6)$ and
E_g = GRP = $2.2(10^6)$,

and the fiberglass dome is roughly six times as stiff as the steel. *(Note that the steel and GRP moduli vary for different formulations; the values used here are considered representative.)* This additional stiffness could make it possible to design a monocoque fiberglass dome that does not require stiffening.

Rubber, which has a relatively small modulus and, therefore, little stiffness, is unsuited as a self-supported monocoque structure. However, it can be designed for a ρc value close to that of water and used in applications for which small transmission losses are required.

Rubber domes can be built using the same principles used for automobile tires, i.e., steel, fiberglass, or other high strength reinforcing cords are added and the rubber is vulcanized to provide a strong material. The dome can be pressurized to hold its shape.The result is improved sound transmission and reduced flow noise excitation.

5.6.3.2 Coincidence Angle

Coincidence angles (see Sections 3.2.5.2 and 3.2.5.5) will exist if the flexural, or compressional, wave speed is faster than the speed of sound in water, i.e., if the wavelength for a given frequency is larger. Therefore (see Section 3.2.2.3), a steel plate would have to be thicker than 1.9 cm for a coincidence angle to exist at 10 kHz, which is much thicker than needed.

To make this applicable to GRP materials, wavelengths must be changed by the ratio

$$\lambda_G/\lambda_S = (E_G/\varrho_G)^{1/4}/(E_S\varrho_S)^{1/4}$$
$$= [(2.2/1.8)/(30/7.7)]^{1/4} = 1.05/1.40 = 0.75,$$

assuming that

$E_G = 2.2(10^6)$,
$E_S = 30(10^6)$,
$\varrho_G/\varrho_\omega = 1.8$,
$\varrho_S/\varrho_\omega = 7.7$, and
ϱ_ω = mass density of water.

Therefore, the wavelength in figure 3.36 for a GRP thickness of 2.5 cm would be equal to that of 2.5 cm of steel multiplied by 0.75. Thus, a fiberglass plate would have to be more than 5 cm thick for a coincidence angle to exist.

The speed of sound in a GRP fiberglass plate is between 2.5 and 4.900 km/sec depending on the formulation; that in steel is 5.03 km/sec. A compressional coincidence angle may exist in both GRP (17° to 37°) and steel(17°).

The compressional coincidence angle can create noise spikes at θ_{cc} for linear arrays behind flat windows. Partially coherent noise can also result when curved GRP or steel domes are used and the geometry will confuse diagnosis. The generation of these waves in the dome plating cause reflections from fixed support points, or other discontinuities; so it is desirable to damp such structures without greatly decreasing their transmission coefficients.

Because of its low modulus and, hence, low sound speed, reinforced rubber is not subject to flexural and compressional coincidence angles.

5.6.3.3. Flow Excitation

Because domes and windows are immediately adjacent to the water flow, they are subject to turbulent flow pulsations (see Section 2.2.7). Therefore, an important flow noise consideration is the roughness of the skin; it triggers the turbulent flow that puts energy into the boundary layer and removes energy from the flowing water at acoustic frequencies (see figure 5.30).

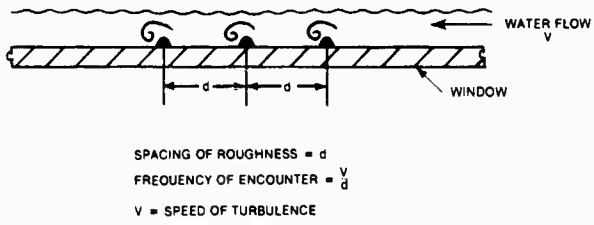

Figure 5.30. Turbulence Effects

Consider speeds of 20 to 30 knots. The speed of the water turbulence may be on the order of 13m/sec. If the concern is with noise in the 2 kHz band, imperfections with 0.65 cm spacing would generate a 2 kHz frequency. Similarly, turbulence eddies 0.65 cm apart that sequentially disturb one protuberance would generate the same frequency. This example is intended to illustrate that excitation at frequencies of interest can readily occur. The quasi-random nature of roughness and eddy formation will generate a wide band of frequencies in turbulent flow similar to those discussed in Section 2.2.7.

Even the smoothest sonar dome surface is subject to biological growth. The most effective treatment is to coat the dome with rubber impregnated with an anti-fouling compound that gradually *leaches* into the surface and inhibits marine growth. The method is applicable to rubber, steel, and GRP materials.

5.6.3.4. Refractions

Sonar domes are usually filled with water. In the rubber domes used onboard surface ships, the water is pressurized and contained; in most other cases it is circulated. Both methods result in acoustic refractions caused by a difference between the speed of sound in two materials. According to Snell's Law (see Section 1.3.6), since the speed of sound in fresh water is ≈ 1481 m/sec and in salt water ≈ 1500 m/sec (if θ = angle from the normal), then

$$(\sin\theta_1)/c_1 = (\sin\theta_2)/c_2 = [\sin(\theta_1 + \Delta\theta)]/c_2$$
$$= (\sin\theta_1 \cos\Delta\theta + \cos\theta_1 \sin\Delta\theta)/c_2,$$

which, for small $\Delta\theta$, i.e., where $\cos\Delta\theta \approx 1$, becomes

$$\Delta\theta = \sin^{-1}(\Gamma_c \tan\theta_1),$$

where $\Gamma_c = (c_2 - c_1)/c_1 = \Delta_c/c_1$. For the above case,

$$\Gamma_c = (1500 - 1481)/1500$$
$$= 19/1500 = 0.0137.$$

Hence, θ = 20, 40, 60; $\tan\theta$ = 0.364, 0.839, 1.732; and $\Delta\theta$ = 0.265, 0.61, 1.26 (degrees).

The refractions depend on the incidence angle and vary at different points on a curved surface. The wave front loses coherence and the signal contains phase fluctuations (see Section 1.11.7).

The variation of sound speed with temperature is given by

$$c = 1499 + 4.59T - 0.053T^2,$$

$$dc/dT = 4.59 - 0.106T,$$

and

$$\Delta c/c_1 = (4.59 - 0.106T)\Delta T/1500,$$

where T = °C. At zero degrees, c becomes

$$\Delta c/c_1 = (4.59)\Delta T/1500.$$

Thus, a temperature difference of 4.1° between the water inside and outside the dome creates velocity difference equal to that of fresh water. The result is that refraction occurs when the ship encounters rapid changes in sea water temperature; e.g., when entering or leaving the Gulf Stream or changing depths, the temperature of the water in the dome changes far more slowly.

5.6.3.5. Reflections

Most domes are subject to reflected acoustic energy from internal structures. Figure 5.31 shows incoherent reflections originating from a rounded bulkhead, which reduce the SNR at the beamformer output. The coherence of the false signals in figure 5.32 is such that a false target on a spurious bearing is displayed (see figure 5.33).

Figure 5.32 illustrates a method used to disperse the coherent reflections. Vertical strips of steel having an acoustic absorber cemented to both sides are randomly spaced to absorb and

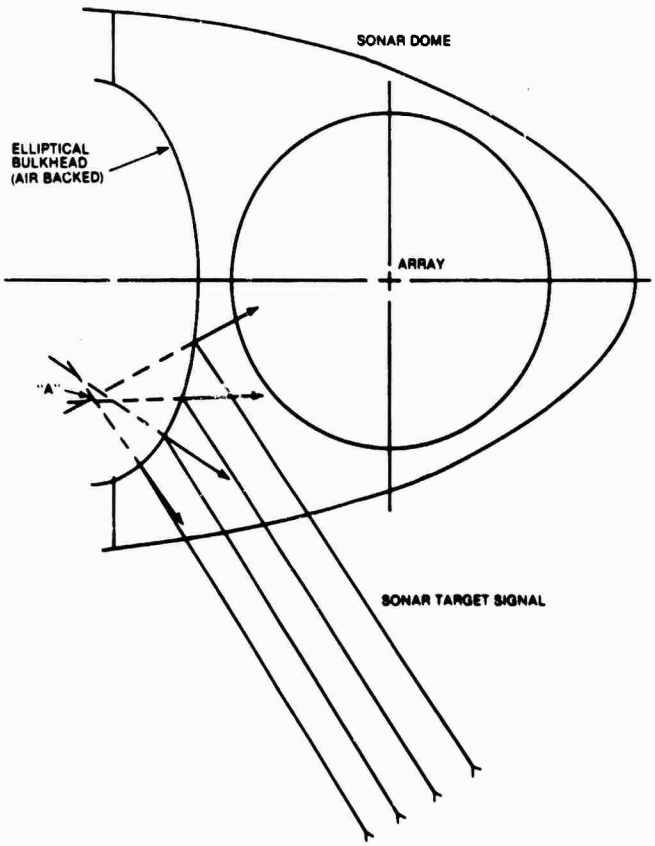

Figure 5.31. Reflections from an Elliptical Bulkhead

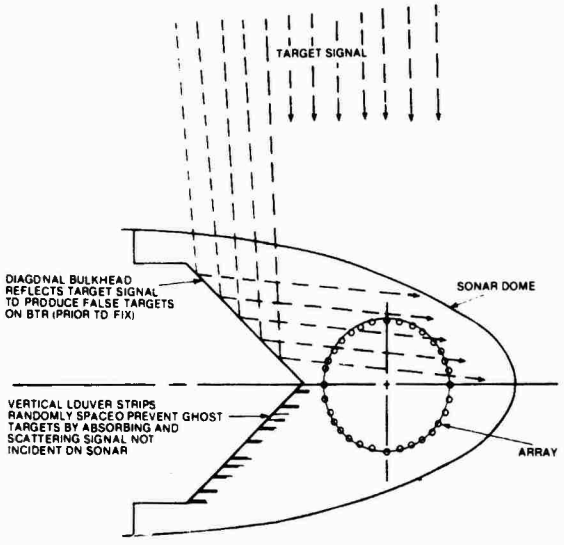

Figure 5.32. Coherent Reflection Compensation

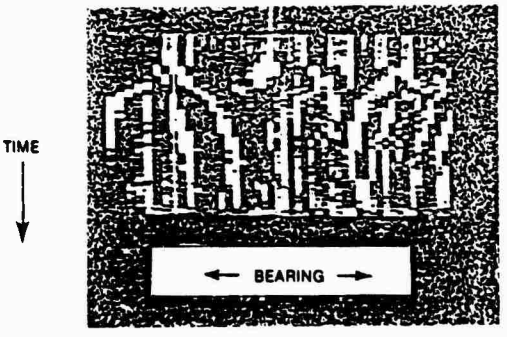

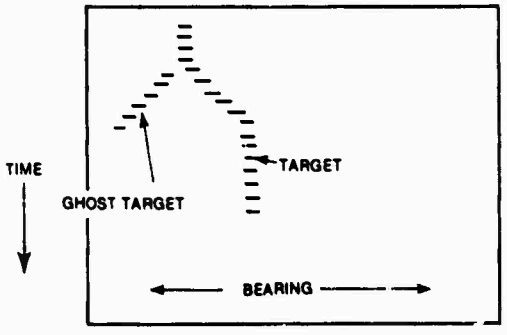

Figure 5.33. Ghost Target Display

scatter signals that are not incident on the sonar array. The random spacing makes the reflected energy incoherent.

The scattering of signal energy from structures or baffles generally create noise that is more coherent than theoretical random noise and causes greater SNR degradation (see Section 1.11.8). Similarly, if there are hydrophones in the ballast tanks, air flasks, structures, and *lead pigs* will cause spurious signals; air flasks resonate and lead pigs cause partly coherent reflections. Figure 5.34 presents various sources of this nature.

5.6.3.6. Structure-Borne Noise

Structure-borne noise directly affects SNR. It is difficult to predict without referring to previous measurements made in similar situations. In relation to domes, such noise is from locally hydrodynamically excited rattles, from machinery noise, or flow induced.

Among the methods to attenuate structure-borne noise is to support the hydrophones on elastomer mounts, as shown in figure 5.35a, or to fix them to a steel plate supported by sound mounts, as shown in figure 5.35b. The sound-mount approach interrupts the acoustic path by two ρc mismatches, one from the plate to the mount and one from the mount to the hydrophone. A baffle between the structure and hydrophones is required to prevent the sound from bypassing this route and reaching the hydrophone through the water.

For high frequencies, a reasonably thick steel plate provides a ρc mismatch and acts as a baffle that will reflect the acoustic energy back to the hull (see Section 3.2.4). The steel plate reflects the signals in-phase (high impedance baffle) and signals at contiguous hydrophone are increased in intensity (see Section 3.2.4.4). However, the steel plate would have to be unrealistically thick for many frequencies of interest.

An alternative to a high impedance baffle is a low weight, low impedance baffle. Here, however, the reflected energy is out-of-phase. A suitable baffle can usually be obtained (see Section 3.2.4.4). Another method of reducing structure-borne noise is to use highly damped structures near the hydrophones.

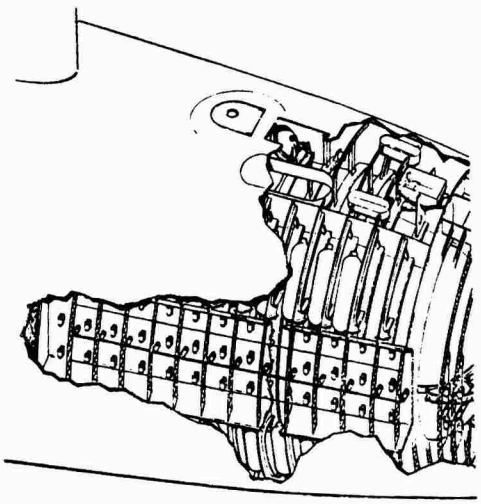

Figure 5.34. Complex Structural Reflective Surfaces

Figure 5.35a. Individual

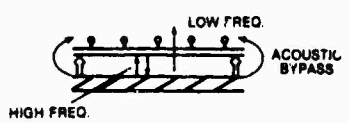

Figure 5.35b. Array

Figure 5.35. Hydrophone Mounting Methods

5.6.3.7. Waterborne Noise

All possible waterborne paths must be considered in dome design. Typical paths are from

1. the structure via the water,
2. machinery via surface or bottom reflection (see figure 5.36),
3. machinery along the hull boundary, and
4. excited dome through the water.

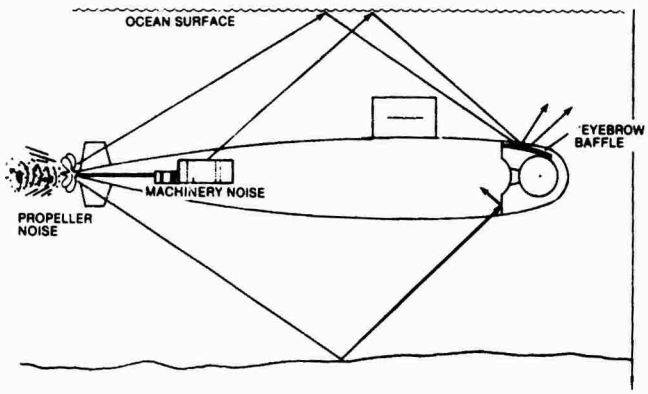

Figure 5.36. Waterborne Noise

The structure to hydrophone path can be attenuated by damping the structures in and near the dome and by baffling. The baffles must be carefully located and designed to prevent signal cancellation at the sensors (see Section 3.2.4.4). Bottom and surface reflections are difficult to attenuate. Arrays are located to avoid these reflections as much as possible and baffles such as those shown in figure 5.36 are employed.

Although it is difficult to explain theoretically, noise does travel along the skin of the ship. Damping and/or baffling adjacent to domes or arrays are used to attenuate such noise.

Excited domes can be a primary source of array noise because of their proximity to the hydrophones (see Sections 2.2.7 and 3.2.5.5). In this case, baffling reduces the signal as well as noise. Damping, without increasing the signal attenuation, appears possible using elastomers.

5.6.3.8. Reverberation

An acoustic wave entering through the dome window or from an adjacent structure reflects from one side to the other in a reverberant fashion. This energy decays by leaking through the window or the hull of the ship. The greatest loss is through the window because the hull is air-backed and, hence, reflective. If the reverberant energy does not decay rapidly, there

will be serious signal degradation. Windows having low transmission loss minimize the reverberation effect.

5.6.3.9. Cavitation

Cavitation (see Section 2.2.5) affects surface ship bow domes and submarine domes when operated near, or on, the surface. It is a monopole source that is a function of hydrodynamic pressures. Careful design and fabrication minimize this problem.

5.6.3.10. Bubbles

Bubbles (see Section 3.3) resonate at sonar frequencies and are extremely efficient scatterers. Also, they greatly reduce the impedance of local water. Hence, bubbles on the face of a transducer or hydrophone cause the impedance match to the water to be lost and output drops dramatically. When they sweep around the sonar dome, their scattering properties attenuate active transmission and passive reception.

5.6.3.11. Anti-Fouling

Marine fouling can seriously degrade sonar system performance by attenuating and distorting incoming signals and by creating turbulence that aggravates flow noise. A rubber layer impregnated with anti-fouling material is the best available defense.

5.6.4. HYDRODYNAMIC FORCES AND STRUCTURAL CONSIDERATIONS

Hydrodynamic forces cause stress in domes and turbulence that excites them. The principal forces usually occur when the ship is moving at an angle to the incident water and the dome is, effectively, a lifting surface. The flow velocity on the dome is often higher than ship speed because its location may be in positions where water velocity is augmented by the flow around the ship (see figure 5.37).

Forces on the dome should be obtained by model testing. In lieu of model testing, however, the basic hydrodynamic force equation can be applied for the lifting force, F_L, i.e.,

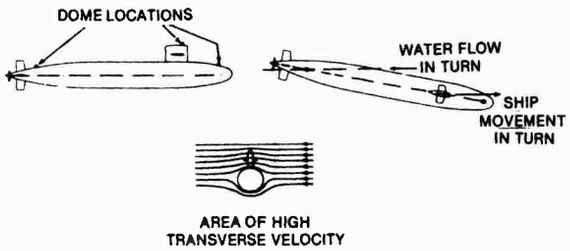

Figure 5.37. Flow Velocity Effects

$$F_L = (\varrho/2)v^2SC_L,$$

where

C_L = lift coefficient,
S = lateral dome area,
v = $1.3(v_S)$, and
v_S = maximum speed.

Figure 5.38 provides lift coefficients for a 20° angle of attack that is a conservative estimate

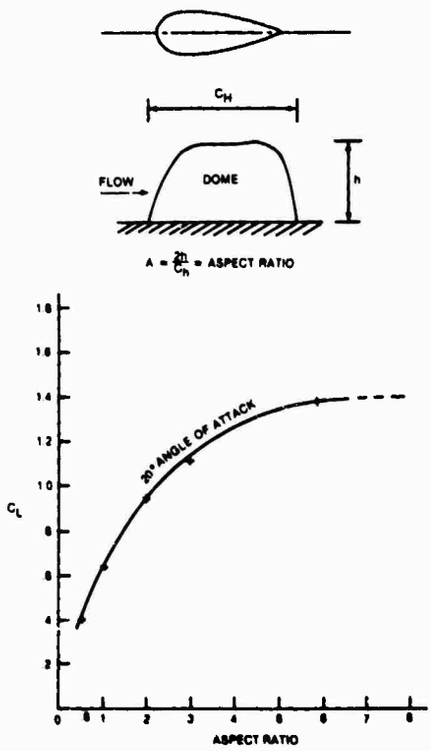

Figure 5.38. Approximate Lift Coefficient for 20° Angle of Attack

for a hard turn. Dome drag can be added, but viscous drag is small compared with lifting force for most streamlined shapes. The estimate is used to determine forces and moments on the dome and its foundation and these data, in turn, are used to determine material stresses. A generous saftey factor should be applied when selecting scantlings for such domes.

Domes should also be able to withstand a *waveslap* load of 4870 kg/m² in any direction. Surface ship domes constructed of steel reinforced, water inflated rubber have proven satisfactory.

5.7. CONFORMAL ARRAYS

Conformal arrays either conform to the shape of the hull or approximate it. Generally they are too large to fit conventional domes and must be located external to the ship. As sonar ranges increase and low frequency passive search becomes more important, the beamforming aperture obtained by conformal arrays provides advantages over those confined to domes. Also, refraction and reflection effects are small for these arrays.

A disadvantage is that the hydrophones are located close to the skin of the ship. In addition, the arrays are so large that portions may extend to high noise areas (see Section 1.11.6).

5.7.1. LOCATION

Comformal array locations are shown in figure 5.39. Figure 5.39a shows a surface ship equipped with a large array on the keel. Figure 5.39b shows a submarine with an array in the ballast tank. The external arrays shown in figure 5.39 c are fastened to the skin of the ship.

Early conformal arrays used minimal acoustic treatment and were subject to large noise variations over their lengths. This degraded performance because the improved SNR that might have been obtained from beamforming was lost to noisy hydrophones.

The arrangement of conformal arrays varies with the ship, the state-of-the- art, and function. They can consist of hydrophones mounted

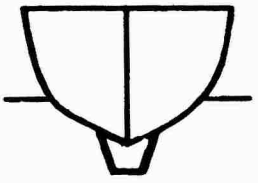

Figure 5.39a. Surface Ship

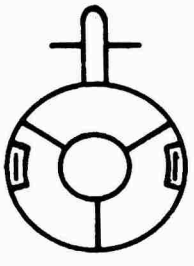

Figure 5.39b. Ballast Tank Array

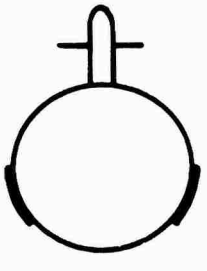

Figure 5.39c. External Array

Figure 5.39. Conformal Arrays

1. in steel bounded recesses in the hull, with sound isolation mounts for the hydrophones;
2. in a line in a main ballast tank;
3. on the hull, with fiberglass protection;
4. on a rubber supported signal conditioning plate, with acoustic baffles behind and a fiberglass window;
5. on an elastically supported signal conditioning plate, with acoustic baffles behind and a rubber window.

5.7.2. BAFFLING

The hydrophones in a large array may be subject to different noise field levels. The approach to this problem is to reduce the self-noise for all of the hydrophones to the lowest operating ambient noise, or at least to maintain the level of the noisiest one to within 3 dB of the general level. Conformal array technology depends heavily on the attenuation of structure-borne noise and flow-noise excitation. It is also desireable to minimize waterborne noise along the skin of the ship.

The lower operating frequencies of these arrays increases the attenuation problem because low frequency noise is difficult to baffle. High and low impedance material used to reflect noise back to the hull also reflects sound on the other side. The placement of the hydrophones is, therefore, critical if nulls at frequency dependent locations are to be avoided.

The field pressure at any point is the sum of the incident and reflected pressure, where the phase and the reduced pressure of the reflected wave caused by transmission or absorption are considered (see Section 3.2.4.4). This applies to all surfaces because the material effects of phase change and reflectivity determine field pressure. The phase change and reflectivity of materials can be derived from the information in figure 3.46 if the real and imaginary parts of the impedance are known.

The curves in figure 3.50 indicate the locations at which reinforcement and cancellation occur. Note that the areas of reinforcement exceed those of cancellation and that satisfactory performance over a wide frequency range is achieved when the standoff distance is selected properly. Increasing the incidence angle effectively decreases the standoff distance to the cosine of the angle multiplied by the distance, i.e.,

$$d_e = d \cos \theta = \text{effective standoff.}$$

At angles approaching grazing, the signal at the pressure release surface is greatly attenuated. This is desirable because noise from grazing angles is discriminated against. The acoustic pattern is of little concern on the noisy side of the baffle because it does not affect performance.

The space, weight, effectiveness tradeoff for conformal array baffles is very complicated. Any practical external baffle adds to the size and weight of a submarine. The required thicknesses for steel baffles (see Section 3.2.5.4) and the large standoff distances required for compliant materials make their use, i.e., the use of one or the other alone, impractical. The best approach is to employ a compliant material on the noisy side and a stiff, dense material on the hydrophone side. This provides good low frequency reflection and reasonably small hydrophone standoff.

5.7.3. FLOW NOISE

Flow noise is important to conformal array design because the hydrophones are located near or at the water interface. Domes (see Section 5.3) are sometimes used to protect conformal arrays. However, elastomers, which provide good shear damping properties, are also employed. Rubber may be used for the window because it is characterized by low modulus and high shear damping. Thus, it is unresponsive to the turbulent flow and inhibits transmission of such energy to the hydrophones. Also, rubber formulated with a ρc product close to that of water provides a low loss, high transmission material at acoustic frequencies.

The flow-noise damping properties of rubber are difficult to quantify, but a few inches are satisfactory for most applications. Small thicknesses, e.g., 1/8 in., provide a definite flow noise reduction when used to coat a fiberglass dome.

5.7.4. FOULING

Fouling of external array surfaces by marine growth causes noise and increases drag. The rough surfaces create severe flow noise problems and seriously degrade sonar performance. Preventive measures include anti-fouling paint or a rubber layer. The rubber layer, which is impregnated with anti-fouling material, is prefered because of its relatively long (5 year) effective life. Also, the layer can be recharged by applying anti-fouling fluid to the skin of the ship.

5.7.5. SOUND ISOLATION

Conformal arrays must sometimes be isolated from the hull to avoid structural noise. The most common approach is to support them on rubber sound isolation mounts or to provide equivalent isolation for the array supports.

5.7.6. TELEMETRY

Conformal arrays require a complex telemetry system. The shielded pairs from each hydrophone in an array module are bundled together. Each bundle is then brought to pin connectors at a hull pressure penetration point.The approach is subject to size and weight penalties because of the number of cables. Also, there are losses at the pin connectors caused by electrical and EMI problems if the shielding is poor.

There are alternative telemetry systems (see Section 1.12) employing fiber optics or conventional copper cable technology. Such systems can greatly reduce cable bulk and the number of hull penetrations.

5.7.7. INSTALLATION

Conformal arrays occupy large areas on the skin of the ship and are, therefore, subject to the same environmental influences as the hull. When choosing a location for the array, designers must consider that the (1) maximum beam is subject to damage from contact with tugboats and piers, (2) keel line and bilge areas are subject to blocking loads in drydock, and (3) forward portion is subject to damage when lowering and hoisting the anchor.

Damaged fiberglass windows can be repaired using localized *lay-up* and epoxy treatment. If the surface of a rubber window is nicked or gouged, a new piece is bonded in place and then coated with an anti-fouling layer. In either case the final surface must be smooth.

It is impractical to rebuild or replace the total conformal array because of the large size. For this reason it is fabricated in sections large enough for reasonable initial installation and small enough for reasonable replacement.

5.7.8. SUMMARY

Because of their size, conformal arrays have much better potential performance than domed arrays. Special attention must be given to baffling to reduce self-noise at the hydrophones and to the window material to reduce flow noise. Their location is important to the overall design of the ship and provisions must be made to deal with immense amounts of data.

5.8. EFFECT OF ADDING EQUIPMENT TO SHIPS

When equipment is added to a ship it adds weight, takes up space, requires utilities, and may increase the number of personnel. If installed on the underwater exterior, it will increase drag. Therefore, shipboard installations must provide the maximum performance and minimum negative impact in order to justify their existence.

Equipment installations will be considered here in the context of post-construction and predesign. Alterations during construction involve schedules, equipment, manpower, and design and cost changes and are beyond the scope of this document.

Adding major equipment after construction eliminates some of the design margin. For example, a surface ship will ride lower in the water than intended and margin lead must be removed when weight is added to a submarine. The location of such equipment is important because its fore/aft position affects trim and its vertical position affects stability. If the weight and location exceed the builder's margin, other equipment is removed or the installation can not be made at all.

Attendant problems include excessive generating equipment loads and demands for cooling water that can result in higher operating temperatures for all equipment. In the extreme, loss of adequate stability can lead to the loss of the ship.

The pre-construction addition of equipment is, of course, easier. Spaces can be made larger, the horsepower of the propulsion plant can be increased, and the generating plant can be expanded. Computer-aided design methods when available may be used to determine the

effects of changes on overall design. The following two paragraphs discuss this subject in general.

5.8.1. EFFECT ON SURFACE SHIP DESIGNS

The size of combat ships is a function of armament, maximum speed and, for non-nuclear vessels, cruising speed and range. The sonar system onboard an ASW surface ship represents a significant portion of its armament. It adds weight, personnel, and volume. It requires electric power, cooling water, air conditioning, and influences the hydrodynamic shape of the hull.

During design, a multiplier effect occurs in each area so, for example, adding 1 ton in the conceptual stage can result in an increased weight of several tons. The influence is greatest for high speed ships and for those that have long range and high cruising speed requirements.

A large bow dome affects hydrodynamic performance and the horsepower for maximum speed and cruising. It also influences seakeeping characteristics and maneuverability.

The weight of a ship is catergorized for accounting and estimation purposes. The U.S Navy uses the following categories:

1. hull structure,
2. propulsion,
3. electrical plant,
4. communication and control,
5. auxiliary systems,
6. outfit and furnishings, and
7. armament.

In addition to these weights, the full load displacement includes variable loads such as

1. crew and effects,
2. ammunition,
3. provisions,
4. general stores,
5. potable water,
6. steam plant feed water,
7. fuel, and
8. lube oil.

To determine the effect of added weight, the relationships between various ship parameters must be known. A large percentage of the weight of a ship is directly related to its size. This includes categories such as structure, anchor and handling machinery, bilge and ballast piping, joiner work, rudder, operating crew and crew dependency weights, and so on. For simplicity, assume that the relationship is linear, i.e.,

$$W_s = C_s W,$$

where W = the weight of the ship and W_s = the weight of the size related elements, and the coefficient is on the order of 42 percent of the total weight.

Crew size is determined by the number of men necessary to operate the ship effectively. Therefore, crew weights are, essentially, a function of required horsepower, combat systems, and ship size. For the purposes of this study, the crew and crew dependency weights are assigned to the functional category that they serve, such as ship operation (W_s), power plant operation (W_p) or combat system (W_c).

Propulsion machinery weight is a function of the maximum shaft horsepower (SHP) required. The SHP is, in turn, a function of maximum speed, size, and hull shape. A simplified curve of drag-to-weight ratio versus Froude number is shown in figure 5.40. For range $0.6 < V/(L)^{1/2} < 1.5$, the curve is represented by

$$D/w = 0.014[V/(L)^{1/2}]^{3.62},$$

where

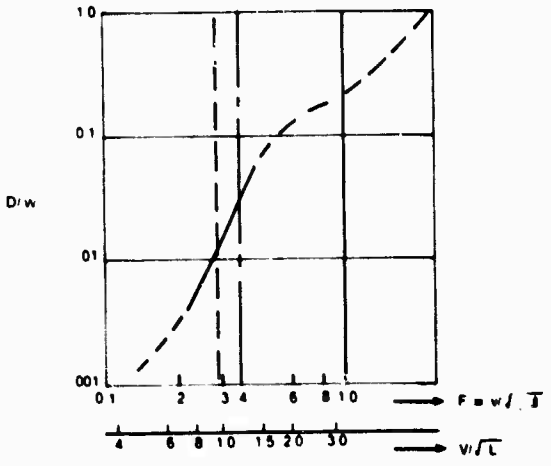

Figure 5.40. Destroyer SHP Drag/Weight Ratio

D = drag (lb), based on installed horsepower,
w = weight (lb),
V = speed (knot), and
L = length (ft).

The required SHP is

$$SHP = 0.014w(1.689V)(V/L^{1/2})^{3.62}/550,$$

i.e.,

$$SHP = (4.3)10^{-5}wV^{4.62}/L^{1.81}$$

since SHP = D(v/550), where v = ft/sec.

Now, assuming that the same type ship is being considered,

$$w = L^3/C$$

or

$$L^{1.81} = (Cw)^{0.60}.$$

Hence,

$$SHP = 4.3 \times 10^{-5}\, wV^{4.62}/(Cw)^{0.60}$$
$$= 4.3 \times 10^{-5}\, w^{0.4}V^{4.62}/C^{0.60}$$

or, if W is in tons, i.e., W = w/2240,

$$SHP = (9.4)10^{-4}W^{0.4}V^{4.62}/C^{0.60}$$

and

$$d(SHP)/dW = (3.76)10^{-4}V^{4.62}/(CW)^{0.60}.$$

Propulsion related weights are a function of the shaft horsepower and the type of propulsion system used. Manufacturing economics dictate that power plants be built in discrete sizes. However, for the purposes of this study, assume that they may be built as a continuous function of the required shaft horsepower. The power plant weight and its derivative with respect to horsepower must be determined from power plant data.

Hence, W_p will be assumed, as well as its derivative, with respect to shaft horsepower, i.e,

$$\delta W_p/\delta(SHP) = F_p,$$

and, thus,

$$\delta W_p/\delta W = F_p(3.76)10^{-4}V^{4.62}/(CW)^{0.60}.$$

Fuel weight (tons) can be obtained by

$$W_F = ES_FSHP_c/(V_c2240),$$

where

E = endurance (nmi),
V_c = cruising speed (knots),
S_F = overall fuel consumption (lb/SHP-hr), and
SHP_c = cruising speed horsepower.

Assuming $V/(L)^{1/2}$ is within the applicable range, the expression for W_F becomes

$$W_F = ES_F(4.192)10^{-7}W^{0.4}V_c^{3.62}/C^{0.60}$$

and

$$\delta W_F/\delta W = 0.4ES_F(4.192)10^{-7}V_c^{3.62}/(CW)^{0.60}$$

or

$$\Delta W_F = [(1.677)10^{-7}ES_FV_c^{3.62}/(CW)^{0.60}]\Delta W.$$

Assuming the weight of the combat system is W_{cs}, the total displacement is now the sum of these categories, i.e.,

$$W = W_s + W_p + W_F + W_{cs}$$

or

$$W = C_sW + W_p$$
$$+ W^{0.4}(4.192)10^7\, E\, S_FV_c^{3.62}/C^{0.60} + W_{cs}.$$

Hence,

$$W(1-C_s) - W_p - W^{0.4}(4.192)10^{-7}ES_FV_c^{3.62}/C^{0.60} = W_{cs}.$$

To find the effect of change in combat system weight, differentiate both sides of the above equation, i.e.,

$$\delta W_{cs}/\delta W = (1-C_s) - \delta W_p/\delta W$$
$$-0.4(4.192)10^{-7}\, ES_FV_c^{3.62}/(CW)^{0.60}$$
$$= (1-C_s) - (3.76)10^{-4}\left(V^{4.62}F_p\right.$$
$$\left. + (4.46)10^{-4}ES_FV_c^{3.62}\right)/(CW)^{0.60}$$

and

$$\delta W = \delta W_{cs}/[(1-C_s) - (3.76)10^{-4}\left(V^{4.62}F_p\right.$$
$$\left. + (4.46)10^{-4}\, ES_FV_c^{3.62}\right)/(CW)^{0.60}]$$

or

$$\delta W = F_m\, \delta W_{cs}$$

where,

$$F_m = 1/[(1-C_s) - (3.76)10^{-4}(V^{4.62}F_p + (4.46)10^{-4}ES_FV_c^{3.62})/(CW)^{0.60}].$$

Since adding any arbitrary weight to the ship has the same weight effect as adding weight to the combat system, F_m applies to any weight added to the ship.

The effect on the weight of changes in speed and endurance is apparent from the above equations. Computer programs used by NAVSEA and other organizations, of course, consider many other factors. Now consider step changes instead of differentials.

Increased volume requirements increase the structure necessary to enclose the space. This may be estimated in terms of tons/ft³. If this value is treated as an arbitrary weight increase and W/100 ft³ = C_v tons, then

$$\Delta W = F_m C_v \Delta(\text{Vol})/100.$$

It is equivalent to increasing maximum and cruising horsepower if an arbitrary drag is added. The additional shaft horsepower is

$$\Delta SHP_m = \Delta D[1.689V/(550)] = 0.0031V\Delta D,$$

where

ΔD = change in drag at maximum speed.

The increase in propulsion plant weight will be

$$\Delta W_p = F_p \Delta SHP_m$$

or

$$\Delta W_p = F_p(0.0031)V\Delta D.$$

The increase in fuel weight at cruising speed is calculated by assuming the added drag is proportional to the velocity squared, i.e.,

$$\Delta D_c = \Delta DV_c^2/V^2.$$

Hence, the increased cruise speed shaft horsepower is

$$\Delta SHP_c = \Delta DV_c^2(0.0031)V_c/V^2$$

and, therefore,

$$\Delta W_F = ES_F\Delta SHP_c/(2240)V_c = ES_F\Delta DV_c^2(0.0031)V_c/V^2(2240)V_c = 1.4(10)^{-6}ES_F\Delta DV_c^2/V^2.$$

The total change, then, is

$$\Delta W_p + \Delta W_F = \Delta D[(0.0031F_pV) + 1.4(10)^{-6}ES_FV_c^2/V^2].$$

This is treated as an added weight and

$$\Delta W = \Delta DF_m[(0.0031F_pV) + 1.4(10)^{-6}ES_FV_c^2/V^2].$$

The addition of one man to the ship, adds 1.14 tons of weight before applying the multiplication factor. Hence,

$$\Delta W = \Delta MF_m(1.14).$$

Additional electrical power requirements can be determined by using, for example, F_E lb/kW for plant weight and F_F lb/(kW-hr)for fuel weight and applying the multiplication factor.

The effect of increasing the top speed is to increase required maximum shaft horsepower and, hence, the power plant weight.

Since $SHP = 9.4(10)^{-4}W^{0.4}V^{4.62}/C^{0.60}$,

$$\delta(SHP)/\delta V = [4.62(9.4\times10^{-4})W^{0.4}V^{3.62}/C^{0.60}]$$

and, since,

$$\delta W_p/\delta(SHP) = F_p,$$

then

$$\delta W = F_p[4.3(10)^{-3}W^{0.4}V^{3.62}/C^{0.60}]\delta V = F_t\delta V$$

and because the effect on ship weight is the added weight multiplied by the multiplication factor, F_M, we have

$$\Delta W = F_m\Delta W_p = F_mF_t\Delta V.$$

The effect of increasing the ship's cruising speed is determined by

$$W_F = ES_F(4.192(10)^{-7})W^{0.4}V_c^{3.62}/C^{0.60}$$

$$\delta W_F/\delta V_c = 3.62ES_F(4.192(10)^{-7})W^{0.4}V_c^{2.62}/C^{0.60}$$

$$\Delta W_F = [(1.52(10)^{-6})ES_FW^{0.4}V_c^{2.62}/C^{0.60}]\Delta V_c$$

and

$$\Delta W = F_m\Delta W_F.$$

The effect of increasing the ships endurance is

$$\Delta W_F = [S_F(4.192(10^{-7})W^{0.4}V_c^{3.62}/C^{0.60}]\Delta E$$
$$\Delta W = F_m\Delta W_F$$
$$= F_m[S_F(4.192)10^{-7}W^{0.4}V_c^{3.62}/C^{0.60}]\Delta E.$$

If we assume a ship for which

W = 6000 tons,
E = 4500 nmi,
V = 33 knots,
V_c = 20 knots,
W_{cs} = 500 tons,
C_s = 0.42,
C = 9,
S_F = 0.82,
F_p = 0.015 tons/SHP,
W_p = 2000, and
C_v = 0.22.

the multiplication factor, F_m, is

$$F_m = 1/(1\text{-}0.42)\text{-}3.76(10)^{-4}$$
$$(33^{4.62} \times .015 + 4.46 \times 10^{-4} \times 4500 \times .82$$
$$\times 20^{3.62})/[(9 \times 6000)^{0.6}]$$
$$= 1/(0.58\text{-}0.13) = 2.22,$$

and it follows that:

For change in volume (ft^3)

$$\Delta W = 0.0022\Delta(\text{vol})2.22 = 0.0049\Delta(\text{vol})$$

For added drag at full speed (lb)

$$\Delta W = \Delta DF_m[.0031F_pV + 1.4 \times 10^{-6}$$
$$ES_FV_c^2/V^2] = \Delta D(2.22)[1.535 \times 10^{-3}$$
$$+ 1.8975 \times 10^{-3}] = .00762\Delta D.$$

For additional personnel (ΔM)

$$dW = 1.14(2.22)\Delta M = 2.53 \text{ tons/man.}$$

For change in maximum speed (knots)

$$\Delta W = F_mF_1\Delta V$$
$$= F_mF_p[4.3 \times 10^{-3}W^{0.4}V^{3.62}/C^{0.60}]\Delta V$$
$$= 2.22 \times 0.015[4.3 \times 10^{-3} \times 6000^{0.4}33^{3.62}/9^{0.6}]\Delta V$$
$$= 390 \text{ tons/knot.}$$

For change in cruising speed (knots)

$$\Delta W = F_m\Delta W_F$$
$$= F_m[1.52 \times 10^{-6}E\,S_FW^{0.4}V_c^{2.62}/C^{0.6}]\Delta V_c$$
$$= [2.22 \times 1.52 \times 10^{-6} \times 4500 \times 0.8 \times 6000^{0.4}$$
$$\times 20^{2.62}/9^{0.6}]\Delta V_c = 277 \text{ tons/knot.}$$

For change in endurance (nmi)

$$\Delta W = [F_mS_F(4.192 \times 10^{-7})W^{0.4}V_c^{3.62}/C^{0.60}]\Delta E$$
$$= [2.22 \times 0.82 \times 4.192 \times 10^{-7}$$
$$\times 6000^{0.4} \times 20^{3.62}/9^{0.6}]\Delta E$$
$$= 0.34 \text{ tons/nmi.}$$

Of course, if ship parameters change, the above factors also change. If, for example, the maximum and cruise speeds are reduced to 29 and 18 knots, respectively, the multiplication factors become

basic multiplication factor = 1.9,
volume = 0.0043 tons/ft^3,
drag = 0.0063 tons/lb,
personnel = 2.2 tons/person,
speed = 209 tons/knot, and
endurance = 0.2 tons/nmi.

5.8.2. EFFECT ON SUBMARINE DESIGNS

Submarine designs are affected differently by volume and weight changes than are surface ship designs.They have rigorous volume and weight constraints and a speed-power curve that is easy to delineate.

A change in equipment can result in a change in speed, with displacement remaining constant, or a change in horsepower, with speed remaining constant. Such changes may

1. be internal or external to the hull,
2. add volume internally or externally,
3. add drag,
4. add power consumption,

5. require more cooling, or
6. change the number of personnel required.

The following discussion will consider general effects of weight and volume changes on submarine design.

If the notations are defined as

($_p$) - Prototype
($_m$) - Modified Design
(sub) - Submerged
(suf) - Surfaced
(pp) - Pressure Proof
(i) - Internal
(ex) - External
(p) - Power plant
(e) - Electric power plant,

then

$$Wsub_p/Wsub_m = Wa_p/Wa_m = Ws_p/Ws_m = Wsuf_p/Wsuf_m = \nabla pp_p/\nabla pp_m,$$

where

W = displacement (tons),
Wa = ships weight in condition "A" which is similar to light ship weight (tons),
Ws = hull structural weight (tons), and
∇ = volume tons, i.e., $ft^3/35$.

This equation assumes that, because of design procedures, these ratios will remain the same as the size of a submarine is changed.

In addition, it is assumed that the internal weight ratio, i.e., the weight of all items of the light ship except for structure, divided by Wa, remains the same as the size changes., i.e.,

$$Ri_p = Ri_m = (Wa-Ws)/Wa.$$

The above assumption is valid if

1. test depth and structural material is constant, so that hull structure weight to pressure-proof volume ratio is constant;
2. main ballast tank capacity to displacement ratio is constant; and
3. variable loads and volume, and free flooded volumes and weights are a constant percentage of total displacement.

The main propulsion horsepower of a submarine is roughly proportional to the displacement to the 2/3 power and its velocity cubed,

$$SHP = K(Wsub)^{2/3}V^3.$$

An example of an expression for the weight of propulsion plant is

$$Wp = 5.5(SHP)^{1/2} + 0.02SHP.$$

From the above, we have

$$\partial Wsub/\partial Wa = Wsub/Wa$$

or

$$\partial Wsub = (Wsub/Wa)\partial Wa.$$

Arbitrary addition of an internal weight increases the internal weight (Wa - Ws) and, since Ri remains constant, Wa increases by the same ratio, i.e.,

$$\partial Wi = \partial(Wa - Ws),$$

and since,

$$(Wa - Ws)/Wa = Ri = \partial(Wa - Ws)/\partial Wa,$$

then

$$\partial Wa = \partial(Wa - Ws)/Ri = \partial Wi/Ri.$$

Also,

$$\partial Wsub = (Wsub/Wa)(\partial Wi/Ri).$$

Arbitrary addition to the internal volume of the ship increases the pressure proof volume and, hence, the weight, Wa, by the same amount, i.e.,

$$\partial Wa = \partial\nabla i$$

and

$$\partial Wsub = (Wsub/Wa)(\partial\nabla i).$$

Weight or volume, whichever provides the larger increase, should be used. If we arbitrarily add weight and volume external to the submarine, i.e., ∂Wex and $\partial\nabla ex$, the added wet weight, Ww is

$$\partial Ww = \partial Wex - \partial\nabla ex$$

and

$$\delta Wa = (\delta Wex - \delta \nabla ex)/Ri.$$

The change in submerged displacement caused by this addition is,

$$\delta Wsub = (Wsub/Wa)(\delta Wex - \delta \nabla ex)/Ri.$$

The change in total submerged displacement from the added external volume is

$$\delta Wsub = \delta \nabla ex.$$

Summing the two, we have

$$\delta Wsub = (Wsub/WaRi)\delta Wex - \delta \nabla ex[(Wsub/WaRi) - 1].$$

Then,

$$SHP = K(Wsub)^{2/3}V^3.$$

If SHP is constant and the above equation is differentiated, we have

$$\delta V = -(2/9)(V/Wsub)\delta(Wsub),$$

which yields the speed change for a given change in submerged displacement.

Now, if the speed is constant and the equation is differentiated with respect to SHP, we have

$$\delta(SHP) = (2/3)(SHP/Wsub)\delta Wsub$$

and

$$Wp = 5.5(SHP)^{1/2} + 0.02SHP.$$

Then, differentiating,

$$\delta Wp = [2.75(SHP)^{-1/2} + 0.02]\delta(SHP)$$

or

$$\delta Wp = K_1\delta(SHP),$$

where $K_1 = 2.75(SHP)^{-1/2} + 0.02$. For the constant speed case, increased horsepower involves additional powerplant weight, increased displacement, increased SHP, and so on.

Since

$$\delta(SHP)_1 = 2/3(SHP/Wsub)\delta(Wsub)_1,$$

and

$$\delta(Wp)_1 = K_1\delta(SHP)_1$$

and, since,

$$\delta Wsub = (Wsub/Wa)(\delta Wi/Ri),$$

then

$$\therefore \delta(Wsub)_2 = [Wsub/Wa][\delta(Wp)_1/Ri].$$

Substituting in the above yields

$$\delta(Wsub)_2 = WsubK_12SHP(\delta Wsub)/(3WaRiWsub)$$

or

$$\delta(Wsub)_2 = K_p[\delta(Wsub)_1],$$

where $K_p = 2/3[K_1SHP/(Wa)(Ri)]$.

The factor K_p applies to each increment of displacement; therefore, the total change in displacement is

$$\begin{aligned}\delta(Wsub)\tau &= \delta(Wsub)_1 + \delta(Wsub)_2 + \delta(Wsub)_3 \ldots \\ &= \delta(Wsub)_1 + K_p\delta(Wsub)_1 + K_p^2\delta(Wsub)_1 \ldots \\ &= \delta(Wsub)_1/(1 - K_p).\end{aligned}$$

Similarly,

$$\delta(SHP)\tau = \delta(SHP)_1/(1 - K_p)$$

or

$$\delta(SHP)\tau = (2/3)(SHP/Wsub)(\delta Wsub)/(1 - K_p).$$

The EHP is the drag multiplied by the velocity and divided by 550 ft/lb/sec/hp. Therefore,

$$EHP = 1.689VD/550 = 0.00307VD$$

and

$$SHP = EHP/PC = (0.00307)VD/PC,$$

where PC = propulsion coefficient.

Hence,

$$V = SHP(PC)/0.00307D$$

and, differentiating with respect to D,

$$\delta V = -[SHP(PC)/0.00307D^2]\delta D$$

or, with constant SHP,

$$\delta V = -[V^2(0.00307)/SHP(PC)]\delta D.$$

Since

$$SHP = 0.00307(VD/PC),$$

differentiating with respect to D yields

$$\delta SHP = 0.00307(V\delta D/PC)$$

and

$$\delta(SHP)_\tau = 0.00307(V\delta D)/PC(1 - Kp).$$

Thus, we have

$$\delta Wp = K_1\delta(SHP)$$
$$= K_1(0.00307)V\delta D/PC(1 - Kp)$$

and, for constant speed,

$$\delta Wsub = (Wsub/Wa)(\delta Wp/Ri)$$
$$= [Wsub/(Wa)(Ri)]$$
$$[K_1(0.00307)V/PC(1 - Kp)]\delta D.$$

As a first approximation for electrical power changes,

$$\delta We = (We/Pe)(\delta Pe),$$

where Pe = electric power capacity.

For constant SHP, we have

$$\delta Wsub = (Wsub/Wa)(We/Pe)(\delta Pe/Ri)$$

and, for constant speed, we have

$$\delta Wsub = (Wsub/Wa)(We/Pe)\delta Pe/Ri(1 - Kp).$$

The above is a first order approximation and does not include the cooling required to remove the heat generated by equipment using the power. A rough estimate of density, We/Ve, is 1.33 Ri (expressed as tons/tons).

Table 5.3 shows possible coefficients for a submarine. In general, the selection of equipment is a function of a tradeoff between the value of the added capability, the cost, and the impact on the ship.

Table 5.3. Example of Impact Coefficients

		Constant SHP		Constant Speed	
1		2	3	4	5
Item	Units	δΔSub Tons	δV Knots	δΔSub Tons	δSHP Horsepower
δWi*	Tons	2.4	-.003	3.0	6.5
δVi*	Tons	1.3	-.001	1.6	3.4
δWex	Tons	2.4	-.003	3.0	6.5
δVex	Tons	-1.4	+.001	-1.8	-3.9
δD	Pounds	----	-.00018	.014	.13
δPe	KW	.10	-.00013	.14	.3
δ(crew)	MEN	5.48	.007	7.0	15.0

5.9. ELECTROMAGNETIC COMPATIBILITY

Electromagnetic compatability (EMC) is ability of shipboard electrical and electronic equipment to perform effectively with minimum mutual interference or degradation of the total electromagnetic (EM) environment. Shipboard space is limited, available bandwidths are restricted, EM energy is difficult to control, and required electrical equipment is increasing with advancing technology. Such factors make effective EMC increasingly difficult. Electrical impulses from any source induce signals in receiving systems. These unwanted signals produce interference that may range from being temporarily inconvenient to rendering the equipment useless.

The atmosphere is the conductor for a vast amount of information. Interference is sometimes eliminated only by the distance between transmitters and by time-sharing channels. Modern transmitters operate in very narrow bandwidths and the atmospheric

channel can, with cooperation between users, convey great amounts of traffic. Therefore, EMC is of an international concern that has resulted in controls on band and channel use.

The U.S. Navy EMC program is a subset of the international program, the ship a smaller subset, and its systems yet smaller subsets. Although the sonar system does not use the atmospheric channel, it is part of the overall EMC program.

In addition to functional electromagnetic emissions, there are incidental emissions from flourescent lighting, commutators, and simple switching devices. It is these seemingly minor, but extremely difficult to eliminate, emissions that present the greatest EMC problems in relation to sonar systems. Electrical equipment may emit radiation that is not only an EMC problem, but is also detremental to its own operation. Proper EMC considerations, then, require that electrical and electronic equipment be designed so that they do not interfere with other equipment or their own operation, and are subject to minimum external interference.

The emission of incidental radiation from a ship is tactically disadvantageous because it provides an adversary with a means of detection. Requirements for EMC in the Fleet and individual ships is provided in publications detailing Navy management and contractor responsibilities.

Because EMC is affected by all electrical equipment and many non-electrical items, coordination of assigned frequencies and establishment of maximum levels of incidental radiation are extremely important. Effective EMC design also includes shielding of susceptible equipment, electromagnetic vulnerability (EMV), electromagnetic pulses (EMP), electromagnetic counter-measures (ECM), electromagnetic counter counter-measures (ECCM) and EM safety.

Acceptable EMC requires intense advance system planning and careful control of the design, construction, and installation of equipment that emits or senses electromagnetic energy in any form. Management guidance for this area is available in MIL-HBK 237.

5.9.1. ELECTROMAGNETIC INTERFERENCE

Electromagnetic interference (EMI) is the principal EMC concern in sonar system installation. It is defined as any radiated or conducted electrical perturbation that degrades the proper operation of electrical or electronic equipment. The causes and effects of EMI are almost as numerous as the types of electrical equipment in use. The subject is of special concern because the number of shipboard equipments and their receiving range and sensitivities (e.g., micro-microwatt ranges) have increased.

Common EMI sources are listed in table 5.4. Their effects are often subtle but, generally, can be minimized by

1. spacial separation, i.e., distance attenuation,
2. shielding,
3. filtering,
4. blanking, or
5. eliminating the source.

Spacial separation is the physical separation of equipment such that attenuation (or, for atmospheric transmissions, over-the-horizon effects) reduces interference. It is used by narrowbeam devices, e.g., microwave antennas, that are constructed to employ narrow sectors for transmission. Shipboard EMI attenuation can result from the effects of bulkheads and decks, but it can also be categorized as shielding.

Shielding is the interposition of a physical barrier between the radiation source and affected equipment. Filters are used if the EMI is conducted by cable. Blanking is essentially a time sharing device, i.e., the equipment causing the interference is not operated when the desired capability is required Other means of eliminating EMI include substituting a non-radiating item to perform the function of the radiating one, and correcting the malfunction causing the radiation.

Because sonar systems operate at relatively low frequencies, they are especially vulnerable to overlapping power system harmonics. This situation is aggravated by space limitations that

Table 5.4. Common Sources of Electronic Interference

Interference Sources	Interference Identification	Reason for Interference
Antennas, communication	Blocking of receiver	Receiving antenna in induction field of transmitting antenna
Antenna, radar	Pulse repetition rate, buzzing interference	Direct radiation from radar antenna to communication antenna
	Spurious traces on PPI scope sector or complete obliteration	Interactions between radars operating near the same frequencies
Antennas, receiving	Grating sound with variations in output signal strength	Loose, corroded, dirty, or damaged antenna hardware
Antennas, transmitting	Broadband hash	Dirty, painted, and cracked or pitted insulators, causing arc-overs and interference by radiation
Cable shield and armors	Hash and clicking	Static discharge caused by ungrounded coaxial cable shields and antenna stays
Circuit breakers	Regular or intermittent clicking	Radiated and conducted power line interference
Code machines and office machines	Regular or intermittent clicking	Interference radiated or conducted along the power lines
Connectors, cable	Hash, popping, or any interference	Armor of cable cut back and loose; cable improperly terminated
Connectors and hardware on stays and antennas	Interference at the sum and difference of frequency	Corroded and/or loose connectors. Interference caused by mixing of signals at connectors which act as detectors arcs across loose connectors.
Console, cabinets, and cases housing radio equipment on shock mounts	Hash-type interference	Cabinets, chassis not bonded to ground
Cross modulation	Audio crosstalk	Conducted or radiated field between closely related and received signals
Degaussing equipment	Hash in sonar receivers	Magnetic or electric coupling between closely related and received signals
Diathermy or other RF heating equipment	Loud sputtering hum	Radiation over great distances
Fathometer	Pulse popping sound	Direct radiation from cable
Fluorescent lights	Hum-modulated hash at twice the power frequency	Radiation to nearby power lines and by conduction through power lines
Ignition systems, vehicles, pumps, and the like	Varying, snapping sound in receiver	Radiated interference
Motors, generators and motor generators	Broadband hash	Radiation of EMI to antenna or cabling of receiver. Conduction of EMI by power lines or cabling
Ordnance radars repetition	Hash, broadband radar rate interference	Radiated and conducted interference
Radar equipment	Audible hash and pulse repetition rate interference; visual, spurious images	Direct radiation. Conduction via power lines and cabling
Radar transmitter	Broadband hash and pulse repetition interference	Poorly shaped trigger pulse
Receiver oscillators	Spurious signals	Radiation to nearby cabinets, antennas, and cables
Relays, thermostats, and switches	Broadband clicks	Radiation and conduction caused by arc across contacts
Rotary converters	Continuous hash	Conduction and induction or radiation between the converter cabling and receiver leads or power leads
Static charges in the atmosphere	Broadband hash	Loosely bonded stays, improper filtering
Synchros	Hum and hash background	Radiated interference to cabling and conducted on power lines
Thyratrons in radar, sonar, and communications equipments	Hash interference modulated at power, or twice power frequency	Conducted interference from thyratrons along power cables to receivers also inductiveiy coupled to receiver
Transmission lines, transmitter, receiver	Hash modulated at power frequency or twice power frequency	On high voltage lines, corona discharge caused by loose and dirty hardware and insulators; improper termination
Transmitters	Broadband hash	Dirty and dusty power amplifier and other rotary coils
Transmitters or audio distribution system	Crosstalk, hash	Over or under modulation, unbalanced audio or mike circuits
Waveguide joints	Spots on scope, hash in receivers	RF energy leaking from joints

cause low amplitude sonar signals to sometimes be transmitted in cable runs connecting other equipment. The most commom approach to the EMI problem is combined shielding and spacial separation. Therefore, consideration must be given to equipment arrangements in terms of cable runs, radiation levels, suseptibility, shielding, and spacial separation.The Handbook of Shipboard Electromagnetic Shielding Practices (NAVSEA 0967-LP-283-5010) provides detailed information on the use, spacing, grounding, and specifications for shielded cables and fittings. Elimination of the EMI source is, in many cases, the most cost effective approach. Unwanted emitters are usually poorly designed, maintained, or installed. The cause can be corrected once the EMI source is identified.

Many equipment changes are made during the life of a ship and each must be reviewed to ensure that minimal EMI is introduced. Also, initial design should minimize the possibility that future modifications will cause EMI problems. Equipment should be tested before installation to determine that internal circuits are properly grounded and shielded, and retested after installation to ensure that interference is not being introduced through power or signal cables. Local equipment should be operated during on-site testing because EMI is an interactive process.

5.9.2. EMI CONCEPTS

One of the most common causes of EMI is cross talk, i.e., induced signal interference. Inductance is very useful in coils, motors, transformers, and tuned circuits, but it is a problem when uncontrolled. A voltage is generated when an electrical conductor is passed through a magnetic field, or is in an expanding and contracting magnetic field. Conductors moving in the earth's magnetic field also generate voltages.

Except when being turned on or off, direct current conductors have constant electromagnetic fields surrounding them. Alternating current conductors, on the other hand, are subject to continuously expanding and contracting fields that generate voltages in adjacent conductors. The magnitude of an induced voltage is expressed as

$$V_{(induced)} = 0.406\ fBA$$

where

f = frequency (Hz)
B = magnetic flux density (Gauss)
A = equivalent loop area (in.^{2})

Application of this formula is described in NAVSEA 0967-LP-283-5010.

Since the rate of change of an alternating current is proportional to the amplitude and frequency, the generated EMI is also proportional. The EMI magnitude varies with that of the interfering flux and its propagation to the receptor. The flux obeys laws including those for refraction and attenuation. Radiation fall-off characteristics vary according to the type of equipment generating the magnetic flux. As mentioned above, the distance between the source and receptor determines the influence of the flux. Shielding, of course, reduces this influence.

5.9.3. SHIELDING

Shielding effectiveness depends on the reaction of the shield to the electric and magnetic radiation fields. The reflection coefficients for a sheet of shielding material are

$$q_E = E^R/E^I = [Z(\ell) - \eta]/[Z(\ell) + \eta] \quad (= k - 1)/(k + 1)$$

and

$$q_H = H^R/H^I = [\eta - Z(\ell)]/[\eta + Z(\ell)] = (k - 1)/(k + 1),$$

where

q_E = electric field reflection coefficient, = $-q_H$,
q_H = magnetic field reflection coefficient,
$k = Z(\ell)/\eta$.
$Z(\ell)$ = impedance (side where $x = \ell$),
E^R = reflected electric field,
E^I = incident electric field,
E^T = transmitted electric field,
η = intrinsic impedance of sheet metal shield,

H^R = reflected magnetic field,
H^i = incident magnetic field, and
H^T = transmitted magnetic field.

The transmission coefficients are

$$P_E = E^T/E^i = 2Z(\ell)/[\eta + Z(\ell)] = 2k/(1 + k)$$

and

$$P_H = H^T/H^i = 2\eta/[\eta + Z(\ell)] \quad 2/(1 + k).$$

The transmission coefficient at the interface of two sheets is

$$P = 4k/(1 + k)^2.$$

The above equations are similar in form to those for acoustic waves at an interface between two media (see Section 3.3.4.2). Shielding of electromagnetic energy, however, is far more complicated than is implied here.

The absorption shielding coefficient which is the predominant shielding factor at low frequencies is

$$A = 3.34t\sqrt{fu_r\sigma_r}\ dB$$

where

f = frequency (Hz)
t = shield thickness (in.)
u_r = relative permeability
σ_r = relative conductivity

The subject of EMC is immense and the reader is referred to the bibliography for this chapter. The significant point for the sonar designer is the threat to SNR posed by the numerous sources of EMI onboard ship. Since the object of installing sonar systems is to collect information, any phenomena that distort or obliterate data are, of course, counter productive. Therefore, implementation of an EMC control plan for each ship design is essential.

5.10. SHIP/SONAR INTERFACE

It is extremely important that the ship designer is knowledgeable about the sonar systems that are to be installed onboard the vessel. He must work with the sonar system designers to determine the best locations for arrays, equipment, hull penetrations, and so on. Also, since more than one type of sonar system is installed, it is necessary to understand the total sonar suite and its internal interfaces. The complete set of sonar systems is referred to as the *underwater surveillance system*.

As a result of such efforts, a clear description of the systems and the interfaces with the ship should develop. Continuous liaison and comunication should be maintained throughout the design, fabrication, installation and testing of the systems. In-service performance feedback is, of course, necessary but will not be discussed herein.

In addition to documented sonar system requirements, the wider concerns of the Naval Architect in relation to total system integration still apply. Since people build, install, operate, and maintain systems, close attention to the human interface is needed. For example, the location and arrangement of CIC must facilitate the flow of information between subsystems and the command watch officer. Operational sequence diagrams (OSDs) are very useful in determining human requirements in terms of particular systems during installation, operation, and maintenance.

An interface description document is tailored for the particular system being installed. Sketches of all system components show their sizes and configurations, cooling water connections, air circulation requirements, mounting locations, maintenance space, and so on.

5.10.1. INTERFACE DESCRIPTION

The introduction to the interface description document should explain its purpose and organization. It should explain the coding of the alpha-numerically designated functional groups and list individual components by name and alpha-numerical designation. Table 5.5 provides such a listing and table 5.6 shows the further breakdown into individual units.

The second section, electronic characteristics, addresses the intra-interface characteristics of the total surveillance system. It is subdivided into categories according to the level of interface addressed, e.g.,

1. underwater surveillance system/ship interfaces,
2. underwater surveillance system intrafaces, and
3. sonar system intrafaces.

Table 5.7 lists underwater surveillance system interfaces. The identification numbers correspond to the interface number in figure 5.41 and those in table 5.8.

There should be an equipment listing defined by the intra-interface tables and a cross-reference to the overall surveillance system functional block diagram (figure 5.41). Tables 5.8 through 5.12 show the variations in a format that describe various interfaces.

The electrical interface tables define the electrical characteristics of equipments that transmit and receive data. *Source* and *load* information are provided to facilitate a comparison of the parameters. *Not applicable* is denoted by *NA* and *to be supplied* by *TBS*. The

Table 5.6. Unit Alpha-Numeric Unit Designators

Alpha Numeric	Unit Name
A-1 - A-4	Amplifier Relay Assembly (4)
A-5	Primary Power Control
A-6A1	Inverse Compensator
A-6A2	D/E Mode Switch
A-6A3	DT Switch
A-7A1, A-7A2	Amplifier Scanner (2)
A 180	Distribution Box
A-11 - A-17	Sonar Transmitters (7)
A-24	Loudspeaker Control
A-26A1	Intercommunication Station
A-26A2	Intercommunication Station
A-26A3	Intercommunication Station
A-26A4	Intercommunication Station
A-33	Loudspeaker
A-34	Loudspeaker
A-37	Megger Test Adapter (Portable)
A-38 - A-40	Emergency Off Switch (3)

Table 5.5. Sonar Set Functional Groups

Group	Function	Equipments Involved
A	Detection and Tracking	System I System II Towed Array Handling Equipment
B	Acoustic Communications	HF/LF Voice/CW Acoustic Communications Equipment
C	Depth/Sound Speed	Sound Velocity Meter
D	Emergency Communications	Emergency Telephone Distress Beacon
E	High Frequency	High Frequency Detection/Tracking Equipment
F	Depth Sounding	Fathometer
G	Expendable BT	Expendable Bathythermograph
H	Recording	Analog Data Recorder Matric Amplifier/Loud Speakers
I	Microfilm Reader/Printer	Printer Portable Reader
J	Acoustic Performance Monitoring	FOM Equipment
K	Performance Measurement	Performance Measurement Equipment

Table 5.7. Interface Designations

Interface Identification Number	Name
	Underwater Surveillance System and Interior Communications System
1	Sonar System II and AN-W1C-x Junction Box
	Underwater Surveillance System and Exterior Communications System
2	Sonar System II and Time of Day Generator
3	Sonar System II and Frequency 11
4	Sonar System II and Time of Day Indicator
	Underwater Surveillance System and Data Processing System
5	Sonar System and Sonar Computer
	The following are an example of Underwater Surveillance System intrafaces. The identification numbers follow in sequence from the interface numbers.
6	Detection and Tracking Group and Sonar System I
7	HF Detection and Tracking Group and Sonar System I
	In addition to these high level interfaces, the lower level intrafaces may be handled as follows.
Intrafaces	
8	Detection and Tracking Group and Recording Group
9	Detection Tracking Group and Depth-Sound Speed Group
10	Detection and Tracking Group and Expendable BT Group
11	Detection and Tracking Group and Depth-Sounding Group
12	Detection and Tracking Group and Acoustic Communication Group
13	Detection and Tracking Group and High Frequency Group
14	High Frequency Group and Acoustic Communication Group
15	High Frequency Group and Recording Group
16	Recording Group and Acoustic Performance Monitoring Group
17	Recording Group and Acoustic Performance Monitoring Group
18	Recording Group and Performance Measurement Group

functions in the tables are not segregated according to cable groupings and, therefore do not define cabling needs.

5.10.2. NAVAL ARCHITECTURAL AND MARINE ENGINEERING INTERFACES

The third section describes system characteristics that affect the naval architecture and marine engineering of the ship.Such knowledge is required for integration of the underwater surveillance system into the total structure and environment of the ship. The characteristics include the space, weight, and environment necessary for equipment units.

Space requirements are divided into inboard and outboard. Inboard requirements include the arrangement and location of equipment comprising the underwater surveillance system. Equipment room drawings are provided to indicate how cabinets will be grouped and to ensure that adequate working space is available. Outboard drawings describe the location, configuration, and alignment of acoustic arrays and sensors mounted outside the pressure hull. Inboard and outboard arrangements, including aperture specifications and array alignment, must be defined.

Space, weight, and ship services requirements are specified for each unit, as shown in table 5.13. Ship services include electrical power, cooling, auxiliary sea water, and hydraulic systems. A summary of installation according to location, such as that shown in table 5.14, shoud be provided.

Ventilation requirements describe the ambient environment that must exist to maintain efficient operation. This section defines the noise, shock, vibration, pressure, and electromagnetic field levels for the particular equipment.

The cabling section defines specifications for internal and external interconnections and the grounding system employed. Another addresses hull penetration. The last section describes the integration of major acoustic arrays and any special installation requirements. In cases where Military Standard Requirements are imposed, the specification should be referenced.

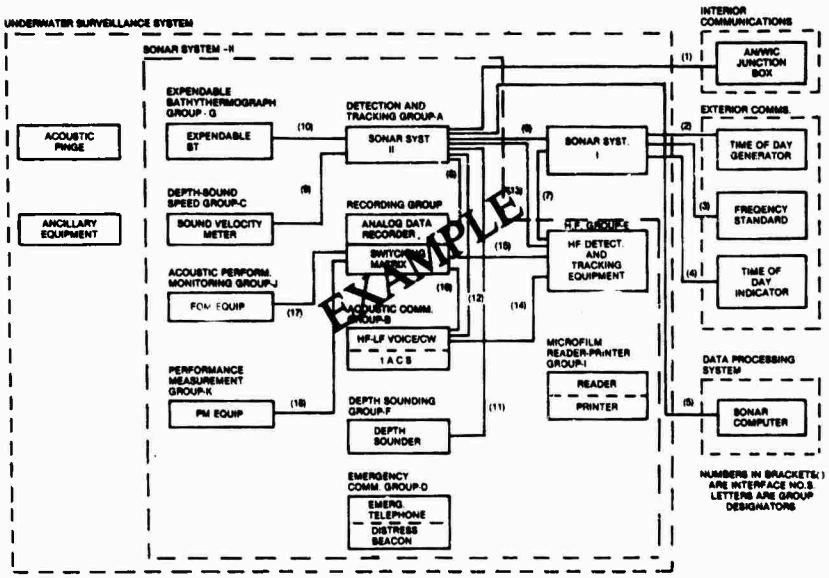

Figure 5.41. Underwater Surveillance System Interfaces

Table 5.8. Electrical Interface Table
Interface 1, *Underwater Surveillance System and Interior Communications System*, Detection Tracking Group A and AN/WIC Junction Box

Source	Load	Function	Impedance Source	Impedance Load	Voltage	Current	Frequency	Remarks
Sonar Supervisor Break in Box Designator H6	AN/WIC Junction Box (J-2730)	27 MC Audio Hi	10 ohms	10 ohms	8.06 VRMS	NA	less than 20 kHz	*Power for detect/ report signals
		27 MC Audio Lo	10 ohms	10 ohms	8.06 VRMS	NA	less than 20 kHz	
		27 MC Control	NA	NA	NA	.5 amps (max.)	NA	
		+28 Vdc*	NA	NA	NA	.5 amps (max.)	NA	
		Ground*	NA	NA	NA	.5 amps (max.)	NA	
		27 MC Lo						
		System Conn Report	NA	NA	+28 VDC	.5 amps (max.)	NA	
		Torpedo Detect	NA	NA	+ 28VDC	.5 amps (max.)	NA	

Table 5.9. Electrical Interface Table
Depth Sounding Group F and Sonar System I, Group A

Source	Load	Function	Synchro Type Source	Synchro Type Load	Impedance Source	Impedance Load	Voltage	Current	Frequency	Voltage Reg. (System)	Remarks
A-7	Unit 1	Apparent Relative Target Bearing (Ba)	TBSS	SCOTT "T"	TBS	TBS	115 VAC	TBS	400 Hz	TBS	1x, 360°P.R.
		Apparent Relative Target Bearing (Ba)	TBS	SCOTT "T"	TBS	TBS	115 VAC	TBS	400 Hz	TBS	36x, 10°P.R.
		Apparent Depression Angle COMP 1 (Eua)	TBS	SCOTT "T"	TBS	TBS	115 VAC	TBS	400 Hz	TBS	1x, 360°P.R.
		Apparent Depression Angle COMP 1 (Eua)	TBS	SCOTT "T"	TBS	TBS	115 VAC	TBS	400 Hz	TBS	36x, 10°P.R.

Table 5.10. Electrical Interface Table
Depth Sounding Group F and Sonar System I, Group A

Source	Load	Function	Impedance Source	Impedance Load	Voltage Level Source	Voltage Level Load	Bandwidth Source	Bandwidth Load	Current	Remarks
AN/BQH-6 Unit 1	A118	Left Half Calibration (Comp 1 and Low Frequency)	TBS	TBS	1 Vrms	NA	TBS	TBS	TBS	Discrete Tones or Broadband Noise
		Sea State Noise Calibration (Comp 1 and Low Frequency)	TBS	TBS	TBS	TBS	TBS	TBS	TBS	Broadband Noise
		Right Half Calibration (Comp 1 and Low Frequency)	TBS	TBS	1 Vrms	NA	TBS	TBS	TBS	Discrete Tones or Broadband Noise
A118 Unit 1	A118	Right and Left Indication (BDI) (Comp 1)	TBS	TBS	-2VDC	+2 VDC	TBS	TBS	TBS	
		Up and Down Indication (UDI) (Comp 1)	TBS	TBS	-2 VDC	+2VDC	TBS	TBS	TBS	
		Right Half Beam Output (Comp 1)	TBS	TBS	TBS	TBS	TBS	TBS	TBS	Broadband Noise to Analog Multiplexer
		Left Half Beam Output (Comp 1)	TBS	TBS	TBS	TBS	TBS	TBS	TBS	Broadband Noise to Analog Multiplexer
		Right Half Beam Towed Array Tracker	TBS	TBS	TBS	TBS	TBS	TBS	TBS	Broadband Noise
		Left Half Beam Towed Array Tracker	TBS	TBS	TBS	TBS	TBS	TBS	TBS	Broadband Noise
		Sum Data Beam	TBS	TBS	TBS	TBS	TBS	TBS	TBS	Sum Audio Output
		Signal to Noise Ratio	TBS	TBS	0	2 V	TBS	TBS	TBS	
		Receive Pulse Data	TBS	TBS	TBS	TBS	TBS	TBS	TBS	Active Emission Detector

Table 5.11. Electrical Interface Table
Depth Sounding Group and Sonar System I, Group A

Source	Load	Function	Impedance Source	Impedance Load	Switching Levels	Accuracy	Resolution	Remarks
A118	Unit 4	Comp 1 D/E ATF Mark	TBS	TBS	TBS	TBS	TBS	
		Comp 1 SNR	TBS	TBS	TBS	TBS	TBS	
		Bearing (True/Relative)	TBS	TBS	TBS	TBS	TBS	
		Pulse Amplitude	TBS	TBS	TBS	TBS	TBS	
		Pulse Width	TBS	TBS	TBS	TBS	TBS	
		Pulse Period	TBS	TBS	TBS	TBS	TBS	
		Frequency	TBS	TBS	TBS	TBS	TBS	
		Test Mode	TBS	TBS	TBS	TBS	TBS	
		Hi/Low	TBS	TBS	TBS	TBS	TBS	
		Torpedo/Target	TBS	TBS	TBS	TBS	TBS	
		Manual Mode	TBS	TBS	TBS	TBS	TBS	
		Classification Symbols	TBS	TBS	TBS	TBS	TBS	
		Mark	TBS	TBS	TBS	TBS	TBS	
		Target Number	TBS	TBS	TBS	TBS	TBS	
A-118		Ocean Temperature	TBS	TBS	TBS	TBS	TBS	
		Ownship Course	TBS	TBS	TBS	TBS	TBS	

Table 5.12. Electrical Interface Table
Depth Sound Speed Group C and Detection Tracking Group A

Source	Load	Function	Impedance Output	Impedance Input	Accuracy	Resolution	Switching Levels	Remarks
C-1	A-118	Date Clock Sound Speed End-of-Transfer	TBS TBS TBS	TBS TBS TBS	TBS	TBS	Logic 0 0< + <2.4 V Logic 1 2.4 V≤V ≤4.5 V I = 40 ma min @ 2.4 V	Output waveforms are shown below. The output consists of 3 separate, serial, and balanced line outputs, to accommodate either positive or negative logic circuitry.

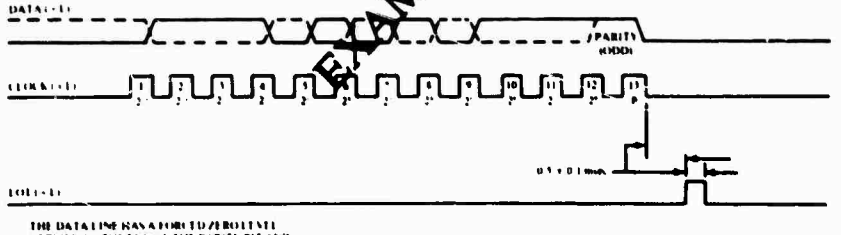

Table 5.13. Unit Descriptions, Detection and Tracking Group A

Alpha-Numeric Designator	Unit Name	No. of Units	Unit Dimensions H x W x D (Inches)	Weight (lbs)	Electrical Power (kW) 115V 3ϕ 60 Hz	3ϕ 400 Hz	1ϕ 60 Hz	1ϕ 400 Hz	Cooling Water GPM	Remarks
A-52	Interconnecting Box	1	15.4 x 27.4 x 7.7	58						
A-56	Active Emission Receiver Processor	1	54.8 x 20 x 20.4	394	1.104					
A-111	Passive F/E/C	1	70.06 x 19.5 x 16.5	933	1.01	0.15			1.59	
A-112	Active F/E/C	1	70.06 x 19.5 x 16.5	933	1.01	0.15			1.79	
A-113	Passive Beamformer	1	70.06 x 19.5 x 16.5	920	2.55	0.15			2.59	
A-114	Active Beamformer	1	70.06 x 19.5 x 16.5	960	2.380	0.15			2.63	
A-115	Passive Broadband Processor	1	65.16 x 19.5 x 16.5	771	1.55	0.15			1.52	
A-116	Active Processor	1	70.06 x 19.5 x 16.5	882	1.975	0.15			2.44	
A-118	Signal Data Converter	1	65.16 x 19.5 x 16.5	815	0.91	0.22			0.89	
A-119	Passive Beamformer	1	70.06 x 19.5 x 16.5	770	0.895	0.15			1.06	
A-124	PM/FL Console	1	22.2 x 53.25 x 23.2	707	TBS	TBS			0.87	
A-125	Electrical Dummy Load	1	53 x 19.5 x 1.65	800					3.89	
A-129	Sonar Receiver	1	69.3 x 21.8 x 15.8	652		1.60				
A-130A A-130B	Classification Processor (MIU/DSA)	1	70.06 x 19.5 x 16.5	930	1.955	0.136			2.04	

Table 5.14. Installation Requirements Summary

Location	Weight (lbs)	Electrical Power (kW) Cooling 115V 3ϕ 60 Hz	3ϕ 400 Hz	1ϕ 60 Hz	1ϕ 400 Hz	Water GPM	Remarks
Sonar Equipment Room	80,428			5.5		64.01	44 kW Ave., 440 V, 3ϕ, 60 Hz, 528 kW Max.
Sonar Control Room						10.63	
Command and Control Center	2,849	2.518	0.106	1.03	0.10	1.57	
Interior of Array	1,588	0.96					
Towed Array Handling Room	5,348			0.085			2 GPM Fresh Water @ 15 psi, 11 GPM Hydraulic @2250-3000 psi
Data Processing Equipment Room	220		1.0				
Maneuvering Room	1						
Adjacent to Midships Wide Aperture Array	500						
Adjacent to AFT Wide Aperture Array	500						
Adjacent to Escape Trunks	194			0.064			
Adjacent to three inch Launcher	70						
External to Pressure Hull							
Totals					0.10	76.21	

5.10.2.1. Inboard Space

Inboard space for the underwater surveillance system should be given for each compartment (e.g., the sonar equipment space, sonar control room, command and control center, and towed array handling space). Units located elsewhere are addressed as other *equipment space requirements.*

A table should provide a summary of the equipment requirements for the sonar equipment room and a figure should show a suggested design. A space will be provided for a work bench, test equipment, and documentation.

5.10.2.2. Outboard Space

Outboard space requirements include those for exterior acoustic arrays and sensors that transmit electrical energy to interior processing equipment or acoustic signals into the water. The location of all such equipment should be illustrated by plan, elevation, and end views of the ship. Other illustrations should show the location, alignment, and configuration of the array in detail. Additional description of array requirements should be provided in accordance with the following example:

The outboard space requirements are based on the four major sonar arrays and the active emission detection sensors supporting the detection and tracking group of sonar set II. These include arrays 1, 2, and 3.

Array 1 is a truncated sphere consisting of transducer elements. It is located in the bow dome area, which is acoustically isolated from own ship noise. The spherical array elements are arranged to cover 360° in azimuth and from + 60° to -80° in D/E. The elements at 180° in azimuth are not installed so there will be room for support structures. The number of azimuthal elements mounted at each D/E angle depends on the distance from the equator.

The interior structure and materials of the ship aft of the array are designed to acoustically isolate the elements from own ship noise and prevent acoustic reflections within the dome. The array baffles are designed to inhibit the transmission of acoustics into the pressure hull when the spherical array is in the active mode. The bulkhead and eyebrow baffles associated with the spherical array are composed of, or covered with, absorbent, reflective, or damping material (see figure 5.12). If the desired aperture is to be maintained, no major structures are installed in front of the forward ballast tank bulkhead, other than the eyebrow baffle.

All air flasks will be mounted aft of the sonar dome. Interfering materials should be minimized within the acoustic viewing angles of the array. The dome enclosure will be filled with fresh water during the shipyard period and the vents will be closed to prevent contaminated water from entering. The vents will be opened underway to permit salt water to replace the fresh.

5.10.3. ARRAY AND SENSOR INSTALLATION

Acoustic arrays and sensors must be properly installed and aligned to provide inputs that are compatible with the inboard electronics. For example, spherical array transducer elements must be mounted for operation at specific azimuthal and D/E angles. Port and starboard line arrays are constructed such that there is an angular offset from a line parallel to the horizontal plane, in order to correspond to beamforming compensation. Active emission detection hydrophones must be aligned parallel to the centerline to within a specified tolerance.

Sonar arrays must not be subject to mechanical interference, e.g., penetration by torpedo tubes. Nor can they be subject to acoustic interference in their apertures, e.g., gas bottles or torpedo ejection equipment. Active sounding elements, such as the secure fathometer transducer, should be separated from active emission detection hydrophones to minimize interference during active depth sounding.

Inboard equipment should be located as close as possible to the outboard equipment it serves in order to minimize cable runs. For example, preamplifier cabinets should be located such that the cable length from the hydrophones is sufficiently short to achieve the desired signal level.

5.10.4. EQUIPMENT WEIGHT

Table 5.13 lists the weight of each inboard unit of the underwater surveillance system. Such tables do not generally include the weight of the spare parts, tools, and test equipment necessary for repairs. Outboard weight requirements are detailed in listings such as that contained in table 5.15, which presents the dry and wet weights of all arrays, sensors, and baffling. Inboard weights are summarized according to locations as in table 5.14 and outboard weights as in table 5.16.

5.10.5. POWER REQUIREMENTS

Detailed power requirements for individual components are specified as shown in table 5.13 and a summary according to location is presented as in table 5.14. Special power considerations should be expressed in accordance with the following example:

Most of the electronic processing equipment requires 115 V, 60 and 400 Hz, 1 and 3 phase supplies. The secure fathometer and some array transmitters require 440 V, 60 Hz, 3 phase supplies. The design of electrical power distribution for the underwater surveillance system must emphasize continuous operation of equipment essential to the mission of the ship. Particular equipment must remain operational in casualty and power casualty situations. Alternating current equipment must be compatible with the interface characteristics and constraints specified in MIL-STD-1399, Section 103.

5.10.6. WATER COOLING

Water cooling requirements for the underwater surveillance system are also summarized in table 5.14 and equipment needs are specified in table 5.13. Special requirements should be expressed in accordance with the following example:

All enclosures requiring water cooling, per MIL-E-16400, will be cooled in accordance with MIL-STD1399, Section 101, and MIL-W-21965. It is desirable to maintain inlet water temperature between 70°F and 75°F but sonar equipment design will tolerate temperatures up to 105°F, per MIL-STD-1399. When sea water temperature exceeds that necessary to maintain 75°F inlet temperature, inlet water cycling will be stopped. All sonar equipment coolant materials will be electro-chemically compatible with those listed in category N of MIL-STD-438 (i.e., they will be, basically, high purity copper). If the water cooling system fails, the air cooling system must sustain the increased heat load for 2 hr.

Table 5.15. Estimated Outboard Sonar System Weight Details — Arrays and Baffles

Spherical Array		
Item	Dry Weight Total (lb.)	Wet Weight Total (lb.)
Array I and Transducers	61,283	32,268
Totals	61,283 lb.	32,268 lb.
	27 long tons	14.4 long tons

Eyebrow Baffle				
Baffle Area: (TBS) sq. ft. fwd, bulkhead (TBS) sq. ft. horizontal member				
Item	Dry Weight lb./sq. ft	Wet Weight lb./sq. ft	Dry Weight Total (lb.)	Wet Weight Total (lb.)
TBS				
Totals				

Table 5.16. Sonar Suite System Weight Estimates

Outboard Summary				
	Dry		Wet	
Item	lb.	Long Ton	lb.	Long Ton
Array I	101,283	45.2	62,268	36.7
Eye Brow Baffle	TBS	TBS	TBS	TBS
FWD Damping and Baffling	TBS	TBS	TBS	TBS
Hull Mounted Line Arrays	6,035	2.69	4,590	2.05
Wide Aperture Arrays	23,610	10.54	18,120	8.09
Wide Aperture Array Damping	TBS	TBS	TBS	TBS
Towed Array and Housing	31,817	14.2	24,071	10.75
Other Array Elements	TBS	TBS	TBS	TBS
Total Outboard				

5.10.7. AUXILIARY SEA WATER AND HYDRAULIC REQUIREMENTS

Sonar units, such as the towed array handling equipment, may require hydraulic and auxiliary sea water supplies for deployment and retrieval (these requirements should be listed in a table such as 5.14). Detailed specifications should be expressed in accordance with the following example:

The hydraulic control panel is a single manifold type having valves to control the speed and direction of the cable drive motors. It interfaces with the main hydraulic power supply, which routes high-pressure fluid to the cable drive motor, reel motor, and hydraulic pressure indicators.

Initial deployment requires that an external force be applied to eject the array from the stowage tube. This is accomplished by a flushing fixture (located between the snubber and stowage tube), which provides the water pressure necessary for ejection. Sea water from the discharge side of the auxiliary sea water cooling system is used for this application. The associated valve assembly is a ball-check type that prevents leakage when the tow cable is severed. Four fresh water flushing fittings are available to cleanse the valve of dirt and cable dust.

Specifications for the hydraulic control panel, flushing fixture, and valve assembly should be provided in the unit description table.

5.10.8. VENTILATION REQUIREMENTS

Sonar equipment space ventilation requirements should be addressed briefly and applicable specifications cited. The discussion should be in accordance with the following example:

The underwater surveillance system ventilation system is designed to maintain the ambient temperature within the operating range of the associated equipment. It must adequately filter, purify, and humidity control the air. The equipment will be protected, per MIL-E16400, at temperatures between 32°F and 90°F and a relative humidity of 95 percent. A specified portion of the ventilation system will be supplied by the vital power supply bus to protect against overheating.

Ducts that are located over equipment must be watertight; therefore, connections should not be made in such areas. Ventilating terminals must also be arranged to prevent water leaks and to prevent short circuit of air between terminals and exhausts. Exhaust terminals must remove heated air from equipment without moving it across work areas.

5.10.9. ENVIRONMENTAL CONDITIONS

Equipment design is subject to constraints imposed on the shipboard environment such as shock, vibration, and so on. The subject should be defined in accordance with the following example:

Underwater surveillance system equipment will be designed, developed, manufactured, and installed to meet natural and induced environmental conditions defined in MIL-E-16400. This includes specifications in relation to the following:

Structure-Borne Noise

Structure-borne noise levels will not exceed those specified for Type 3 equipments in MIL-STD-740B, Notice 1, except for the Fault Status/Fault Localization Printer, which shall not exceed 87 Adb/10^{-3} cm/sec^2 over the frequency range and the PDR, which shall not exceed 105 Adb/10^{-3} cm/sec^2 when hard mounted. These units will transfer minimal structure-borne noise.

Air-Borne Noise

Air-borne noise levels measured in accordance with NASI Standard S1.2 will not exceed the levels specified.

Shock Mounting

Sonar equipment will not be installed on shock mounts if the design does not specifically

include them. Shock mounts will not be used if the equipment is installed in a shock mounted cabinet, rack, or console. Installed shock and rigid mounts will not be replaced with another type or size. If shock mounts are utilized, adequate equipment to equipment, and equipment to bulkhead clearance must be provided for excursion.

All sonar system equipment will satisfy shock requirements for Grade A or B equipment in accordance with MIL-S-901 for

1. *type A,*
2. *hull and deck mounted,*
3. *classes I and II, and*
4. *weight classification per MIL-S-901.*

Grade A equipment should be designed for minimal performance degradation following shock loading. Grade B equipment can be subject to some performance degradation but cannot present a hazard to personnel or other equipment. Grade C equipment has no shock requirements but must not be hazardous after a shock. Table 5.17 shows the shock classification for underwater surveillance system equipment.

Vibration

All sonar equipment will meet the vibration requirements in MIL-E-16400 and the Type I vibration tests in MIL-STD-167B for the 4 to 33 Hz range.

Table 5.17. Shock Requirements

Equipment	Shock Classification	Remarks
Group A	Grade A	
Group B	Grade A	
Group C	Grade A	
Group D	Grade A	
Group E	Grade B	
Group F	Grade A	
Group G	Grade A	
Group H	Grade A	Recording Tape is Grade C
Group I	Grade A	
Group J	Grade A	
Group K	Grade A	
Acoustic Pinger	Grade A	
Test equipment	Grade B	

Pressure

All sonar system components that may be exposed to external sea pressure will withstand continuous hydrostatic pressure of X psi. Other equipment will be capable of operation over an atmospheric pressure range of from 24 to 36 in. of mercury. Hydrophones and transducers will be designed to withstand pressure transients of X psi/sec superimposed on a hydrostatic pressure of X psi, thereby providing a peak pressure environment of X psi. No leakage into the pressure hull, or mechanical or electrical degradation shall result from exposure to this pressure environment.

Magnetic Fields

Except for the high frequency array group, active emission receiver/processor, and loudspeakers, the sonar equipment will withstand an ambient steady-state magnetic field of from X to XX oersteds with a maximum change rate of X oersteds/sec. The equipment will be capable of operating in an alternating current magnetic field defined by the RS-01 narrowband limit of MIL-STD-461. When an ambient magnetic field of X oersteds exists, the equipment will be operational, but the CRT displays will have a maximum distortion displacement of 1/16 in.

Electrical Fields

Except for high frequency array group, active emission receiver/processor, and loudspeakers, the equipment will operate in the electric field defined by the RS-03 limit in MIL-STD-461 to an upper limit of 10 MHz. It will also withstand the conducted interference defined by the CS-01 limit in MIL-STD-461.

5.10.10. CABLING, GROUNDING AND PENETRATION REQUIREMENTS

Special cabling, grounding, and hull penetration requirements should be described in accordance with the following example:

Cables for sonar equipment interconnection, power, audio, and similar applications will be in accordance with

MIL-E-16400 or MIL-C-17. All receptacles for interconnection of separately mounted enclosures and equipment with shipboard support systems will be selected from MIL-STD-242 as specified in MIL-E-16400. Connector backshells for equipment interconnections will be specified by the shipyard. Internal sonar equipment cabling and connectors will be selected from MIL-STD-242. Cabling between a hydrophone and the respective preamplifier will be no longer than 100 ft unless capacitor or loss discrepancy compensated. Differences in cable lengths between hydrophones and preamplifiers in a single array will not exceed 10 ft to ensure comparable signal transmission characteristics. Additional requirements are imposed on cables that transmit signals that are more susceptible to EMI or high impedance losses. All inboard cabling is to be shielded, per Handbook of Submarine Electromagnetic Shielding Practices NAVSHIPS 0967-283-5010, Section 6. High frequency sonar cabling will be designed to meet the following constraints:

1. Outboard hydrophone cables from the hull penetration should be of equal length (within 5 percent) and as short as possible (not to exceed 50 ft).

2. Inboard cables from the hull penetration to the amplifier control group should not exceed 100 ft.

3. The total cable run from outboard gear to the dummy load should not exceed 150 ft.

The cable length of the interconnection between the depth sounder processor and transducer will not exceed 150 ft. The cabling distance from the data processing system sonar computer to associated peripherals, such as the control display consoles and signal data converter, will not exceed 150 ft to ensure accurate digital data transmission. Other critical distances involving cabling between units in the sonar equipment space, e.g., MIU/DSA Unit A to MIU/DSA Unit B, will be accomplished by appropriate cabinet arrangement.

All equipment enclosures will be furnished with provisions for securing bond straps to the cabinets. The location, design, and number of bonding points will conform to MIL-STD-1310C. A digital equipment signal ground system will connect to all digital units of the underwater surveillance system, including digital-to-analog conversion equipment. The one-point ground system will be used as specified in MIL-STD-1310C.

Electrical interconnections between acoustic sensors and inboard processing equipment require the installation of watertight hull penetrations. The two methods of penetration are the Portsmouth and British hull penetrators. The British penetrator consists of 18 leads in a polyethylene mold. Because a standard 18 leads are included for each British penetrator, a number of spare leads may exist.

The Portsmouth penetrator, which contains conductors arranged in concentric rings, does not use a standard number of channels; the number of leads depends on the application. A watertight fitting screws over the penetrator and provides the interconnection between the concentric ring conductors and exterior cabling. Cables are attached to the exterior fitting in a spider-like arrangement. The inboard fitting will be connectorized to facilitate testing and removal of the cable. Table 5.18 summarizes the number of channels and projected number of hull penetrations required for each array. It should be noted that the actual number of channels indicated for each array is not always the same as the number of hull penetrators. The eventual number of penetrators required is subject to further refinement during detailed ship design.

5.10.11. SONAR DOME INSTALLATION

Installation requirements for conformal appendage domes (see Section 5.3) are provided. The information needed for the installation interface includes the location and shape of the dome, fastening details, and special handling problems. Each dome is listed and drawings for each are provided.

Table 5.18. Hull Penetrations

Array	Channels	Penetrations
Array I	1241	1241
Array II	92	6
Array III	16	16
Towed	1	1
Active Emission Detection Sensor	3	3
Acoustic Monitor Sensors	10	10
Acoustic Communication	4	4
Distress Beacon	2	2
Depth/Sound-Speed Group	2	2
Depth Sounder	1	1
Emergency Underwater Telephone	2	2
High Frequency Detection/Tracking Group	13	7
Deep Ocean Transponder	2	2
Acoustic Pinger	1	1
Totals	1390	1384

5.10.12. SONAR/DATA PROCESSING INTERFACE

The functional data transmitted between the underwater surveillance system and data processing system should be described. Both inter- and intra-face functions should be addressed. The interface description defines the information transmitted between units and the control method. Simple formating can be included, but complicated formating and data control requires a separate document. The discussion should be in accordance with the following example:

The data processing system controls the transfer of digital data between the fire control and underwater surveillance systems. A computer receives data from the sonar, processes the data, and returns the functions. Functions required by the data processing system, such as software interrupts, are not addressed here but may be components of the sonar/data processing interface.

5.10.13. UNDERWATER SURVEILLANCE SYSTEM INTERFACE

Interface functions between fire control and the underwater surveillance system should be listed and described. Specific equipment should be defined for each group of functions listed.

5.10.13.1. Fire Control System

Many of the functions generated by the underwater surveillance system are required by the fire control system to support target motion analysis. The manner in which such functions are provided should be clearly defined. A table should list examples of the functional transmission requirements and an equipment applicability matrix to provide a convenient way of stating requirements.

Each sonar array generates target information on the target. These functions are supplied to the fire control system to provide multiple information for target analysis. Examples of sonar system inputs concerning the target are

1. apparent relative bearing,
2. apparent relative bearing rate,
3. apparent D/E angle,
4. apparent range,
5. apparent range rate,
6. SNR (azimuth) and SNR (D/E),
7. time delays,
8. apparent bearing error,
9. apparent range error,
10. mark signals,
11. localization channel, and
12. identification and classification.

Target data from one array can be compared with data from another to provide a passive ranging calculation by triangulation. Triangulation functions supplied to fire control include

1. target apparent range,
2. data confidence measure,
3. spherical array apparent relative bearing,
4. spherical array D/E angle,
5. spherical array tracker identification,
6. spherical array SNR,
7. towed array steered angle,
8. towed array tracker identification,

9. towed array SNR,
10. error status,
11. target identification, and
12. maneuver time to complete.

5.10.13.2. Underwater Surveillance System

The fire control system uses data from other systems to generate functional parameters for the underwater surveillance system to support target tracking and localization. Functions transferred from the fire control system through the sonar/data processing interface are the generated

1. true target bearing,
2. true target bearing rate,
3. target horizontal range,
4. target horizontal range rate,
5. base frequency (frequency line tracking),
6. target number,
7. clock word, and
8. own ship course, pitch, and roll.

The recording device requires functional data from the fire control system to provide a permanent record of target data for evaluation at land-based sites. These functions should also be listed.

The underwater surveillance system may be complemented by a data processing system to provide digital processing in support of sonar functions. Digital data may be input into computer subprograms dedicated to sonar related tasks. The subprograms provide output data to display or support sonar signal processing. The input/output functions associated with these subprograms constitute the underwater surveillance system/data processing interface functions.

Specific input/output parameters should be defined in the computer program performance specification (CPPS) and computer program design specification (CPDS). A detailed description of all input/output data for each subprogram is contained in the CPPS detailed functional requirements. The specified programming approach to implement the computer program is contained in a CPDS summary of input/output parameters for each subprogram. The input data should be defined in terms of the underwater surveillance system source equipment, and the output data should be defined in terms of the destination.

5.10.14. INTEGRATED LOGISTIC SUPPORT

This section defines the test equipment, spare parts, tools, technical manuals, and working space required to support the sonar system. The space, weight, and location of such materials should be specified to ensure that adequate storage facilities will exist.

5.10.14.1. Test Equipment

Sonar test equipment is categorized as general or special purpose. General purpose test equipment measures parameters common to two or more equipments, or systems, that are of essentially different design. Special purpose test equipment is used to measure parameters that are peculiar to a particular equipment or system.

Basically, general purpose test equipment consists of devices that measure electrical parameters. A table summarizing the quantity, space, and weight requirements for such equipment should be provided. There should also be a table summarizing the requirements for special purpose test equipment. Much of it will be housed in the sonar set-kits containing cable assemblies and extender modules.

5.10.14.2. Tools

Sonar systems tools are required for disassembly, repair, and reassembly of damaged units. They should be easily accessible but contained to prevent them from becoming a hazard. A table specifying the space, weight, and location requirements for such should be included in the interface description.

5.10.14.3. Spare Parts

A variety of spare parts and electronic modules must be carried onboard to ensure that the system can be repaired. Certain components deteriorate with time and others are susceptible to damage from overheating. These, of course, are the items that should be carried in the greatest abundance.

5.10.14.4. Technical Manuals

A complete set of technical manuals for all sonar system equipment is required to troubleshoot and repair damaged units. They should be in the form of microfilm to conserve space. A list of such manuals should be supplied for the particular system.

5.10.14.5. Storage and Working Spaces

Required storage and working spaces should be provided.

5.11. TEMPORARY INSTALLATIONS

Temporary installations are made either for research purposes or to meet special mission requirements. They may range in size from the three-story high MACS antenna that was installed onboard USS NAUTILUS to small electronic boxes installed to test new circuit designs.

All such installations, no matter how minor, influence the ship in some way. Temporary installation work must be done in accordance with approved plans and must meet current U.S. Navy specifications for the ship. This applies particularly to *sub-safe* requirements for submarines and *weight-stability* requirements for all types of ships. Although certain requirements may be waived for short period installations, safety must never be compromised.

5.11.1. INITIATING A TEMPORARY INSTALLATION

The individual or organization requesting a temporary installation usually has a reasonably good idea of the impact on the ship, i.e., where the equipment will be located, how large it is, the amount of power required, the cooling load, and the number of personnel required. Discussions should be undertaken with the design group to review the feasibility of the job, the cost, and the schedule.

5.11.2. SHIP CHECK

A designer should visit the ship assigned for the temporary installation to determine the requirements. Other specialists may be required if the installation is complex, i.e., if extensive foundations or modifications to the power supply are required. If it is decided that the vessel meets the need, a study should be made of the relevant dimensions and power supply capabilities through actual measurements and reference to ship's drawings. It should be noted here that there will usually be differences between the measurements and the original drawings.

5.11.3. INSTALLATION DESIGN

The installation design is based upon the information obtained during the ship check. There is a manual for temporary submarine installation techniques (*Pearson, 1977*) that provides a detailed description of the requirements. General installation considerations are

1. sub-safe requirements,
2. noise radiation,
3. electrical security,
4. cable selection and runs,
5. EMI,
6. grounding,
7. welds,
8. inactivated systems,
9. restoration,
10. classified material,
11. shock,
12. increased drag,
13. increased weight,
14. stability,
15. integrity, i.e., effects on diving depth, electrical penetrations, watertightness, and
16. on- and off-loading equipment.

At the conclusion of the design, a report is prepared describing the installation and the impact on the ship. This document provides the information required to determine whether or not the installation will be approved.

5.11.4. INSTALLING ACTIVITY

While the details of the installation are being worked out, it is necessary to meet with members of the installing activity to discuss the availability of pier space, crane facilities, and special requirements (e.g., cable reels, refuse oil facilities, divers). The supplier of materials,

manpower resources, and security provisions are also determined at this time. A written description of separate responsibilities is good practice.

5.11.5. PRE-INSTALLATION CHECK

After the installation is approved the temporary equipment, cable connectors, hull and bulkhead penetrators, structural steel, piping, fittings, and other necessary materials must be acquired. It is best to assign this responsibility to a single individual in order to maintain the highest degree of control. All equipment should, of course, be tested for proper operation before the installation.

5.11.6. COORDINATION

As soon as possible after a ship has been assigned, senior project personnel should meet with the senior ships officers to explain the purpose of the installation and the extent to which it will affect the vessel. This provides the opportunity for shipboard personnel to define problems that may have been overlooked during installation design and to plan for inconveniences that the installation may entail. Such an approach is also likely to create a spirit of cooperation among the principals.

5.11.7. INSTALLATION

The installation coordinator must ensure that the necessary equipment and materials are onboard and that the work progresses as smoothly as possible. Among a host of other duties,he must be available to answer questions concerning the installation plans and location of required materials.

5.11.8. TESTING

When the installation is completed, the equipment is *lit off* and tested for proper operation, strength, watertightness, and so on. If necessary the equipment is calibrated at this time. If there are no problems, the installation is ready for at-sea operation.

5.11.9. REMOVAL

Most temporary installations are not complete until they have been removed and the ship has been restored, as nearly as possible, to its original condition. There are instances, however, in which the equipment is left onboard because it adds a desired capability.

BIBLIOGRAPHY

Beranek, L. L., *Noise and Vibration Control*, McGraw Hill Book Company, New York, 1971.

Cook, I., "The Ship-Sonar Interface," *Naval Engineering Journal*, June 1969.

Cramer, W. S., "Anechoic Coatings-Present Status and Future Problems," *U.S. Navy Journal of Underwater Acoustics*, vol. 20, January 1970.

DeJarnette, H. M. and H. J. Demattia, "Electromagnetic Interference Considerations for Shipboard Electronics Systems," *Naval Engineer's Journal*, June 1966.

Graham, C., "The Impact of Subsystems on Naval Ship Design,"*Naval Engineer's Journal*, December 1975.

Hamlin, N. A., *Evaluation of Environmental Degradation of a Surface Ship's Sonar Performance*, Technical Report B6-2, Webb Institute of Naval Architecture, Glen Cove, N.Y., April 1969.

Hoerner, S. F., *Fluid Dynamic Drag*, Published by Author, 148 Busteed Drive, Midland Park, N.J. 07432.

Laskey, M., "Historical Review of Underwater Acoustic Technology: 1939-1945 With Emphasis on Undersea Warfare," *U.S. Navy Journal of Underwater Acoustics*, vol. 25, October 1975.

Libuha, J. J. and W. F. Wardle, *Blanket Hydrophones: Their Design, Development and Application*, NUSC Technical Report 4023, 22 December 1970.

Loeser, H. T., "Transient Towline Configurations During Ship Maneuvering," NUSC Technical Memorandum EA131-104-74, 19 November 1974.

Loeser, H. T., "Guide to Calculating the Hydrodynamic Forces on Protruding Dome Appendages on Ships," NUSC Technical Memorandum 781121, 19 June 1978.

Pearson, E.B. and W. Helton, *Guidance Manual for Temporary Submarine Installation Techniques*, NUSC Technical Document 5657, 6 September 1977.

MIL-STD-1472B, *Human Engineering Design Criteria for Military Systems*, 31 December 1974.

MIL-HDBK-237-A, *EMC Management Guide for Platforms Systems and Equipment*, 2 February 1981.

NAVSEA 0967-LP-283-5010, *Shipboard Electromagnetic Shielding Practices*.

NAVSEA 0900-LP-089-5010, *Resilient Mount Handbook*.

Principles of Sonar Installation

CHAPTER VI
FUTURE TECHNOLOGY

CHAPTER VI
FUTURE TECHNOLOGY

6.0 INTRODUCTION

The thrust of sonar development has been, and probably will continue to be, the development of more effective platforms and sonar systems. The trend in sonar has been toward specialized systems to satisfy needs as they develop, and toward larger arrays that exploit the low frequency ranges. The capability to control acoustic energy, mainly through the use of elastomers, is resulting in larger, more effective arrays. The increased number of hydrophones in arrays is, in turn, forcing the development of more complex digital beamformers.

The trend toward specialization is also apparent in sonar platforms. A subset of ships, the ASW escort, has evolved from the all-purpose destroyer escort. A new concept offers the possibility of mobile surveillance ships, operated by civilians, that would tow very large arrays at slow speeds. Also, high speed hydrofoil, SWATH, and SES platforms are being reviewed for sonar suites adapted to their particular requirements.

The persistent effort to acoustically and electromagnetically quiet ASW ships has led to quieter platforms and, therefore, more effective sonar systems. The need for detection and classification of over-the-horizon targets has added impetus to the installation of long range, passive sonar systems onboard missile carrying ships.

The ever increasing data available to the Tactical Command Officer is inspiring new presentation methods, e.g., prescreening to select only important data for display, presentation of information at the proper time, and reporting system degradation only when it effects the particular operation. While these and other efforts result in higher performance, the sonar ship impact on the ship grows and the sonar/ship interface problem increases.

6.1. ADVANCED SONAR

Large arrays provide advantages that suggest their use will increase. They permit the formation of narrow beams and lower side lobes for better SNR. The improved SNR requires reduced self-noise with increased array size.

Sound isolation experiments have shown encouraging results for area arrays fixed to the outer hull of the ship. The method provides a baffle against noise emanating from the hull, maximizes the signal at the hydrophone, and attenuates flow noise. As information on the acoustic behavior of materials and combinations of materials is obtained, arrays having far better self-noise characteristics may be developed. Figures 6.1 and 6.2 illustrate the types of conformal arrays that could result from this technology.

Data processing for large arrays is extremely complex. However, improved microprocessing techniques are eliminating the problem of prohibitive equipment, size, cost, and impact.

Quality control of elastomeric materials is currently based on manufacturing methods and crude post-fabrication tests. A better understanding of the acoustic processes involved in absorption, reflection, decoupling, and damping will require more precise specification of material properties. For example, the real and imaginary dynamic compliance as a function of acoustic frequency should be known for each material used. Instruments to measure surface impedance and loss tangents in shear

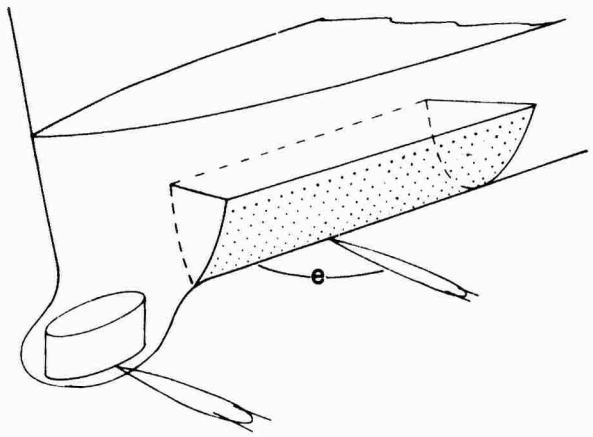

Figure 6.1. Surface Ship Conformal Array

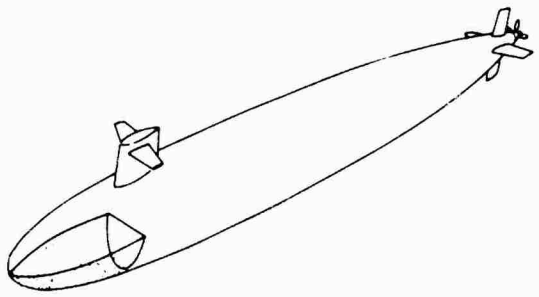

Figure 6.2. Submarine Conformal Array

and compression must be developed so that the dynamic surface properties of an acoustic treatment can be determined.

Improved projectors and hydrophones are also being developed. Wider band projectors will be required as frequency bands become wider to improve performance and permit the use of several active bands. Fiber optic light modulation and improved piezoelectric and moving coil devices are being developed for hydrophone applications. Light modulation techniques may eliminate electrical conductors for low level signal stages and, thus, eliminate some EMI problems.

Exploitation of the acoustic spectrum continues to increase the types of specialized sonar systems, especially onboard submarines. Higher frequencies are used to sense the environment at different ranges and in different detail. Acoustic signals for communication will probably be developed for longer ranges. The parametric sonar, which has a narrow beamwidth and very low side lobes, is a candidate for this application.

The reliable acoustic path (RAP) is difficult to exploit because it requires that sensors be located in deep water, but it can be used by towed and suspended arrays. Increased use of RAP will probably involve towing from displacement ships or *sprint and dip* tactics using hydrofoils or SES vessels.

Development of fiber optic technology for telemetering information and low cost electro-optical transducers and repeaters opens a new area of possible sonar applications. The tow cable would be smaller, transmitted data would increase by an order of magnitude, and the low cost would permit the use of expendable units.

Possible applications are

1. long towed arrays having many hydrophones,
2. expendable anti-trail hydrophones deployed astern,
3. expendable RAP depth sonobouys,
4. expendable line arrays deployed down wind,
5. covert monitoring of deployed hydrophones from great distances,
6. expendable arrays monitored by a fiber optic umbilical, and
7. fiber optic shipboard telemetering to reduce space requirements, cost, and EMI.

The EMC management guide recognizes that management of technology is as important as its development, and that the benefits of improved technology do not automatically improve performance. Only continued emphasis on EMC through specification and management at all levels will increase the quality of the information data processors provide CIC.

6.2. ADVANCED PLATFORMS

Various advanced ship designs have been proposed as ASW platforms. The U.S Navy currently uses the conventional destroyer hull, submarines, patrol aircraft, carrier aircraft, and helicopters as primary ASW platforms.

The *high performance* platforms under consideration include hydrofoil, SES, and SWATH vessels. Hydrofoils have a high speed capability and a smooth ride that employs electronic control. However, they have a relatively small payload, short range, and high cost per ton of payload. When foil-borne, the water-jet propelled type is relatively quiet but the drag of acoustic domes or towed fish is costly in terms of performance.

Suggested ASW uses have included the installation of a small high frequency attack sonar on the strut or foil in conjunction with detection and localization by another platform, a towed array, or deployed sonobuoys. The high speed attack advantage would thus be retained while the detection, tracking, and localization functions were accomplished elsewhere.

When not foil-borne, hydrofoils have relatively long ranges at low speeds and can be used effectively for local ASW patrols. However, because the acoustic sensor system is of little use when foil-borne, operation with other types of ships is advisable.

Most of the above discussion applies to the SES type platform. The SES can achieve higher speeds and its engine noise is decoupled from the water because it rides on an air cushion. The high speed capability of hydrofoils and SES vessels permits them to use the RAP propagation mode. This requires that the array be lowered deep into the ocean, but the high sprint capability permits a reasonably high speed of advance.

The SWATH platform (see figure 6.3) can be designed for high speed operation and is, for its size, a very good seagoing vessel. The small waterplane area results in a very low frequency response to waves. If the ship's frequency remains below the seaway spectrum, the SWATH will not respond to the wave excitation. Figure 6.4 shows a typical seaway spectrum. A frequency below 0.2 results in a ship that responds very little to the sea. The design provides for the infrequent low frequency waves that may be encountered.

This relatively stable, seagoing platform can accommodate any type sonar system. Twin hull construction permits the deployment of heavy surveillance and towed arrays. The SWATH might best be employed as an on-station monitor that relays data via satellite to a shore station.

None of the ships discussed above has, as yet, been established as a convincing ASW platform. However, advanced technology may yet find such a use for them.

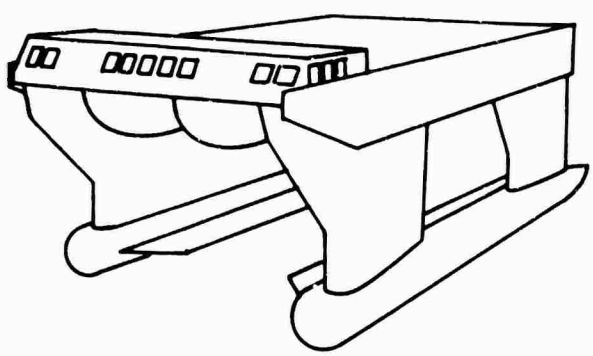

Figure 6.3. SWATH Platform

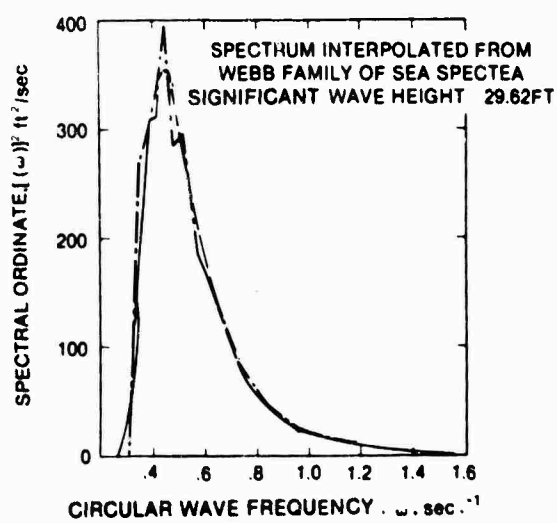

Figure 6.4. Typical Seaway Spectrum

BIBLIOGRAPHY

Graham, C., LCDR, USN, "The Impact of Subsystems on Naval Ship Designs," *Naval Engineer's Journal* vol. 87, no. 6, pp. 15-25, December 1975.

Graham, C., F. Fahy, and J. Grostick, "A Comparative Analysis of Naval Hydrofoil and Displacement Ships, *SNAME Trans.*, 1976.

Howell, J. and C. Graham, "Marginal Weight Factors for Surface Combatant Ships," 13th Annual ASE Technical Symposium, March 1976.

Kennel, B. and G. Colen, "Small Waterplane Area, Twin-Hull (SWATH) Combatant Ship Parametric Study," *Naval Engineer's Journal*, October 1979.

Meeks, T.L. and P. J. Mantle, "Evaluation of Advanced Naval Vehicle Concepts," *AIAA/SNAME*, no. 78-846.

Meeks, T.L., C. Graham and R. Chu, "Combat Systems for the Advanced Naval Vehicles Concepts Evaluation," *Naval Engineer's Journal*, October 1978.

Surface Warfare Magazine, January 1977.

Initial Distribution List

ADDRESSEE	NO. OF COPIES
CINCLANTFLT	1
CINCPACFLT	1
COMSECONDFLT	1
COMTHIRDFLT	1
COMSIXTHFLT	1
COMSEVENTHFLT	1
COMASWFORSIXTHFLT	1
COMNAVSURFLANT	1
COMNAVSURPAC	1
COMSUBLANT	1
COMSUBPAC	1
COMTRALANT	2
COMTRAPAC	2
COMOPTEVFOR	1
OICNLONTEVDET	1
DEPCOMOPTEVFORPAC	2
COMFLTRAGRU PEARL	2
COMFLTRAGRU SDGO	2
COMFLTRAGRU WSTPC	2
COMFLETRAGRU GTMO	2
COMCRUDESGRU 1	1
COMCRUDESGRU 2	1
COMCRUDESGRU 3	3
COMCRUDESGRU 5	1
COMCRUDESGRU 8	1
COMCRUDESGRU 12	1
COMSURFWARDEVGRU	1
COMSUBRON	1
COMSUBRON 2	1
COMSUBRON 3	1
COMSUBRON 4	1
COMSUBRON 6	1
COMSUBRON 7	1
COMSUBRON 10	1
COMSUBRON 14	1
COMSUBRON 15	1
COMSUBRON 16	1
COMSUBRON 18	1
COMSUBGRU 5	1
COMSUBDEVGRUONE	1
COMSUBDEVRON 12	1
OASN (M. G. Cann)	1
CNO, OP-22, -39, -951, -951D, -951E, -37, -981F, -981G1, -981H, -982F	10
CNM, MAT-08T, -08T1 (Dr. J. Probus), -08T21, -08T22, -08T23, ASW-122,-111, -10, -24, -53, PM-18, ASW-14	12
NAV SURFACE WEAPONS CENTER, WHITE OAK LABATORY	1
DWTNSRDC ANNA	1
DWTNSRDC CARD	1
NRL	1
NRL, USRD	1
NRL, AESD	1
NORDA (Dr. R. Goodman, 110)	1
USOC, Code 241, -240	2
SUBASE LANT	1
NAVSUBSUPACNLON	1

NAVSEASYSCOM, SEA-00, -001, -003, -03, -03R, -04, -05, -05D, -05H, -05L,-05R, -511, -06, -06C, -06D, -06R, -06V, -06Z, -61, -61R, -611, -613, -614, -62, -62R, -63, -63R, -63R-1, -63R-13, -63X, -631X,-631Y, 632X, 632Y, -92, -92R, -393, -395, -396, -921, -93, -996,	42
Naval Sea Systems Detachment, Norfolk, VA,	1
NOSC, Code 6565 (Library)	2
DTNSRDC	1
NAVCOASTSYSLAB	1
CIVENGRLAB	1
NAVSURFWPNCEN	1
CHESNAVFACENGCOM, FPO-1P3	1
NAVSHIPYD PUGET	1
Carr Inlet Acoustic Range (Puget Sound)	1
NAVSHIPYD CHASN	1
NAVSHIPYD LBEACH	1
NAVSHIPYD PEARL	1
NAVSHIPYD PHILA	1
NAVSHIPYD PTSMH	1
NAVSHIPYD NORVA	1
NAVSHIPYD MARE	1
NUWES, KEYPORT	1
NUWES San Diego Detachment	1
NUWES Hawaii Detachment	1
NISC	1
CNT, Code 017	
NAVSUBTRACENPAC	1
FLTASWTRACENPAC Tactical Library	1
FLTASWTRACENLANT	5
NAVSUBSCOL	1
NAVTRAEQUIPCEN	1
NAVPGSCOL	1
NAVWARCOL	1
NETC	1
SWOSCOLCOM	1
NAVTRAEQUIPCENT, Technical Library	1
APL/UW, SEATTLE	1
ARL/PENN STATE, STATE COLLEGE	1
CENTER FOR NAVAL ANALYSES (ACQUISITION UNIT)	1
DTIC	2
DARPA	1
NOAA/ERL	1
NATIONAL RESEARCH COUNCIL	1
WOODS HOLE OCEANOGRAPHIC INSTITUTION	1

SUPPLEMENTARY

INFORMATION

DEPARTMENT OF THE NAVY
NAVAL SEA SYSTEMS COMMAND
2531 JEFFERSON DAVIS HIGHWAY
ARLINGTON VA 22242-5160

IN REPLY REFER TO

5510 - 1
Ser: 118/351/09T1F/MISC
18 FEB 1994

ERRATA

0033

00043.5

From: Commander, Naval Sea Systems Command
To: Commander, Naval Undersea Warfare Center, Detachment New London (Attn: J. L. Foster) 39 Smith Street, New London, CT 06320-5594

Subj: RELEASE OF NUSC TD 6059 B063 220

5511

Ref: (a) Your ltr 5500 Ser: 40233/67 of 26 Jan 94
(b) Naval Postgraduate School ltr of 3 Jan 94
(c) NUSC TD 6059 "Principles of Sonar Installation"

1. In reply to references (a) and (b), our review has determined that assignment of Distribution Statement "A" is appropriate for reference (c). Cite this letter as your authority for remarking and notify all holders.

2. Any questions regarding this matter may be directed to T. M. Napper (SEA 09T1F) at (703) 602-3784 (ext. 108).

ERRATA

E. R. HAINES
Director,
Office of Security

Copy to:
Naval Postgraduate School (Attn: R. Keolian)

40F11
U94/2125